

A STUDY OF THE EFFECT OF EMBEDMENT AND RELATED FACTORS ON THE DYNAMIC BEHAVIOUR OF FOOTINGS

BY

N. R. KRISHNASWAMY

CE
1972
D
KRI
STU

TH
CE/1972/D
K8975



DEPARTMENT OF CIVIL ENGINEERING

INDIAN INSTITUTE OF TECHNOLOGY KANPUR

APRIL 1972

A STUDY OF THE EFFECT OF EMBEDMENT AND RELATED FACTORS ON THE DYNAMIC BEHAVIOUR OF FOOTINGS

**A Thesis Submitted
In Partial Fulfilment of the Requirements
for the Degree of
DOCTOR OF PHILOSOPHY**

**BY
N. R. KRISHNASWAMY**

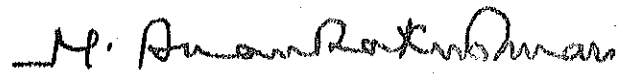
17133

to the

**DEPARTMENT OF CIVIL ENGINEERING
INDIAN INSTITUTE OF TECHNOLOGY KANPUR
APRIL 1972**

CERTIFICATE

This is to certify that the thesis entitled
'A Study of the Effect of Embedment and Related Factors on
the Dynamic Behaviour of Footings' by N.R. Krishnaswamy, for
the award of the Degree of Doctor of Philosophy, of the
Indian Institute of Technology, Kanpur is a record of
bonafide research work carried out by him under my
supervision and guidance. The thesis work, in my opinion
reached the standard fulfilling the requirements for the
Doctor of Philosophy Degree. The results embodied in this
thesis have not been submitted to any other University or
Institute for the award of any degree or diploma.




(M. ANANDAKRISHNAN)

Professor

Department of Civil Engineering
Indian Institute of Technology, Kanpur.

April 1972.

POST GRADUATE OFFICE

This thesis has been approved
for the award of the Degree of
Doctor of Philosophy (Ph.D.)
in accordance with the
regulations of the Indian
Institute of Technology Kanpur
Dated: 5/10/72 

JUNE '76

A 22155

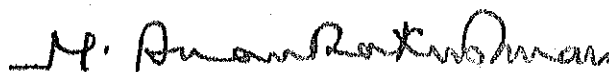
I. I. T. KANPUR
CENTRAL LIBRARY
A 221545

5 JAN 1973

CE-1972-D-KRI-STU

CERTIFICATE

This is to certify that the thesis entitled
'A Study of the Effect of Embedment and Related Factors on
the Dynamic Behaviour of Footings' by N.R. Krishnaswamy, for
the award of the Degree of Doctor of Philosophy, of the
Indian Institute of Technology, Kanpur is a record of
bonafide research work carried out by him under my
supervision and guidance. The thesis work, in my opinion
reached the standard fulfilling the requirements for the
Doctor of Philosophy Degree. The results embodied in this
thesis have not been submitted to any other University or
Institute for the award of any degree or diploma.



(M. ANANDAKRISHNAN)

Professor

Department of Civil Engineering
Indian Institute of Technology, Kanpur.

April 1972.

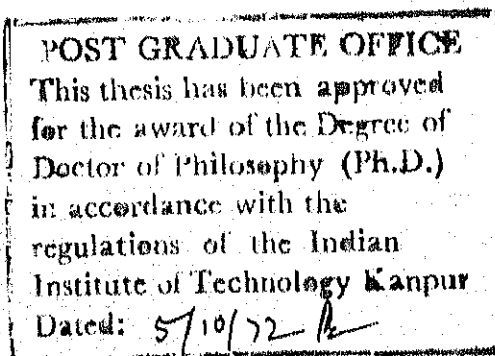


TABLE OF CONTENTS

	Page
ACKNOWLEDGMENT	iii
LIST OF TABLES	viii
LIST OF FIGURES	ix
NOTATION	x v
SYNOPSIS	xviii
CHAPTER 1 INTRODUCTION	1
1.1 General	1
1.2 Background	3
1.3 Scope	5
1.4 Presentation	7
CHAPTER 2 THEORETICAL BACKGROUND AND REVIEW OF PREVIOUS INVESTIGATIONS	12
2.1 General	12
2.2 Mass-Spring-Dashpot System	14
2.2.1 Free Vibrations	14
2.2.2 Forced Vibrations with Constant Forcing Function	16
2.2.3 Forced Vibrations with Rotating-Mass-Type-Excitation	18
2.3 The Elastic Half-Space Theory	19
2.3.1 General	19
2.3.2 Results of the Elastic Half-Space Theory	21

	Page
2.4 Reorganization of Half-Space Solution	25
2.4.1 Geometrical Damping	25
2.4.2 Hsieh's Equations	26
2.4.3 Lysmer's Analogue	27
2.4.4 Hall's Analogues	29
2.5 Limitations of the Half-Space Theory	30
2.5.1 General Remarks	30
2.5.2 Nonlinearity	30
2.5.3 Embedment	31
2.6 Previous Experimental Investigations	36
CHAPTER 3 FIELD VIBRATORY INVESTIGATIONS	43
3.1 General	43
3.2 Test Site	44
3.2.1 Test Footings	47
3.3 Instrumentation	48
3.3.1 Mechanical Vibrator	48
3.3.2 Transducers	52
3.3.3 Vibration Recording	53
3.3.4 Steady State Vibratory Tests	56
3.3.5 Surface Seismic Investigations	61
3.3.6 Cross-Hole Seismic Investigations	68
CHAPTER 4 RESULTS OF SEISMIC INVESTIGATIONS	85
4.1 General	85

	Page
CHAPTER 8 THE PROPOSED THEORETICAL MODEL	193
8.1 General	193
8.2 Effect of Embedment	194
8.3 The Proposed Theoretical Model	195
8.3.1 General Remarks	195
8.3.2 Forced Vibrations with Constant Forcing Function	197
8.3.3 Forced Vibrations with Rotating-Mass-Type Excitation	203
8.4 Evaluation of the Constant Frictional Force	206
8.5 Comparison with Experiments	209
CHAPTER 9 CONCLUDING DISCUSSIONS WITH RECOMMENDATIONS	262
9.1 General	262
9.2 The Effect of Embedment	263
9.3 The Effect of Surcharge	266
9.4 The Effect of Base Size and Shape	267
9.5 The Effect of Variation of Soil Properties	269
9.6 The Effect of Moisture in Soils	270
9.7 The Effect of Soil Under Large Dynamic Force Levels	271
CHAPTER 10 SUMMARY AND CONCLUSIONS	272
REFERENCES	275
APPENDIX A	285
APPENDIX B	291
VITA	293

LIST OF TABLES

		Page
TABLE 3.1	PHYSICAL PROPERTIES OF THE CONCRETE FOOTINGS TESTED IN THE PRESENT INVESTIGATION	72
TABLE 4.1	RESULTS OF CROSS-HOLE SEISMIC INVESTIGATIONS AT CHAKERI SITE	95
TABLE 4.2	CONFINING PRESSURE CALCULATIONS BASED ON PRANGE'S SOLUTIONS (For $\mu = 0.25$)	96
TABLE 5.1	PREDICTED RESPONSE OF TEST FOOTINGS BY LYSMER'S ANALOGUE	123
TABLE 5.2	RESULTS OF ANALYSES OF EXPERIMENTAL FREQUENCY-DISPLACEMENT RESPONSE CURVES	124
TABLE 6.1	RESULTS OF ANALYSES OF EXPERIMENTAL FREQUENCY-DISPLACEMENT CURVES FOR VARIOUS DEPTHS OF EMBEDMENT	149
TABLE 8.1	COMPARISON BETWEEN THE PREDICTED AND OBSERVED DYNAMIC RESPONSE OF EMBEDDED FOOTINGS	213

LIST OF FIGURES

Figure No.		Page
1.1	SIX MODES OF VIBRATION FOR A BLOCK FOUNDATION	11
1.2	FOUR MODES OF VIBRATION FOR A CIRCULAR FOUNDATION	11
2.1	RESPONSE CURVES FOR ONE-DEGREE-OF-FREEDOM MASS-SPRING-DASHPOT-SYSTEM (a) For constant amplitude of exciting force (b) For rotating mass type exciting force	42
3.1	SOIL PROFILE FOR THE TEST AREA AT I.I.T. KANPUR	73
3.2	SOIL PROFILE FOR THE TEST AREA AT CHAKERI, KANPUR	74
3.3	SITE PLAN OF TEST AREA AT I.I.T.KANPUR	75
3.4	SITE PLAN OF TEST AREA AT CHAKERI, KANPUR	76
3.5	SCHEMATIC DIAGRAM OF FIELD VIBRATOR AND FOOTING WITH INSTRUMENTATION	77
3.6	SCHEMATIC DIAGRAM OF INSTRUMENTATION FOR SEISMIC REFRACTION SURVEY	78
3.7	SCHEMATIC DIAGRAM OF INSTRUMENTATION FOR CROSS HOLE SEISMIC INVESTIGATIONS	79
3.8	A PHOTOGRAPHIC VIEW OF THE EXCAVATED PIT WITH BASE-1	80
3.9	A PHOTOGRAPHIC VIEW OF THE VIBRATOR-FOOTING SYSTEM WITH ASSOCIATED INSTRUMENTATION	81
3.10	A PHOTOGRAPHIC VIEW OF VIBRATOR AND BASE-3 IN A PARTIALLY EMBEDDED CONDITION	82
3.11	A PHOTOGRAPHIC VIEW OF BASE-4 IN A FULLY EMBEDDED CONDITION	83

Figure No.		Page
3.12	A PHOTOGRAPHIC FLAN VIEW SHOWING BASES-2,3 and 4	84
4.1	SAMPLE TRAVEL TIME GRAPH FOR THE TEST SITE AT I.I.T. KANPUR	97
4.2	SAMPLE TRAVEL TIME GRAPH FOR THE TEST SITE AT I.I.T. KANPUR	98
4.3	TYPICAL PHOTOGRAPHIC RECORDS OF OSCILLOSCOPE TRACES OBTAINED DURING REFRACTION SURVEYING	99
4.4	CROSS HOLE SEISMIC INVESTIGATIONS ACROSS BASE-3	100
4.5	CROSS HOLE SEISMIC INVESTIGATIONS ACROSS BASE-5	101
4.6	TYPICAL PHOTOGRAPHIC RECORDS OF THE OSCILLOSCOPE TRACES OBTAINED DURING CROSS-HOLE SEISMIC INVESTIGATIONS ACROSS BASE-3	102
4.7	TYPICAL PHOTOGRAPHIC RECORDS OF THE OSCILLOSCOPE TRACES OBTAINED DURING CROSS HOLE SEISMIC INVESTIGATIONS ACROSS BASE-5	103
4.8	DISTRIBUTION OF AVERAGE CONFINING PRESSURE, $\bar{\sigma}_0$, BENEATH THE PERIPHERY OF BASES-1,2,3,4 AND 5.	104
5.1	FREQUENCY VS DISPLACEMENT, BASE-1 AT HIGHER DYNAMIC FORCE LEVELS	128
5.2	FREQUENCY VS DISPLACEMENT, BASE-3 AT HIGHER DYNAMIC FORCE LEVELS	129
5.3	FREQUENCY VS DISPLACEMENT, BASE-1	130
5.4	FREQUENCY VS DISPLACEMENT, BASE-2 WITHOUT BACKFILL	131
5.5	FREQUENCY VS DISPLACEMENT BASE-3 WITHOUT BACKFILL	132

Figure No.		Page
5.6	FREQUENCY VS DISPLACEMENT, BASE-4, WITHOUT BACKFILL	133
5.7	FREQUENCY VS DISPLACEMENT BASE-5	134
5.8	FREQUENCY VS DISPLACEMENT, CHAKERI-BASE	135
5.9	DECREASE OF SPRING CONSTANT, K, WITH INCREASE OF DYNAMIC FORCE LEVELS DURING DRY AS WELL AS WET SOIL CONDITIONS	136
5.10	DECREASE OF DAMPING FACTOR, D, WITH INCREASE OF DYNAMIC FORCE LEVELS, DURING DRY AS WELL AS WET SOIL CONDITIONS	137
6.1	FREQUENCY VS DISPLACEMENT, BASE-2, BACKFILLED BY SAND 6 $\frac{3}{4}$ " DEEP	156
6.2	FREQUENCY VS DISPLACEMENT, BASE-2 BACKFILLED BY SAND, 13 $\frac{1}{2}$ " DEEP	157
6.3	FREQUENCY VS DISPLACEMENT, BASE-2, BACKFILLED BY SAND, 20 $\frac{1}{4}$ " DEEP	158
6.4	FREQUENCY VS DISPLACEMENT, BASE-2, BACKFILLED BY SAND 27" DEEP	159
6.5	FREQUENCY VS DISPLACEMENT, BASE-3, BACKFILLED BY SAND 1' DEEP	160
6.6	FREQUENCY VS DISPLACEMENT, BASE-3, BACKFILLED BY SAND, 2' DEEP	161
6.7	FREQUENCY VS DISPLACEMENT, BASE-3, BACKFILLED BY SAND, 3' DEEP	162
6.8	FREQUENCY VS DISPLACEMENT, BASE-3, BACKFILLED BY SAND, 4' DEEP	163
6.9	FREQUENCY VS DISPLACEMENT, BASE-4, BACKFILLED BY SAND- 6 $\frac{3}{4}$ " DEEP	164
6.10	FREQUENCY VS DISPLACEMENT, BASE-4, BACKFILLED BY SAND- 13 $\frac{1}{2}$ " DEEP	165
6.11	FREQUENCY VS DISPLACEMENT, BASE-4, BACKFILLED BY SAND- 20 $\frac{1}{4}$ " DEEP	166

Figure No.		Page
6.12	FREQUENCY VS DISPLACEMENT, BASE-4, BACKFILLED BY SAND- 27" DEEP	167
6.13	COMPARISON OF RESPONSE CURVES FOR BASE-2 WITH DIFFERENT EMBEDMENT FACTORS	168
6.14	COMPARISON OF RESPONSE CURVES FOR BASE-3 WITH DIFFERENT EMBEDMENT FACTORS	169
6.15	COMPARISON OF RESPONSE CURVES FOR BASE-4 WITH DIFFERENT EMBEDMENT FACTORS	170
6.16	OBSERVED AMPLITUDE REDUCTION FACTOR VS EMBEDMENT FACTOR	171
6.17	OBSERVED FREQUENCY INCREASE FACTOR VS EMBEDMENT FACTOR	172
6.18	OBSERVED INCREASE IN THE EFFECTIVE STIFFNESS OF THE SOIL-FOUNDATION SYSTEM WITH EMBEDMENT	173
6.19	OBSERVED INCREASE IN THE EFFECTIVE VISCOUS DAMPING OF THE SOIL-FOUNDATION SYSTEM WITH EMBEDMENT	174
7.1	FREQUENCY VS DISPLACEMENT, BASE-5 WITH 1 LAYER OF SURCHARGE	181
7.2	FREQUENCY VS DISPLACEMENT, BASE-5 WITH 2 LAYERS OF SURCHARGE	182
7.3	FREQUENCY VS DISPLACEMENT, BASE-5 WITH 3 LAYERS OF SURCHARGE	183
7.4	FREQUENCY VS DISPLACEMENT, BASE-5 WITH 4 LAYERS OF SURCHARGE	184
7.5	FREQUENCY VS DISPLACEMENT, BASE-5 WITH 5 LAYERS OF SURCHARGE	185
7.6	FREQUENCY VS DISPLACEMENT, BASE-5 WITH 6 LAYERS OF SURCHARGE	186
7.7	FREQUENCY VS DISPLACEMENT, BASE-5 WITH 7 LAYERS OF SURCHARGE	187

Figure No.		Page
7.8	EFFECT OF SURCHARGE ON MAXIMUM AMPLITUDES AT RESONANCE, BASE-1	188
7.9	EFFECT OF SURCHARGE ON MAXIMUM AMPLITUDES AT RESONANCE, BASE-2	189
7.10	EFFECT OF SURCHARGE ON MAXIMUM AMPLITUDES AT RESONANCE, BASE-2	190
7.11	EFFECT OF SURCHARGE ON MAXIMUM AMPLITUDES AT RESONANCE, BASE-5	191
7.12	EFFECT OF SURCHARGE ON RESONANT FREQUENCIES	192
8.1	THE ELASTIC HALF-SPACE MODEL AND THE EQUIVALENT SINGLE-DEGREE-OF-FREEDOM ANALOGUE a) A RIGID CIRCULAR FOOTING ON SURFACE OF SOIL b) A RIGID CIRCULAR FOOTING EMBEDDED IN SOIL	229
8.2	AMPLITUDE-FREQUENCY RELATIONS FOR A LUMPED MASS-SPRING SYSTEM WITH COMBINED VISCOUS AND COULOMB FRICTION DAMPING FOR CONSTANT AMPLITUDE EXCITING FORCE	230
8.3	AMPLITUDE-FREQUENCY RELATIONS FOR A LUMPED MASS SPRING SYSTEM WITH COMBINED VISCOUS AND COULOMB FRICTION DAMPING FOR EXCITING FORCE DUE TO ECCENTRIC ROTATING MASSES	240
8.4	DECREASE OF MAXIMUM AMPLITUDES AT RESONANCE WITH COULOMB FRICTION FACTOR FOR CONSTANT AMPLITUDE OF EXCITING FORCE	250
8.5	DECREASE OF RESONANT FREQUENCY WITH COULOMB FRICTION FACTOR FOR CONSTANT AMPLITUDE OF EXCITING FORCE	251
8.6	DECREASE OF MAXIMUM AMPLITUDES AT RESONANCE WITH COULOMB FRICTION FACTOR FOR EXCITING FORCE DUE TO ECCENTRIC ROTATING MASSES	252

Figure No.		Page
8.7	INCREASE OF RESONANT FREQUENCY WITH COULOMB FRICTION FACTOR FOR EXCITING FORCE DUE TO ECCENTRIC ROTATING MASSES	253
8.8(a)	CORRELATION BETWEEN THE PREDICTED AND OBSERVED AMPLITUDES AT RESONANCE FOR AN EMBEDDED FOOTING (BASE-2)	254
8.8(b)	CORRELATION BETWEEN THE PREDICTED AND OBSERVED AMPLITUDES AT RESONANCE FOR AN EMBEDDED FOOTING (BASE-3)	255
8.8(c)	CORRELATION BETWEEN THE PREDICTED AND OBSERVED AMPLITUDES AT RESONANCE FOR AN EMBEDDED FOOTING (BASE-4)	256
8.8(d)	CORRELATION BETWEEN THE PREDICTED AND OBSERVED AMPLITUDES AT RESONANCE FOR EMBEDDED FOOTINGS, DATA FROM FRY (1963) and novak (1970)	257
8.8(e)	CORRELATION BETWEEN THE PREDICTED AND OBSERVED RESONANT FREQUENCIES FOR AN EMBEDDED FOOTING (BASE-2)	258
8.8(f)	CORRELATION BETWEEN THE PREDICTED AND OBSERVED RESONANT FREQUENCIES FOR AN EMBEDDED FOOTING (BASE-3)	259
8.8(g)	CORRELATION BETWEEN THE PREDICTED AND OBSERVED RESONANT FREQUENCIES FOR AN EMBEDDED FOOTING (BASE-4)	260
8.8(h)	CORRELATION BETWEEN THE PREDICTED AND OBSERVED RESONANT FREQUENCIES FOR EMBEDDED FOOTINGS, DATA FROM FRY (1963) AND NOVAK (1970)	261

NOTATION

A_i and A_j	= Arbitrary Constants
a_i	= Dimensionless Parameter in Eq. 2.40
a_0	= Dimensionless Frequency Factor
B	= Lysmer's Modified Dimensionless Mass Ratio
b	= Nondimensional Mass Ratio
b_i	= Dimensionless Parameter in Eq. 2.41
C	= Coefficient of Viscous Damping
C_a	= Wall Adhesion Under Dynamic Conditions
C_c	= Critical Damping Coefficient
c	= Cohesive Strength of the Soil
D	= Nondimensional Viscous Damping Factor
D_h	= Nondimensional Viscous Damping Factor for an Embedded Footing
E	= Young's Modulus
e	= Eccentricity of the Rotating Mass
e'	= Void Ratio
F	= Constant Frictional Force
F_1 and F_2	= Components of Lysmer's Displacement Functions
f_1 and f_2	= Components of Reissner's Displacement Functions
G	= Shear Modulus
H	= Height of Foundation Contact with Surrounding Soil
I	= $2 \beta D S + \beta^2 (1 + R)$
i	= $(-1)^{1/2}$
K	= Spring Constant

K_h	= Spring Constant for an Embedded Footing
K_o	= Coefficient of Lateral Earth Pressure at Rest
L	= Perimeter Length of the Foundation
M	= Total Mass of the Foundation and the Vibrator
m_o	= Total Mass of the Rotating Eccentric Weights
P	= Periodic Force Acting on Elastic Body
P_o	= Amplitude of Periodic Force Acting on Elastic Body
Q_o	= Amplitude of External Force
$Q(t)$	= Time Dependent Exciting Force
q	$= \left[\left(\frac{\beta^2 - 1}{\beta^2} \right)^2 + \left(\frac{2D}{\beta} \right)^2 \right]^{1/2}$
R	= A Function Independent of Constant Friction, F
r_o	= Radius of the Foundation Base
S	= A Function Independent of Constant Friction, F
t	= Time
V_p	= Compressional Wave Velocity
V_s	= Shear Wave Velocity
X	= Time Dependent Displacement of the mass, M
\dot{X}	= Time Dependent Velocity of the Mass, M
\ddot{X}	= Time Dependent Acceleration of the Mass, M
X_f	= F/K
X_o	= Amplitude of Displacement of the Mass, M
X_{or}	= Resonant Amplitude of Displacement of the Mass, M
$X_{or,h}$	= Resonant Amplitude of Displacement of the Embedded Footing

α	= Coefficient of Apparent Mass Increase
β	= ω_n/ω
γ	= Density of the Soil Surrounding the Foundation
δ	= Logarithmic Decrement
μ	= Poisson's Ratio
μ_f	= Coefficient of Kinematic Friction
ϵ	= Phase Angle as Described in Eq. 8.6
ϕ	= Angle of Internal Friction of the Soil
ω	= Circular Frequency of Excitation
ω_d	= Damped Natural Circular Frequency
ω_n	= Natural Circular Frequency
ω_r	= Resonant Circular Frequency
$\omega_{r,h}$	= Resonant Circular Frequency of the Embedded Footing
ρ	= Mass Density of the Soil
ψ	= Phase Angle between the Displacement and force Vector
π	= 3.1459...
σ_o	= Average Effective Normal Stress or Effective Octahedral Normal Stress
τ	= Shear Stress
exp	Used for Base of Natural Logarithms

SYNOPSIS

N.R.Krishnaswamy,
Ph.D.Thesis,
Indian Institute of Technology, Kanpur,
April 1972
'A STUDY OF THE EFFECT OF EMBEDMENT AND RELATED FACTORS
ON THE DYNAMIC BEHAVIOUR OF FOOTINGS'

Results of a series of field vibratory tests on massive concrete footings in conjunction with a relevant seismic investigation of the test sites are presented.

The data obtained from steady-state vibration tests are analysed and the effects of the following parameters on the dynamic response of footings are critically evaluated: a) embedment of the footing into soil, b) surcharge around the periphery of the footings c) shapes and sizes of the foundation base, d) increasing intensities of dynamic force application, e) extremely moist conditions of the soil below the footing, and f) properties of the soil layer on which the footing is directly resting.

A single-degree-of-freedom mass-spring-dashpot analogue with the inclusion of a Coulomb friction damper is suggested to explain analytically the dynamic behaviour of embedded foundations. A simple procedure is described for the case of an embedded footing undergoing vertical vibrations, by which the constant frictional force of the Coulomb friction

damper can be estimated. The suggested procedure takes into consideration the depth of embedment, the area of side contact with the soil, the density of the surrounding soil and the physical characteristics of the interface between foundation walls and the surrounding soil.

The field test data obtained from the present investigation as well as those published by other investigators elsewhere are compared with the values predicted by the proposed theoretical model. The theoretical solutions of the proposed model are graphically presented in nondimensional form so as to render them useful for purposes of design and analyses.

CHAPTER 1

INTRODUCTION

1.1 GENERAL

In recent years, important new advances have been made in our knowledge concerning the vibrations of soils and foundations. This knowledge is of great significance to engineers dealing with design problems of machine foundations, highway and airport pavements, railway embankments, bridges, radar towers, missile launching pads and other civil engineering structures which are required to resist dynamic loads such as those due to vibrating machinery, periodic or intermittent wind forces, traffic, blasts, earthquakes etc. The main purpose in the design of any of these structures is to limit motions to values which are permissible. The basis for determining the permissible values, however, depends on the criteria for failure of the design function of the structure in question. For example, the permissible value of motions for design of a particular machine foundation may be the one which would not cause distress to couplings or wear of bearings and parts of the machine, leading to unsafe operations. In some cases, the criteria may be to limit motions transmitted into the ground which may otherwise cause discomfort to persons or damage to adjacent structures by vibration and settlement.

In soil dynamics, a great deal of effort is directed towards understanding the behaviour of a foundation subjected to periodic forces. This, no doubt, directly helps in solving foundation problems involving dynamic loads generated by several kinds of industrial machinery such as compressors, reciprocating machines and rotating engines. The same principles and concepts can be utilized for problems involving random or transient force pulses due to impacts, blasts and earthquakes.

The design of a machine foundation subjected to harmonic exciting forces usually involves the prediction of maximum amplitudes that might occur when the frequency of exciting forces generated by the machine coincides with the natural frequency of the soil-foundation system. The frequency at which the maximum amplitude occurs is usually called the resonant frequency in soil dynamics literature. The design of a machine foundation is invariably done by keeping the operating frequency of the machine as much away from the resonant frequency as possible. In addition, the response of the foundation block is of interest since the machine is to frequently go from a standing start to the operating frequency.

Machine foundations can be either block foundations or framed foundations. Turbines require framed foundations

whose columns supporting the foundation table act as springs, thereby introducing several degrees of freedom to the system. A discussion on the behaviour of framed foundations is beyond the scope of this dissertation. The focus of attention will, therefore, be limited to the analysis of block foundations in direct contact with the supporting soil.

A massive block foundation resting directly on the soil may be considered to possess six degrees of freedom because of its ability to vibrate in vertical, longitudinal, or lateral translation and the rotational modes of rocking, pitching, or yawing. These motions are illustrated in Figure 1.1. Although a rigid body possesses six degrees of freedom, the positioning of the coordinate axes in an equivalent axially symmetric case results in only four independent modes of motion, denoted by vertical, horizontal, rocking and torsional modes of vibration as shown in Figure 1.2. The axially symmetric representation of the rigid body or the massive block foundation lends itself more easily to rigorous mathematical treatments of the problem. In machine foundations vertical, rocking and some type of coupled motions involving both rocking and sliding vibrations are very common.

1.2 BACKGROUND

One of the earliest approaches to the study of foundation vibrations in any one of above mentioned modes, considered

the oscillating foundation-soil system to behave as a lumped mass supported by a weightless spring and subjected to viscous damping. The simple theory, however, was too inadequate to explain the available results of field vibratory tests.

Therefore, the theory of a rigid mass oscillating on the surface, of a linearly elastic, isotropic and homogenous half-space, which is more rational, has become the basis for many of the existing analyses of the dynamics of foundations. Reissner(51) formulated this mixed boundary value problem during 1930's to give an analytical solution for the periodic vertical displacement at the centre of a circular loaded area assuming uniform pressure distribution. The theory was later extended by Quinlan(50) and Sung(57) to cover various contact pressure distributions under the footing. Further improvements were made by Bycroft(9) by considering the weighted average of the displacements beneath the footing and taking into account the internal friction in the soil. He solved the problem for other types of motion besides the vertical one. The problem of a rigid mass oscillating on the half-space has also been solved by Borodatchev(8) and Awojobi and Grootenhuis(3) as a contact problem without any assumed type of pressure distribution under the base. The problem of vertical and torsional oscillations of a rigid

mass supported on an elastic layer which in turn is supported by a semi-infinite rigid body has been treated by Arnold, Bycroft and Warburton(2), Bycroft(9) and Warburton(61).

Though the half-space theory has been vastly developed to get the best possible estimates of the response of a vibrating footing, it is still preferable to use the concepts and formulae derived from the single-degree-of-freedom mass-spring-dashpot system. This is especially true since the development of the simplified lumped system analogues(31, 17, 42, 22) wherein the results of the elastic half-space theory are expressed in terms of the parameters of a single-degree-of-freedom system.

1.3 SCOPE

In spite of all the above mentioned developments, foundations in practice pose several problems which are not fully explained by the existing theoretical models. The serious departures from the theory encountered in practice are mainly due to the nonlinear nature of the response of footings with higher dynamic force levels, the effects of variation of soil properties with depth, the effects of base size and shape and the effects due to embedment of the footing and the surrounding surcharge.

The scope of this dissertation is to examine, in general, the above deviations from the theory with the help

of data obtained from a comprehensive programme of field vibratory tests on massive concrete footings in conjunction with a thorough seismic investigation of the test site. The present study, however, attempts to examine the effects due to embedment of the footing in greater detail.

One of the simplified assumptions of the current theoretical models is that the vibrating body rests on the surface of the soil or the so called 'half-space'. However, in practice, foundations are always partially or fully embedded into the soil with the result that their vibratory responses are greatly affected.

The problem of the vibrations of embedded foundation has not received wide attention, probably because the design calculations with respect to amplitudes of motion would err on the conservative side when the effect of embedment is neglected. However, a realistic assessment of the effect of embedment, in quantitative terms, will lead to more economic and safe designs besides narrowing the present gap between theoretically predicted values and experimentally observed data.

In this dissertation, a single-degree-of-freedom lumped system analogue with the inclusion of a Coulomb friction damper has been proposed to describe the effects due to

embedment in an independent manner. A simple method has been evolved to calculate the kinematic frictional force that is likely to be mobilized as a result of embedment, taking into consideration the physical characteristics of the interface between the foundation wall and the surrounding soil. The correlation between the values predicted by the proposed theoretical model and the experimental results has been discussed herein with the help of data obtained from a comprehensive programme of field vibratory tests on embedded concrete footings.

This dissertation deals exclusively with steady-state vertical vibrations and does not include other modes of vibration. The proposed theoretical model, however, can be used for transient excitation also, if desired.

1.4 PRESENTATION

A review of relevant literature relating to previous investigations on foundation vibrations are presented in Chapter 2. This review briefly describes the development of the mass-spring-dashpot models, the elastic half-space models and the subsequent lumped parameter analogue models. This is followed by a review of theoretical investigations pertaining to embedded foundations. Finally the results of some previous field investigations of similar nature are briefly discussed.

Chapter 3 is devoted to bring out the essential features of the two programmes of field vibratory tests conducted at Indian Institute of Technology, Kanpur, and Chakeri, Kanpur. This includes the site plans of the test areas, the soil profiles at the test sites and a description of the sequence of instrumentation and related measurements. Details of surface seismic investigations and steady-state vibratory tests are also elucidated in Chapter 3.

Chapter 4 discusses the results of seismic investigations in terms of the in situ dynamic soil properties. A method to obtain the approximate value of dynamic shear modulus of soil on the basis of confining pressure is also described in Chapter 4.

The results of steady-state vibratory tests are presented in Chapter 5 wherein the nonlinear nature of the subgrade resistance with higher dynamic force levels, the effect of moisture in soils, the effect of size and shape of the footings on the dynamic response of the footings are discussed.

The observed dynamic response of the test bases with various heights of contact with the backfilled soil is presented in Chapter 6. The results of field vibratory tests on embedded footings conducted by other investigators

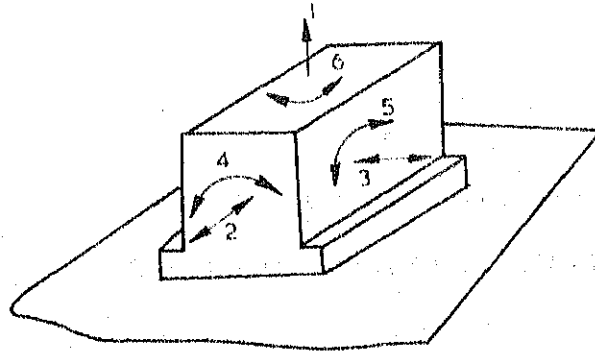
elsewhere are also included in the same Chapter.

In order to understand the effect of frictionless surcharge around the periphery of the vibrating footing, some special tests were conducted wherein the interface between the vertical walls of the footing and surrounding backfilled soil was eliminated by means of a rigid box-like enclosure. The results of these tests are elucidated in Chapter 7.

Chapter 8 is devoted to demonstrate the versatility of the proposed single-degree-of-freedom lumped mass-spring-dashpot model with the addition of a Coulomb friction damper in describing the effect of embedment in an independent manner. The theoretical solutions of the proposed model are graphically presented so as to render them useful for purposes of design and analyses. A simple procedure to evaluate the constant frictional force that is likely to be mobilized as a consequence of embedment of the footing into the soil is described in the same Chapter. A comparison of the experimentally observed values with those of the values predicted by the proposed lumped parameter analogue is also included in Chapter 8.

The findings of the present study are discussed in a comprehensive manner along with a set of recommendations for further studies in Chapter 9.

A brief summary consisting of some useful conclusions which have been arrived at as a result of this investigation, is presented in Chapter 10.



TRANSLATIONAL MODES

- 1-VERTICAL
- 2-LONGITUDINAL
- 3-LATERAL

ROTATIONAL MODES

- 4-ROCKING
- 5-PITCHING
- 6-YAWING

FIG. 1.1 SIX MODES OF VIBRATION FOR A BLOCK FOUNDATION

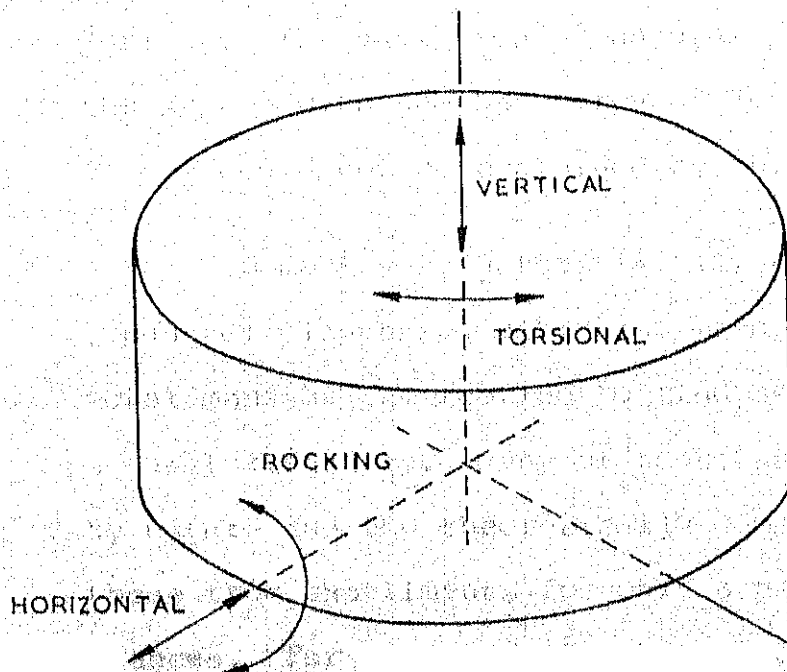


FIG. 1.2 FOUR MODES OF VIBRATION FOR A CIRCULAR FOUNDATION

CHAPTER 2
THEORETICAL BACKGROUND AND
REVIEW OF PREVIOUS INVESTIGATIONS

2.1 GENERAL

One of the first attempts to solve the problem of foundation vibrations was made by assuming that the soil-foundation system consisted of a linear, weightless spring and a dashpot with the mass of the foundation block representing the total vibrating mass. The validity of this simple theory was questioned as early as 1933 when the experimental findings of Hertwig, Fröh and Lorenz (29) were published in Germany. The variation of natural frequency and damping of the system with the base area of the footing and the exciting forces could not be explained by the simple theory.

Some investigators (4, 11, 48) suggested that a certain amount of 'in-phase' vibrating mass of soil be added to the total mass of the footing to find agreement with regard to natural frequency. Many of these attempts were empirical by nature and the theoretically computed values agreed with those from experiments for only a particular set of circumstances. For instance, Crockett and Hammond (11) and Balakrishna Rao and Nagaraj (4) attempted the problem in

which the estimation of the apparent mass of in-phase soil was based on the volume of a certain pressure bulb under the foundation. These methods do not take into consideration the effect of variation of certain important parameters such as, Poisson's ratio of the soil, the pressure distribution under the base, etc. Pauw (48) developed a method for calculating the apparent mass of in-phase soil by considering the foundation mass to be supported by a truncated mass of soil springs. These methods, however, failed to provide satisfactory answers for design purposes. For many similar reasons, the mass-spring-dashpot model was considered to have lost its potential as a research tool to analyse foundation vibrations.

It is rather interesting to note the parallel development of the theory of an oscillating body resting on the surface of an elastic half-space, published by Reissner (51) as early as 1936, in the context of foundation vibration. The elastic half-space theory provides a more rational method of determining the response of a foundation subjected to dynamic loading than the simple mass-spring-dashpot model. The theory can accommodate the effects of varying the shear modulus, Poisson's ratio, the density of the soil, the pressure distribution and the mass and radius of the foundation. The evolution of the theory by different

stages and the organisation of the theory into a useful form are briefly reviewed in Section 2.3.

Since the development of the so called lumped system analogues wherein the results of the elastic half-space theory are expressed in terms of the parameters of a single-degree-of-freedom system, there is a significant revival of interest in the potentialities of the mass-spring-dashpot model. The formulae and concepts derived from a single-degree-of-freedom mass-spring-dashpot system are profusely referred for practical calculations in the present investigation also. Therefore, the theoretical aspects of the single-degree-of-freedom system is briefly presented in the following Section.

2.2 MASS-SPRING-DASHPOT SYSTEM

2.2.1 Free Vibrations

A mass attached to a weightless spring and a dashpot as shown in Figure 8.1(a) has an equation of free vibration given by

$$M \ddot{X} + C \dot{X} + K X = 0 \quad (2.1)$$

where

X = time dependent displacement of the mass, M ;

\dot{X} = time dependent velocity of the mass, M ;

\ddot{X} = time dependent acceleration of the mass, M ;

K = the spring constant; and

C = the coefficient of viscous damping.

The undamped natural circular frequency of the system is given by

$$\omega_n = \sqrt{K/M} \quad (2.2)$$

The solution of Eq. 2.1, in order that the mass can undergo oscillations whose amplitudes decay with time is given by

$$X = \exp(-\omega_n D t) (A_1 \sin \omega_n t \sqrt{1-D^2} + A_2 \cos \omega_n t \sqrt{1-D^2}) \quad (2.3)$$

where A_1 and A_2 are arbitrary constants; t is the time and D is the nondimensional damping factor which is defined as

$$D = C/C_c \quad (2.4)$$

where C_c is called the critical damping coefficient and is given by

$$C_c = 2\sqrt{KM} \quad (2.5)$$

It may be noted that the frequency of free vibrations in the damped case is less than the undamped natural circular frequency and is given by

$$\omega_d = \omega_n \sqrt{1-D^2} \quad (2.6)$$

A convenient way to determine the amount of damping present in a system is to measure the rate of decay of free

oscillations. This is conveniently expressed by a term called 'logarithmic decrement' which is defined as the natural logarithm of the ratio of any two successive amplitudes of motions, or

$$\delta = \ln \frac{x_{o1}}{x_{o2}} = \frac{2\pi D}{\sqrt{1-D^2}} \quad (2.7)$$

2.2.2 Forced Vibrations with Constant Forcing Function

The differential equation of motion for a viscously damped, lumped mass-spring system, excited by a force $Q(t) = Q_o \sin(\omega t)$, as shown in Figure 8.1(a) can be written as

$$M \ddot{X} + C \dot{X} + K X = Q_o \sin(\omega t) \quad (2.8)$$

where Q_o is the amplitude of the harmonic exciting force and ω is the circular frequency of harmonic excitation.

Since the free vibration of a damped system eventually approaches zero after a number of oscillations, only the steady-state response remains to be considered. The part of the solution which remains then is the particular solution corresponding to the steady-state vibration. The particular solution may be taken as

$$X = X_o \sin(\omega t - \psi) \quad (2.9)$$

in which X_o is the amplitude of displacement of the mass, M and ψ is the phase angle between the force and the resulting motion.

By substituting the value of X from Eq. 2.9 into Eq. 8, one obtains

$$-M\omega^2 X_0 \sin(\omega t - \psi) + C\omega X_0 \cos(\omega t - \psi) + K X_0 \sin(\omega t - \psi) = Q_0 \sin \omega t \quad (2.10)$$

Setting $(\omega t - \psi) = 0$ and $(\omega t - \psi) = \pi/2$, two relationships between the unknowns X_0 and ψ , giving

$$C\omega X_0 = Q_0 \sin \psi \quad (2.11)$$

$$(K - M\omega^2) X_0 = Q_0 \cos \psi \quad (2.12)$$

Solving for X_0 and ψ gives

$$X_0 = \frac{Q_0}{\sqrt{(K - M\omega^2)^2 + C^2 \omega^2}} \quad (2.13)$$

$$\tan \psi = \frac{C\omega}{K - M\omega^2} \quad (2.14)$$

Substitution of the expressions for D and ω_n in Eqs. 2.13 and 2.14 gives

$$\frac{X_0}{Q_0/K} = \frac{1}{\sqrt{\left[1 - (\omega/\omega_n)^2\right]^2 + (2D\omega/\omega_n)^2}} \quad (2.15)$$

$$\tan \psi = \frac{2D(\omega/\omega_n)}{1 - (\omega/\omega_n)^2} \quad (2.16)$$

Eq. 2.15 defines the dimensionless amplitude factor and is plotted against the frequency ratio, ω/ω_n for various values

of the damping factor, D , in Figure 2.1(a). It can be verified that the maximum value of X_0 in Eq. 2.15 is located at a frequency

$$\omega_r = \omega_n \sqrt{1 - 2D^2} \quad (2.17)$$

and has a maximum amplitude of

$$X_{Or} = \frac{Q_0/K}{2D \sqrt{1 - D^2}} \quad (2.18)$$

Throughout the remainder of the text, the resonant frequency, ω_r will be referred to as the frequency which corresponds to the maximum amplitude of motion.

2.2.3 Forced Vibrations with Rotating-Mass-Type Excitation

In many types of machinery the vibrations are produced by forces from unbalanced rotating components. The amplitudes of such forces vary directly as the square of the frequency of oscillations. The harmonic exciting force caused by an eccentric rotating mass, which is typical of many existing machinery and of vibration testing machines, can be represented as

$$Q(t) = m_0 e \omega^2 \sin \omega t \quad (2.19)$$

in which m_0 is the eccentric mass and e is the radius of eccentricity of the rotating mass.

The steady-state solution of Eq. 2.8 with the forcing function described by Eq. 2.19, can be written in the form of dimensionless amplitude factor as

$$\frac{M X_0}{m_0 e} = \frac{(\omega/\omega_n)^2}{\sqrt{\left[1 - (\omega/\omega_n)^2\right]^2 + (2D\omega/\omega_n)^2}} \quad (2.20)$$

and is plotted against the frequency ratio, ω/ω_n , for various values of the damping factor, D , in Figure 2.1(b).

It can be verified that the maximum value of X_0 in Eq. 2.20 occurs at a frequency

$$\omega_r = \frac{\omega_n}{\sqrt{1 - 2D^2}} \quad (2.21)$$

and has a maximum amplitude of

$$X_{or} = \frac{m_0 e / M}{2D \sqrt{1 - D^2}} \quad (2.22)$$

2.3 THE ELASTIC HALF-SPACE THEORY

2.3.1 General Remarks

The behaviour of a foundation block vibrating on soil can be approximated by a mass vibrating on the surface of an elastic semi-infinite medium or the so called 'elastic half-space' as shown in Figure 8.1(a). It is then possible to

develop a mathematical theory to obtain the dynamic response of the mass resting on the elastic medium, which is considered as homogeneous and isotropic.

The origin of the development of this approach can be traced to Lamb (38) who derived a solution to the problem of a harmonic point loading on a semi-infinite medium in 1904. Reissner (51) found the solution for the periodic vertical displacement of a vibrating body by integrating Lamb's solution over a circular area. He assumed that the pressure distribution was uniform. Quinlan (52) established equations for contact pressures which vary across a diameter of the contact area with a parabolic distribution, with a uniform distribution and with the distribution corresponding to a rigid-base case. He developed solution only for the rigid base case. Sung (57) also established the basic equations for the pressure distributions and presented solutions for each case. Bycroft (9), Borodatchev (8), Awojobi and Grootenhuis (3) and others also have solved the axially symmetric problem for the case of vertical vibration. All of the solutions differ depending on the researcher's assumptions as to the pressure distribution under the footing and the deformation considered in the solution for the cases when the footing is not considered rigid. The following section presents the salient features

of the general solution of the half-space as solved by Reissner (51) and other previously mentioned researchers.

2.3.2 Results of the Elastic Half-space Theory

In their actual studies of the problem, Reissner (51), Quinlan (50) and Sung (57) considered the contact area between the oscillating body and the half-space to be circular and of radius, r_0 . The response of the oscillating mass on the half-space was found to depend on the following parameters:

- 1) the radius, r_0 of the contact area and the total mass, M of the oscillating body or the footing and vibrator assembly which rests on the surface of the elastic half-space;
- 2) the amplitude of the total dynamic force applied, Q_0 ;
- 3) the distribution of the contact pressure on the circular contact area; and
- 4) the shear modulus, G , the Poisson's ratio, μ and the mass density, ρ of the soil.

In developing the solutions, Reissner (51) found it convenient to establish two dimensionless parameters which relate the physical quantities involved. They are:

- 1) the dimensionless frequency factor expressed as

$$a_0 = (\omega r_0) / \sqrt{\rho/G} \quad (2.23)$$

where ω is the circular frequency of excitation; r_0 is the radius of the contact area; ρ is the mass density of the elastic body or soil; and G is the shear modulus of elasticity of the soil.

2) the dimensionless mass ratio expressed as

$$b = M / \rho r_0^3 \quad (2.24)$$

where M is the total mass of the vibrating footing and the exciting mechanism, which rests on the surface of the elastic half-space.

After complicated mathematical computations, which are omitted here, but may be found in the papers by Quinlan (50) or Sung (57), the vertical displacement, X at the centre of the circular loaded area of the surface is given by

$$X = \frac{P_0 \exp(i\omega t)}{G r_0} (f_1 + i f_2) \quad (2.25)$$

where P_0 is the amplitude of the total periodic force acting on the circular contact area of the elastic half-space; and f_1 and f_2 are the time-independent amplitude functions depending on the dimensionless frequency factor, a_0 and Poisson's ratio, μ .

It may be noted that in Eq. 2.25, displacement, X and the force, P_0 are considered as positive while in the downward direction.

The expression for the amplitude of displacement is given by

$$x_o = \frac{Q_o}{G r_o} \sqrt{\frac{f_1^2 + f_2^2}{(1 - b a_o^2 f_1)^2 + (b a_o^2 f_2)^2}} \quad (2.26)$$

where Q_o is the amplitude of the external force acting on the circular footing.

The phase angle ψ between the external force, $Q = Q_o \exp(i\omega t)$, and the displacement, x can be expressed as

$$\tan \psi = \frac{f_2}{-f_1 + b a_o^2 (f_1^2 + f_2^2)} \quad (2.27)$$

Sung (57) established values for the displacement functions f_1 and f_2 used in Eq. 2.25, for values of $\mu = 0, 1/4, 1/3$ and $1/2$ and for each of the three base-pressure distributions over the range of a_o from 0 to 1.5. Richart (54) put the half-space solutions of Sung (57) in a form which is convenient for finding the resonant frequency and the amplitude of motion at the resonant frequency.

Analytical solutions for vertically vibrating loads on a rectangular surface of the elastic half-space were attempted by integrating Lamb's solution by Kobori (36), Thomson and Kobori (59) and recently by Elorduy, Nieto and Szekely (14).

Analytical solutions for the torsional oscillations of a circular footing resting on the surface of the elastic half-space were developed by Reissner (52) and Reissner and Sagoci (53). The theoretical solutions for the torsional oscillations revealed that the energy is dissipated by propagation of elastic shear waves and that the torsional oscillation is an uncoupled motion which can be treated independently of the possible vertical motion of the footing. It is of interest to note that torsional oscillations are not influenced by Poisson's ratio.

Analytical solutions for the rocking oscillation of footings resting on the elastic half-space were presented by Arnold, Bycroft and Warburton (2) and by Bycroft (9). The problem of horizontal translation or sliding oscillations of a circular disc on the half-space, which can exist only in a mathematical sense, was solved by Arnold, Bycroft and Warburton (2) and Bycroft (9).

Reissner (52) outlined the method of solution for the case of torsional oscillation of a circular footing on a layered system and Arnold, Bycroft and Warburton (2) and Bycroft (9) presented some solutions to this problem. The problem of vertical oscillations of the rigid circular footing on the elastic layer was treated by Arnold et al. (2),

Bycroft (9), and Warburton (61). A detailed discussion on the findings of the above mentioned investigators is beyond the scope of the present dissertation. However, an excellent review on the development of the elastic half-space theory and the significant contributions by several investigators has been published by Richart, Hall and Woods (55).

2.4 REORGANIZATION OF HALF-SPACE SOLUTION

2.4.1 Geometrical Damping

Observation of the response curves of the half-space solution as given by Eq. 2.26 shows motions of finite amplitude at all frequencies even though no damping is considered in the material itself. This is because the energy loss takes place by the propagation of elastic waves away from the source of vibrations. There can be no reflection of these waves as the medium is considered infinite in extent. Thus, the wave will continue to propagate outward while carrying off the input energy. The consequent damping effect is referred to in the literature as 'geometric damping'. This aspect of the half-space solution has prompted several researchers like Hsieh (31), Lysmer (40), Hall (22) and others to rearrange the half-space solution into a form similar to that of a single-degree-of-freedom system. Their works are reviewed by Richart, Hall and Woods (55) and the following condensation is presented.

2.4.2 Hsieh's Equations

The solution of the half-space theory is given by Eq. 2.25. By differentiating Eq. 2.25 with respect to time, Hsieh obtained

$$\dot{X} = \frac{P_0 \omega \exp(i\omega t)}{G r_0} (i f_1 - f_2) \quad (2.28)$$

combining Eq. 2.25 and Eq. 2.28 one obtains

$$f_1 \omega X - f_2 \dot{X} = \frac{P_0 (\omega)}{G r_0} (f_1^2 + f_2^2) \exp(i\omega t) \quad (2.29)$$

putting $P = P_0 \exp(i\omega t)$, one obtains

$$P = - \frac{G r_0}{(\omega)} \frac{f_2}{(f_1^2 + f_2^2)} \dot{X} + G r_0 \frac{f_1}{(f_1^2 + f_2^2)} X \quad (2.30)$$

The equation of motion of a mass on a half-space may be written as

$$M \ddot{X} = Q - P \quad (2.31)$$

where $Q = Q_0 \exp(i\omega t)$.

Eqs. 2.30 and 2.31 can be combined and written as

$$M \ddot{X} + C \dot{X} + K X = Q_0 \exp(i\omega t) \quad (2.32)$$

$$\text{where } C = (r_0^2 / a_0) \sqrt{(G/\rho)} \left(\frac{-f_2}{f_1^2 + f_2^2} \right) \quad (2.33)$$

$$\text{and } K = G r_0 \frac{f_1}{(f_1^2 + f_2^2)} \quad (2.34)$$

Eq. 2.32 has the same general form as the equilibrium equation for the damped single-degree-of-freedom system except that both C and K are functions of the frequency of vibration.

2.4.3 Lysmer's Analogue

The vertical motion of a rigid circular footing was studied by Lysmer (40) by considering a footing made up of a series of concentric rings. By applying uniform pressures of different magnitudes on each ring, he was able to develop a constant deflection under the footing and to evaluate the dynamic response of the footing. In his calculations, he used new displacement functions, F_1 and F_2 which were obtained by multiplying the displacement functions f_1 and f_2 by a factor, $4 / (1 - \mu)$, in order to render them essentially independent of Poisson's ratio, μ . Lysmer calculated the values of F_1 and F_2 curves over the range of frequency factor ($0 < a_0 < 8.0$) whereas the previous investigators considered the displacement functions upto $a_0 = 1.5$. Lysmer developed response curves by introducing a modified dimensionless mass ratio

$$B = \frac{(1 - \mu)}{4} b = \left(\frac{1 - \mu}{4} \right) \left(\frac{M}{\rho r_0^3} \right) \quad (2.35)$$

which essentially eliminated the influence of Poisson's ratio. He developed the response curves by introducing the modified

expressions of F_1 and F_2 , and B into Eq. 2.26 for cases corresponding to a constant force excitation Q_0 and rotating mass excitation, $Q_0 = m_0 e(\omega)^2$.

After studying the variations of the effective damping and spring terms with frequency term, a_0 in Eqs. 2.33 and 2.34, Lysmer discovered that constant values of these quantities which are independent of frequency, could be used to get satisfactory response curves. He chose the spring constant equal to the static value

$$K = \frac{4 G r_0}{1 - \mu} \quad (2.36)$$

and found the best fit for the damping term in the range $(0 < a_0 < 1.0)$ to be

$$C = \frac{3.4 r_0^2}{(1 - \mu)} \sqrt{\rho G} \quad (2.37)$$

Because the agreement between the response curves obtained by using Eqs. 2.36 and 2.37 in Eq. 2.32 with those obtained by using Eqs. 2.33 and 2.34 in Eq. 2.32 is so remarkable, it is sufficient to use the approximate expressions in Eqs. 2.36 and 2.37 in Eq. 2.32 to describe the vertical oscillations of the rigid circular footing on the elastic half-space. Thus, the differential equation of motion for the foundation-soil system illustrated in Figure 8.1(a) can be written as

$$M \ddot{X} + \frac{3.4 r_o^2}{(1-\mu)} \sqrt{\rho G} \dot{X} + \frac{4 G r_o}{(1-\mu)} X = Q(t) \quad (2.38)$$

and is known as Lysmer's analogue.

The dimensionless damping factor, D as described in Eq. 2.4, according to Lysmer's analogue, is given by

$$D = \frac{0.425}{\sqrt{B}} \quad (2.39)$$

The direct consequence of Lysmer's study was in establishing the bridge between the elastic half-space theory and the mass-spring-dashpot system and providing values of damping and spring constants which are independent of frequency of vibrations.

2.4.4 Hall's Analogues

Following the success of Lysmer in developing a mass-spring-dashpot analogue to the vertical vibration of a footing resting on the half-space, Hall (22) followed this approach to study the same problem for rocking, sliding and coupled rocking and sliding modes of vibrations. The mathematical treatment will not be repeated here, but it may be found in the original paper or in the reviews of Richart, Hall and Woods (55).

2.5 LIMITATIONS OF THE HALF-SPACE THEORY

2.5.1 General Remarks

Inspite of its rationality and usefulness there are still questions which the elastic half-space theory leaves unanswered. The effect of embedment of the footing is not considered since the theory is built on the assumption that the vibrating mass rests on the surface of the elastic half-space. Similarly, the effects of the nonlinearity and inelastic behaviour of the soil subgrade are not considered since the theory depends on an ideal elastic half-space.

The half-space theory can, however, be used as the basis for developing simpler models such as the single-degree-of-freedom lumped parameter models which closely approximate the half-space behaviour but allow extension into other areas such as nonlinearity and inclusion of interfacial damping due to embedment. These are the subjects of study described in subsequent chapters.

2.5.2 Nonlinearity

There are several theories and procedures which treat the behaviour of foundations resting on nonlinear media. The usefulness of these procedures become imminent to describe the behaviour of foundation-soil systems under higher strain amplitudes when the foundation under question

is subjected to large dynamic forces. Lorenz (39) attempted the problem by suggesting a nonlinear resistance function which could be analysed graphically. Robson (58) thought that the resistance curve of the soil might be represented by a numerical series. Novak (46) has suggested the development of a nonlinear theory of a lumped mass system allowing for nonlinear restoring force as well as nonlinear damping. Alpan (1) presented as extension of the procedure suggested by Lorenz (39) into the range of the natural frequencies and considered the effect of damping also. Funston and Hall (18) have attempted the problem by describing two types of resistance curves which exhibit nonlinear softening characteristics. The usefulness of many of the above procedures is not being fully explored since standard methods for identifying the nonlinear behaviour of soils under large strain amplitudes are not easily available.

2.5.3 Embedment

The theoretical formulation for the problem of embedded foundation-soil system has been attempted by some investigators following two distinctly different approaches. One of the approaches retains the original concept that the soil can be represented by a linearly elastic, isotropic and homogeneous half-space or semi-infinite medium. The other approach treats the infinite media as a finite model to get

solutions by numerical methods.

The former approach has been adopted by some investigators and is reviewed by Novak (47). Baranov (5), for example, attempted to get an approximate theoretical solution of the effect of embedment by considering the dynamic reaction below the foundation base as well as along the foundation sides which are in contact with the surrounding soil. The dynamic reaction below the base was calculated by treating the base to rest on the surface of a semi-infinite elastic medium while a system of horizontal infinitesimally thin layers were assumed to estimate the dynamic forces along the sides of the foundation. The theoretical solutions worked out by Baranov (5) included all basic types of motion and confirmed that the effect of embedment is to reduce the maximum amplitudes and increase the resonant frequencies. Toshkov (58) attempted the same problem by assuming a hemispherical footing.

The effect of embedment was studied by Kaldjian (34) using the latter approach. He prepared a solution for the problem by finite element method in terms of a finite static model and demonstrated the changes in the vertical spring constant for circular footings with embedment. He considered the case of footing mobilizing skin frictional resistance along the sides as well as resistance by pressure on the base.

He also considered the case of footing developing resistance by the pressure of base alone by neglecting the skin frictional resistance along the sides. Kaldjian (35) has recently demonstrated the changes in the torsional stiffness for embedded footings by following a similar approach.

The problem of embedment was more rigorously treated by Lysmer and Kuhlemeyer (41) by considering a finite dynamic model. This dynamic model is more rational in the sense that proper boundary conditions ensuring almost complete absorption of wave energy at specified boundaries have been analytically found out.

As the numerical methods are not directly applicable to infinite systems, Lysmer and Kuhlemeyer (41) evolved a general method through which an infinite system may be approximated by a finite system with a special viscous boundary condition. In doing so, they investigated different possibilities for expressing this boundary condition analytically and found that the viscous boundary condition defined by

$$\sigma = a_1 \rho v_p \dot{w} \quad (2.40)$$

and

$$\tau = b_1 \rho v_s \dot{u} \quad (2.41)$$

is a nearly perfect absorber of harmonic elastic waves, in which σ and τ are the normal and shear stress,

respectively; \dot{w} and \dot{u} are the normal and tangential velocities; ρ is the mass density; V_p and V_s are the velocities of P and S waves, respectively; and a_1 and b_1 are dimensionless parameters. The proposed boundary condition corresponded to a situation in which the convex boundary was supported on infinitesimal dashpots oriented, normal and tangential to the boundary. The boundary, when $a_1 = b_1 = 1$ resulted in 95 % absorption of S wave energies and has been referred to as the standard viscous boundary by the investigators (41).

Lysmer and Kuhlemeyer (41) found that it was possible to design a viscous boundary for steady-state problems which can completely absorb Rayleigh waves. The required boundary was similar to the viscous boundary defined in Eqs. 2.40 and 2.41 except that the parameters a_1 and b_1 varied with the distance from the free surface. The mathematical expressions involved to obtain the variation of a_1 and b_1 with the distance from the free surface is omitted here and can be found in the original paper by Lysmer and Kuhlemeyer (41). They, however, concluded that at depths greater than one-half wave length, the parameters a_1 and b_1 approached constant values.

The above method was applied by Lysmer and Kuhlemeyer (41) to the axisymmetric foundation problem wherein a finite model of the infinite system was formed by replacing the far

field with the suggested viscous boundary conditions. The finite model was used to obtain the dimensionless displacement functions, F_1 and F_2 , described in Section 2.4.3, by means of finite element method.

Lysmer and Kuhlemeyer (41) have reported numerical results which were obtained with two basic models: 1) A small model with 238 nodal points and a distance to the viscous boundary of $3/4$ times the wave length of Rayleigh waves; and 2) a large model with 632 nodal points and a distance to the boundary of $1\frac{1}{2}$ times the wave length of Rayleigh waves. They have reported that the total processing time required, in a CDC 6400 computer, to obtain a value of F_1 and F_2 at one frequency was 2 minutes for the small model and 8 minutes for the large model. Good agreement was reported only with the large model when comparisons were made between the values obtained from the finite model and those from the existing infinite models.

Lysmer and Kuhlemeyer (41) adopted the large model, mentioned above, and also solved the problem of a rough rigid footing, embedded in half-space. The problem, which was solved by the finite element method, yielded displacement functions, F_1 and F_2 , for two ratios of foundation depth, H to the footing radius, r_0 . They were for the cases when $H/r_0 = 0.5$ and 1.0 respectively. The response of an

embedded footing for the above mentioned two cases was found out using the concepts and formulae described in Section 2.3.2.

2.6 PREVIOUS EXPERIMENTAL INVESTIGATIONS

One of the earliest experiments in the field of foundation vibrations were carried out by the German Research Society for Soil Mechanics, known as DEGEBO during the early 1930s. This group developed a rotating mass mechanical vibrator with four eccentric masses to excite test bases into vertical and torsional modes of vibration. A report on the findings of DEGEBO was published by Hertwig, Fröh and Lorenz (29). The experiments carried out by DEGEBO indicate that it is very difficult to fit the test results into a single-degree-of-freedom mass-spring-dashpot system. This was because the damping constant was different for different tests. The experiments revealed that dynamic response was nonlinear and settlements developed during tests on sand. The report included a table of natural frequencies of soils which led many people to believe that soil has a natural frequency which depended only on the type of soil involved but not on either the geometry of the foundation or the intensity of load applications.

Crockett and Hammond (11) conducted some tests by striking a foundation with a sudden blow in order to measure the so called ' natural frequencies of soils ' which were

thought by many to be characteristics of the type of soil involved. They also conducted some steady-state vibration tests and observed the results contradicting the linear theory of the single-degree-of-freedom systems. Therefore they suggested a specific value of the apparent mass of soil, in-phase with the vibrations, which is influenced by the weight of soil within a certain 'bulb of pressure'.

Jones (33) conducted some field investigations in order to measure the in situ dynamic properties of soil. He showed that steady-state Love waves could be used to determine the shear wave velocity in the upper medium of a layered half-space and also the thickness of the upper layer. Jones also conducted some steady-state vibratory tests to determine the resonant frequency of a small electro-magnetic vibrator, excited to vertical vibrations, on the surface of the soil. He analysed the observed dynamic response of his tests using the elastic half-space theory. Jones confirmed the observation that the modulus of a soil is higher under a high confining pressure by adding more dead weight to the vibrator.

Heukelom and Foster (30) demonstrated the possibilities of vibratory tests to determine the dynamic properties of underlying strata of pavements. They were able to measure three different Rayleigh wave velocities in the four layer highway profile. They used an electro-magnetic type of

Vibrator in their investigations.

The U.S. Army Engineers Waterways Experiment Station at Vicksburg, Mississippi conducted one of the most exhaustive and complete sets of field vibratory tests during the early 1960s. The report of these investigations, prepared by Fry (16), contains extensive data about the tests which were conducted by constructing circular concrete bases of various contact areas and subjecting them to vertical, torsional, and rocking modes of vibration by means of a mechanical vibrator. The tests were conducted to determine the effects of base size, the static intensity of pressure below the base and the intensities of dynamic force application. Two series of tests were performed, one at the WES base on a silty clay (loess) soil and the other at Eglin Air Force Base, Florida, on a uniform fine sand. It should be noted that one set of tests was conducted on a circular foundation with a diameter of 87.6 inches which was embedded in the sandy soil at Eglin. This test was conducted, however, for a single depth of embedment, i.e. the surface of the base was at ground surface elevation.

Maxwell and Fry (43) have described the procedure for determining elastic moduli of in situ soils by dynamic techniques on the basis of several seismic investigations conducted by the U.S. Army Engineer Waterways Experiment

Station (WES) at numerous sites. The procedure involved the use of both small electromagnetic vibrators as well as heavy mechanical vibrators for the generation of sustained vibrations and measuring the propagated wave velocities.

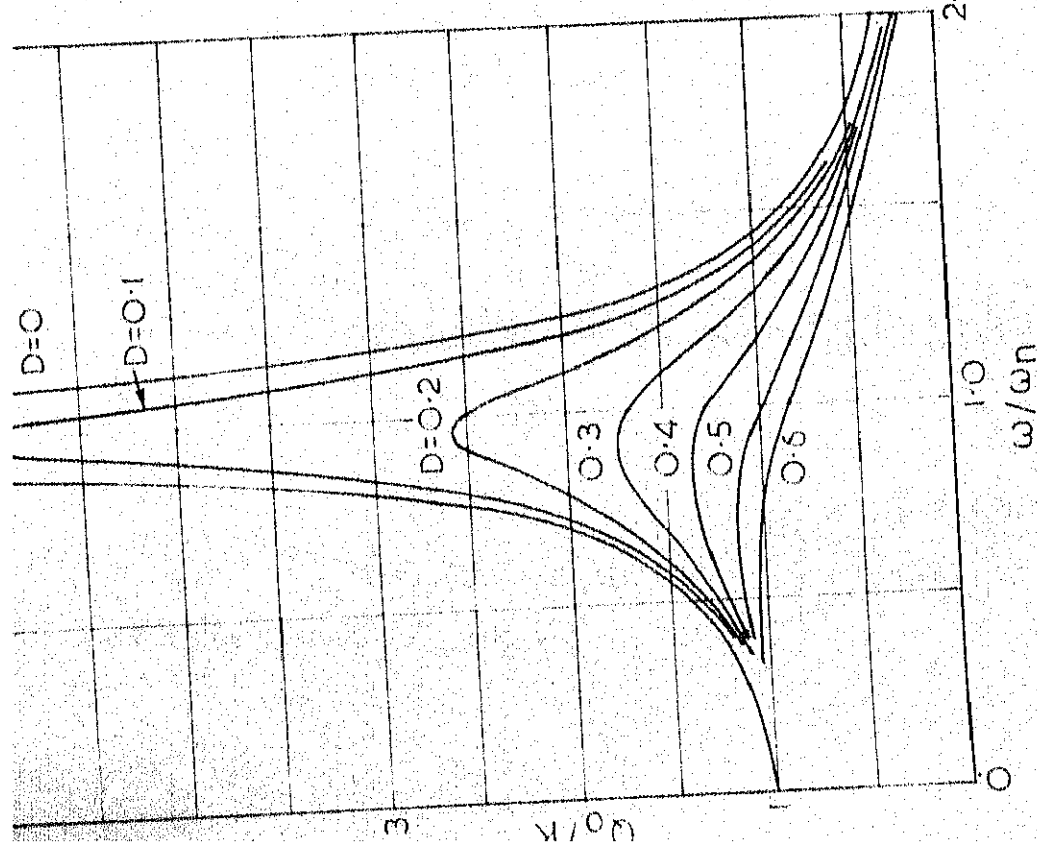
Novak (45) has reported another series of steady-state vibratory tests which were carried out with a steel test body allowing for changes in the foundation square base area, and weight of the test body. The main series of tests were carried out on degraded loess loam. Novak (45) has also reported another series of tests which were carried out on concrete footings, founded below the natural surface of a loess loam soil. These tests were conducted to get response curves of a foundation at various depths of embedment. He demonstrated the importance of the nature of side contact with the surrounding soil by conducting the tests with undisturbed as well as compacted backfilled soil around the footing.

Many significant contributions concerning the behaviour of soils and foundations during vibrations have been made by laboratory investigations. For instance, the development of resonant column testing to study various dynamic soil parameters was possible by the works of Hardin and his associates (23, 24, 25, 26, 27 and 28). A review

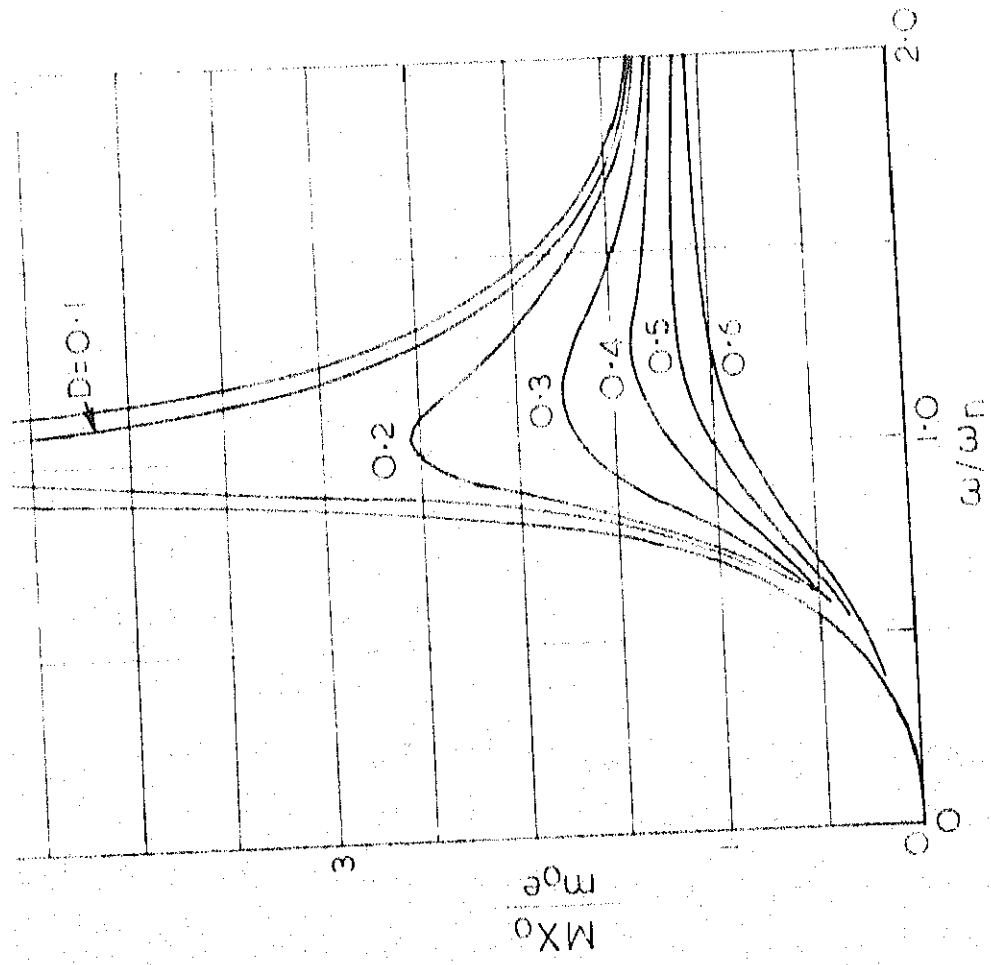
of the experimental investigations conducted in a laboratory scale is, however, beyond the scope of the present dissertation. Nevertheless, a brief account of the study of embedment of footings by laboratory investigations is reviewed in the following paragraph.

Chae (10) conducted an experimental investigation to study the dynamic behaviour of embedded foundation-soil systems in the laboratory by means of an electro-magnetic type of oscillator capable of producing a harmonic force of constant amplitudes. He chose five footings of various shapes, sizes and weights made of one inch thick steel plates. The footings were embedded in sand contained in a bin of inside dimensions: 4.8 feet by 4.8 feet and 4.0 feet in height. Chae concluded that the maximum amplitude of motion of an embedded footing was greatly reduced by the additional shearing resistance along sides of the footing and the rate of decrease became smaller and smaller as the depth of embedment was increased. He also noted that embedment did not significantly change the resonant frequency which he attributed to a greater mass associated with the footing vibration. Chae observed that the amplitude reduction coefficient, which is the ratio of amplitude of the footing embedded to that at the surface, was independent of the

mass ratio when plotted as a function of the embedment factor, which is the ratio of embedment depth to the radius of the footing. He also suggested an empirical relation between the amplitude reduction coefficient and the embedment factor in an attempt to describe the complicated phenomena of the vibrations of an embedded footing.



(a) For constant amplitude of exciting force



(b) For rotating mass type exciting force

FIG. 2.1 RESPONSE CURVES FOR ONE-DEGREE-OF-FREEDOM MASS-
SPRING-DASHPOT SYSTEM

CHAPTER 3

FIELD VIBRATORY INVESTIGATIONS

3.1 GENERAL

Field vibratory tests on massive cement concrete footings, cast in situ, were carried out for the purpose of obtaining data to examine the effect of the following parameters on the dynamic response of footings:

- a) embedment of the footing into the soil with different heights of contact with the surrounding soil;
- b) surcharge around the periphery of the footing in which there is no contact between the walls of the footing and the surrounding surcharge;
- c) shapes and sizes of the foundation base;
- d) increasing intensities of dynamic force application;
- e) extremely moist conditions of the soil at the test site due to, say, heavy rainfall; and
- f) properties of the soil layer on which the footing is directly resting.

The parameters listed above are arranged in the order of specific significance devoted while planning the execution of this investigation.

Surface seismic investigations were made in the test site area to obtain the velocities of compressional and shear waves of the soil. The main purpose of surface seismic investigations was to arrive at an average value of the dynamic shear modulus of the soil in the test site area.

Cross-hole seismic investigations were carried out across some concrete footings which had been constructed for the purpose of conducting steady-state vibratory tests. The aim of cross-hole seismic investigations was to ascertain the variation of the dynamic shear modulus of the soil with respect to depth.

3.2 TEST SITE

Uniformity of subsurface conditions is always the main consideration in the selection of a test site. This is because the tests performed on a relatively more homogeneous soil would exclude unknown parameters that might creep in if performed on heterogeneous materials. It is, however, very difficult to come across ideally homogeneous soils upto great depths in real nature. The best one can do is to avoid abrupt changes in the soil stratas at shallow depths.

The area where the present investigations were carried out, forms a part of the Gangetic plain. It is composed of deposits of gravel, sand, silt and clay-all of

an alluvial origin. The sand horizons are thin and are a result of widespread braided stream deposition in the geological past. Vast inter-fluvial flood basins were thought to have been responsible for the silt and clay accumulation. Because of the complex meandering pattern of the streams, the resulting thickness and the grain size of the sand horizons also vary extensively.

The general sequence at shallower depths, which is of interest for foundation problems, is one with silt (and occasional kankar or lime-stone nodules) and silty clay material. However, at depths like 80 feet, thin sand horizons were evidenced from bore hole data published by Gokhale (19).

The site selected in the present case was on a level area situated at the Indian Institute of Technology, Kanpur. The soil at the site is classified as a silty clay (CL) as per Indian Standards Institution Classification system. Borings were made and samples obtained to determine uniformity of the soil conditions. A typical log of a bore hole is illustrated in Figure 3.1 along with the information about the Atterberg limits and the natural moisture content. Data from the bore hole samples indicated reasonably uniform conditions except for the presence of kankar or limestone nodules in the silty clay at a depth of about 4 feet from the

ground level. The presence of kankar was noticed in all the bore holes and the layer of silty clay containing these nodules was about 6 inches in thickness.

As the main purpose of the tests was to study the effect of embedment of the footing, it was required to found the footings inside large excavated pits, below the surface of the ground. Obviously, the pits were excavated deep enough, in each case, so that the base of the footing was well below the layer of silty clay containing kankar. However, a special footing was constructed on the natural surface of the soil to find the effect of the silty clay layer with limestone nodules, located at a depth of about 4 feet below the base, on the dynamic response.

Field vibratory investigations were also carried out at another test site, near Chakeri, about 12 miles away from the main test site at Indian Institute of Technology, Kanpur. The soil at the Chakeri test site is essentially the same as the soil at I.I.T. test site. The concrete footing at this site was constructed in a large excavated pit and its base was founded directly on the silty clay layer containing kankar or limestone nodules to find the effect of this layer on the dynamic response of the footing subjected to steady-state vibrations. A typical log of a bore hole at Chakeri

site is illustrated in Figure 3.2 along with the information about Atterberg limits and the natural moisture content.

3.2.1 TEST FOOTINGS

The physical dimensions as well as the force limitations of the oscillator which might be used in performing the tests will have the maximum influence in deciding the base size of a footing. As for the shape of the footing, the circular base is ideal from the analysis point of view as well as from the fact that a circular base would not tend to generate erratic waves from an angular interface as might be the case with square or rectangular shapes. However, footings of both circular and square bases were adopted in the present investigation in order to study the effect of base size as well as shape on the dynamic response of foundation-soil systems.

Initially, four cement concrete bases were constructed on the levelled surface of each of the four pits excavated to a depth of 5 feet below the natural surface. The size of each of the pits, square in shape, was chosen to be about three times the lateral dimension of the corresponding footing so that any effects of soil surcharge adjacent to the periphery of the base would be precluded. The two circular concrete footings, designated as Base-1 and Base-2, were 36 and 48 inches in diameter respectively. The two square

concrete footings, designated as Base-3 and Base-4 were having lateral dimensions of 32.0 and 42.5 inches respectively. An additional cement concrete footing was later constructed on the levelled natural surface to compare with the responses of footings constructed inside the excavated pits. This additional footing, designated as Base-5, was also square in shape with a lateral dimension of 32 inches. Each of the bases 1, 3 and 5 was 48 inches in height and had the same base area. Both of the bases 2 and 4 were 27 inches in height and had the same base area. The site plan showing the pertinent characteristics of the footings and their locations are shown in Figure 3.3. The physical properties of all the concrete footings are described in Table 3.1. The sixth concrete footing was constructed at Chakeri test site, and is designated as Chakeri-Base. The Chakeri-Base was also square in base shape with lateral dimension of 32 inches and a height of 48 inches. The Chakeri-Base was identical to Base-3 with respect to physical dimensions as well as weight. The layout of the test area is shown in Figure 3.4.

3.3 INSTRUMENTATION

3.3.1 Mechanical Vibrator

Field vibratory tests on massive footings require the services of a mechanical vibrator which can generate sinusoidally varying dynamic force. Though the generation of a

sinusoidal forcing function is not an absolute necessity, analyses of data become rather complicated with any other forcing function. In addition, the choice of a suitable vibrator depends on the capability of the vibrator for reaching and surpassing the resonant frequency of the soil-foundation system being tested. Obviously, the vibration generator should be able to produce forces of sufficient magnitude to yield measurable responses on the recording instruments.

A mechanical vibrator, by the name 'Lazan oscillator', which satisfied the above mentioned requirements, was used in the present investigation. This vibrator utilises the centrifugal force of unbalanced masses to generate a sinusoidally varying dynamic force. The vibrator has two shafts which are geared together and which rotate in opposite directions. Each shaft has three eccentric weights which are so mounted such that the horizontal components of their centrifugal forces cancel out the corresponding components of the eccentric weights on the other shaft of the machine and vice versa. This gives a condition where vertically the forces of the two shafts add, resulting in a sinusoidal force only in the vertical plane. The magnitude of this force depends on the phase angle between the two smaller but equal eccentric weights and the larger eccentric weight located on

each shaft. The actual force adjuster is located on one of the shafts and consists of a screw, a key and a helical slotted sleeve. The axial position of the key in the force adjuster shaft determines the angular position of the large eccentric weight with respect to the shaft and the smaller eccentric weights. The phase angle between the eccentric weights on the other shaft changes correspondingly by means of a gear. For a constant position of the eccentric weights, their centrifugal forces increase with the square of the speed of rotation of the shafts. Both the eccentric weights as well as the phase angle between the weights can be changed to produce the required dynamic force levels. The magnitude of the sinusoidal force output of the vibrator in pounds at different phase angles between the eccentric weights is given by the following equation

$$Q(t) = 2.0 (\omega/2\pi)^2 \sin(\theta/2) \sin(\omega t) \quad (3.1)$$

in which $Q(t)$ is the time dependent exciting force in pounds, θ is the phase angle between eccentric weights, ω is the circular frequency of the rotating shafts and t is the time.

The amplitude of the dynamic force, Q_0 in pounds for a particular setting of the eccentric weights would, thus, be given by

$$Q_0 = 0.05066 \sin(\theta/2) \omega^2 \quad (3.2)$$

However, it is customary to represent the dynamic force generated by a rotating mass type of vibrator by the following expression

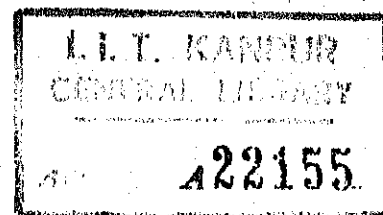
$$Q_0 = m_0 e \omega^2 \quad (3.3)$$

in which m_0 is the total eccentric mass of the vibrator and e is the radius of eccentricity or the radius from centre of gravity of rotating part to centre of rotation.

Thus, the eccentricity moment, $m_0 e$ and the phase angle, θ , between the eccentric weights of the Lazan vibrator used in the present investigation are related by the expression

$$m_0 e = 0.05066 \sin (\theta/2) \quad (3.4)$$

The mechanical vibrator used in the present investigation had a maximum capacity of generating a sinusoidal force amplitude of 1600 pounds and could be operated upto 3600 revolutions per minute. The phase angle, θ between the eccentric weights could be varied by means of a mechanical arrangement provided in the vibrator so that tests could be conducted at various dynamic force levels. However, the phase angle, θ , was so chosen as to keep the maximum acceleration of the vibrator, which was rigidly fixed to the test footing, below 0.5 g throughout the test programme.



The mechanical vibrator was driven by a 3.5 H.P. variable speed motor whose speed could be smoothly varied from 375 to 3750 revolutions per minute. The motor could be connected to the mechanical vibrator through a flexible shaft.

3.3.2 Transducers

A transducer is a device which can convert such quantities as displacement, velocity, acceleration, pressure, strain, force etc. into a usable output such as a voltage which is proportional to the quantity being measured.

The selection of proper type of transducers to measure the movement of the foundation when subjected to vibratory force has to be given careful consideration. The choice has to be made from among linearly variable differential transformer-type transducers, velocity transducers and acceleration transducers. In an investigation of the present nature, differential transformer-type transducers have to be ruled out due to the difficulty of providing a stable reference base. The velocity transducers are very well suited for the measurement of the motion of a foundation primarily because of the ease with which data can be reduced to actual displacement units.

Velocity transducers are mostly of the electromagnetic type in which a change of magnetic flux induces an electromotive

force in a conductor. The relative motion of a moving coil across the magnetic field of a permanent magnet can cause a change in the magnetic flux. The velocity transducers are commercially available in designs having a stationary magnet and a moving coil as the sensing element or a stationary coil and moving magnet as the sensing element.

The velocity transducers, used in the present investigation, consist of a coil moving across a magnetic field. These transducers are designed on the basis of a single-degree-of-freedom system with a natural frequency of 4.75 cycles per second. These transducers had a flat response above its natural frequency. Prior to use, these transducers were calibrated in the laboratory through the associated instrumentation.

3.3.3 Vibration Recording

In order to record the vibrations of a footing in terms of both amplitudes of displacement and frequency, the output signals from the velocity transducers, fixed rigidly to the vibrating body, have to pass through several electronic systems. These are: attenuating and calibrating circuits, frequency cutoff filters, amplifiers, galvanometers, integrating circuits etc.

A practical requirement for the above systems to be used in field operations is that they be in a ruggedly

compact form and capable of easy transportation. This requirement is easily met by several commercially available vibration meters and oscillographs.

In the present investigation, a vibration meter with facilities to amplify the output signals from four velocity transducers was used. The signals from the transducers could finally be read in terms of displacement, velocity and acceleration. The minimum values of displacement, velocity and acceleration that could be recorded from the vibration meter was 0.00005 inch, 0.001 inch per second and 0.1 g respectively. The maximum values of displacement, velocity and acceleration which could be recorded from the vibration meter was 1.0 inch, 1000 inches per second and 1000 g respectively.

The wave form of the output signals was studied by means of a dual trace storage-type oscilloscope and a Polaroid camera. It may be noted that an oscilloscope is an indispensable instrument for investigations of the present kind because of the ability of the device to provide a visual display of the wave form being measured. This is especially true since the geometry of the displayed wave form can be reconverted into measurements of voltage and time.

An oscilloscope essentially consists of a cathode ray tube where in a beam of electrons illuminates a spot on its screen which is phosphor-coated. The spot on the screen is capable of accurate adjustments both in the horizontal and vertical directions as the beam of electrons passes through pairs of deflection plates across which a variable voltage can be applied. The time scale is provided on the screen of the cathode-ray tube by an arrangement wherein a calibrated sawtooth voltage is applied to the horizontal-deflection plates so that the beam moves from left to right at a known velocity and then turns back swiftly to the left side of the tube to repeat its sweep from left to right. The amplification of the signal to be measured is done by varying the voltage across the vertical-deflection plates. Thus, an accurate information about amplitudes and frequencies of vibration can be obtained in terms of voltages and time by means of an oscilloscope. A dual-trace oscilloscope has the advantage of studying separate signals from two transducers simultaneously, thereby, facilitating the determination of phase relationships between the two signals. A storage-type oscilloscope has the advantage of storing the wave forms for a great length of time so that they may be studied carefully and accurately. A Polaroid camera facilitates in taking permanent photographic record of a vital information.

The details regarding the name of the manufacturer and other relevant technical specifications of each of the instruments used in the present investigation are given in Appendix B.

3.3.4 Steady-state Vibratory Tests

The concrete bases were subjected to vertical mode of vibration by means of the rotating mass type of mechanical vibrator described in Section 3.3.1. The centre of gravities of the oscillator and the base were made to lie on the same vertical line to avoid any tendency of the base to rocking motions. This could be achieved when the oscillator was symmetrically centred on top of each base and rigidly secured by four foundation bolts with double lock nuts. The foundation bolts had been previously set in place during construction of the base. The transducers were located at the centre of the base and on the four equidistant corner points of the footing to ascertain whether the amplitude of motion will be equal at all points and in-phase. This could be done by a comparison of amplitudes of motion as well as phase relationships between any two output signals from the transducers. In this manner, it was possible to judge whether or not the vibrations were predominantly in the vertical direction.

The total weight of each of the test bases including the weight of the vibrator and the associated fastenings was kept at 4500 pounds throughout the programme of steady-state vibration tests. The sinusoidal forces were applied by means of the vibrator over a range of frequencies, usually between 375 and 3600 revolutions per minute, as permitted by the limitations of the vibrator as well as the variable speed motor which was connected to the driving shaft of the vibrator through a flexible shaft. Each of the test bases was tested at four positions of the eccentric masses which corresponded to 30, 35, 40 and 45 degrees in terms of phase angles between the eccentric weights or 0.0131, 0.0152, 0.0174 and 0.0194 pound-second² in terms of eccentricity moments, m_0e , respectively. These eccentric settings were selected primarily due to the wider frequency range available while giving consideration to the fact that the maximum acceleration of 0.5 g should not be exceeded at any stage of the test. However, two series of tests were conducted on Base-1 and Base-3, as exceptions, wherein four positions of the eccentric masses which corresponded to 45, 60, 75 and 90 degrees in terms of phase angles or 0.0194, 0.0253, 0.0308 and 0.0358 pound-second² in terms of eccentricity moments respectively, were used. These two series of tests were specially conducted in order to examine the effect of

increasing intensities of force application on the dynamic response of the test footings. The base at Chakeri was tested at five positions of the eccentric masses which corresponded to 36, 45, 54, 63 and 72 degrees in terms of phase angles between the eccentric weights or 0.0156, 0.0194, 0.0230, 0.0265 and 0.0298 pound-second² in terms of eccentricity moments, m_0e , respectively. Thus, for a specific eccentric setting of the vibrator, records of the movement of the footing caused by the exciting force for each frequency over the entire range used, were obtained.

The first series of tests were conducted on bases, 1, 2, 3 and 4 without any backfilling of the excavated pits. In other words, the excavated pits were empty but for the centrally constructed concrete footings. A corresponding series of tests were conducted on Base-5 which was constructed on the natural surface of the ground at I.I.T. test site. Also, another series of tests of similar nature, were conducted on the base at Chakeri test site which was constructed directly on the silty clay layer with kankar or limestone nodules. As mentioned earlier, each of the footings was tested at several settings of the eccentric masses to produce different intensities of force application. Thus, several frequency response spectras were obtained for each of the footing under a given static loading condition.

The observed amplitude-frequency relations are illustrated in Figures 5.1 to 5.8 and will be discussed in subsequent Chapters.

The extent to which the moisture content of the soil can affect the dynamic response of the soil-foundation system, was studied by taking advantage of the natural rainfall at the test site. The heavy down pour at the test site provided conditions close to saturation of the soil up to 1.5 to 2.0 feet below the base level of the footings constructed in the excavated pits. One set of dynamic tests were conducted on Base-1 under these conditions. The observed amplitude-frequency relations under these wet conditions are compared with those obtained under dry conditions in Figure 5.1.

The second series of steady-state vibration tests were undertaken to investigate the effect of embedment on the dynamic response of the footings. This was done by the backfilling with well graded sand into the pit in layers of specified depth. Each layer of sand was compacted to the same density by vigorous tamping followed by vibratory compaction. The effect of embedment was studied in this manner on Base-2, 3 and 4. Each of the bases was tested for every layer of the compacted fill at the same exciting force levels as was done before. The observed amplitude-frequency relations of each of the bases for various heights

of the backfilled material at different settings of the eccentric masses of the vibrator are illustrated in Figures 6.1 to 6.15. The observed phenomena will be discussed in greater detail in Chapter 6.

The third series of tests were conducted on Base- 1, 2, and 5 with a view to study the effect of surcharge around the immediate vicinity of the periphery of the footing in which there is no interfacial contact between the walls of the footing and the surrounding surcharge. This was done by two different methods. In one of the methods, the interface between the sides of the footing and the backfilled sand was eliminated with the help of a rigid box barrier whose dimensions were slightly more than that of the footing under test. The air gap between the box barrier and the sides of the footing was kept around an inch. The surcharge was increased in regular increments by the backfilling of sand into the space between the periphery of the rigid box enclosure and the reexcavated pit. The dynamic response of the footing for various depths of surcharge was obtained for the same eccentric setting of the eccentric masses as explained before.

In the other method, sand bags were placed all around the footing so that the gap between the footing and edge of

the sand bags was approximately six inches. The surcharge was increased in regular increments by piling up sand bags, layer above layer. The dynamic response of the footing for various layers of surcharge consisting of sand bags was obtained in the same manner as described above. The observed results are illustrated in Figures 7.1 to 7.12 and discussed in Chapter 7.

Throughout the test programme, a number of special tests were performed to determine the reproducibility of data and the effects of time and weather conditions.

The schematic diagram of the instrumentation sequence for a typical steady-state vibratory test is illustrated in Figure 3.5. Photographic views showing the excavated pit containing Base-1, the experimental set up indicating the vibrator-footing system with transducers and recording units, Base-3 in a partially embedded condition, Base-4 in a fully embedded condition, and a plan view indicating Base-2, 3 and 4 are illustrated in Figures 3.8, 3.9, 3.10, 3.11 and 3.12 respectively.

3.3.5 Surface Seismic Investigations

Seismic methods consist in measuring the reactions of certain ground points to artificially induced vibrations. The vibrations are detected at various distances and

directions from the source of energy by means of seismometers which are commonly called geophones or detectors. The geophones are mostly velocity transducers whose outer casings are specially designed so that they may be driven into the soil and held in position firmly. The resulting vibrations can be recorded on a storage-type oscilloscope for further studies.

Determination of in situ dynamic soil properties by means of seismic methods is based on the assumption that the soil satisfies all the conditions of an absolutely elastic body. As the subject of foundation vibrations is developed on the assumption that the soil is an isotropic, homogeneous, elastic body, seismic methods are well suited for obtaining information about the dynamic soil properties at specified locations of a test site.

A disturbance of equilibrium conditions produced by a sudden stress or shock at any point in an elastic half-space will cause elastic waves to be propagated. The three elastic waves whose velocities of propagation are of interest are: (a) the compressional or the P-waves in which the particle motion is a push-pull motion parallel to the line of propagation, (b) shear or the S-waves in which the motion of particles is at right angles to the direction of

propagation, and (c) Rayleigh wave in which the particle motion is made up of both horizontal and vertical components. The P and S waves are called body waves and propagate radially outward from a source located on the surface, along a hemispherical wave front. The Rayleigh wave propagates radially outwards from the source along a cylindrical wave front. These waves have been exhaustively discussed and their significance in the study of vibrations of soils and foundations is clearly brought out by Richart, Hall and Woods(55).

The refraction method of seismic surveying can be effectively employed to determine the above elastic wave velocities in the soil at shallow depths which in turn are related to the dynamic elastic constants: Young's modulus, E , the shear modulus, G and the Poisson's ratio, μ . The method of evaluating these dynamic constants from the observed seismic wave velocities will be discussed in the next Chapter. In the refraction method, measurements are made of the elapsed time between the impact of a hammer blow on a selected reference point on the surface of the soil, called the impact station and the arrival of the first seismic wave fronts at several points along a line called the refraction survey line. Geophones, placed at measured distances along the line, can send information about arrival

of the first wave front and the subsequent arrivals to an oscillograph and thus a continuous record of the arriving seismic waves can be obtained.

The compressional wave travels at the highest speed and the mode detected in the first-arrival refraction surveying, therefore, is the P-wave. The velocity of shear wave is slower than that of P-wave and the velocity of Rayleigh wave is slightly slower than that of the shear wave. For the investigation of properties of materials, it is quite instructive to determine the velocity of shear wave or even the Rayleigh wave.

In most conventional, shallow refraction survey work, a vertical impact on a small steel plate is caused by a sledge hammer. The amount of shear produced in the soil medium from such a blow is small compared to the change in volume. Therefore, the most easily distinguishable arrival is that of the direct P-wave. The shear wave arrival will be hardly noticeable on the oscillograph. This difficulty can be overcome if a predominantly shear-type of disturbance is caused at the impact station. The arrival of shear and Rayleigh waves can be easily distinguished if two geophones one for measuring the vertical components and the other for measuring the horizontal components of the arriving wave

fronts, are used simultaneously at every receiving station along the survey line. In this way, the time of arrival of all the three wave fronts at several receivers or geophones kept at increasing distance along the refraction survey line from the impact station can be noted and the velocity of these waves can be determined.

In the present investigation, a long wooden board, 8 feet long, 1 foot wide and 4 inches thick, was employed for the generation of a predominantly shear disturbance. The board was secured firmly to the ground by means of 12 numbers of 8 inch long bolts. The ground below the board had been cleared of the grass and other loose material before fixing the same. One end of the wooden board had been reinforced by means of steel angles so that sledge hammer blows could be imparted to the board without causing the board any damage. It was possible to generate a predominantly shear disturbance by hitting the reinforced end of the wooden board by means of a sledge hammer, in a horizontal direction, along the longitudinal axis of the wooden board. It is very essential that the contact between the base of the wooden board and the ground is maintained during the impact of the hammer blow. This was done by letting the front axle wheels of an automobile rest on the wooden board throughout the field operations.

A traverse line was aligned in the direction perpendicular to the longitudinal axis of the wooden board. Receiving stations for the arrival of seismic wave fronts were established at every five feet along the traverse. Two velocity transducers were selected as geophones to record the vertical and horizontal disturbances of the ground at every receiving station. The two geophones were connected to the upper and lower channels of a dual-trace storage-type oscilloscope by means of two-conductor shielded, long cables. The two-conductor shielded cables are best suited to eliminate electrostatic noise from the traces.

The measurement of the time interval from the hammer-blow against the longitudinal edge of the wooden board to the first and subsequent wave fronts received by the geophone, is done by triggering the horizontal sweep of the oscilloscope with a signal generated by the impact of the hammer. In the present investigation, the triggering signal was generated by a piezoelectric acceleration transducer which was rigidly fixed on a central point of the wooden board. The electric signal generated by the transducer, and amplified through a vibration meter, proved a very convenient method of triggering the horizontal sweep of the oscilloscope. Immediately after the impact of the hammer blow, the oscilloscope is triggered and a trace appears on the screen of the

oscilloscope which can be stored. The travel time of the first and subsequent wave fronts can be obtained by multiplying the sweep rate of the oscilloscope by the distance from the beginning of the trace point to the point of corresponding arrivals. In the present investigation, the hammer impacts were repeated and several traces were stored and viewed simultaneously by changing slightly the vertical position of the sweep between consecutive impacts of the hammer. The use of upper and lower half of the screen to the traces obtained from vertically and horizontally mounted geophones, rendered possible the recognition of all the three wave fronts at a particular receiving station.

Thus, the traverse was completed along the alignment by noting down the travel time of each wave front at each receiving station in the manner described and typical time-distance graphs are illustrated in Figures 4.1 and 4.2. Two traverses were undertaken in the test site area whose alignments were perpendicular to each other. The location of the impact stations with geophone positions and their alignments are illustrated in the layout of the site plan shown in Figure 3.3. The reduction of data to get the pertinent soil properties are described in Chapter 4. A schematic diagram of the instrumentation sequence is illustrated in Figure 3.6.

3.3.6 Cross-hole Seismic Investigations

This is one of the most useful of seismic methods by which the elastic properties of the underlying materials between any two points of a test site can be accurately determined. The method is not only useful for a preliminary investigation of the soil at a test site but also for suggesting corrective measures to the performance of machines or other structures whose foundations were designed by the rule of thumb or without thorough study.

The cross-hole seismic investigation is similar to the surface seismic investigation, described in Section 3.3.5, in all respects except that the tests are conducted between two drill holes. The cross-hole seismic tests are performed by creating a disturbance at the bottom of a drill hole and measuring the arrival time of resulting seismic wave fronts by means of a geophone located at the bottom of another drill hole. In order to obtain an accurate profile of the dynamic soil properties with respect to depth at a site, it is convenient to perform the tests between the bottoms of two drill holes of equal depth. Seismic wave velocities between the drill holes have to be established at every 6 or 12 inches depth. Thus, the investigation comprises of alternate operations of drilling and seismic shooting until the desired depth of drilling is reached.

The technique by which the disturbance is created at the bottom of drill hole has to be modified in the cross-hole test. The source of impact or a disturbance at the bottom of the hole may be an explosive charge. As mentioned earlier, the disturbance has to be created repeatedly to get several traces of the earth vibrations in order to clearly distinguish the first arrivals. Therefore, the use of explosive charges becomes rather too expensive and time consuming for an investigation aiming to obtain the dynamic soil properties upto a depth, say, ranging between 20 to 40 feet. The method of explosives may prove convenient when the drill holes are very deep and far apart as is the case with some oil exploration surveys. In view of these practical difficulties, the hammer-blow method has to be modified and used in the cross-hole investigations also.

In the present investigation, impact of the hammer blow was communicated to the bottom of one of the holes by means of an assembly of mild steel pipes, to the lower end of which a flat steel plate was attached. The velocity transducer, which triggered the oscilloscope, was encased in a rugged and compact steel casing. The steel casing had been so designed as to receive hammer blows on top of the casing without causing any damage to the velocity transducer inside the casing. This rugged and compact assembly was rigidly

connected to the other end of the assembly of pipes, protruding out from the drill hole. Thus, an impact of the hammer on top of the steel casing was transmitted to the bottom of the drill hole through the assembly of pipes besides triggering the horizontal sweep of the dual trace storage type oscilloscope. A geophone, connected to the lower end of another assembly of pipes and stuck to the bottom of another drill hole, received the resulting earth vibrations. The wave fronts, sensed by the geophone, were displayed and stored on the screen of the oscilloscope. By changing slightly the vertical position of the sweep of the oscilloscope between consecutive impacts of the hammer, several traces were stored and viewed simultaneously to calculate the time of arrival of the seismic wave fronts. The position of the geophone and the impact assemblies were interchanged and another set of traces were stored to calculate the time of arrival of the seismic wave fronts in the opposite direction. This improved the accuracy of the observations.

The method described above proved quite versatile as new lengths of pipe could be easily assembled depending on the progress of the drill holes downwards. It may, however, be noted that when the length of the assembly of pipes is large enough, depending on the depth of the drill holes, a correction has to be applied for all travel-time

computations, to take into effect the time of impact energy travelling from the top end of the assembly of pipes to the bottom of the drill hole, the velocity of elastic waves in steel being 17000 feet per second.

The cross-hole investigations, as described above, were carried out across Base-5 and Base-3, the distance between the drill holes, in each case being 10 and 24.5 feet respectively. The location of these drill holes are shown in the layout of the site plan illustrated in Figure 3.3. Cross-hole investigations were also carried out at Chakeri test site between two drill holes, 25 feet apart. The location of the drill holes are shown in the layout of the test area, illustrated in Figure 3.4.

Typical oscillograph recordings are illustrated in Figures 4.6 and 4.7. The reduction of data to get the pertinent soil properties is described in Chapter 4. A schematic diagram, showing the instrumentation sequence, is illustrated in Figure 3.7.

TABLE 3.1 PHYSICAL PROPERTIES OF THE CONCRETE FOOTINGS
TESTED IN THE PRESENT INVESTIGATION

Base Description	Base Shape	Lateral Dimensions in Feet	Height in Feet	Total Weight of Footing and Vibrator	Base Area in Sq.Ft.	Perimeter Length, L in Feet	Mass Ratio $\frac{b}{L}$
Base-1	Circular	3.0 dia	4.0	4500	7.1	9.42	12.1
Base-2	Circular	4.0 dia	2.25	4500	12.56	12.56	5.1
Base-3	Square	2.67 by 2.67	4.0	4500	7.1	10.68	12.1
Base-4	Square	3.54 by 3.54	2.25	4500	12.56	14.16	5.1
Base-5	Square	2.67 by 2.67	4.0	4500	7.1	10.68	12.1
Chakeri-Base	Square	2.67 by 2.67	4.0	4500	7.1	10.68	12.6

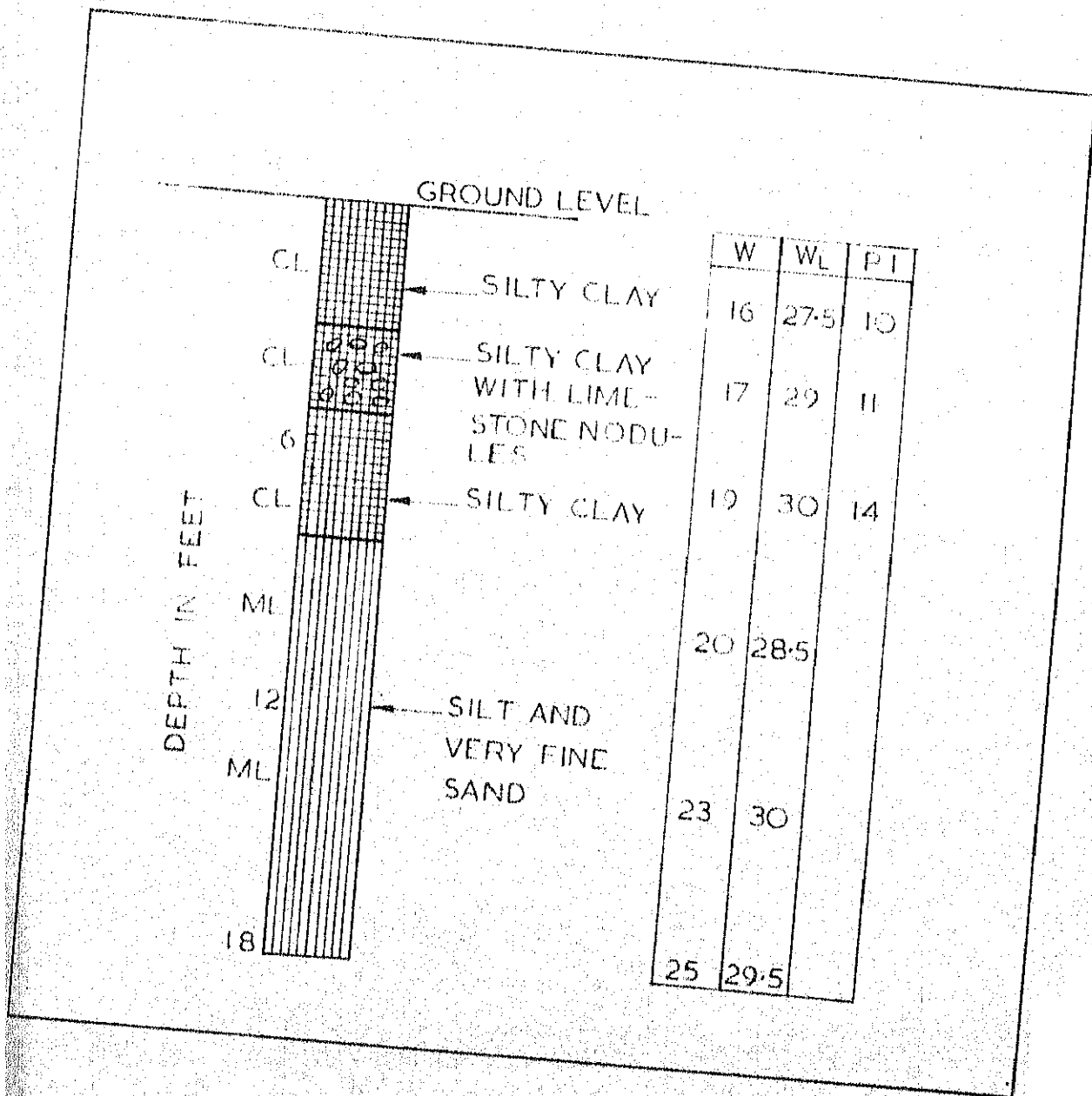


FIG. 3.1 SOIL PROFILE FOR THE TEST AREA AT I.I.T. KANPUR.

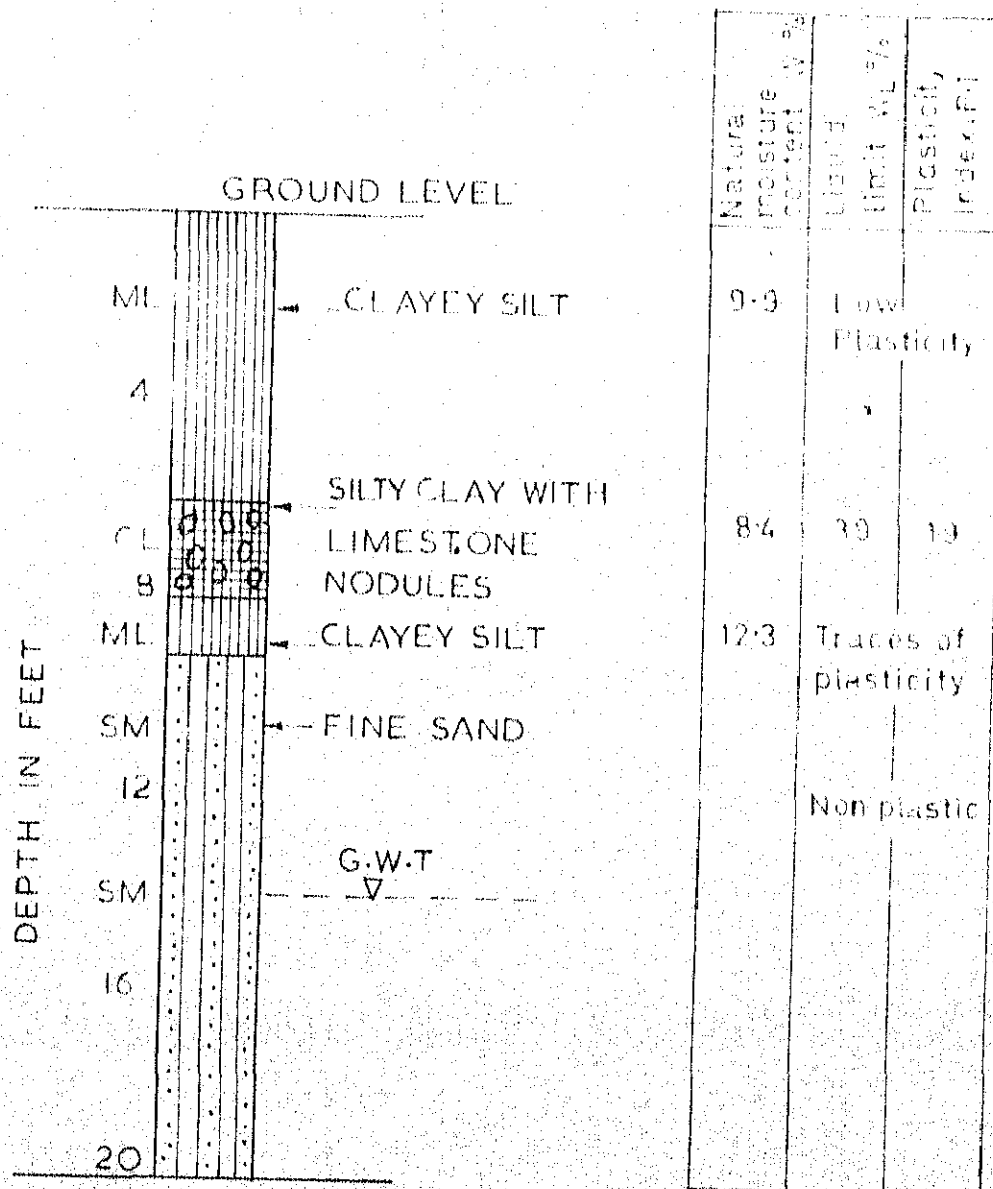


FIG. 3-2 SOIL PROFILE FOR THE TEST AREA AT CHAKERI, KANPUR.

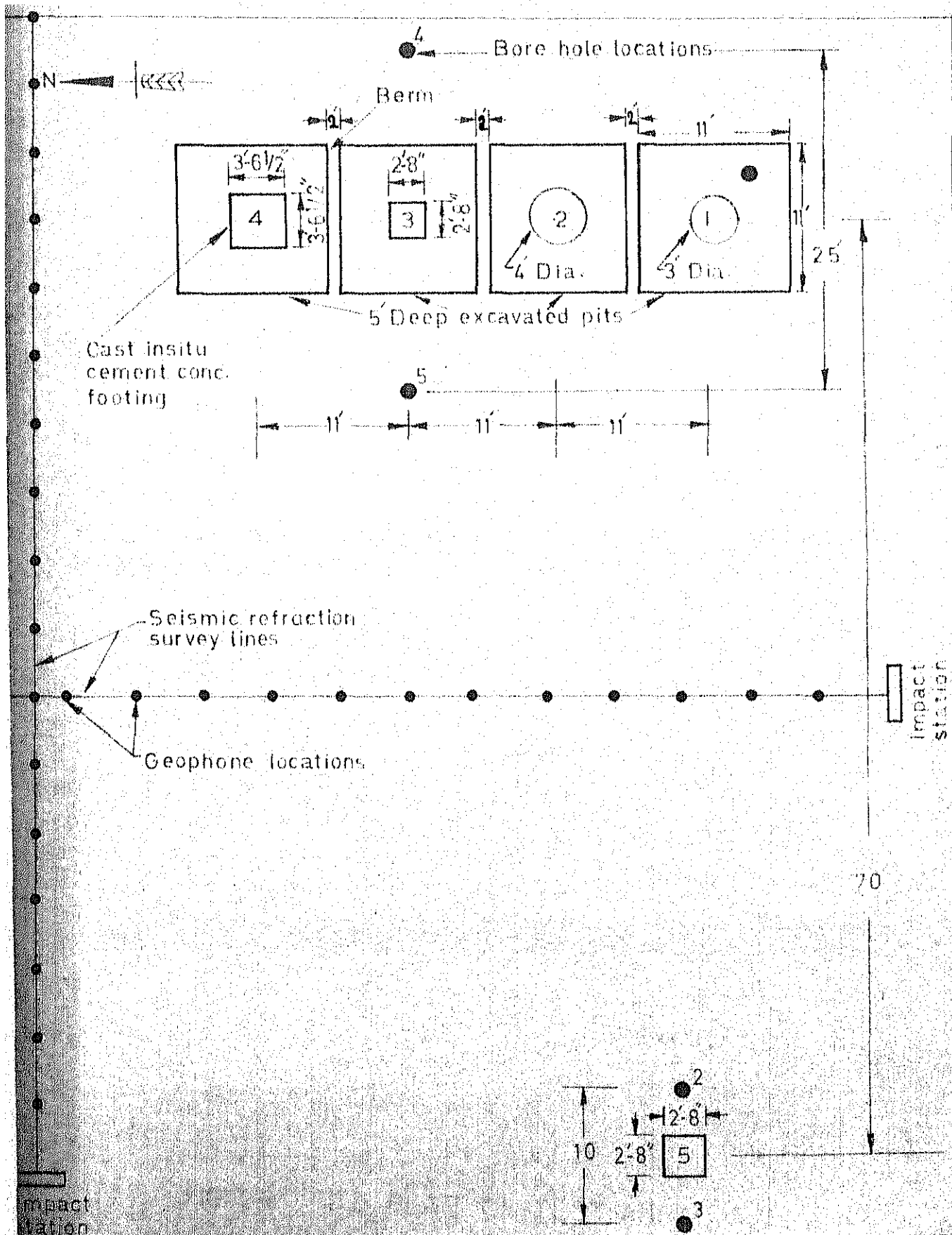


Fig. 3.3 SITE PLAN OF TEST AREA AT I.I.T. KANPUR.

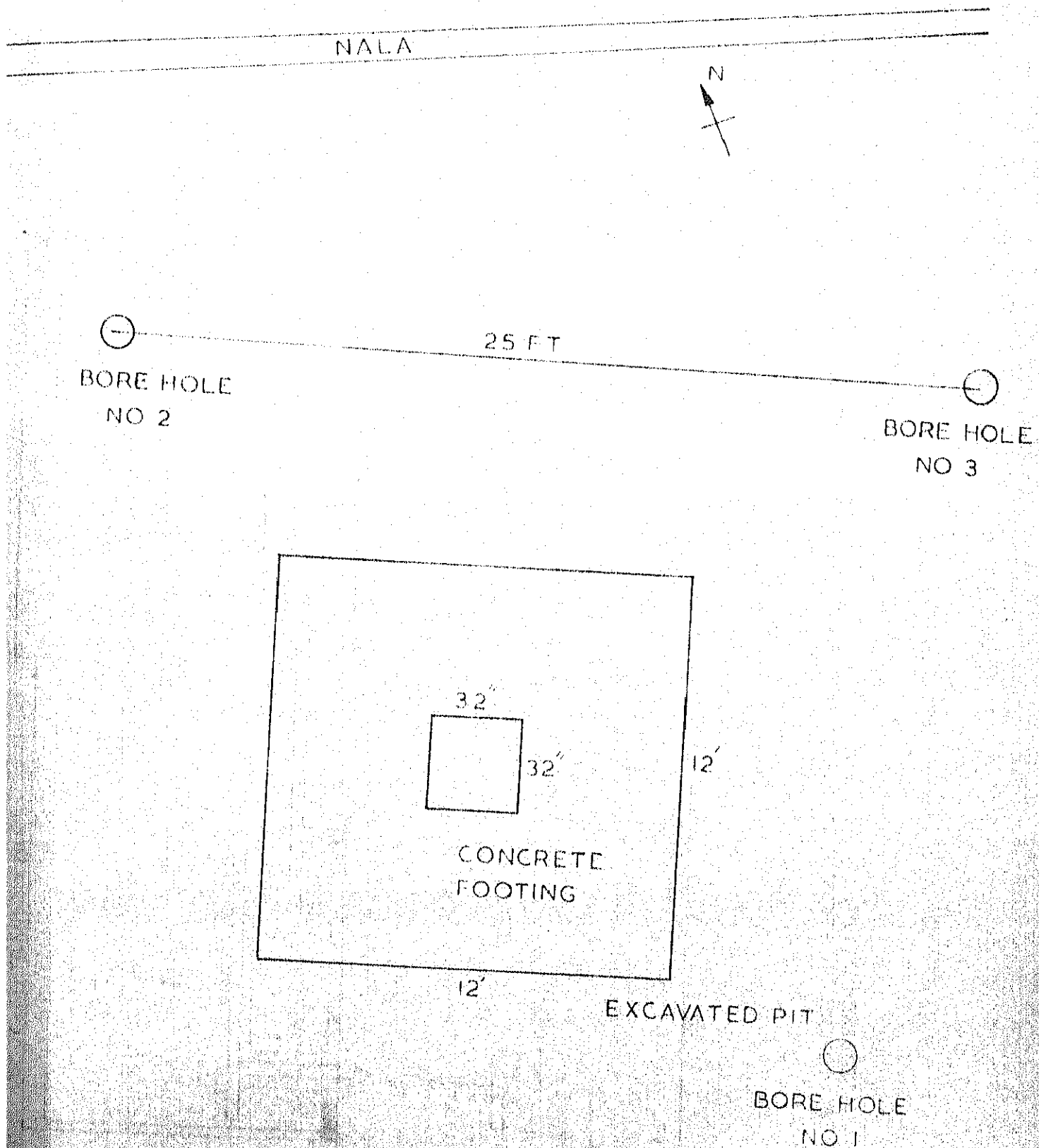


FIG. 3-4 SITE PLAN OF TEST AREA AT CHAKERI, KANPUR

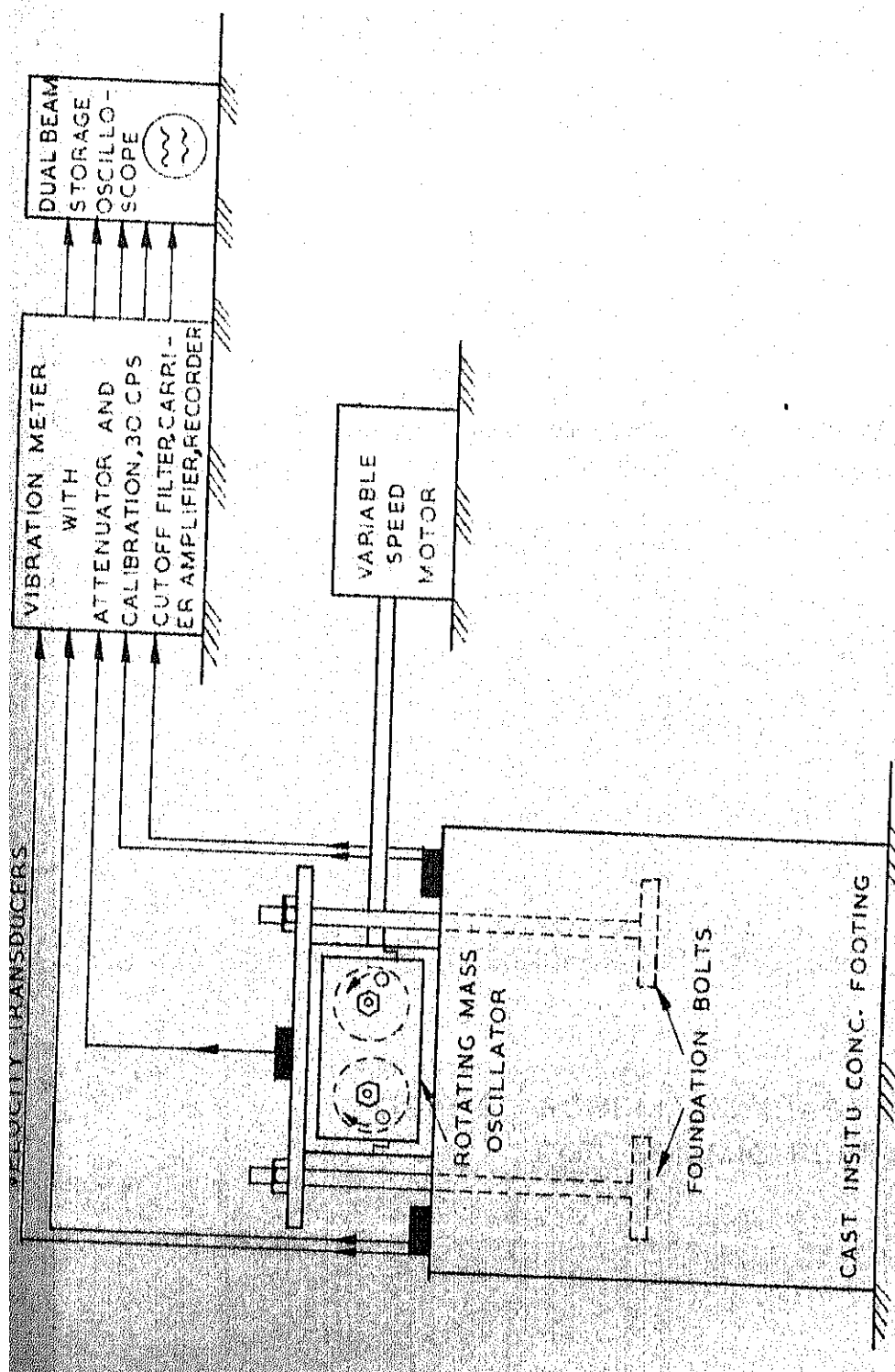


FIG. 3.5 SCHEMATIC DIAGRAM OF FIELD VIBRATOR AND FOOTING WITH INSTRUMENTATION.

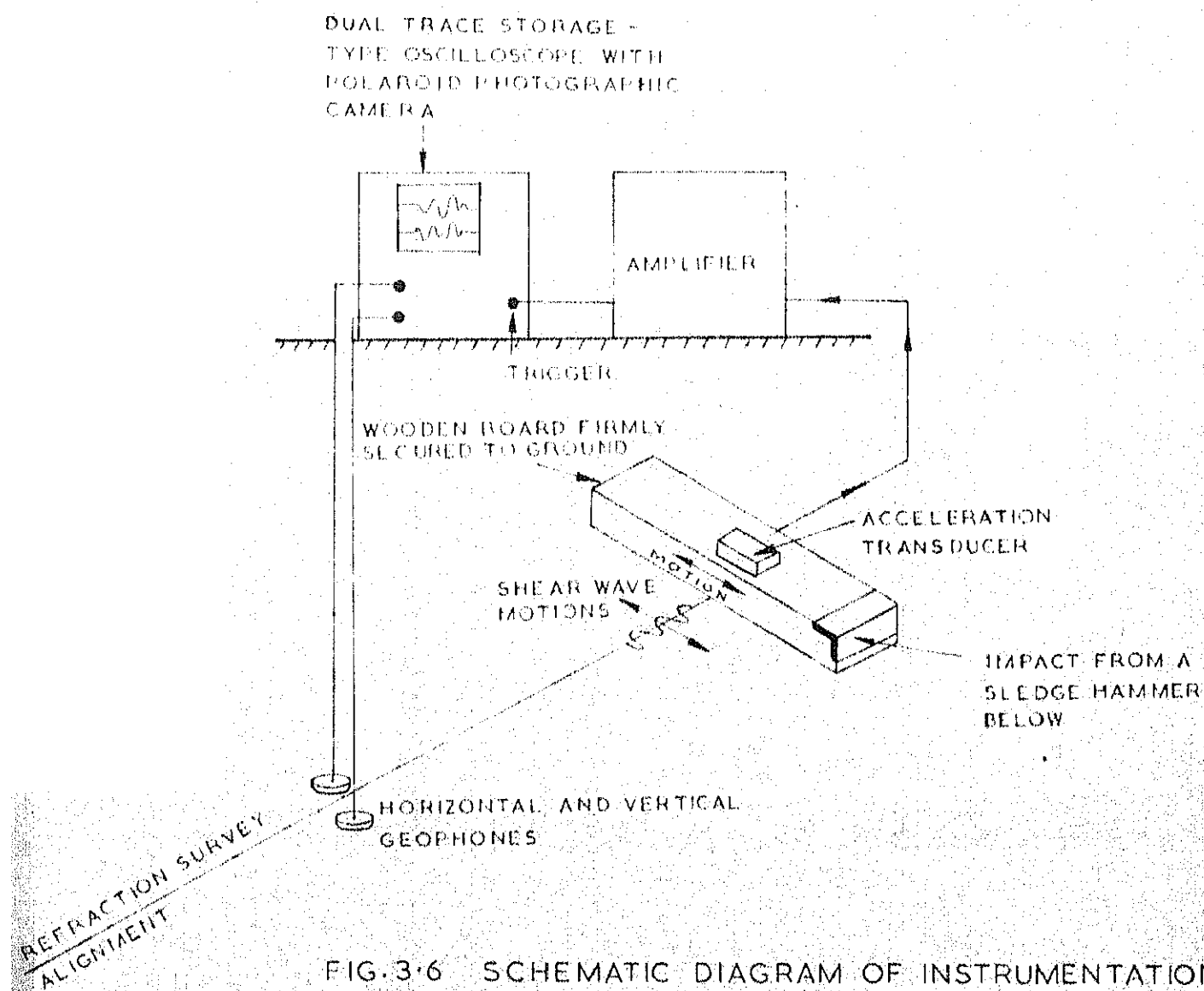


FIG. 3.6 SCHEMATIC DIAGRAM OF INSTRUMENTATION
FOR SEISMIC REFRACTION SURVEY

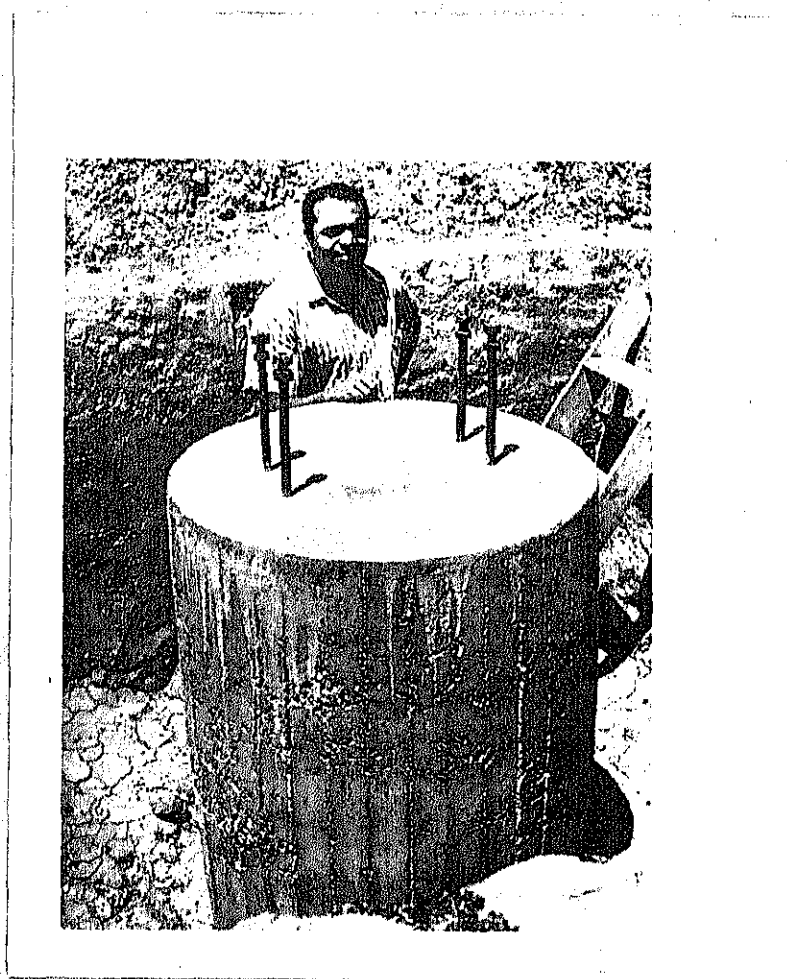


FIG. 3.8 A PHOTOGRAPHIC VIEW OF THE EXCAVATED PIT WITH BASE-1

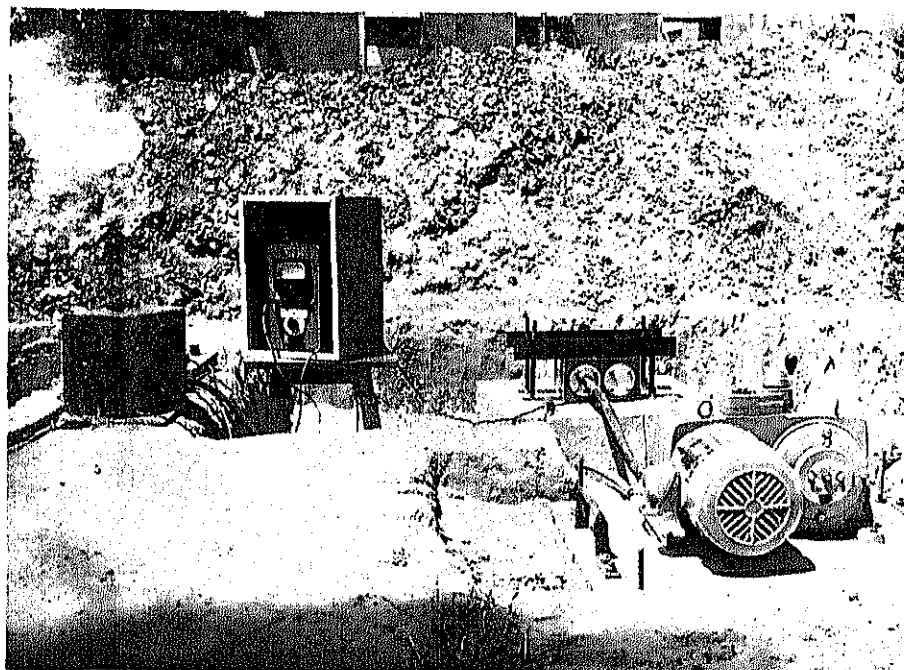


FIG. 3.9 A PHOTOGRAPHIC VIEW OF THE VIBRATOR-FOOTING SYSTEM WITH ASSOCIATED INSTRUMENTATION.

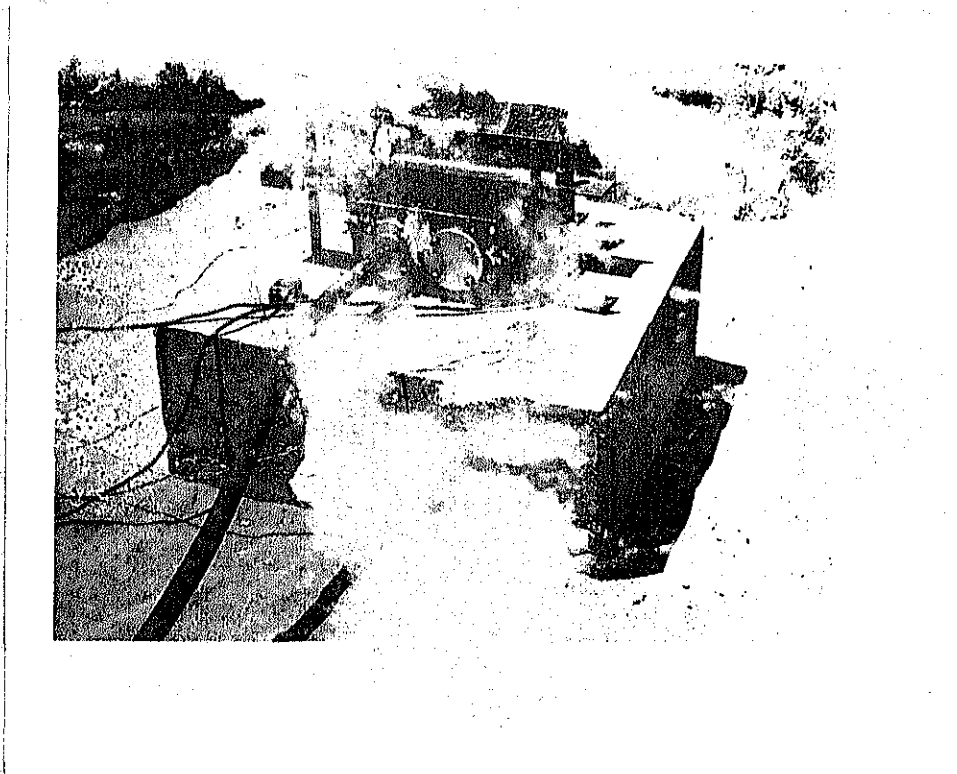


FIG. 3.10 A PHOTOGRAPHIC VIEW OF VIBRATOR AND BASE-3 IN A PARTIALLY EMBEDDED CONDITION.

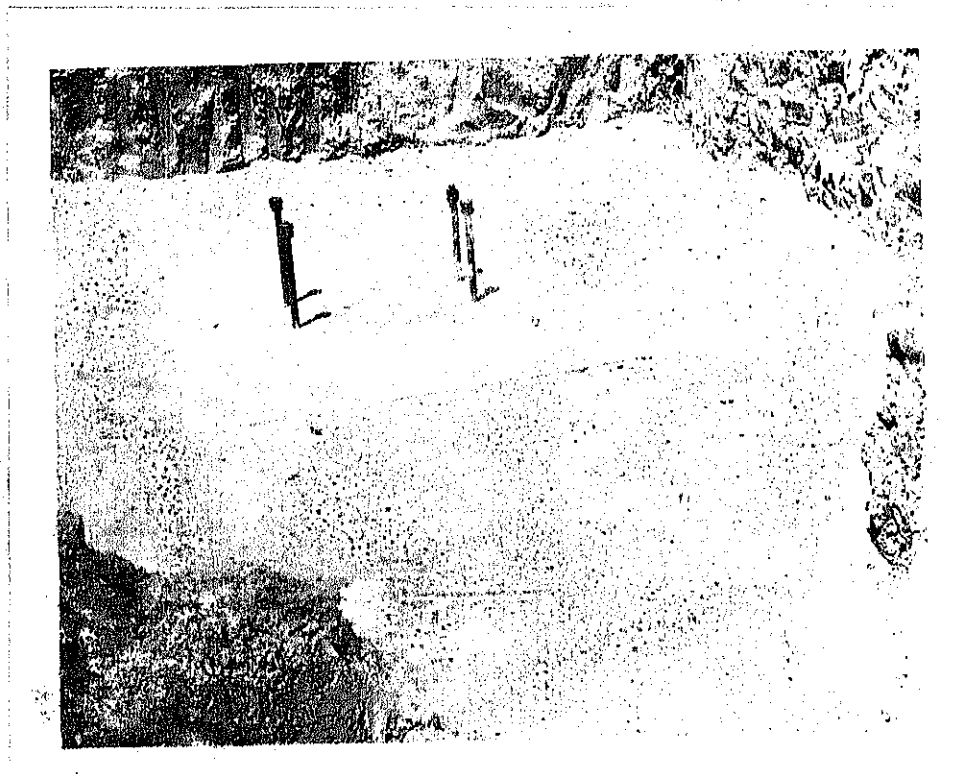


FIG. 3.11 A PHOTOGRAPHIC VIEW OF BASE-4 IN A FULLY EMBEDDED CONDITION.

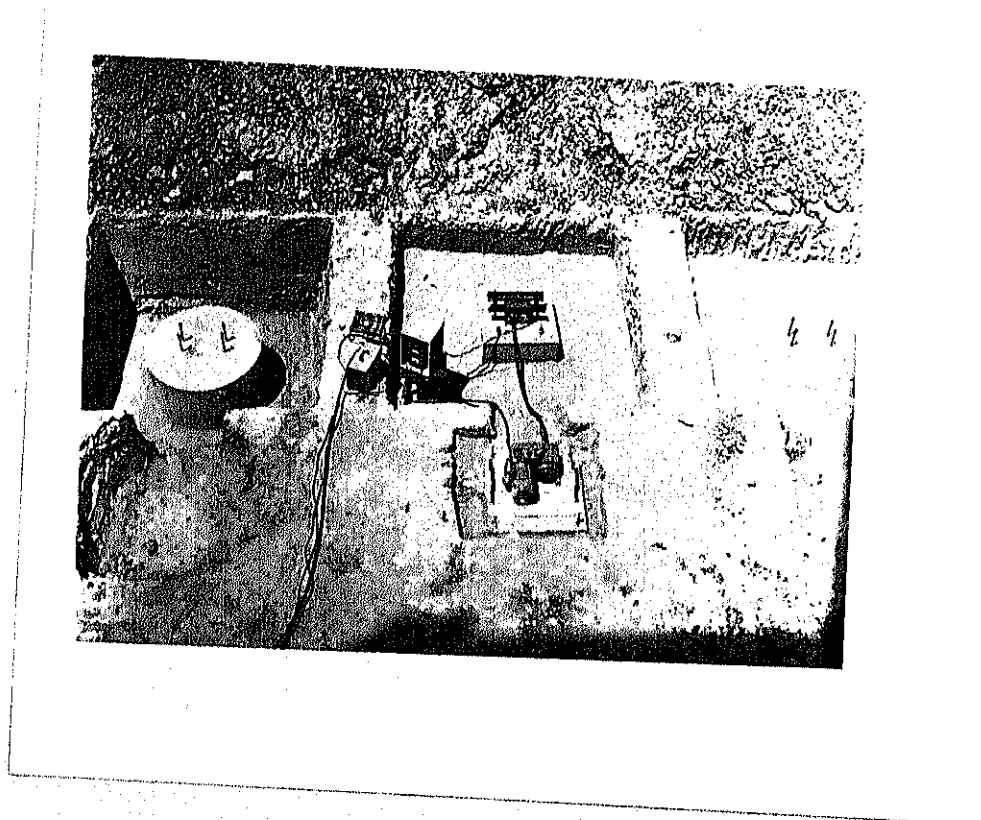


FIG. 3.12 A PHOTOGRAPHIC PLAN VIEW SHOWING BASES-2,3 AND 4.

CHAPTER 4

RESULTS OF SEISMIC INVESTIGATIONS

4.1 GENERAL

It has been described in Section 3.3.5 how a storage-type oscilloscope can be used in conjunction with horizontal and vertical component geophones for the measurement of shear and compressional wave velocities. These velocities can furnish valuable data on the engineering properties of the soil. The ratio of shear wave to compressional wave velocity gives an indication of Poisson's ratio for the material. When Poisson's ratio and the in situ density of the soil are known, dynamic values for the Young's modulus and shear modulus of elasticity of the soil can be computed. These calculations are based on the theories of wave propagation in elastic media.

The theory of propagation of waves in a homogeneous, isotropic, elastic semi-infinite medium gives the following relationships between the various dynamic moduli of the material and the propagation velocities of seismic waves in the material. The mathematical derivations to arrive at these relationships have been treated in detail by many authors (60, 37, 15, 20) and hence not presented here.

$$V_p^2 = \frac{E (1 - \mu)}{(1 + \mu) (1 - 2\mu)} \quad (4.1)$$

$$V_s^2 = \frac{G}{\rho} \quad (4.2)$$

$$\mu = \frac{V_p^2 - 2 V_s^2}{2 (V_p^2 - V_s^2)} \quad (4.3)$$

where V_p = compressional wave velocity;
 V_s = shear wave velocity;
 μ = Poisson's ratio;
 G = dynamic shear modulus of the soil;
 E = dynamic Young's modulus of the soil; and
 ρ = in situ mass density of the soil.

Thus, if seismic wave velocities can be measured and if in situ soil densities are known, all corresponding dynamic elastic properties of the soil can be determined. It should, however, be noted that the dynamic values obtained apply to small amplitude vibrations within elastic range in the average idealized mass.

4.2 RESULTS OF REFRACTION SURVEY

Refraction surveying can provide information about the velocities of two or three stratas or layers of materials whenever a higher velocity medium is encountered below a lower velocity medium. This technique can also indicate the depth of the first strata. The mathematical derivations to

yield the depth of the layer are described by several authors (15, 21) and is not of interest for the purpose of obtaining the average velocities of compressional or shear wave in the top most layer. Besides, techniques like the cross-hole seismic investigations can furnish more precise information about the variation of the dynamic properties of the soil with depth and the existence of layers of different composition at any specified location.

The travel-time graphs, obtained for the test site at two selected refraction survey lines, indicated in the layout of the site plan of Figure 3.3, are illustrated in Figure 4.1 and Figure 4.2. Typical photographic recordings of the oscilloscope tracings, obtained at particular receiving stations along the traverse, are illustrated in Figure 4.3. It may, however, be noted that the Polaroid photographic prints, obtained by instant developing, were redrawn on tracing papers to facilitate the production of several copies.

The shear wave velocity, V_s , for the top few feet of the soil at the test site was 470 feet per second along the East-West refraction line and 462 feet per second along the North-South refraction line. The compressional wave velocity, V_p , for the top few feet of the soil at the test site was 800 feet per second along the East-West refraction line and 690 feet per second along the North-South refraction

line. The density of the soil was determined by obtaining soil samples at several locations, at an average depth of about 2 feet below the natural surface. The in situ density for the top 2 feet of the soil was found to lie between 108 to 112 pounds per cubic feet and an average value of 110 pounds per cubic feet was adopted in all the calculations.

The calculation of Poisson's ratio, μ by means of Eq. 4.3 is seldom met with success. The main reason being that these computations involve small differences of rather large numbers. However, the combination of shear wave velocity, $V_s = 470$ feet per second and compressional wave velocity, $V_p = 800$ feet per second yielded a Poisson's ratio = 0.236 which is fairly reasonable. It may be of interest to note that other combinations of these velocities obtained from cross-hole seismic investigations as well as from North-South refraction data yielded absurd values of Poisson's ratio. In view of these practical difficulties some authors (55) have suggested to assume a suitable value of Poisson's ratio which usually vary from 0.25 to 0.45 in the case of soils, for computational purposes. The value of Poisson's ratio = 0.25, which is quite close to the value of 0.236, as determined from the seismic wave velocities, was adopted in all the calculations.

The dynamic shear modulus of soil was found to be 5250 psi and 5100 psi as per the shear wave velocities determined from the East-West and North-South refraction surveys respectively. These values were found by substituting the observed shear wave velocities and the in situ mass density of the soil in Eq. 4.2. The mass density of the soil was obtained by dividing the in situ densities of the soil, expressed in pounds per cubic foot, by acceleration due to gravity, $g = 32.0$ feet per second.²

4.3 RESULTS OF CROSS-HOLE SEISMIC TESTS

The observed velocities of compressional or primary or P-waves and the shear or S-waves between the two bore holes across Base-3, at various depths, are illustrated in Figure 4.4. The distance between the bore holes across Base-3 was 24.5 feet. The oscilloscope traces of the seismic wave fronts were obtained at every two feet interval and a total depth of 18 feet was examined between the two bore holes across Base-3. Typical photographic recordings of the oscilloscope tracings, obtained at particular depths below the natural surface are illustrated in Figure 4.6. As the length of the pipe assembly used across these bore holes was finally as long as 20 feet, suitable corrections were applied in all travel-time computations to take into effect the time of impact energy travelling from the top

end of the assembly of pipes to the bottom of the drill holes. The corrected wave velocities are illustrated by the broken lines in Figure 4.4.

The observed velocities of compressional and shear waves between the two bore holes across Base-5, at various depths, are illustrated in Figure 4.5. The distance between the bore holes across Base-5 was 10 feet. The oscilloscope traces of the earth vibrations were obtained at every two feet interval and a total depth of 10 feet was examined between the two bore holes across Base-5. Typical photographic recordings of the oscilloscope tracings are illustrated in Figure 4.7. The correction for the travel time in the pipe assembly was not applied in this case as the length involved was only 10 feet.

Similarly, the results of Cross-hole seismic investigations conducted at Chakeri test site are elucidated in Table 4.1.

It may be observed that the velocities of the elastic waves increase with respect to depth. This can be expected as the soils at greater depths are subjected to greater overburden pressures resulting in better consolidation and higher densities. Besides, a soil mass at greater depth is subjected to higher confining pressure which results in higher

shear modulus. Hence the increase of velocities of elastic waves with respect to depth.

4.4 CONFINING PRESSURE AND SHEAR MODULUS

The dynamic shear modulus can also be estimated by a procedure described by Hardin and Richart (28) who demonstrated the predominant influence of void ratio and confining pressure on the shear wave velocities of clean granular materials over the range of $(0.37 < e' < 1.26)$. Hardin and Black (25) later demonstrated that the shear wave velocity in sands depended on the confining pressure, $\bar{\sigma}_0$ which is the normal stress on the octahedral plane and was essentially independent of the state of shearing stress in the sample. This established that $\bar{\sigma}_0$ is the principal quantity to be estimated for a particular bed of sand in order to evaluate V_s or the shear modulus, G for use in the dynamic analysis.

Empirical expressions have been developed for the velocity of shear waves, V_s and the shear modulus, G for round grained as well as angular grained materials on the basis of the above mentioned investigations. These are discussed in detail and reviewed by Richart, Hall and Woods (55). The relationships developed in the case of angular grained materials are given below.

$$V_s = \left[159 - (53.5) e' \right] (\bar{\sigma}_0)^{0.25} \quad (4.4)$$

and

$$G = \frac{1230 (2.97 - e')^2 (\bar{\sigma}_o)^{0.5}}{1 + e'} \quad (4.5)$$

where V_s = velocity of shear waves in feet per second;

G = shear modulus in pounds per inch²;

e' = void ratio; and

$\bar{\sigma}_o$ = confining pressure in pounds per foot² in Eq. 4.4
and pounds per inch² in Eq. 4.5

Hardin and Black (26) ran resonant column tests on clay samples and concluded that for normally consolidated clays of low surface activity, the shear wave velocity is adequately predicted by Eq. 4.4 for small strain amplitudes. According to Richart, Hall and Woods (55), this conclusion for certain normally consolidated clays is a significant aid to the designer, even if it represented only a first approximation. They also concluded that the dynamic shear modulus of cohesive soils, if found by Eq. 4.5, was adequate for a first estimate.

With this in view, the shear modulus of the soil beneath the concrete footings constructed at the test site was found using Eq. 4.5. For an approximation to the pressure developed below the periphery of the footing, the theoretical solution obtained by Prange (49) for a

rigid circular footing on the isotropic, homogeneous, elastic half-space was used. These relations are given in Table 4.2 for Poisson's ratio, $\mu = 0.25$. Figure 4.8 shows how the average confining pressure, $\bar{\sigma}_o$ caused by the contact pressure of each of the footings decreases with depth below the periphery of the footing according to Prange's solution.

The vertical and horizontal stresses at a depth in the soil mass are given by

$$\bar{\sigma}_z = \gamma z \quad (4.6)$$

$$\text{and } \bar{\sigma}_x = \bar{\sigma}_y = \frac{\mu}{1-\mu} \bar{\sigma}_z \quad (4.7)$$

These stresses established $\bar{\sigma}_{os} = (61)z$ and is illustrated in Figure 4.8.

The total average confining pressure at any depth below the perimeter of a footing is the sum of $\bar{\sigma}_{oq}$ and $\bar{\sigma}_{os}$, as shown in Figure 4.8. The minimum value of $\bar{\sigma}_o$ and the void ratio of the soil at the test site ($e' = 0.50$) were introduced into the equation for the dynamic shear modulus, described in Eq. 4.5. By this procedure, value of $G = 5800$ and 5260 psi were obtained for the soil directly beneath the Bases- 1, 3, 5 and 2, 4 respectively. These values are reasonably close to those obtained by seismic methods in spite of the daring approximations involved.

Thus, the dynamic shear modulus for the soil at the test site was obtained by three different methods described in Sections 4.2, 4.3 and 4.4 respectively. The values of dynamic shear modulus, $G = 5500$ psi and Poisson's ratio, $\mu = 0.25$ were finally selected as the most probable values for the soil of the test site at Indian Institute of Technology, Kanpur.

TABLE 4.1 RESULTS OF CROSS-HOLE SEISMIC INVESTIGATIONS AT CHAKERI SITE. (Distance between Bore Holes=25 Ft.)

Depth from Ground Level in Feet.	Soil Classification.	In-Situ Density in lbs./ft. ³	Travel Time of S-Wave in Milli-Seconds.	Shear Wave Velocity in Feet/Sec.	Dynamic Shear Modulus in lbs./Sq.in.
GL	Clayey Silt ML	98.7	53.0	472	4750
2.0	Clayey Silt ML	99.5	50.5	495	5250
7.0	Silty Clay with Kankar CL	105.2	44.0	567	7300
8.5	Clayey Silt ML	107.7	41.5	604	8450
10.25	Fine Sand SM	100.2	41.0	610	8175

TABLE 4.2 CONFINING PRESSURE CALCULATIONS BASED ON PRANGE'S SOLUTIONS. (For $\mu = 0.25$)

z/r_0	$\frac{q_0}{W/\pi r_0^2}$	Applicable for Bases-1,3,5 and Chakeri-Base		Applicable for Bases-2 and 4	
		Depth Below Base in Feet (Z)	\bar{q}_0 in lbs.per Sq.Feet	Depth Below Base in Feet (Z)	\bar{q}_0 in lbs.per Sq.Feet
0.1	0.642	0.15	407	0.2	230
0.2	0.440	0.30	279	0.4	158
0.4	0.293	0.60	186	0.8	105
0.6	0.222	0.90	141	1.2	79.5
0.8	0.178	1.20	113	1.6	63.7
1.0	0.147	1.50	93	2.0	52.6
1.5	0.096	2.25	61	3.0	34.4
2.0	0.067	3.00	42.5	4.0	24.0
3.0	0.037	4.50	23.4	6.0	13.25
		$W/\pi r_0^2 = 634$ lbs./Sq.Ft.		$W/\pi r_0^2 = 358$ lbs./Sq.Ft.	

Seismic wave observed travel time, in milliseconds

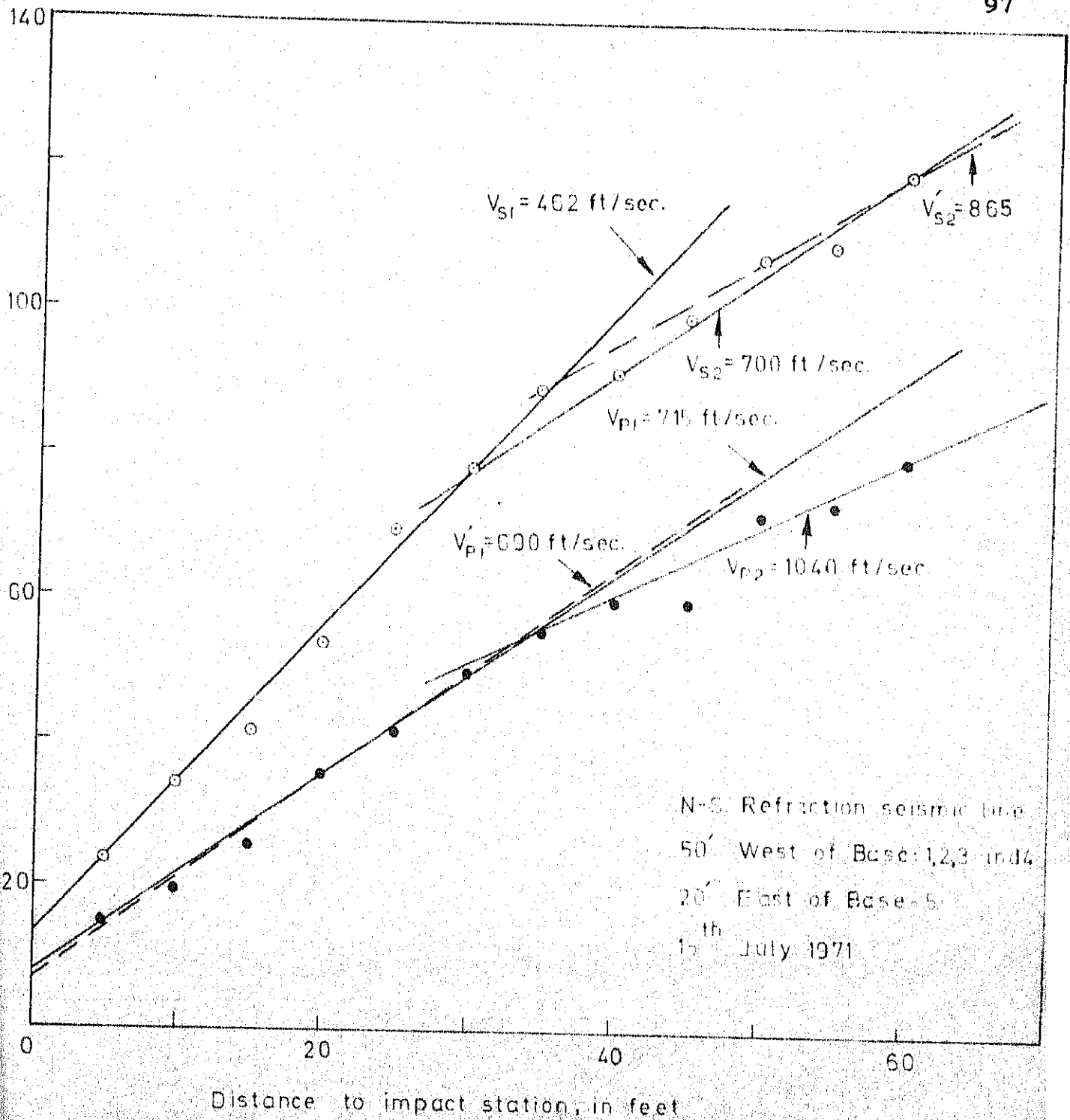


FIG. 4.1 SAMPLE TRAVEL TIME GRAPH FOR THE TEST SITE AT I.I.T. KANPUR

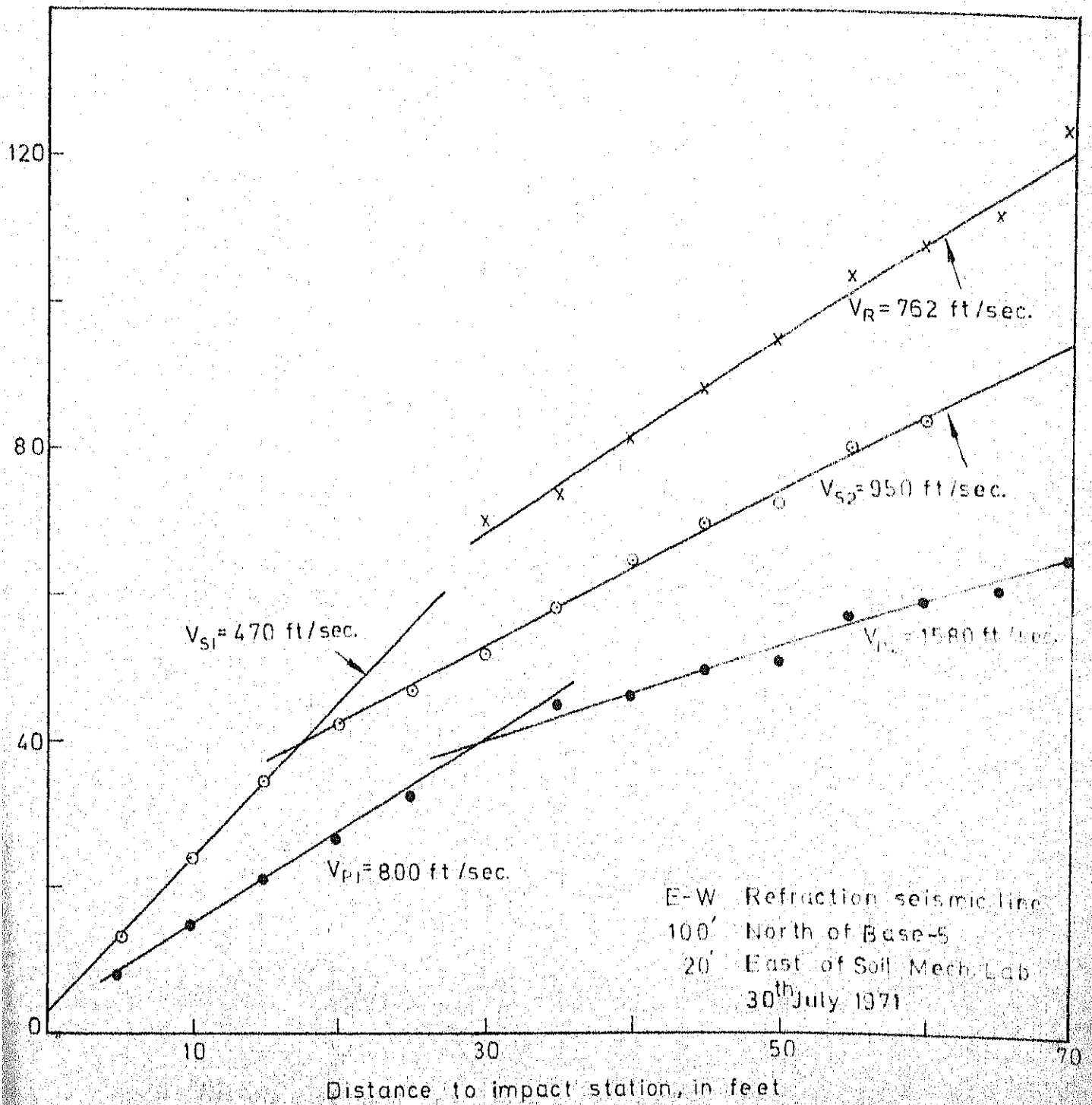
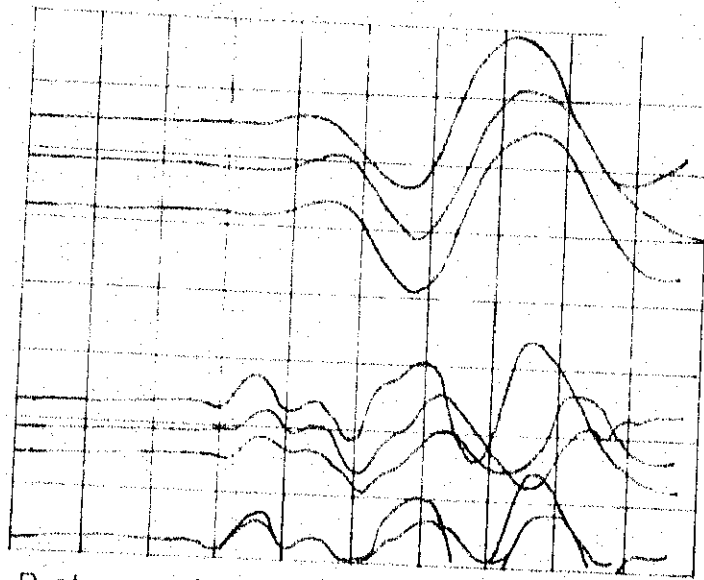
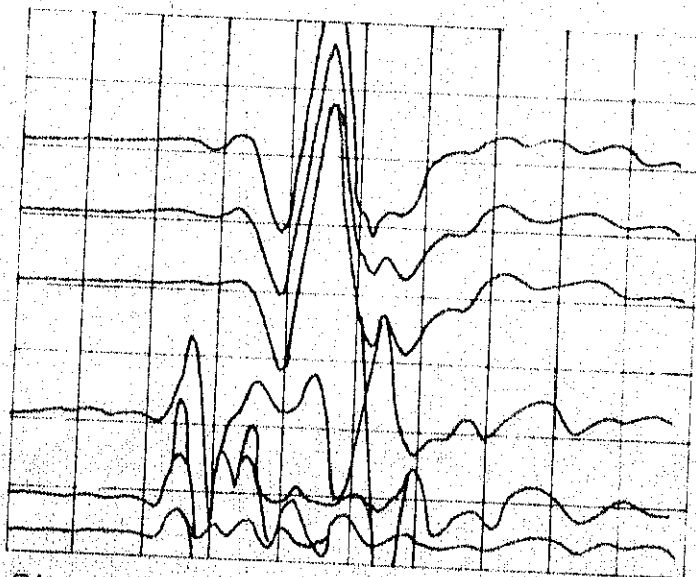


FIG. 4.2 SAMPLE TRAVEL TIME GRAPH FOR THE TEST SITE AT I.I.T. KANPUR



(a) Distance of geophones from impact station=10'
Horizontal sweep=5 milli sec./cm; Soil type=CL



(b) Distance of geophones from impact station=15
Horizontal sweep=10 milli sec./cm; Soil type=CL

FIG. 4.3 TYPICAL PHOTOGRAPHIC RECORDS OF OSCILLOSCOPE TRACES OBTAINED DURING REFRACTION SURVEYING

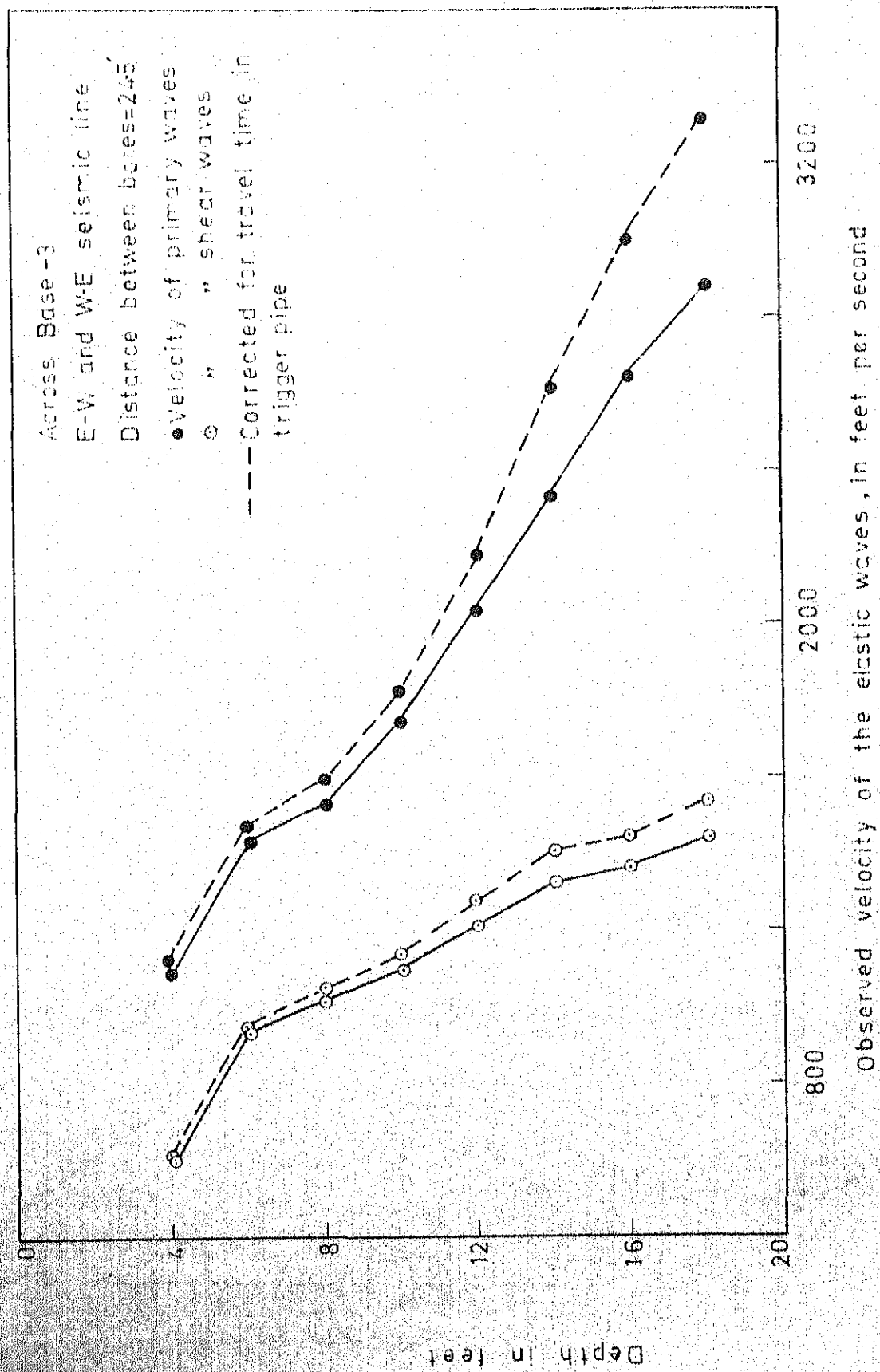


FIG. 4.4 CROSS HOLE SEISMIC INVESTIGATIONS ACROSS BASE-3

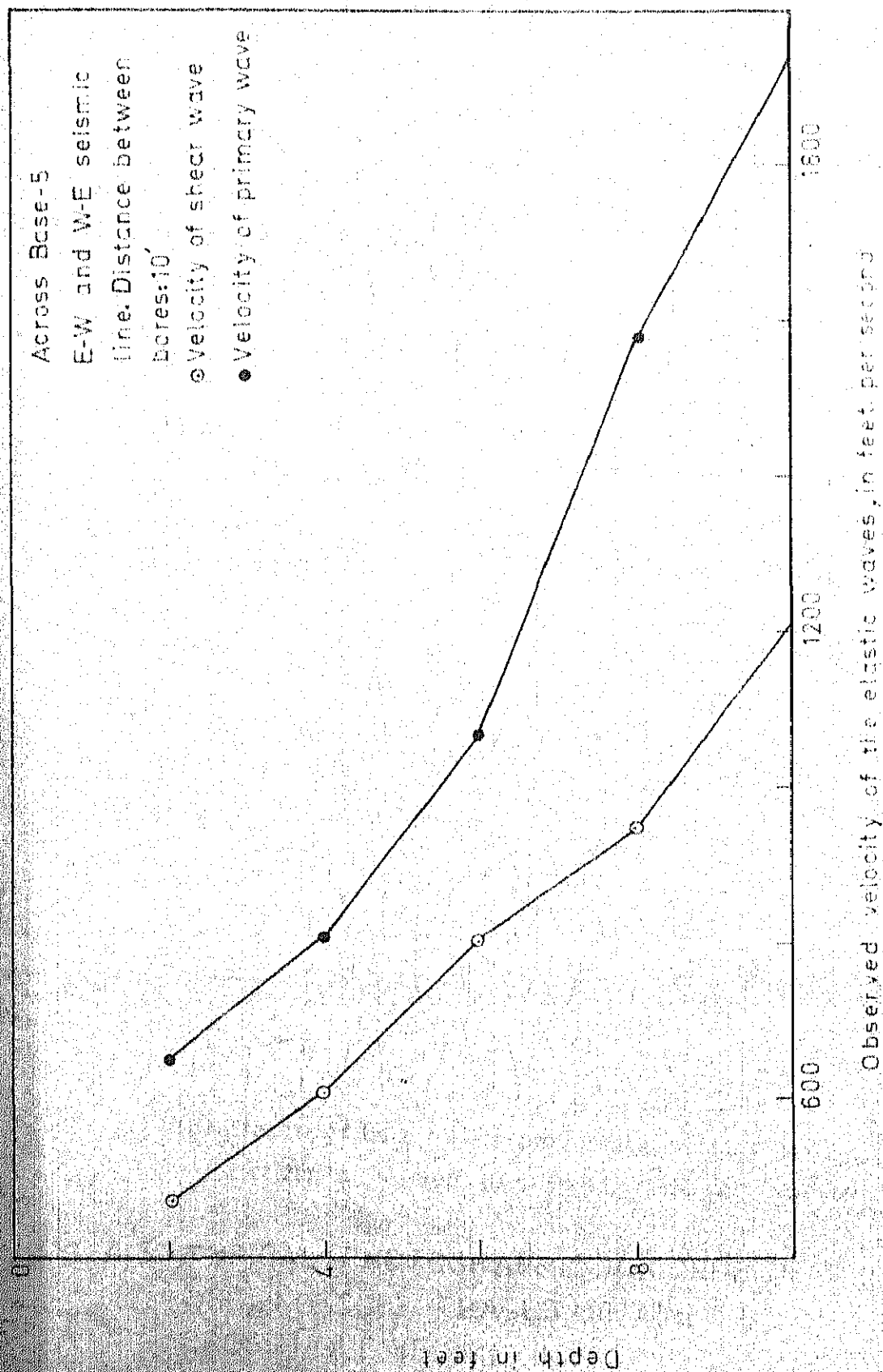
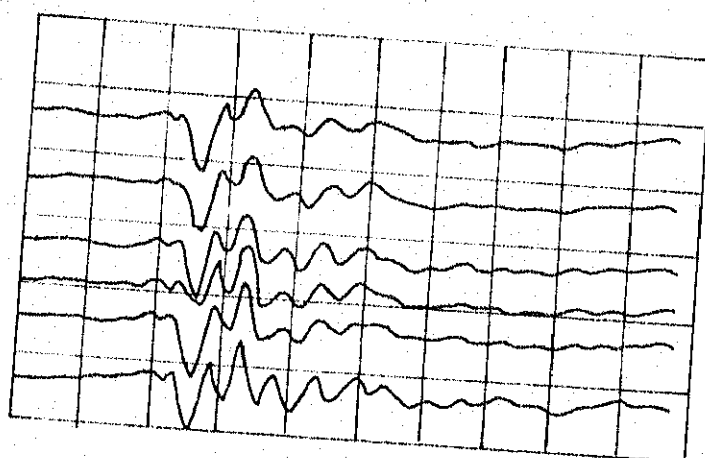
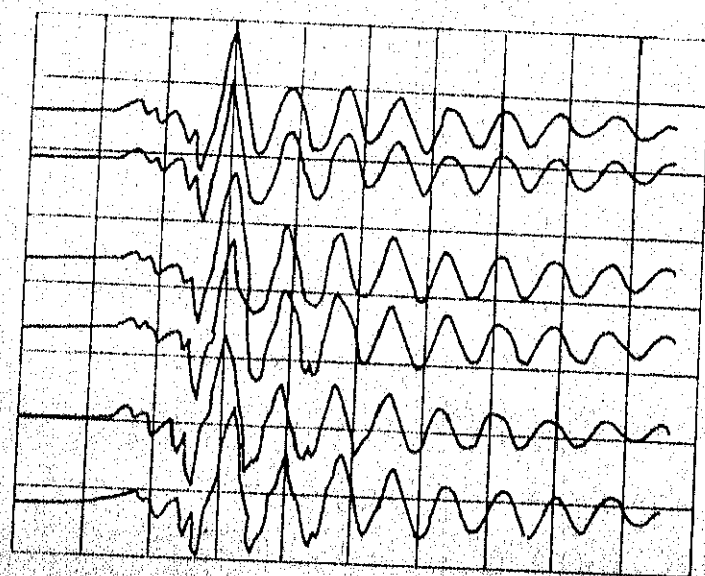


FIG. 4.5 CROSS HOLE SEISMIC INVESTIGATIONS ACROSS BASE-5

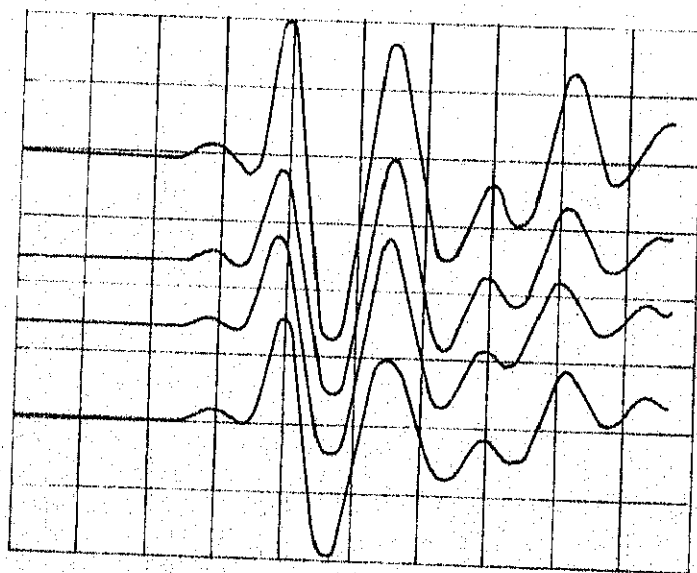


(a) Depth of bore hole from natural surface=10'
Horizontal sweep 10 milli sec./cm soil type=ML



(b) Depth of bore hole from natural surface=14'
Horizontal sweep 10 milli sec./cm soil type=ML

FIG. 4.6 TYPICAL PHOTOGRAPHIC RECORDS OF THE
OSCILLOSCOPE TRACES OBTAINED DURING
CROSS-HOLE SEISMIC INVESTIGATIONS ACROSS
BASE-3



Depth of bore hole from natural surface=4'

Horizontal sweep = 5 milli sec./cm; soil type=CL

FIG. 4.7 TYPICAL PHOTOGRAPHIC RECORDS OF THE OSCILLOSCOPE TRACES OBTAINED DURING CROSS HOLE SEISMIC INVESTIGATIONS ACROSS BASE-5

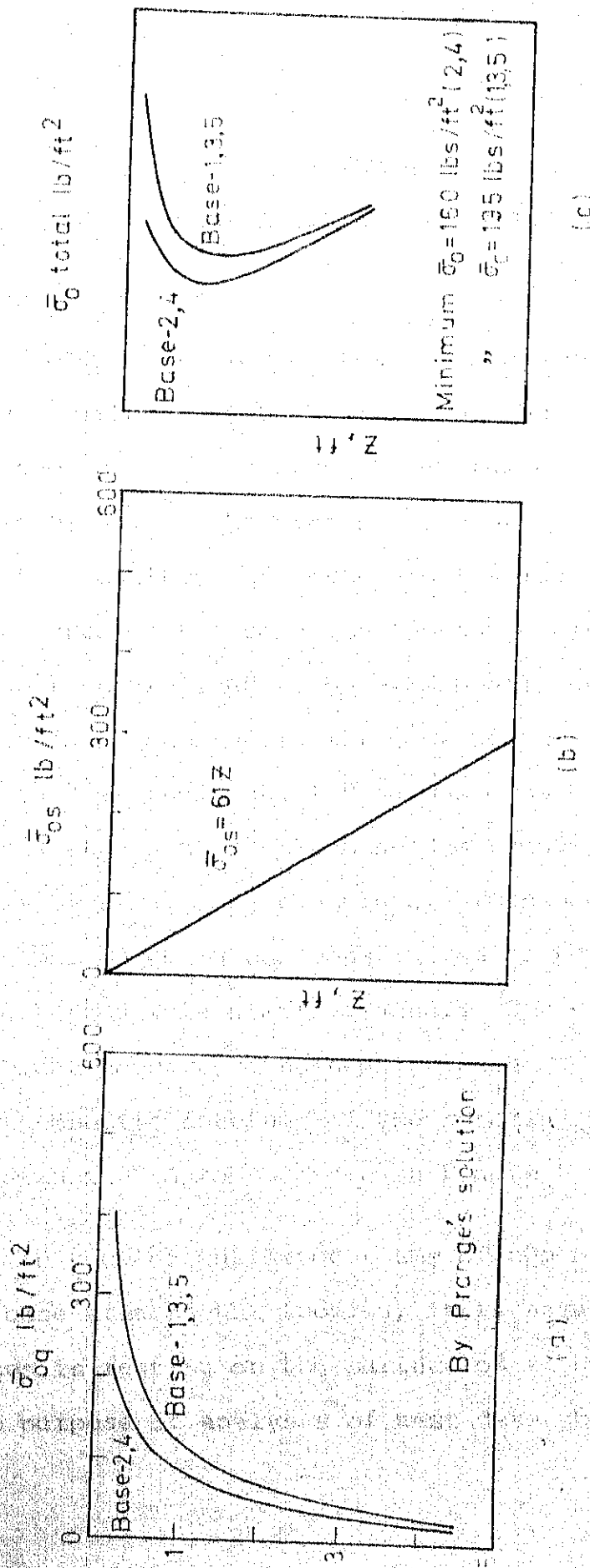


FIG. 4.8 DISTRIBUTION OF AVERAGE CONFINING PRESSURE, $\bar{\sigma}_0$, BENEATH THE PERIPHERY OF BASES - 1,2,3,4 AND 5. (a) $\bar{\sigma}_{0q}$ FROM FOOTING LOAD. (b) $\bar{\sigma}_{0s}$ FROM UNIT WEIGHT OF SOIL (c) TOTAL $\bar{\sigma}_0 = \bar{\sigma}_{0q} + \bar{\sigma}_{0s}$

CHAPTER 5

RESULTS OF STEADY-STATE VIBRATORY TESTS

5.1 GENERAL

The first series of tests was conducted on Base-1, 2, 3 and 4 without any backfilling of the excavated pits. Each of the bases was tested at several positions of the eccentric masses of the mechanical vibrator to produce different intensities of force application. Similar tests were conducted on the concrete footing constructed at Chakeri. This base is equivalent to Base-3 in all respects and is designated as Chakeri-Base for convenience. As explained in Section 3.2, the Chakeri-Base was also constructed in a large excavated pit and its base was founded directly on the layer of silty clay containing limestone nodules or kankar. Base-5 which was constructed on the natural surface was also tested in a similar manner. The various frequency-displacement spectras obtained for each of the footings, at various eccentric settings of the rotating masses are illustrated in Figure 5.1 through Figure 5.8.

In view of the large sizes of the pits in relation to the base area of the footing, it is assumed that each of the bases is resting on the surface of an elastic half-space for the purpose of analysis of test data obtained without

any backfilling. The lumped parameters, spring constant, K and the damping factor, D have been evaluated for each of the footings by three different ways for purposes of comparison and the method of analysis is explained below.

5.2 METHOD OF ANALYSIS

5.2.1 Prediction of Footing Response by Lysmer's Analogue

One of the approaches consisted in using the value of shear modulus, G , Poisson's ratio, μ and the in situ mass density, ρ of the soil as determined from the seismic investigations in the test site area. These dynamic soil properties were used in Eq. 2.36 and Eq. 2.39 of Lysmer's analogue, explained in Section 2.4.3 of Chapter 2, for evaluating the spring constant, K and the damping factor, D respectively. The resonant frequency and the maximum amplitudes of motion at resonance for each of the bases at the corresponding exciting force levels can be predicted using the formulae derived for the single-degree-of-freedom mass-spring-dashpot system, as explained in Section 2.2.3 of Chapter 2. Thus values of resonant frequency and maximum amplitude of motion at resonance were computed using Eq. 2.21 and Eq. 2.22 respectively. These predicted values are tabulated in Table 5.1 for each of the footings of corresponding exciting force levels, which are also indicated in Table 5.1.

The numerical steps involved for one set of computations are illustrated in Appendix A as an example.

5.2.2 Evaluation of K and D by Frequency Response Curves

In this approach, the response curves which show the resonant frequencies and maximum amplitudes of motion for each of the bases, at the given exciting force levels, are analysed using Eq. 2.21 and Eq. 2.22. For example, the damping factor, D can be evaluated from Eq. 2.22 when the magnitude of the amplitude of displacement at resonance, X_{or} , the total mass of the footing and the vibrator, M and eccentricity moment, $m_0 e$ of the vibrator are known. The damping factor, D, thus found out, can be used in Eq. 2.21 to estimate the natural frequency, $(\omega)_n$ of the system and hence the spring constant, K.

The estimation of damping factor, D and the natural frequency, $(\omega)_n$, from Eqs. 2.22 and 2.21 involves some uncertainties. The effective in-phase mass of the soil participating in the vibrations, for instance, must be either neglected or included. As mentioned earlier, some investigators (4, 11, 48) tried to estimate the amount of in-phase mass by empirical means but without much success. The later refinement was to find out a suitable coefficient of mass increase, α , and a damping factor, D so that the lumped mass theory yielded the same maximum response as did

the half-space theory. These values of coefficient of apparent mass increase α_c , are derived for vertical and other kinds of motion by Whitman (62), Hsieh (31), Funston (17) and others.

In the present study, the field test data have been analysed by considering a suitable coefficient of apparent mass increase, α_c , as given by Funston (17) as well as by ignoring the same. The selected values of α_c corresponded to the rigid base type of pressure distribution. The results of the analyses of these data are tabulated in Table 5.2.

The numerical steps involved for one set of computations are illustrated in Appendix A as an example.

Thus, three different damping factors can be assigned to the same footing if computations are carried out with different assumptions or approaches. Though there is nothing sacrosanct about these numerical values, there is, at least, a definite indication about the lower and upper bounds of these quantities and hence the presentation of results by three different methods. It is of interest to note here that one of the assumptions of the proposed theoretical model to describe the dynamic response of embedded footings, which will be explained in Chapter 8, is that no change is effected either in the spring constant, K

or the damping factor, D as a result of embedment of the footing. Therefore, it is important to estimate these quantities as correctly as possible.

5.3 NONLINEARITY OF OBSERVED RESPONSE

Typical experimental response curves obtained from steady-state vibration tests on Base-1 and Base-3, without any backfilling of the pits, are illustrated in Figure 5.1 and Figure 5.2. These tests were specially conducted at four positions of the eccentric masses which corresponded to 45, 60, 75 and 90 degrees in terms of phase angles between the eccentric weights or 0.0194, 0.0253, 0.0308 and 0.0358 pound-second² in terms of eccentricity moments, m_0e respectively, in order to achieve higher intensities of force application. It can be seen from Figure 5.1 and Figure 5.2 that the resonant frequency of the system decreases with every increase in the eccentricity of the rotating masses. For example, there was a decrease of five cycles per second in the resonant frequency by increasing the eccentricity moment from 0.0194 to 0.0358 pound-second².

The data illustrated in Figure 5.1 and Figure 5.2 were, however, analysed by the method described in Section 5.2.2. The spring constant, K and the damping factor, D were evaluated using Eq. 2.22 and Eq. 2.21 respectively. The computations were carried out with the same assumption

of coefficient of mass increase, α as was done in the case of previous computations. Such an analysis qualitatively indicated a continuous decrease in the value of spring constant, K with every increase in the eccentricity moments, $m_0 e$ or dynamic force levels. The analysis also revealed that the damping factor, D decreased continuously with every increase in the dynamic force levels. These results are tabulated in Table 5.2.

Obviously, the method of analysis which is applicable for linear systems only cannot be expected to explain the nonlinear behaviour which was observed in the present investigation. However, such an attempt can reveal the trends in the variation of dynamic soil parameters, spring constant, K and damping factor, D during large strain amplitudes. Thus, for instance, the analysis of observed data by the linear mass-spring-dashpot model revealed the decrease of both K and D with higher angles of eccentricity, θ as shown in Figure 5.9 and Figure 5.10. The trend in the variation of the parameters, K and D suggests that a nonlinear theory of a lumped mass system allowing for a nonlinear spring and a nonlinear dashpot are required to explain the foundation behaviour whenever large dynamic stress levels are encountered.

The nonlinear nature of the dynamic response of the foundation-soil system was similarly felt in the results presented by Jones (33) and the Waterways Experiment Station (16). The results of the above mentioned investigations also indicated the decrease of resonant frequency as the amplitude of the exciting force increased, a trend confirmed by the present investigation. The decrease of K with the angle of eccentricity, Θ , shown in Figure 5.9, suggests that the foundation-soil system appears to behave as though it were a softening system in which the restoring force depends not merely on the dynamic force levels and the frequency but also on the amplitudes of displacement.

Though several theoretical models have been developed by many investigators (17, 38, 56, 46) to explain the nonlinear nature of the dynamic response, the exact cause as to why the response is nonlinear is not yet known. Some possible causes have been put forward by a few investigators as to why the response is nonlinear. Richart (54), for instance, felt that some of the test vibrators might have jumped free of the ground each cycle when the accelerations exceeded 1.0 g, thereby acting as a compactor. This, he thought, caused a change in the pressure distribution which resulted in the increase of amplitude of vibrations and the consequent nonlinear behaviour found in some tests.

Funston (17) reasoned that the nonlinear behaviour could be explained, atleast in part, by the fact that soils generally exhibit a nonlinear behaviour under static loading. Novak (46) observed nonlinearity in damping besides the nonlinearity in the spring characteristic with experiments, particularly on cohesive soils. He thought some of the effects might depend on the history of preceding loading or stress history with clays. He concluded that the nonlinearity of experiments on some cohesive soils could not be described by any single perfectly elastic nonlinear behaviour but may be most likely attributed to their visco-elastic and elastoplastic properties.

5.4 EFFECT OF MOISTURE IN SOILS

The assumption in most of the theories up to date that the soil medium can be approximated as an isotropic, homogeneous and elastic half-space poses some serious obstacles. Soil is infact a rheological material whose properties are greatly affected by the presence of moisture besides its dependance on the state of stress and other factors. The extent to which the moisture content in the soil can affect the dynamic response of the soil-foundation system was studied by taking advantage of the natural rainfall at the test site. The heavy down-pour at the test site provided conditions close to saturation of the soil up to

1.5 to 2.0 feet below the base level of the footing constructed in the excavated pits. One set of dynamic tests were conducted on Base-1 under such wet conditions. The graph of dotted lines shown in Figure 5.1 describes the response of Base-1 under near saturation conditions, at the same exciting force levels as those adopted during the prevailing dry conditions. The resonant frequencies were observed to be less than those observed for tests during dry conditions. Also, the resonant amplitudes were slightly more than those observed for tests during dry conditions. The analysis by the lumped parameter model indicated an appreciable decrease in the spring constant and a slight decrease in the damping factor due to saturation. The results of these tests are tabulated in Table 5.2. The decrease in the spring constant as a result of excessive moisture is illustrated in Figure 5.9. This behaviour can be intuitively explained by the fact that a cohesive soil of the type encountered at the test site, loses its strength to an appreciable degree with increasing moisture content.

It is of interest to briefly review the theory of wave propagation in porous saturated solids at this state. Biot (7) considered the general three-dimensional propagation of both P and S waves in a fluid-saturated porous medium. Biot's theory has been reviewed by Richart, Hall

and Woods (55) in the context of vibrations of soils and foundations. Biot's theory clearly points out the strong influence of the structural coupling, due to the stiffnesses of solid and fluid components of the system, involved in the compressional waves and lack of structural coupling for the shear wave. Therefore, Richart, Hall and Woods (55) have suggested that field measurements of shear waves in saturated soils may be taken as the actual shear wave velocity in the soil structure. Also, the steady-state response of a vibrating footing is closely associated with the shear modulus of the soil on which it is resting, as can be noted in Section 2.3. In view of the above arguments, the shear modulus of the soil and hence the spring constant, is not expected to change appreciably with water saturation. The contradiction in the observed results may be due to one or many of the following reasons:

- 1) partial saturation of the soil;
- 2) presence of excessive moisture in the top few feet of the soil and the lack of excessive moisture in the soil below, might have converted the soil mass below the footing into a complicated layer system;
- 3) buoyancy effects on unit weight of the soil ; and
- 4) physico-chemical changes in the soil structure of the silty clay soil due to the presence of excessive moisture.

Further research, under more controlled conditions is necessary to verify the implications of Biot's theory in the field of soil dynamics.

5.5 EFFECT OF SIZE AND SHAPE

The responses of Bases-1, 2, 3 and 4 are comparable with regard to the effects of size and shape since they were constructed inside excavated pits of same dimensions, at the same elevation below the natural surface, with soil conditions below each of these footings remaining uniformly same. As mentioned earlier, the main series of tests were conducted on these four footings at four positions of the eccentric masses corresponding to 30, 35, 40 and 45 degrees in terms of phase angles between the eccentric weights. This enabled to keep the level of the maximum amplitudes of acceleration below 0.5 g through out the programme of tests in this series. Consequently, the nonlinearity in the observed dynamic response of footings was kept at a minimum possible level. The observed frequency-displacement curves for each of the bases at the corresponding exciting force levels are illustrated in Figure 5.3 through Figure 5.6.

The frequency spectras illustrated in Figures 5.3, 5.4, 5.5 and 5.6 reveal that the responses of circular footings and the square footings of equivalent base area

show good agreement as long as the static intensity of stress below the footing is same. This is clear by a comparison of the responses of Base-1 with Base-3 and Base-2 with Base-4 respectively.

The changes in the response of footings with foundation base size is another important factor that should be borne in mind for any attempts of extrapolating test results to the design calculations of larger foundations. The deviation of the theoretically predicted changes in the dynamic response with respect to base size from the actual trends observed in the field, is often considerable. For example, the observed increase in the resonant frequencies of Base-2 and Base-4 with those of Base-1 and Base-3, as per the response curves illustrated in Figures 5.3 to 5.6, is of the order of 26.9 %. Similarly, the observed decrease of maximum amplitudes of Base-2 and Base-4 with those of Base-1 and Base-3, at various eccentricity moment values, ranges between 46.0 % and 48.0 %. However, the theoretically predicted values which are tabulated in Table 5.1, show an increase of 34.5 % in the predicted values of resonant frequencies between Base-2 and Base-1 or Base-4 and Base-3. Similarly, the corresponding, theoretically predicted decrease of resonant amplitudes between Base-2 and Base-4 with those of Base-1 and Base-3 is of the order

31.0 %. The theoretically predicted values, tabulated in Table 5.1, were computed by means of Lysmer's analogue, as described in Section 5.2.1.

Novak (45) published the results of his experiments, supplemented by the field test data published by Fry (16) of Waterways Experiment Station. He noticed that the experimentally observed variations in the natural frequencies with footings of increasing base area were much greater than the theoretically predicted ones and they seemed to diverge with increasing base area. According to the experimental findings of Fry (16) and Novak (45), the observed resonant amplitudes of footings were found consistently larger than the theory of a rigid body oscillating on the elastic half-space indicated. Some such observations have been confirmed from the present investigation also. A comparison of the theoretically predicted damping factors, tabulated in Table 5.1, with those obtained from the observed frequency-displacement relations, tabulated in Table 5.2, reveals that the effective damping of real footings is always less than that predicted by the elastic half-space theory. A similar observation has been reported by Novak (45) also.

The deviation of test results from the theoretically predicted values may be attributed to the changes in the soil

5.6 RESPONSE OF BASE-5

As mentioned in Section 3.3 an additional concrete base, designated as Base-5, was constructed on the natural surface and the same is indicated in the layout of the site plan illustrated in Figure 3.3. Base-5 was also tested under steady-state vertical vibrations at four different positions of the eccentric masses corresponding to 30, 35, 40 and 45 degrees in terms of phase angles, ϕ between the eccentric weights. Typical frequency-displacement curves are illustrated in Figure 5.7.

It is of interest to note that both Base-5 and Base-3 are geometrically identical. Yet there is a marked difference between the natures of the dynamic response of both the footings. The frequency response curves of Base-5 reveal a higher resonant frequency and a slightly lesser amplitude of motion at resonance. These frequency response curves have been analysed to yield values of lumped parameters, K and D by the method described in Section 5.2.2. These results have been tabulated in Table 5.2. It can be seen that both the spring constant, K and the damping factor, D are somewhat higher in comparison with the values evaluated for Base-3 by the same method. It may also be noted the observed dynamic response of Base-5 is nearer to the theoretically predicted response, as tabulated in Table 5.1.

This can be expected as Base-5 was constructed on the natural surface of the soil, which closely approximated the assumption on which the elastic half-space theory is developed. It is rather intriguing that the layering effect described in the previous section was not noticed in the dynamic response of Base-5, in spite of the presence of the silty clay layer containing kankar or limestone nodules about five feet below the base of footing. This was perhaps due to the fact that the limestone nodules whose average effective diameters ranged between half inch to one and a half inch, were so loosely distributed as to cause any appreciable change in the wave propagation characteristics of the medium. The presence of the kankar, however, might have contributed towards the overall stiffness of the system which is felt as an increase in the spring constant, K .

5.7 RESPONSE OF CHAKERI-BASE

As mentioned in Sections 3.2 and 3.3 of Chapter 3, a sixth concrete footing was constructed at Chakeri test site which is designated as Chakeri-Base. The concrete footing at this site was constructed in a large excavated pit of lateral dimensions: 12 feet by 12 feet; and its base was founded directly on the silty clay layer containing kankar or limestone nodules. The layout of the test area is shown in Figure 3.4. It can be recalled that Chakeri-Base is

geometrically identical to Base-3 and Base-5. Chakeri-Base was tested under steady-state vertical vibrations at five positions of the eccentric masses which corresponded to 36, 45, 54, 63 and 72 degrees in terms of phase angles between the eccentric weights or 0.0156, 0.0194, 0.0230, 0.0265 and 0.0298 pound-second² in terms of eccentricity moments, $m_0 e$, respectively. Typical frequency-displacement curves are illustrated in Figure 5.8.

Though the Bases-3 and 5 and Chakeri-Base were geometrically identical and had the same mass, Chakeri-Base registered relatively lower amplitudes of motion at resonance than those registered by either Base-3 or Base-5. Also, the observed resonant frequencies of Chakeri-Base at all positions of the eccentric masses were higher than those registered by either Base-3 or Base-5.

The observed frequency-displacement curves for Chakeri-Base, illustrated in Figure 5.8, were analysed to yield values of lumped parameters, K and D , by the method described in Section 5.2.2. These results have been tabulated in Table 5.2. It can be seen that both the spring constant, K and the damping factor, D are higher in comparison with the values evaluated in the same way for either Base-3 or Base-5. This shows that the effective stiffness as well as

damping of the soil beneath the Chakeri-Base was at its highest as the concrete footing was directly constructed on top of the relatively hard layer of silty clay with kankar. It can be recalled that this particular layer of soil registered a shear wave velocity of about 567 feet per second as per the findings of the cross-hole seismic investigations, conducted at Chakeri test site, the results of which are tabulated in Table 4.1. It may also be noted that the subsequent layers of clayey silt and fine sand located below the silty clay layer with kankar registered higher shear wave velocities by virtue of their depths below the natural surface.

The presence of silty clay layer with kankar was noticed below both Base-5 and Chakeri-Base. A comparison of the responses of both Base-5 and Chakeri-Base reveals that it is advantageous to locate the base of the footing directly on the relatively harder layer of silty clay with kankar, in order to achieve the maximum overall stiffness of the soil below the base.

TABLE 5.1 PREDICTED RESPONSE OF TEST FOOTINGS BY LYSMER'S ANALOGUE.

Applicable for	Bases-1,3 and 5	Bases-2 and 4
M (lbs./in./sec ²)	11.65	11.65
Effective, r_o (in.)	18.0	24.0
G (lbs./in ²)	5500	5500
γ (lbs./ft ³)	110	110
	0.25	0.25
B	2.27	0.96
D	0.282	0.434
K (lbs./in.)	5.28×10^5	7.04×10^5
ω_n (rads./sec.)	213	246
ω_r (rads./sec.)	232	312
$\frac{M X_{or}}{m_o e}$	1.848	1.279
X_{or} (in.) when $m_o e = 0.0194$	0.00308	0.00213
X_{or} (in.) when $m_o e = 0.0174$	0.00276	0.00191
X_{or} (in.) when $m_o e = 0.0152$	0.00241	0.00167
X_{or} (in.) when $m_o e = 0.0131$	0.00208	0.00144

TABLE 5.2 RESULTS OF ANALYSES OF EXPERIMENTAL FREQUENCY-DISPLACEMENT RESPONSE CURVES.

Base No.	m_{oe} in lbs.-sec ²		Observed x_{or} in Inches	Observed ω_r in rads. per sec.	D	ω_n in rads. per sec.	K in lbs. per inch	Refer Fig. No.
(1)	(2)	(3)	(4)	(5)	(6)	(7)	(8)	(9)
1	0.0358	1.09	0.00990	192	0.144	187.5	446645	5.1 (dry)
1	0.0308	1.09	0.00800	199	0.153	193.7	476611	-Do-
1	0.0253	1.09	0.00600	214	0.168	207.4	546077	-Do-
1	0.0194	1.09	0.00440	223	0.176	215.9	591999	-Do-
1	0.0358	1.09	0.01025	182	0.139	179.2	407785	5.1 (wet)
1	0.0308	1.09	0.00850	192	0.144	187.5	446564	-Do-
1	0.0253	1.09	0.00650	192	0.155	186.9	443455	-Do-
1	0.0194	1.09	0.00415	199	0.187	191.4	465069	-Do-
3	0.0358	1.09	0.0100	192	0.142	187.6	447037	5.2
3	0.0308	1.09	0.0080	199	0.153	193.7	476611	-Do-
3	0.0253	1.09	0.00615	207	0.164	201.5	515964	-Do-
3	0.0194	1.09	0.00435	220	0.178	212.7	574529	-Do-

Contd.....

Table 5.2 contd...

(1)	(2)	(3)	(4)	(5)	(6)	(7)	(8)	(9)
1	0.0194	1.09	0.0044	220	0.176	212.8	575440	5.3
1	0.0174	1.09	0.00395	222	0.178	214.2	582691	-Do-
1	0.0152	1.09	0.00330	224	0.184	216.7	596554	-Do-
1	0.0131	1.09	0.00290	226	0.181	218.6	606674	-Do-
1	0.0194	1.00	0.00440	220	0.193	211.5	521014	5.3
1	0.0174	1.00	0.00395	222	0.195	212.7	527380	-Do-
1	0.0152	1.00	0.00330	224	0.201	215.2	539370	-Do-
1	0.0131	1.00	0.00290	226	0.198	217.1	548872	-Do-
2	0.0194	1.21	0.00235	283	0.307	254.5	913128	5.4
2	0.0174	1.21	0.00210	283	0.309	254.2	911125	-Do-
2	0.0152	1.21	0.00182	283	0.311	253.8	908617	-Do-
2	0.0131	1.21	0.00157	283	0.310	253.9	909278	-Do-
2	0.0194	1.00	0.00235	283	0.383	237.4	656831	5.4
2	0.0174	1.00	0.00210	283	0.385	236.9	654043	-Do-
2	0.0152	1.00	0.00182	283	0.388	236.3	650546	-Do-
2	0.0131	1.00	0.00157	283	0.387	236.5	651468	-Do-

Contd.....

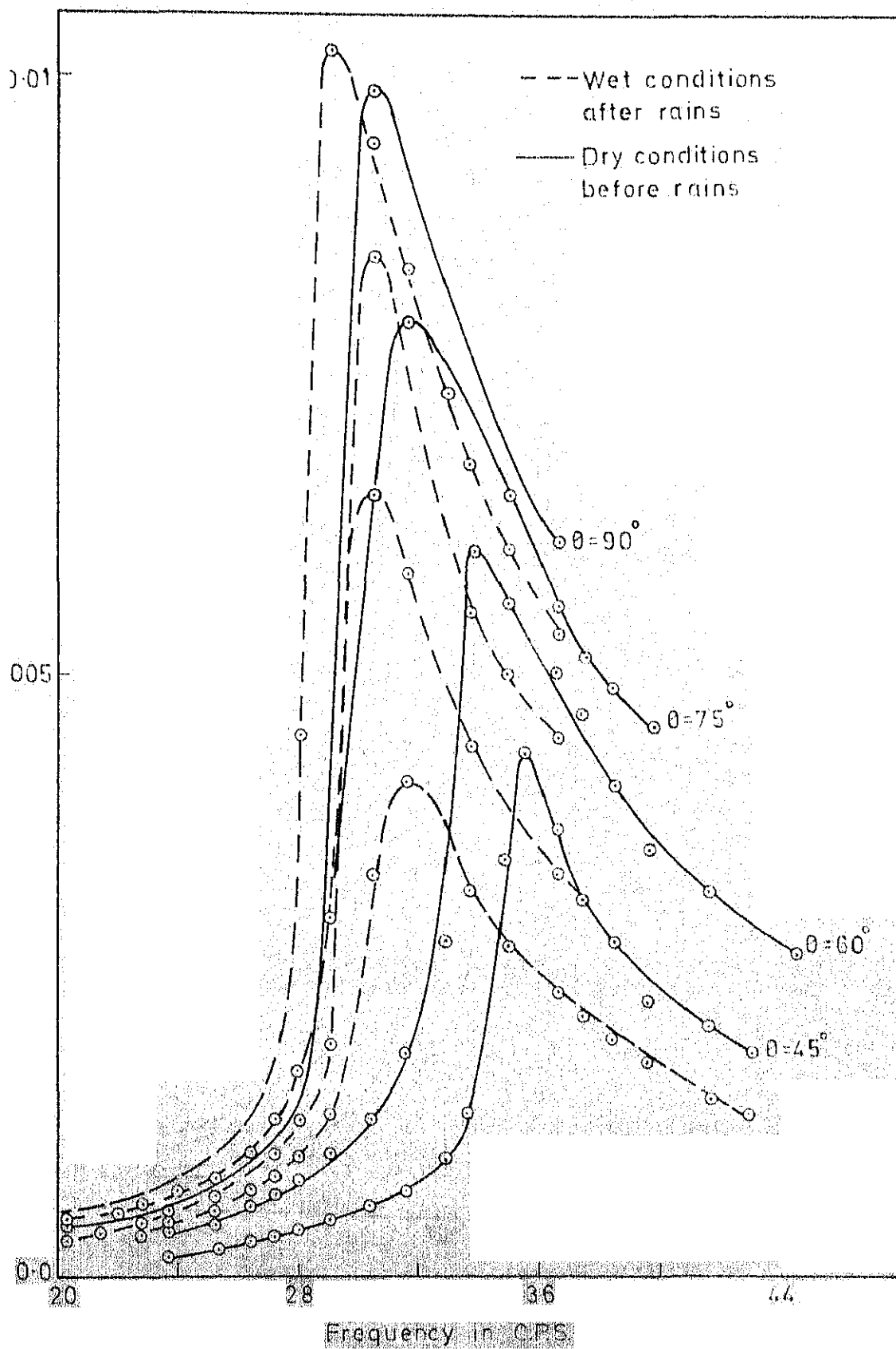
Table 5.2 contd.....

(1)	(2)	(3)	(4)	(5)	(6)	(7)	(8)	(9)
3	0.0194	1.09	0.00435	220	0.178	212.7	574529	5.5
3	0.0174	1.09	0.00385	220	0.181	212.5	573397	-Do-
3	0.0152	1.09	0.00325	224	0.187	216.5	595152	-Do-
3	0.0131	1.09	0.00285	226	0.184	218.3	605117	-Do-
3	0.0194	1.00	0.00435	220	0.195	211.3	520007	5.5
3	0.0174	1.00	0.00385	220	0.198	211.0	518757	-Do-
3	0.0152	1.00	0.00325	224	0.205	214.8	537818	-Do-
3	0.0131	1.00	0.00285	226	0.201	216.7	547150	-Do-
4	0.0194	1.21	0.00225	283	0.323	251.4	891262	5.6
4	0.0174	1.21	0.00195	283	0.336	248.7	871890	-Do-
4	0.0152	1.21	0.00170	283	0.337	248.5	870706	-Do-
4	0.0131	1.21	0.00145	283	0.341	247.6	864541	-Do-
4	0.0194	1.00	0.00225	283	0.404	231.8	626077	5.6
4	0.0174	1.00	0.00195	283	0.422	226.5	598177	-Do-
4	0.0152	1.00	0.00170	283	0.424	226.3	596451	-Do-
4	0.0131	1.00	0.00145	283	0.430	225.0	590125	-Do-

Contd.....

Table 5.2 contd...

(1)	(2)	(3)	(4)	(5)	(6)	(7)	(8)	(9)
5	0.0194	1.09	0.00330	236	0.238	221.7	624427	5.7
5	0.0174	1.09	0.00300	242	0.235	228.1	660467	-Do-
5	0.0152	1.09	0.00275	244	0.223	232.4	685885	-Do-
5	0.0131	1.09	0.00255	244	0.207	234.2	696710	-Do-
5	0.0194	1.00	0.00330	236	0.261	218.8	557914	5.7
5	0.0174	1.00	0.00300	242	0.258	225.2	590631	-Do-
5	0.0152	1.00	0.00275	244	0.245	229.8	615174	-Do-
5	0.0131	1.00	0.00255	244	0.226	232.0	627221	-Do-
Cha- keri Base	0.0298	1.09	0.00435	291	0.281	266.0	898876	5.8
	0.0265	1.09	0.00380	292	0.287	266.0	898629	-Do-
	0.0230	1.09	0.00345	294	0.273	270.4	928381	-Do-
	0.0194	1.09	0.00280	296	0.284	270.2	927461	-Do-
	0.0156	1.09	0.00230	297	0.278	272.4	942033	-Do-
Cha- keri Base	0.0298	1.00	0.00435	291	0.309	260.7	792047	5.8
	0.0265	1.00	0.00380	292	0.315	260.4	790105	-Do-
	0.0230	1.00	0.00345	294	0.300	265.4	820547	-Do-
	0.0194	1.00	0.00280	296	0.313	264.7	816169	-Do-
	0.0156	1.00	0.00230	297	0.306	267.1	831034	-Do-



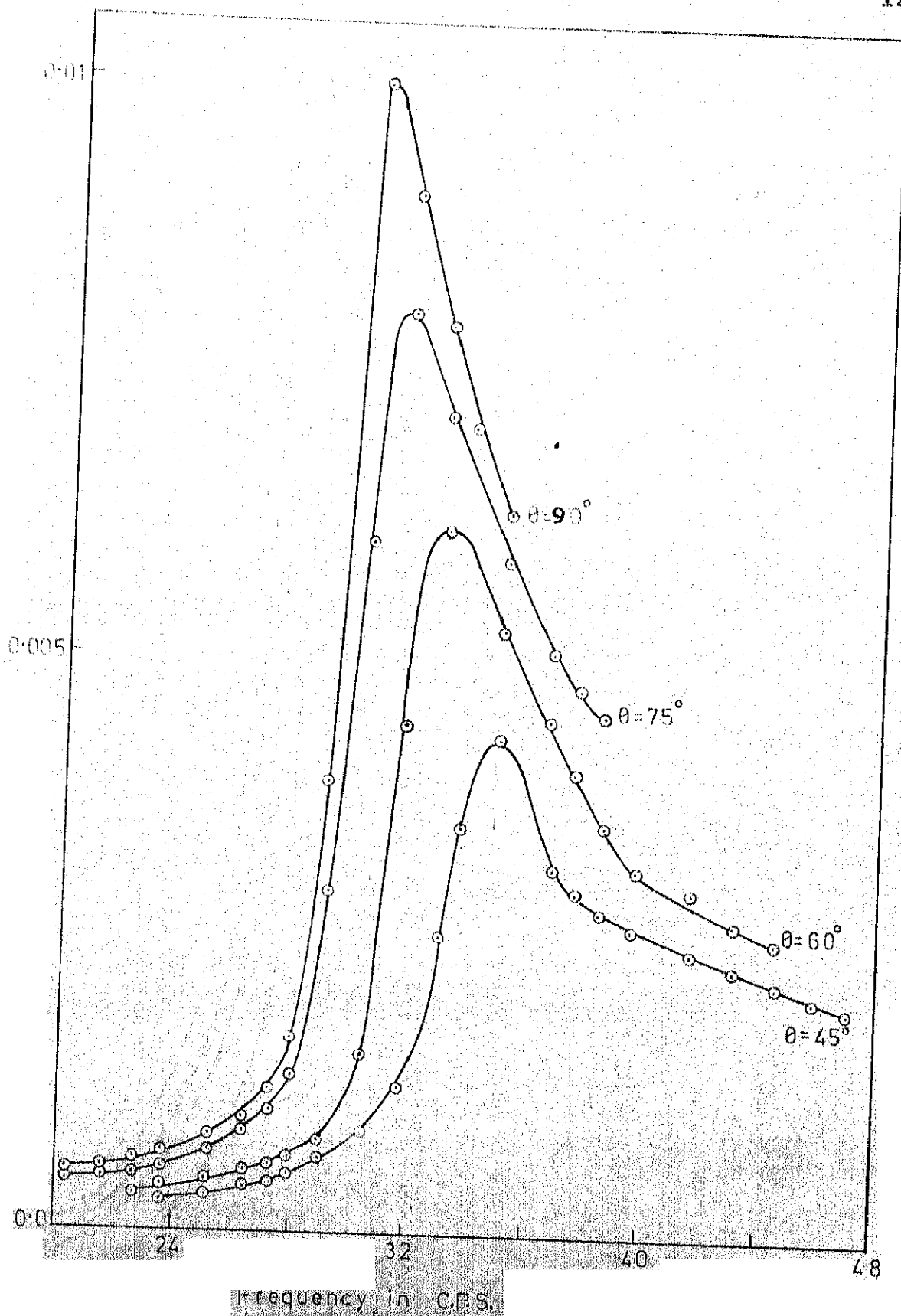


FIG. 5.2 FREQUENCY VS DISPLACEMENT, BASE-3
AT HIGHER DYNAMIC FORCE LEVELS

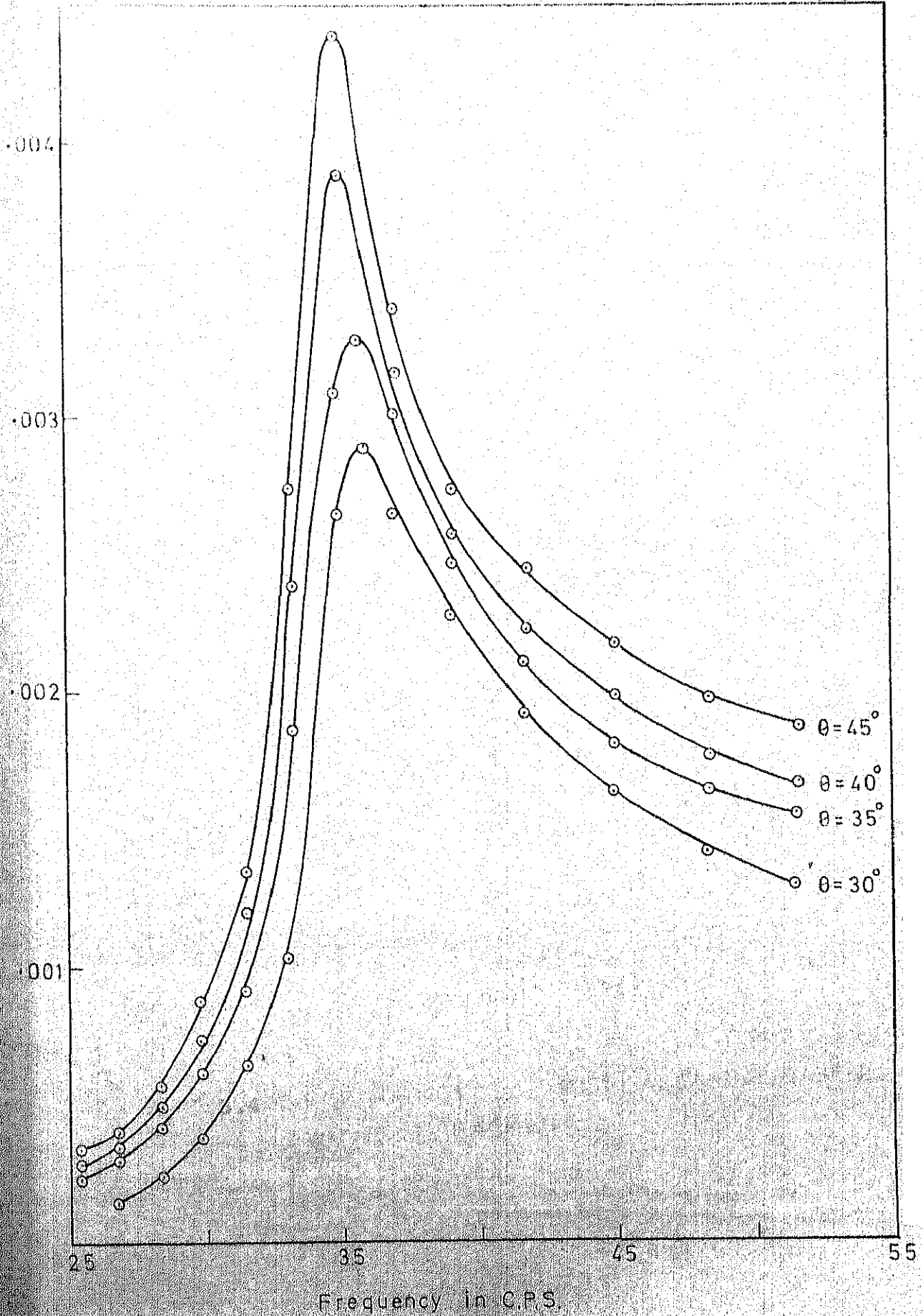


FIG. 5.3 FREQUENCY VS DISPLACEMENT, BASE-1

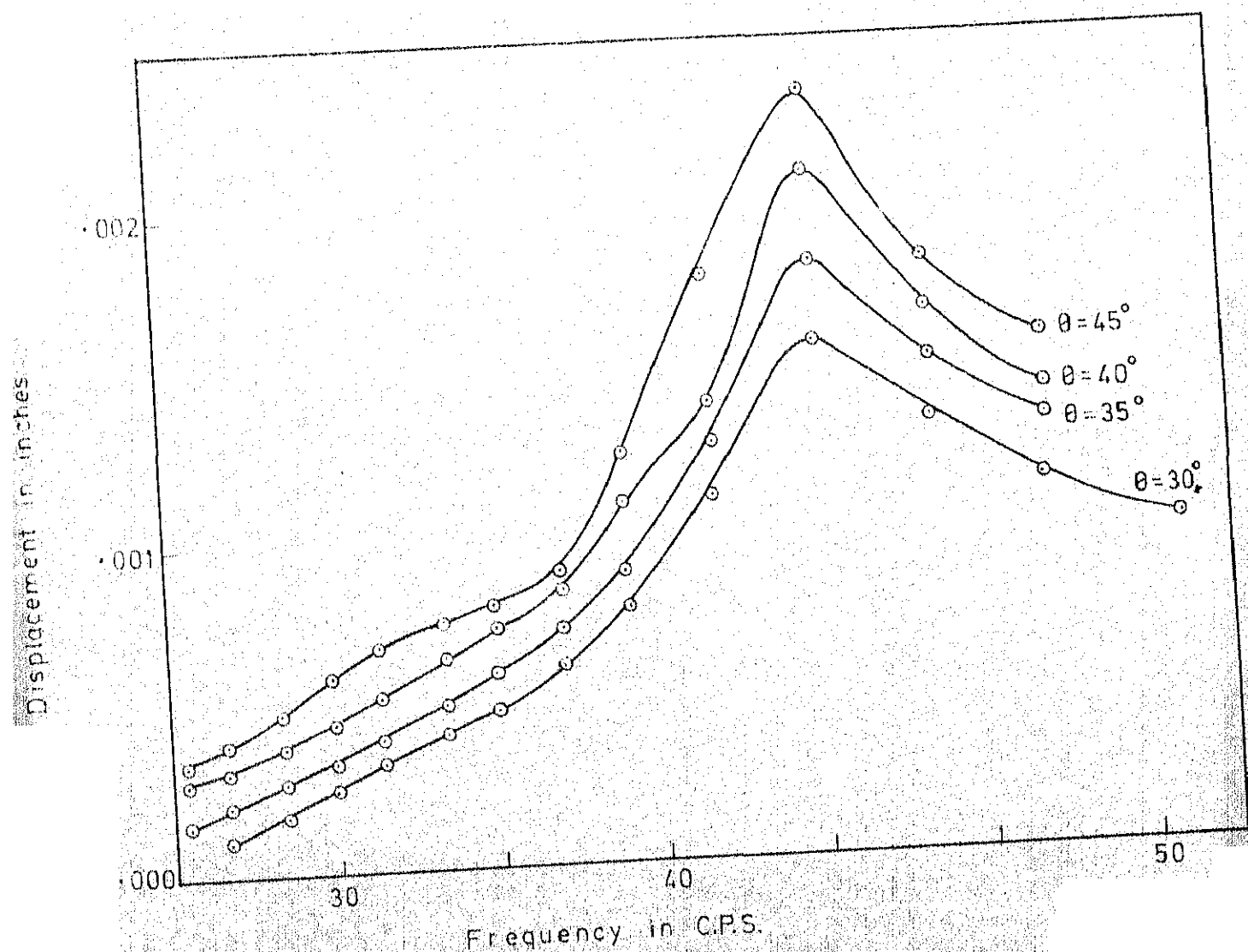


FIG 5.4 FREQUENCY VS DISPLACEMENT, BASE-2 WITHOUT BACKFILL

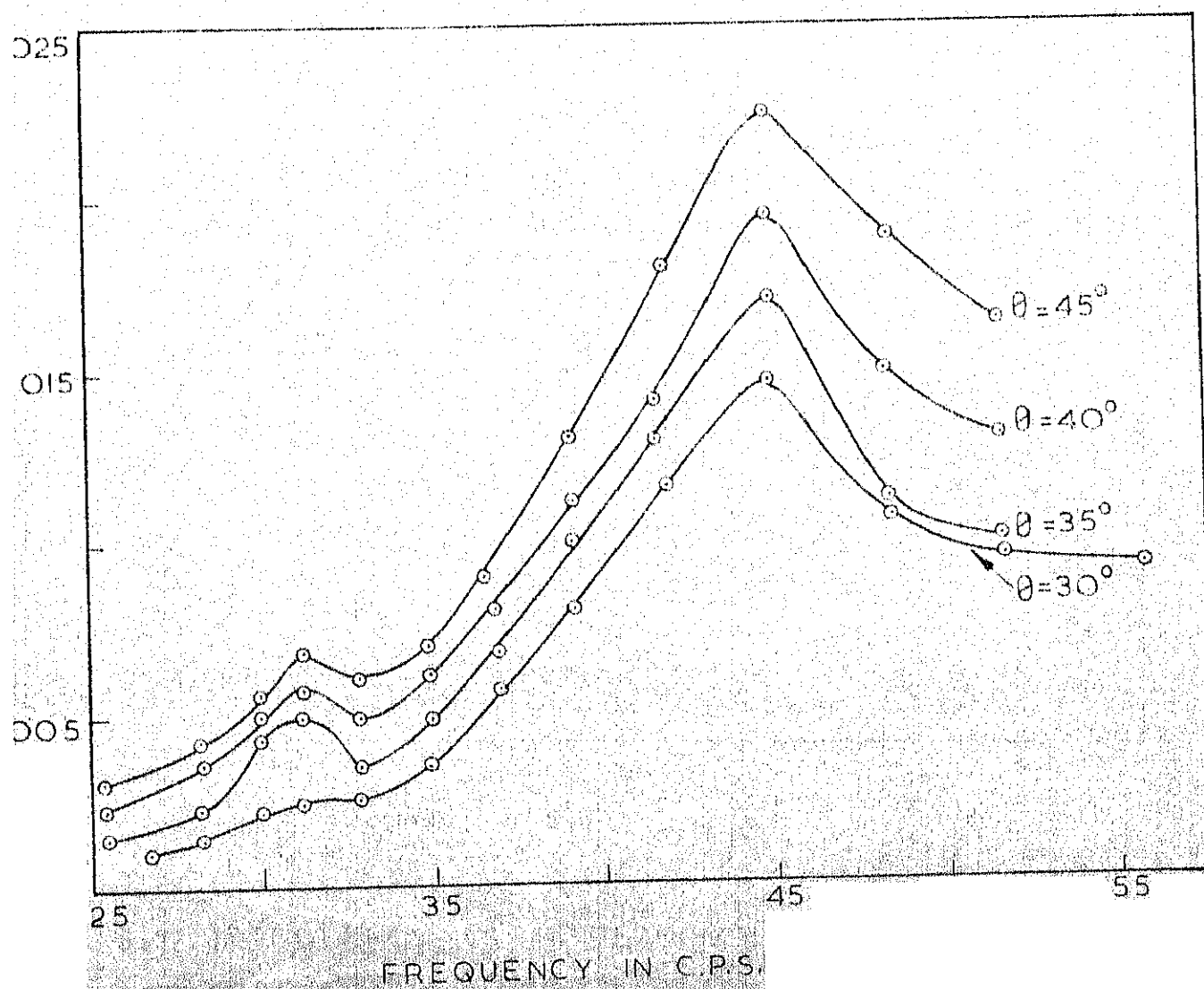


FIG. 5.6 FREQUENCY VS DISPLACEMENT, BASE-4, WITHOUT BACKFILL

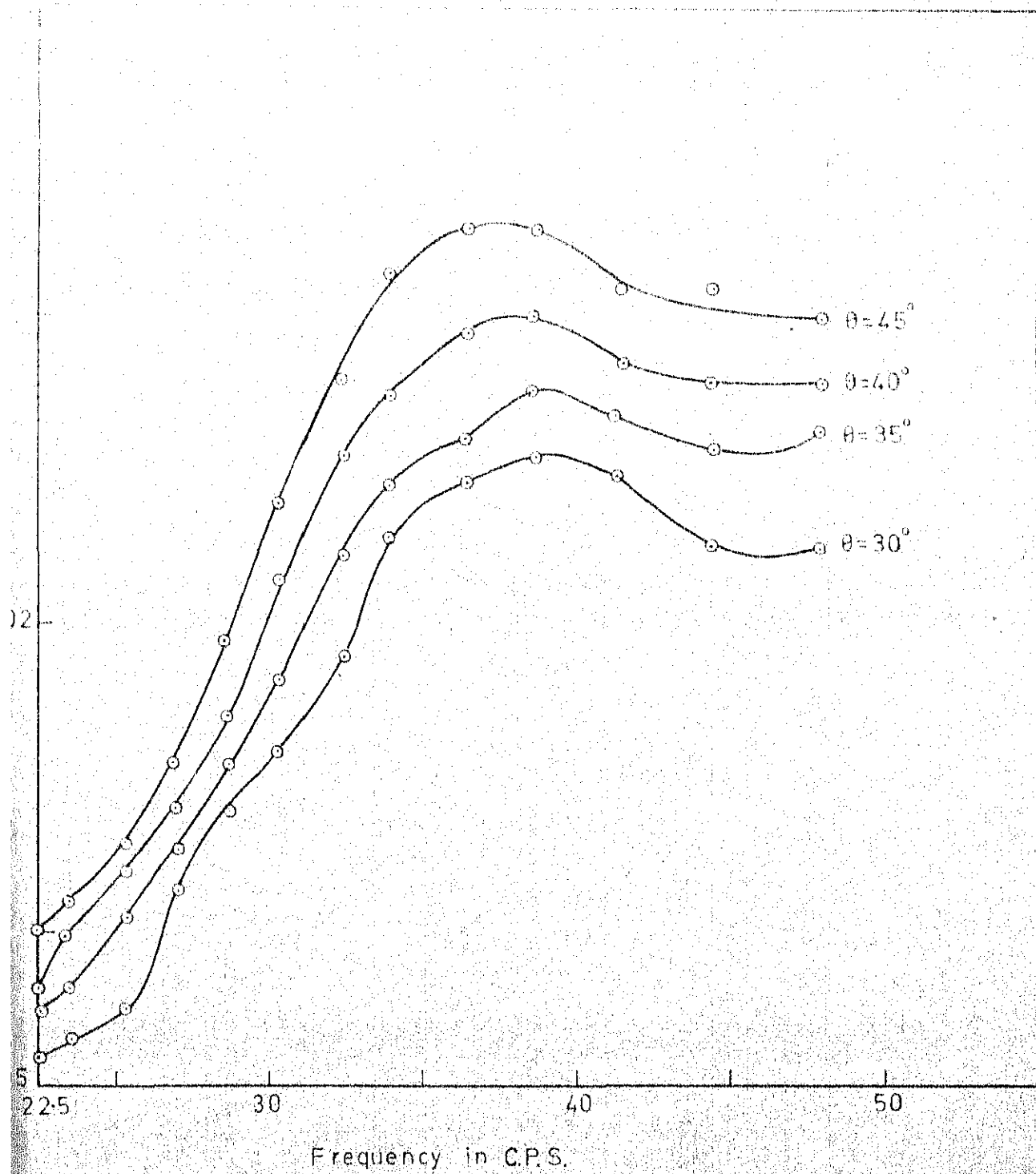


FIG. 5.7 FREQUENCY VS. DISPLACEMENT, BASE-5

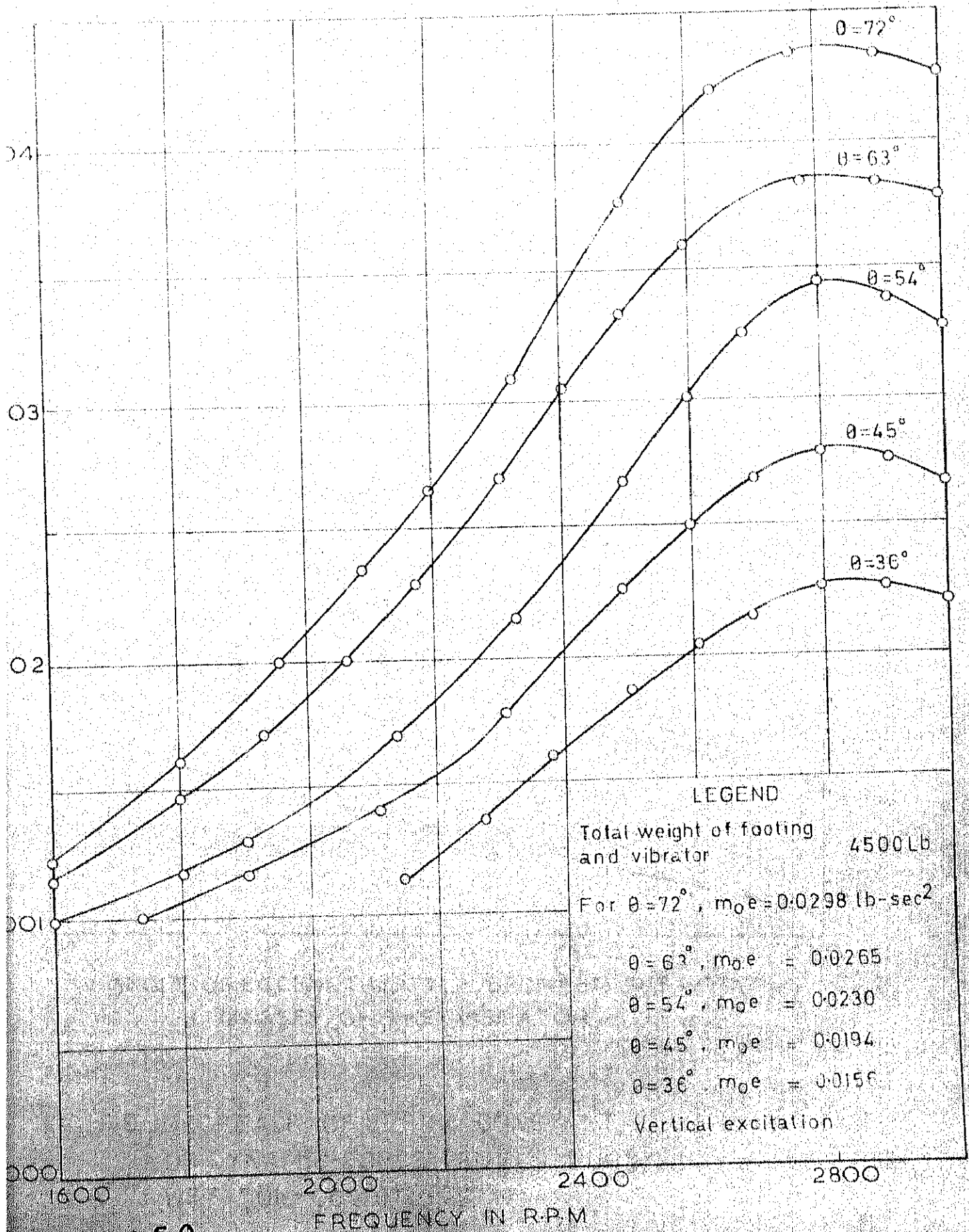


FIG. 5-8.

FREQUENCY VS. DISPLACEMENT, CHAKERI-BASE

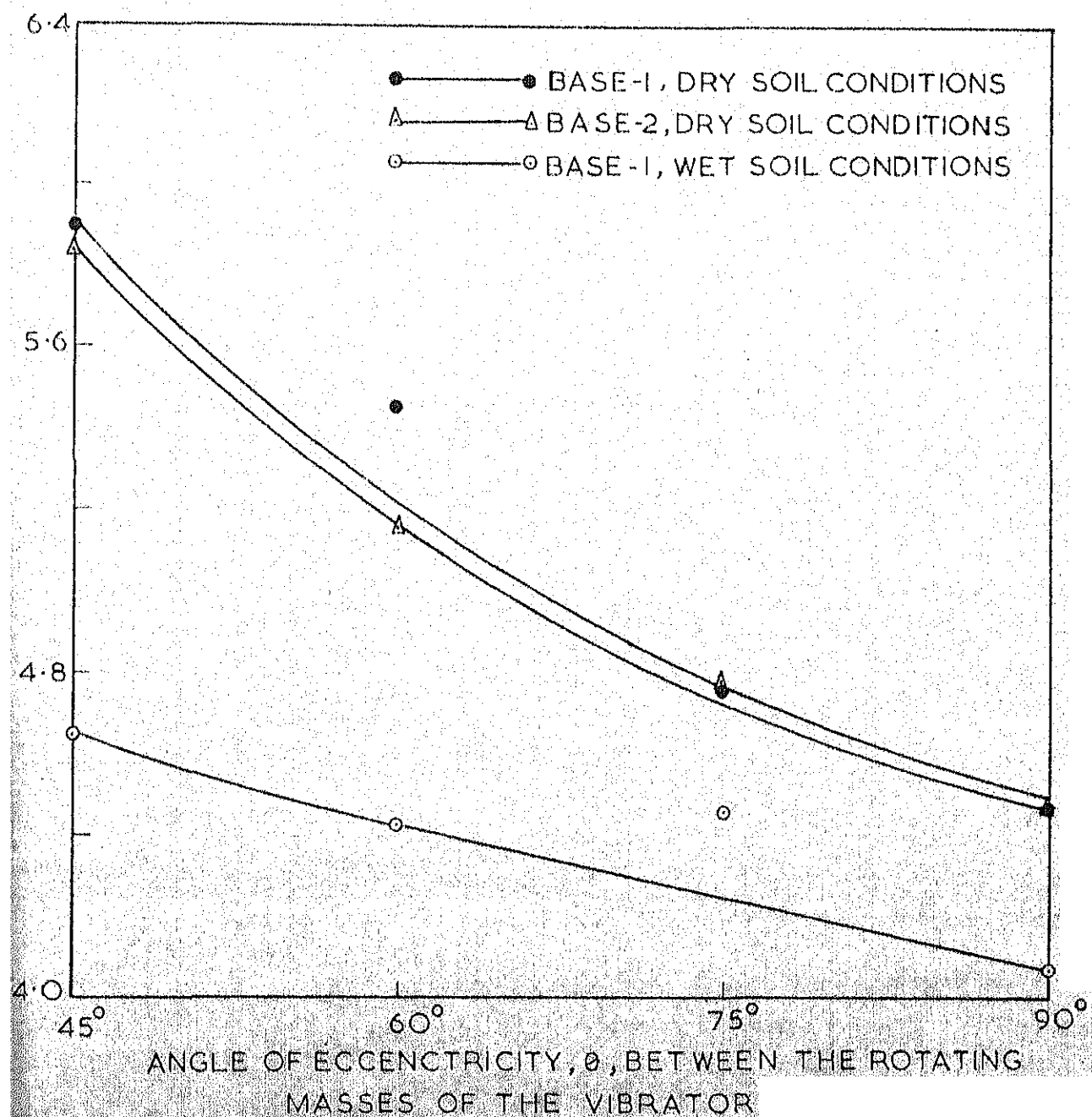


FIG. 5.9 DECREASE OF SPRING CONSTANT, K , WITH INCREASE OF DYNAMIC FORCE LEVELS DURING DRY AS WELL AS WET SOIL CONDITIONS

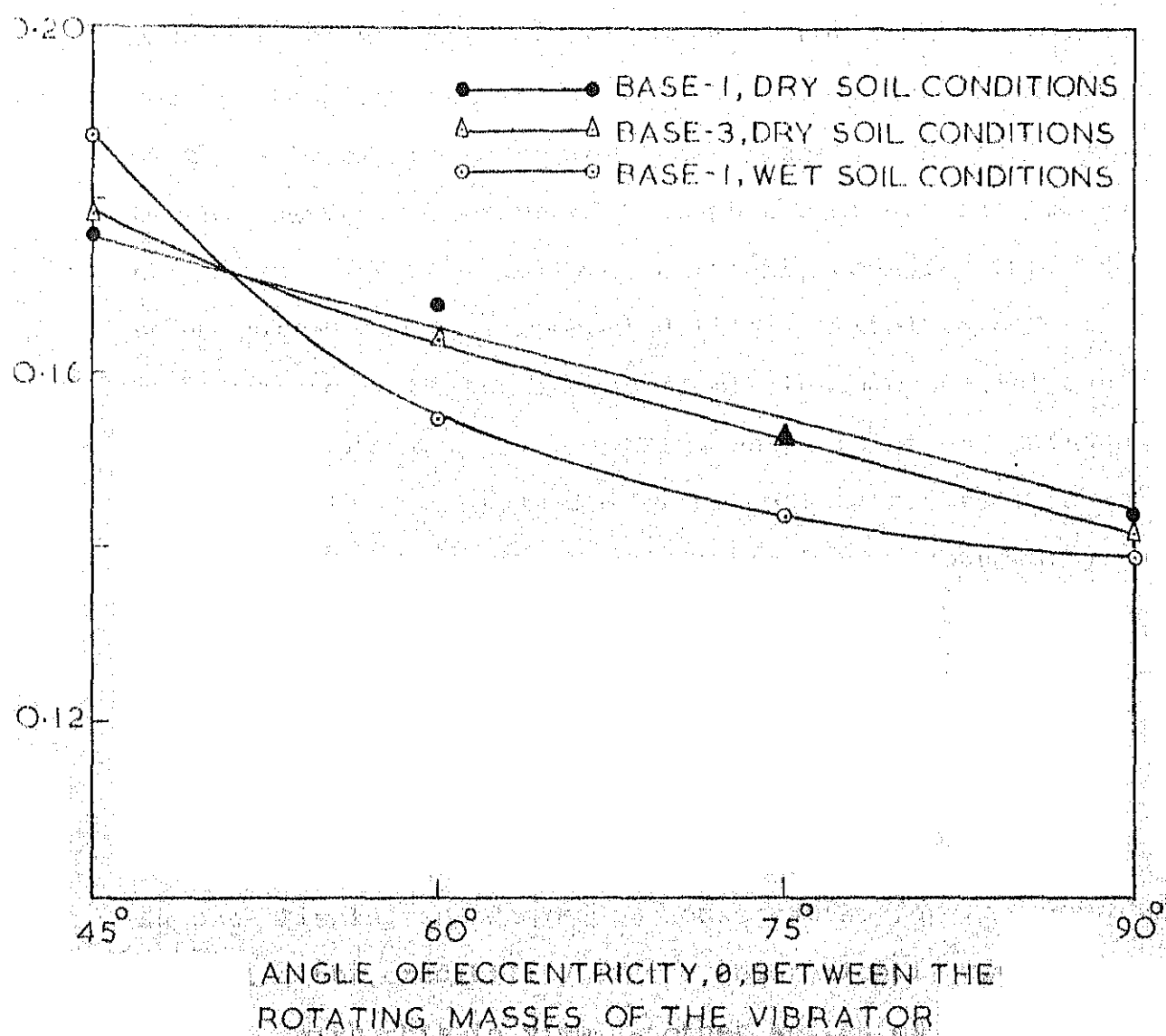


FIG. 5.10 DECREASE OF DAMPING FACTOR, D , WITH INCREASE OF DYNAMIC FORCE LEVELS, DURING DRY AS WELL AS WET SOIL CONDITIONS

CHAPTER 6

TESTS ON EMBEDDED FOOTINGS

6.1 GENERAL

One of the main assumptions of the existing theoretical models which attempt to describe the vibrations of foundation-soil systems is that the vibrating body rests on the surface of the soil or the so called 'half-space'. The real foundations, however, are founded beneath the ground surface so that they are either fully or partially embedded into the soil, surrounded by a compacted fill material in normal circumstances or by undisturbed soil in some special cases. The dynamic response of a footing which is either surrounded by a compacted fill material or by undisturbed soil is quite different from that of a footing which is surrounded by an air gap or resting on the natural surface of the soil. On many an occasion, the effect of embedment is ignored as the design calculations with respect to amplitudes of motion would err on the conservative side. However, a realistic assessment of the effect of embedment, may, at least, help in establishing the degree of conservatism involved besides enhancing the credibility of the theoretically predicted values. With this in view, another series of steady-state vibration tests were conducted to determine the effect of embedment on the vibration characteristics of massive concrete

footings founded below the ground surface. The results of these experiments are discussed in the following sections.

6.2 PRESENTATION OF RESULTS

The effect of embedment was studied on Base-2, 3 and 4 by the backfilling of well graded sand into the respective pits in layers of specified depths. Each layer of sand was compacted to the same density by vigorous tamping, followed by vibratory compaction. The steady-state tests, in the vertical mode of vibration, were then conducted on each of the bases in the manner described in Section 3.3.4. Each of the bases was tested, for different depths of embedment in compacted fill, at four different exciting force levels corresponding to 30, 35, 40 and 45 degrees in terms of phase angle between the eccentric weights of the vibrator. The observed dynamic responses of each of the footings for various heights of the compacted fill material, in terms of frequency-displacement spectras, are illustrated in Figures 6.1 through 6.15.

In general, backfilling which in other words amounts to embedment of the footing, resulted in the decrease of resonant amplitudes of motion and increased the resonant frequencies. This trend can be clearly seen from the frequency-displacement curves illustrated in Figures 6.13,

6.14 and 6.15. For convenience of interpretation, the observed experimental results are presented in the form of dimensionless factors. The height of the backfill is expressed in terms of an embedment factor, H/r_0 which is the ratio of the depth of embedment, H , to the radius, r_0 of the footing. The reduction in amplitudes of displacement at resonance is expressed in terms of an amplitude reduction factor, $X_{or,h} / X_{or}$ which is the ratio of the amplitude of displacement of the embedded footing, $X_{or,h}$ to the amplitude of displacement, X_{or} of the footing which is not embedded. The increase in resonant frequency is expressed in terms of a frequency-increase factor, $\omega_{r,h} / \omega_r$ which is the ratio of the resonant frequency, $\omega_{r,h}$ of the embedded footing to the resonant frequency, ω_r of the footing which is not embedded.

The field test results are illustrated in Figures 6.16 and 6.17 where the amplitude reduction factors and the frequency-increase factors are plotted against the embedment factor. It can be seen from Figure 6.16 that the rate of decrease in the maximum amplitudes with the depth of embedment becomes smaller as the depth of embedment is increased. The results of some field investigations of similar nature, but on different types of soils, have been reported by Barkan (6), Fry (16) and Novak (45). Some of the numerical data published by Novak (45) and Fry (16) are also indicated

in Figures 6.16 and 6.17.

The results show that the mass ratio, b , of the footing plays an important part at large embedment factors. It is of interest to note here that Chae (10) who conducted a laboratory investigation of embedded footing using an electro-magnetic type of oscillator, producing a sinusoidal force of constant amplitudes, concluded that the amplitude reduction factor is independent of the mass ratio. The error involved in such an inference may be insignificant for small embedment factors. However, the effect of mass ratio, b , becomes more pronounced for larger embedment factors as is evident from Figure 6.16.

Similarly, the increase in the observed resonant frequency of the system is shown by a plot of frequency-increase factor against the embedment factor in Figure 6.17. Numerical data published by Fry (16) and Novak (45) are also indicated in the same figure. The increase of resonant frequency with embedment is quite significant. It is, however, important to note that rotating-eccentric-mass type of oscillators were used to obtain the field test data plotted in Figure 6.17.

Chae (10) who employed a constant force type of excitation, observed that the changes in the resonant frequencies were insignificant with the depth of embedment

of the footings. A similar investigation, employing constant force type of excitation, was conducted by Jain (32) on small concrete footings embedded in sand wherein a decrease of resonant frequencies with increase in the depth of embedment has been reported.

Therefore, it can be concluded that the maximum amplitudes decrease with embedment irrespective of the type of excitation. However, the increase or the decrease in the resonant frequencies with embedment depends on the type of excitation.

6.3 ANALYSIS OF TEST RESULTS

An attempt was made to analyse the data obtained from tests on embedded footings by means of the single-degree-of-freedom lumped mass-spring-dashpot model as described in Section 5.2.2. The lumped parameters viz., the spring constant, K and the damping factor, D were calculated from each of the response curves obtained for various depths of embedment. In all the calculations, the mass associated with the vibrations of the embedded footing was assumed to be same as that of the footing which was not embedded. Such an analysis of each response curve, obviously, yields different values of the spring constant, K and the damping factor, D for every change in the depth of embedment. Though broad conclusions cannot be drawn from these numerical

quantities, the results, however, describe qualitatively the trend in the variation of the lumped parameters. For instance, both the spring constant, K and the damping factor, D have been found to increase, rather irregularly in the case of K , with the depth of embedment as shown in Figure 6.18 and Figure 6.19. The variation of the spring constant, K with embedment was expressed in terms of a stiffness-increase factor, K_h/K which is the ratio of the spring constant, K_h of the embedded footing to the spring constant, K of the footing which is not embedded. Similarly, the variation of the observed viscous damping factor, D was expressed in terms of a damping-increase ratio, D_h/D which is the ratio of the viscous damping factor, D_h of the embedded footing to the damping factor, D of the footing which is not embedded. The stiffness and damping-increase factors, as obtained from an analysis of observed frequency-displacement curves, are plotted against embedment factors and are illustrated in Figure 6.18 and Figure 6.19. The numerical results are tabulated in Table 6.1.

Kaldjian (34) demonstrated the increase of static spring constant with embedment by finite element idealisation of the soil media. Results reported by Kaldjian (34) are also plotted in Figure 6.18 to examine the extent of

correlation of observed data with those of the theoretically indicated values. The scatter of data at low embedment factors is too much to draw any conclusion. The increase in the observed stiffness factor at embedment factors greater than 0.8 is well defined. However, the theoretical curve and the experimentally obtained curve diverge with increasing embedment factors.

This raises some serious doubts as to the utility of single-degree-of-freedom mass-spring-dashpot model in either analysing or predicting the response of an embedded footing. As discussed earlier, the magnitude of uncertainties involved in actual practice, even in the absence of embedment, is too much for the single-degree-of-freedom mass-spring-dashpot model to explain. In view of all these practical difficulties, a separate parameter which can describe the effects of embedment in an independent manner is very desirable.

6.4 DISCUSSION ON TEST RESULTS

As mentioned previously the embedment of a footing resulted in the reduction of the amplitude of motion at resonant peaks and increased the resonant frequencies. However, it should be noted that rotating mass type of vibrators were used in all the field investigations from where the above observations were noticed. Barkan (6)

presented examples in which embedment of footings decreased the vertical motions at resonance considerably. In one particular case a footing with a base area of 1.0 m^2 placed on silty clays, registered an amplitude reduction factor of 0.3 due to the backfilling of the foundation excavations to a depth of 2 m. Barkan (6) attributed this aspect of the steady-state vibrations of an embedded footing to an increase in the effective damping force. Richart, Hall and Woods (55) attributed the same phenomena to an increase in the effective spring constant as well as a probable increase in the effective damping force. The reduction in motion of an embedded foundation was attributed by Chae (10) to the additional shear resistance along sides of the footing and to a shift in the contact pressure distribution caused by the surcharge around the footing. Chae (10) suggested that the effect of embedment should be evaluated in terms of embedment depth (or the amount of surcharge), the weight and size of the footing. McNeill (44) thought that the effect of embedment was to increase the stiffness of the system. He attributed the increase of stiffness to three sources: 1) resistance to deformation due to the embedment; 2) side friction between the soil and the foundation; and 3) increased soil stiffness due to the confinement or overburden. McNeill (44) indicated that the first two effects could be estimated for vertical motions by the use of curves

developed by Kaldjian (34) and reproduced in Figure 6.18. McNeill (44) suggested that the effect of confinement or overburden could be taken into account in the laboratory testing programme by performing tests at a confining pressure equal to the average of the principal stresses in the design configuration. Novak (45) felt that the dynamic response of an embedded footing depended on the relative height of the backfilled material as well as the density of the fill material. He also thought that the foundation response very much depended on the quality and nature of the foundation contact with the surrounding soil.

The above discussion indicates how difficult it is to integrate the view points of each investigator into a rigorous mathematical theory like the elastic half-space theory. However, experimental evidence suggests that the physical characteristics of the interface between the sides of the footing and the surrounding fill material plays a major role in the complicated phenomena of vibrations of an embedded footing. It is also felt that any attempt at formulating a theoretical model should be such as to allow the study of embedment as an independent parameter. Such a flexible approach facilitates the study of the effects of several associated factors such as 1) different fill materials, 2) foundation sides with varying degrees of roughness,

3) foundation shapes allowing for various perimeter areas,
4) different intensities of surcharge etc. on the dynamic response of an embedded footing even while assuming that the base of the footing is resting on the surface of an elastic half-space. One such attempt is elucidated in Chapter 8.

TABLE 6.1 RESULTS OF ANALYSES OF EXPERIMENTAL FREQUENCY-
DISPLACEMENT CURVES FOR VARIOUS DEPTHS OF
EMBEDMENT.

Base-2 ; $\alpha = 1.21$							
$m_o e$ in lbs.- Sec ²	H/ r_o	Observed X_{or} in inches	Observed ω_r in radians per second	D	ω_n in radians per second	K lbs. per inch	Refer Fig. No.
(1)	(2)	(3)	(4)	(5)	(6)	(7)	(8)
0.0194	0.281	0.00215	305	0.340	267.0	1005483	6.1
	0.562	0.00205	316	0.359	271.8	1041341	6.2
	0.843	0.00190	325	0.394	270.0	1027612	6.3
	1.125	0.00180	350	0.421	281.0	1113176	6.4
0.0174	0.281	0.00190	305	0.346	265.6	994589	6.1
	0.462	0.001825	316	0.363	270.9	1034471	6.2
	0.843	0.001675	325	0.402	267.2	1006972	6.3
	1.125	0.00160	350	0.426	279.1	1098113	6.5
0.0152	0.281	0.001675	316	0.342	276.1	1074686	6.1
	0.562	0.00160	316	0.361	271.3	1037591	6.2
	0.843	0.00145	338	0.407	276.0	1074435	6.3
	1.125	0.00140	367	0.425	293.5	1214205	6.4

Contd.....

Table 6.1 contd....

(1)	(2)	(3)	(4)	(5)	(6)	(7)	(8)
0.0131	0.281	0.00145	316	0.341	276.5	1078035	6.1
	0.562	0.00140	325	0.355	281.1	1114031	6.2
	0.843	0.00125	338	0.407	276.1	1074784	6.3
	1.125	0.00120	367	0.428	292.3	1204444	6.4
Base-2 ; $\alpha = 1.00$							
0.0194	0.281	0.00215	305	0.428	242.3	684150	6.1
	0.562	0.00205	316	0.456	241.1	677310	6.2
	0.843	0.00190	325	0.509	225.7	593488	6.3
	1.125	0.00180	350	0.556	215.8	542826	6.4
0.0174	0.281	0.00190	305	0.437	239.5	668036	6.1
	0.562	0.001825	316	0.461	238.2	666699	6.2
	0.843	0.001675	325	0.523	218.6	556938	6.3
	1.125	0.00160	350	0.566	209.5	511226	6.4
0.0152	0.281	0.001675	316	0.432	249.9	727536	6.1
	0.562	0.00160	316	0.459	240.1	671530	6.2
	0.843	0.00145	338	0.531	222.9	579127	6.3
	1.125	0.00140	367	0.564	221.2	570149	6.4

Contd.....

Table 6.1 contd..

(1)	(2)	(3)	(4)	(5)	(6)	(7)	(8)
0.0131	0.281	0.00145	316	0.429	250.7	732474	6.1
	0.562	0.00140	325	0.450	250.8	733013	6.2
	0.843	0.00125	338	0.531	223.1	579775	6.3
	1.125	0.00120	367	0.570	217.1	549054	6.4
Base-3 ; $\alpha = 1.09$							
0.0194	0.667	0.00330	261	0.238	246.0	768434	6.5
	1.334	0.00290	282	0.274	260.6	862313	6.6
	2.000	0.00245	303	0.330	268.0	911951	6.7
	2.668	0.00220	315	0.374	267.0	905156	6.8
0.0174	0.667	0.00295	261	0.239	245.8	767628	6.5
	1.334	0.00250	282	0.286	258.5	848383	6.6
	2.000	0.00220	303	0.330	268.0	912330	6.7
	2.668	0.00195	315	0.380	265.4	894587	6.8
0.0152	0.667	0.00255	261	0.242	245.5	765377	6.5
	1.334	0.00215	287	0.291	261.9	870894	6.6
	2.000	0.00190	303	0.334	267.0	905624	6.7
	2.668	0.00170	325	0.381	273.6	950750	6.8

Contd.....

Table 6.1 contd....

(1)	(2)	(3)	(4)	(5)	(6)	(7)	(8)
0.0131	0.667	0.00220	261	0.241	245.5	765603	6.5
	1.334	0.00190	294	0.283	269.0	919312	6.6
	2.000	0.00165	303	0.331	267.7	910109	6.7
	2.668	0.00150	325	0.370	276.6	971981	6.8
Base-3 ; $\alpha = 1.00$							
0.0194	0.667	0.00330	261	0.261	242.7	686581	6.5
	1.334	0.00290	282	0.301	255.7	761914	6.6
	2.000	0.00245	303	0.365	259.6	784933	6.7
	2.668	0.00220	315	0.416	254.4	754166	6.8
0.0174	0.667	0.00295	261	0.262	242.6	685680	6.5
	1.334	0.00250	282	0.315	253.1	746111	6.6
	2.000	0.00220	303	0.364	259.6	785374	6.7
	2.668	0.00195	315	0.422	252.3	741448	6.8
0.0152	0.667	0.00255	261	0.265	242.2	683158	6.5
	1.334	0.00215	287	0.320	256.1	764355	6.6
	2.000	0.00190	303	0.369	258.3	777573	6.7
	2.668	0.00170	325	0.424	259.9	787283	6.8

Contd.....

Table 6.1 contd...

(1)	(2)	(3)	(4)	(5)	(6)	(7)	(8)
0.0131	0.667	0.00220	261	0.241	245.5	765603	6.5
	1.334	0.00190	294	0.283	269.0	919312	6.6
	2.000	0.00165	303	0.331	267.7	910109	6.7
	2.668	0.00150	325	0.370	276.6	971931	6.8
Base-3 ; $\alpha = 1.00$							
0.0194	0.667	0.00330	261	0.261	242.7	686581	6.5
	1.334	0.00290	282	0.301	255.7	761914	6.6
	2.000	0.00245	303	0.365	259.6	784933	6.7
	2.668	0.00220	315	0.416	254.4	754166	6.8
0.0174	0.667	0.00295	261	0.262	242.6	685680	6.5
	1.334	0.00250	282	0.315	253.1	746111	6.6
	2.000	0.00220	303	0.364	259.6	785374	6.7
	2.668	0.00195	315	0.422	252.3	741448	6.8
0.0152	0.667	0.00255	261	0.265	242.2	683158	6.5
	1.334	0.00215	287	0.320	256.1	764355	6.6
	2.000	0.00190	303	0.369	258.3	777573	6.7
	2.668	0.00170	325	0.424	259.9	787283	6.8

Contd.....

Table 6.1 contd...

(1)	(2)	(3)	(4)	(5)	(6)	(7)	(8)
0.0131	0.667	0.00220	261	0.265	242.2	683411	6.5
	1.334	0.00190	294	0.311	263.6	809431	6.6
	2.000	0.00165	303	0.366	259.2	782792	6.7
	2.668	0.00150	325	0.411	264.1	812795	6.8
Base-4 ; $\alpha = 1.21$							
0.0194	0.281	0.00195	305	0.381	256.5	927388	6.9
	0.562	0.00185	316	0.407	258.1	939250	6.10
	0.843	0.00175	325	0.437	255.6	921025	6.11
	1.125	0.00170	350	0.454	268.2	1014280	6.12
0.0174	0.281	0.00170	305	0.395	252.6	899662	6.9
	0.562	0.00165	316	0.410	257.1	932077	6.10
	0.843	0.001575	325	0.435	256.2	925353	6.11
	1.125	0.00150	350	0.464	263.7	980768	6.12
0.0152	0.281	0.00150	316	0.390	263.1	976361	6.9
	0.562	0.00142	325	0.418	254.6	913952	6.10
	0.843	0.00137	338	0.437	265.2	991431	6.11
	1.125	0.00130	367	0.470	274.6	1063595	6.12

Contd....

Table 6.1 contd...

(1)	(2)	(3)	(4)	(5)	(6)	(7)	(8)
0.0131	0.281	0.00130	316	0.387	263.9	982135	6.9
	0.562	0.00125	325	0.407	265.8	996289	6.10
	0.843	0.00120	338	0.428	268.5	1016791	6.11
	1.125	0.00115	367	0.453	282.0	1121520	6.12
Base-4 ; $\alpha = 1.00$							
0.0194	0.281	0.00195	305	0.489	219.8	563127	6.9
	0.562	0.00185	316	0.531	208.5	506506	6.10
	0.843	0.00175	325	0.588	180.6	380169	6.11
	1.125	0.00170	350	0.631	157.8	290281	6.12
0.0174	0.281	0.00170	305	0.511	210.5	516192	6.9
	0.562	0.00165	316	0.536	205.7	493077	6.10
	0.843	0.001575	325	0.584	183.1	390540	6.11
	1.125	0.00150	350	0.674	106.4	131924	6.12
0.0152	0.281	0.00150	316	0.503	221.6	572398	6.9
	0.562	0.00142	325	0.550	198.2	457894	6.10
	0.843	0.00137	338	0.589	186.4	404862	6.11
	1.125	0.00130	367	-	-	-	6.12

Contd.....

Table 6.1 contd...

(1)	(2)	(3)	(4)	(5)	(6)	(7)	(8)
0.0131	0.281	0.00130	316	0.499	223.5	582190	6.9
	0.562	0.00125	325	0.531	214.8	537432	6.10
	0.843	0.00120	338	0.570	199.5	463511	6.11
	1.125	0.00115	367	0.629	168.2	329517	6.12

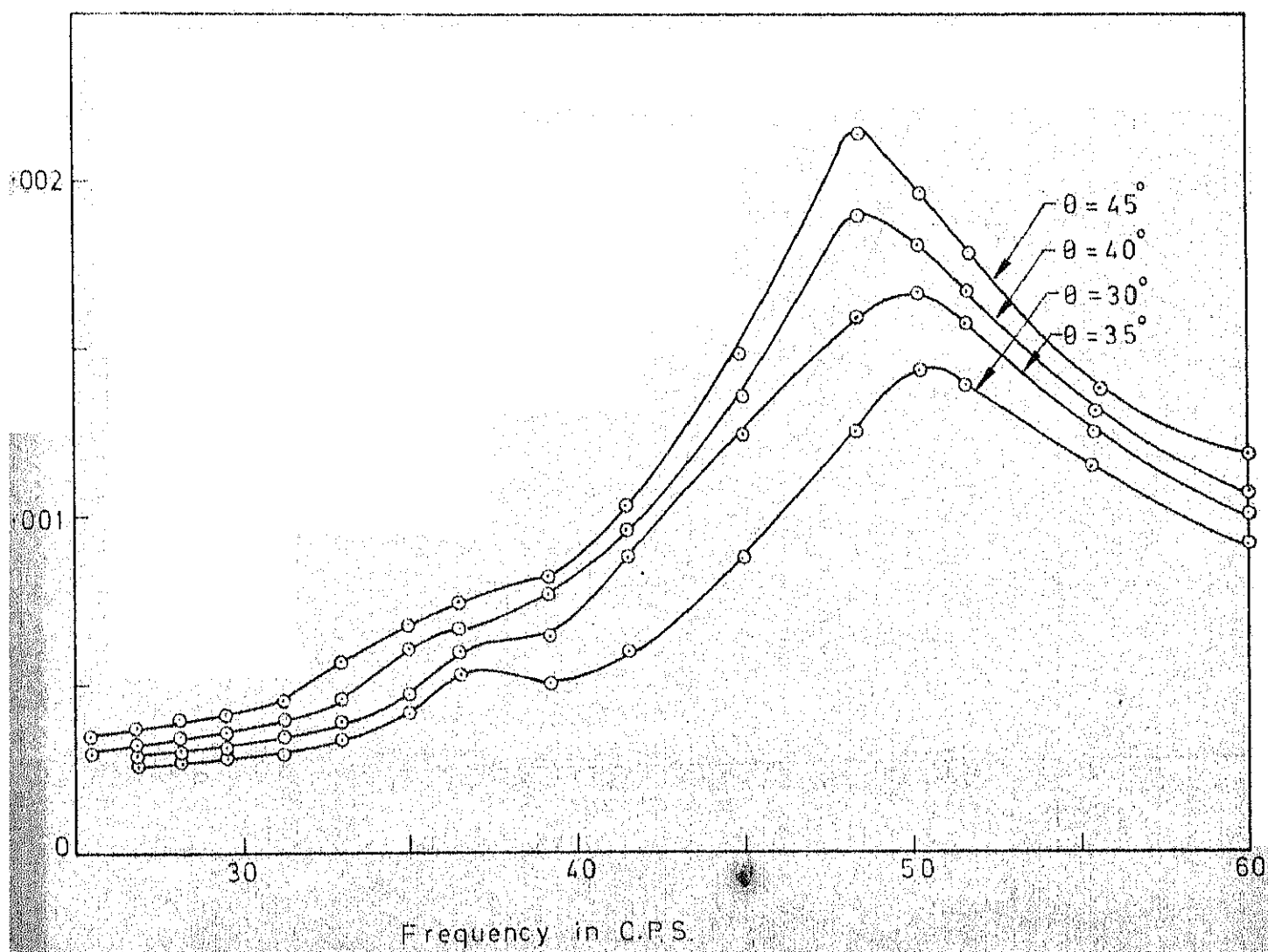


FIG. 6.1 FREQUENCY VS. DISPLACEMENT, BASE-2, BACKFILLED BY SAND 6 ³/₄ DEEP

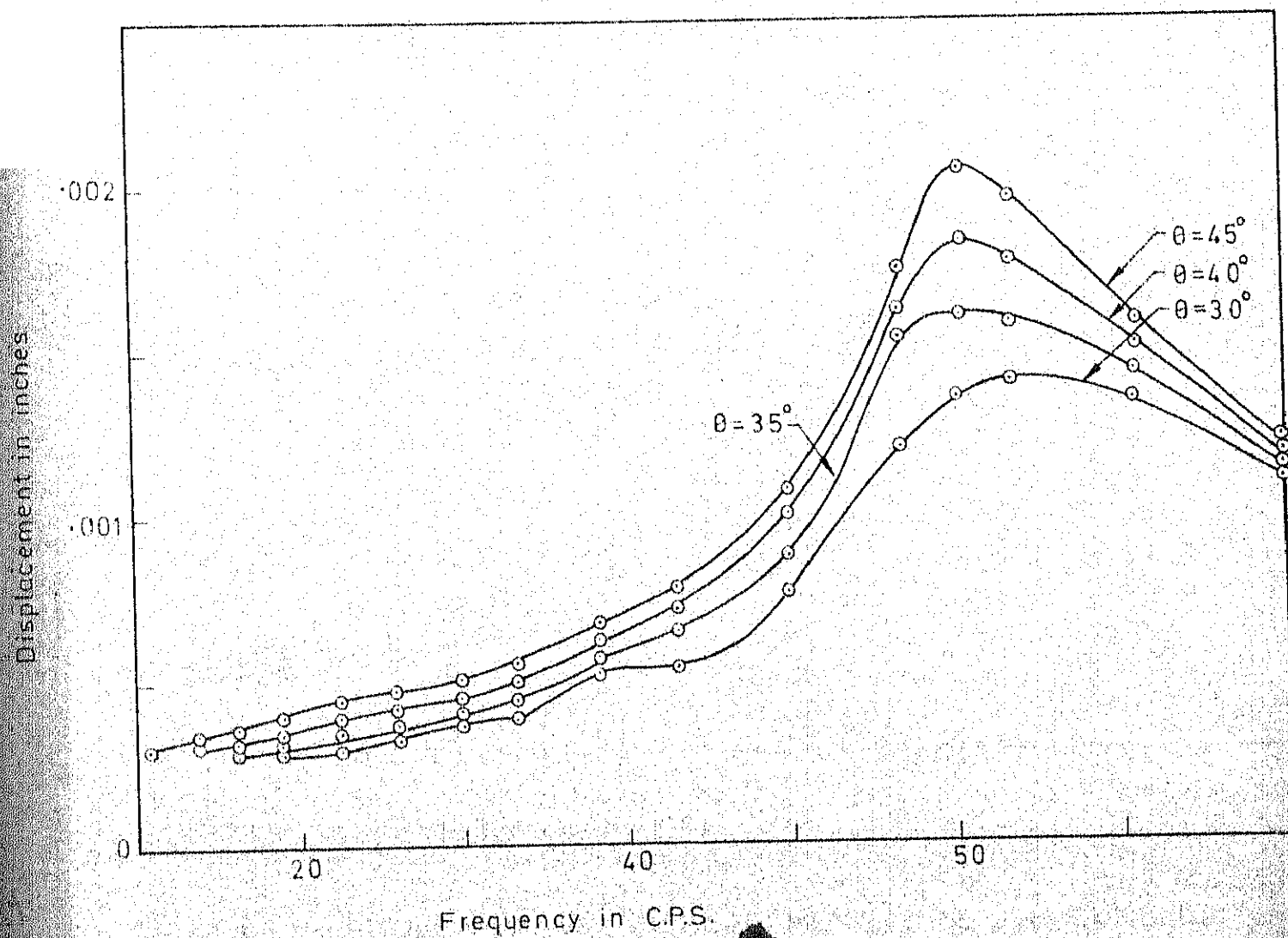


FIG. 6.2 FREQUENCY VS. DISPLACEMENT, BASE-2, BACKFILLED BY SAND, $1\frac{3}{2}$ " DEEP

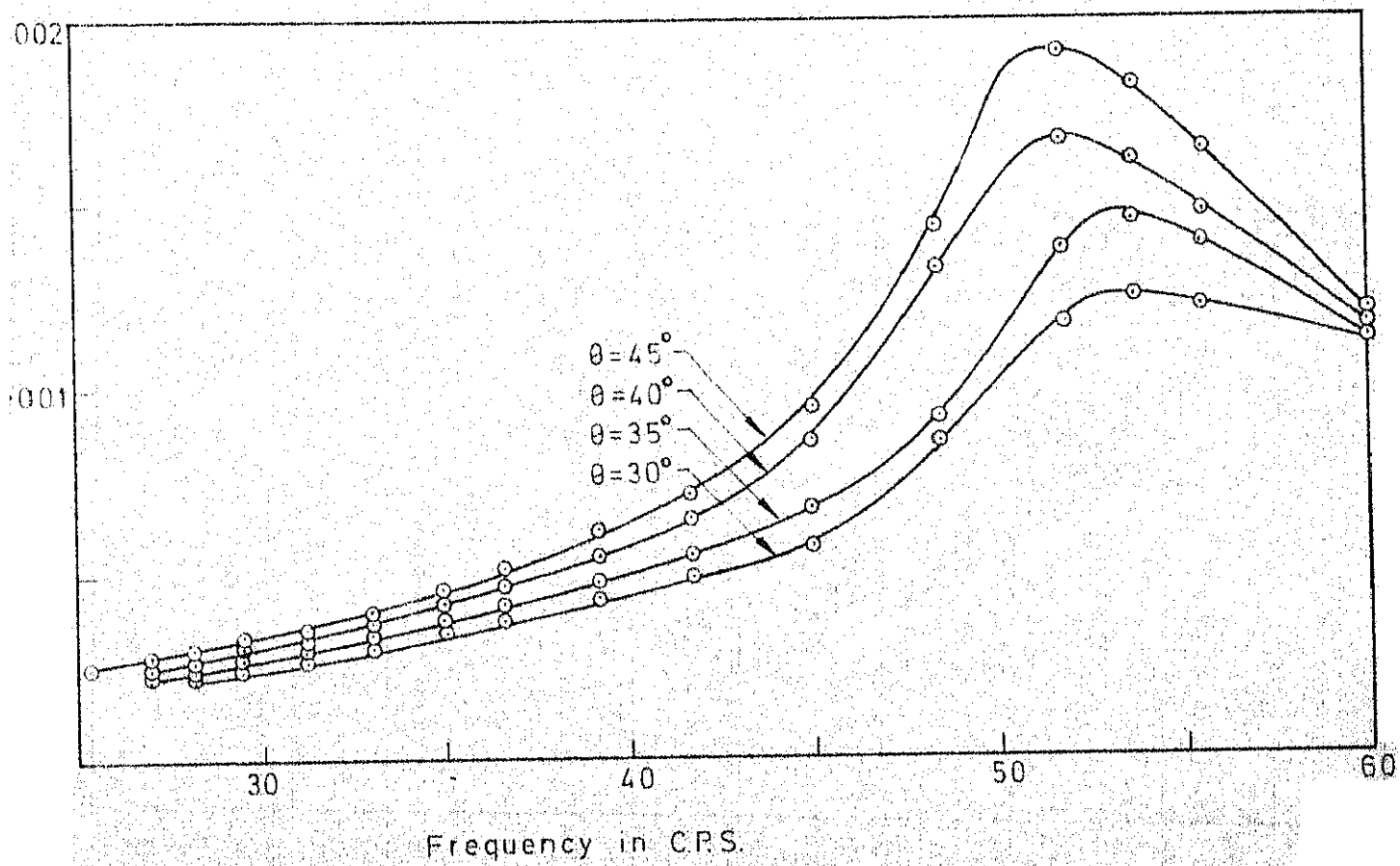


FIG. 6.3 FREQUENCY VS DISPLACEMENT, BASE-2, BACKFILLED BY SAND, 20 1/4" DEEP

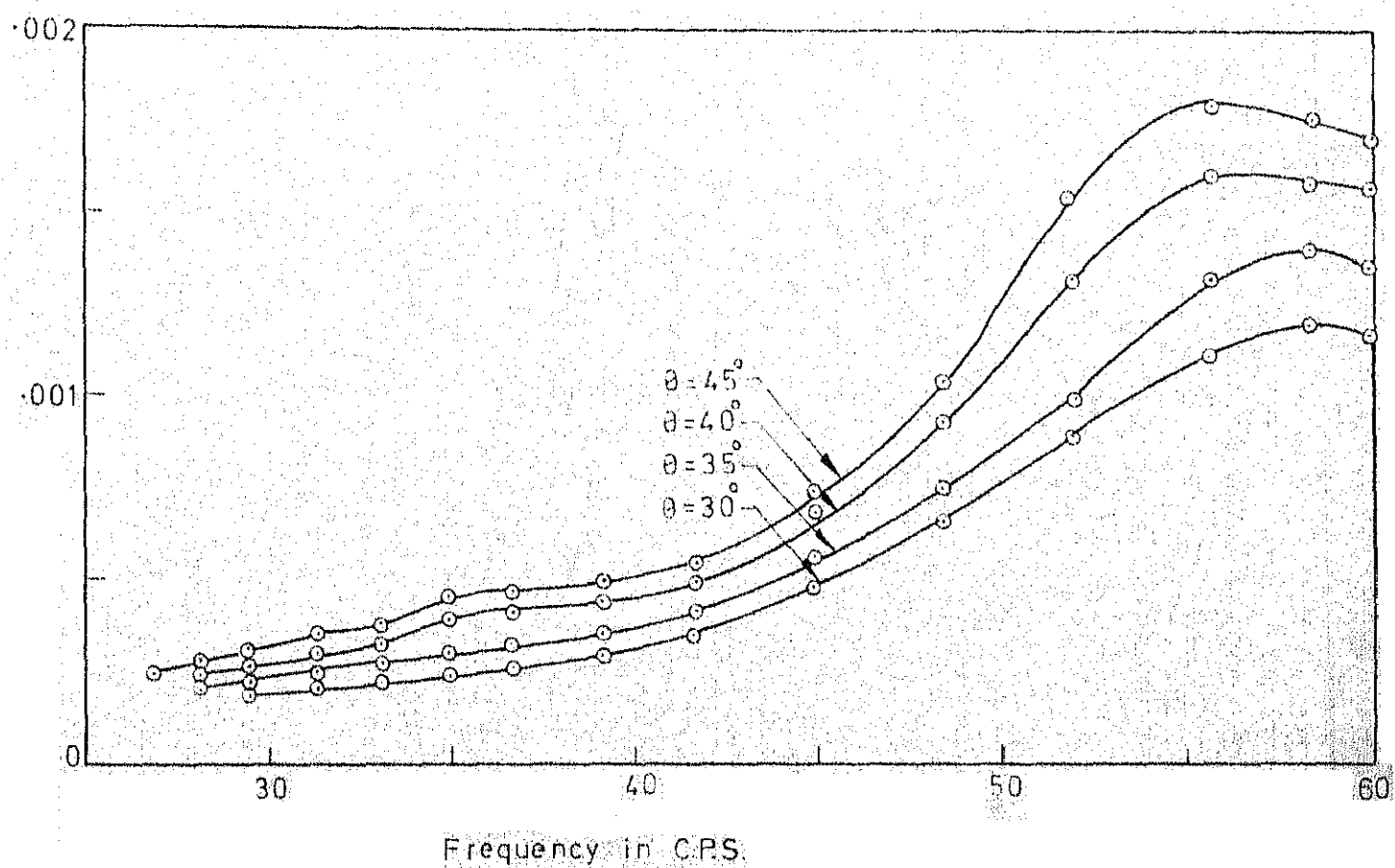


FIG. 6.4 FREQUENCY VS DISPLACEMENT, BASE-2, BACKFILLED BY SAND 27' DEEP

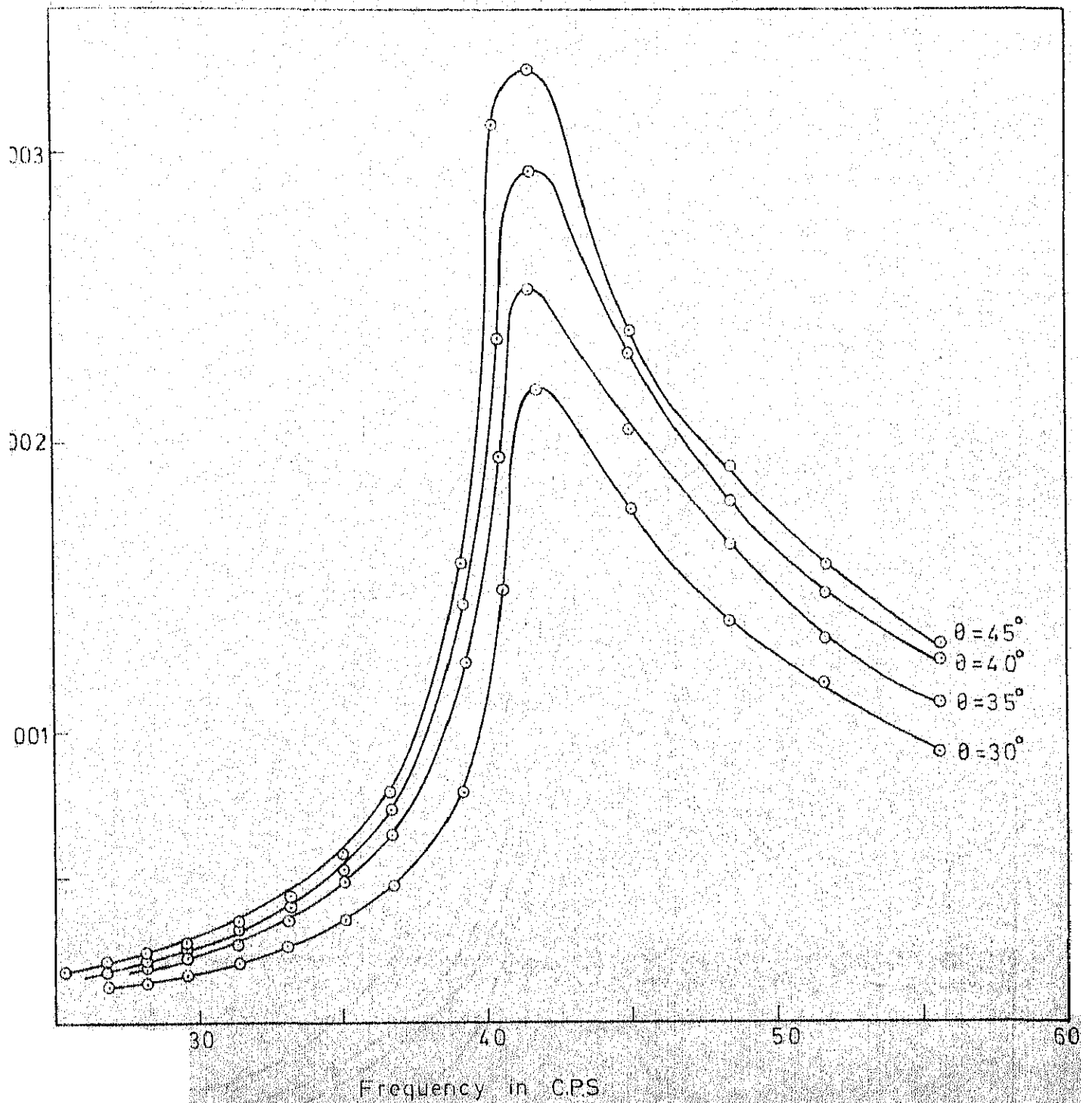


FIG. 6.5 FREQUENCY VS DISPLACEMENT, BASE-3, BACKFILLED BY SAND 1 DEEP

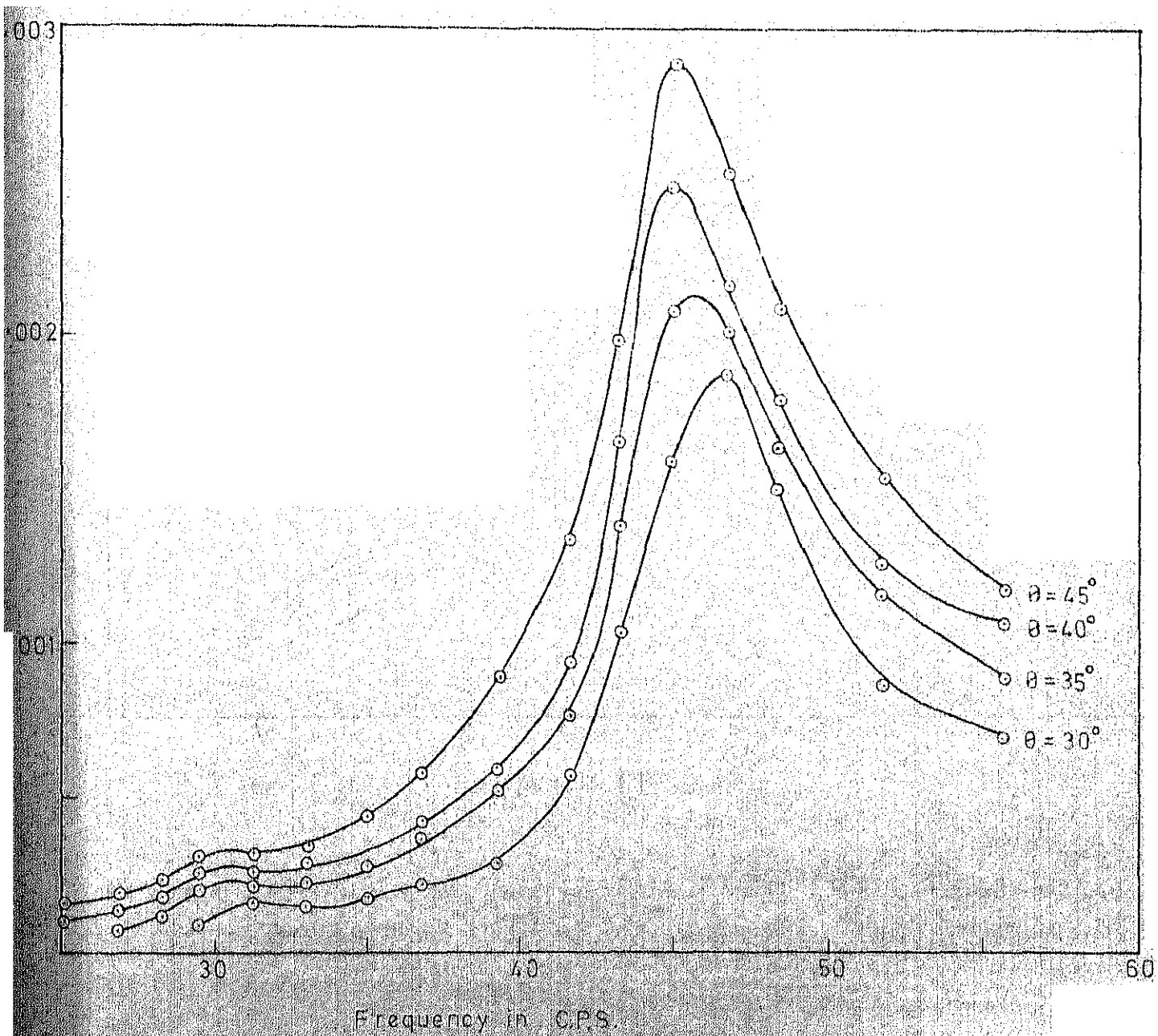


FIG. 6.6 FREQUENCY VS DISPLACEMENT, BASE-3, BACKFILLED BY SAND, 2 DEEP

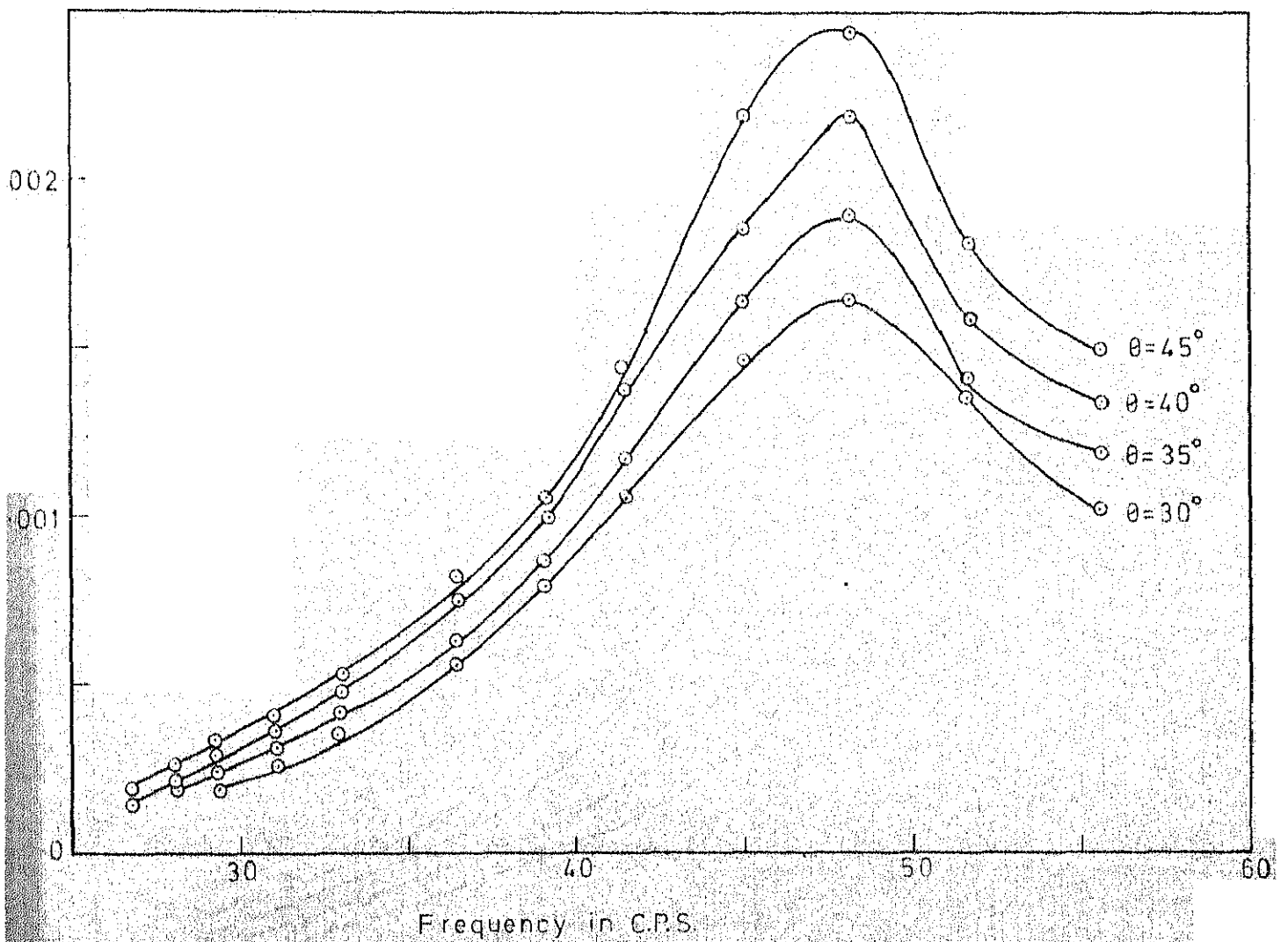


FIG. 6.7 FREQUENCY VS. DISPLACEMENT, BASE-3, BACKFILLED BY SAND, 3' DEEP

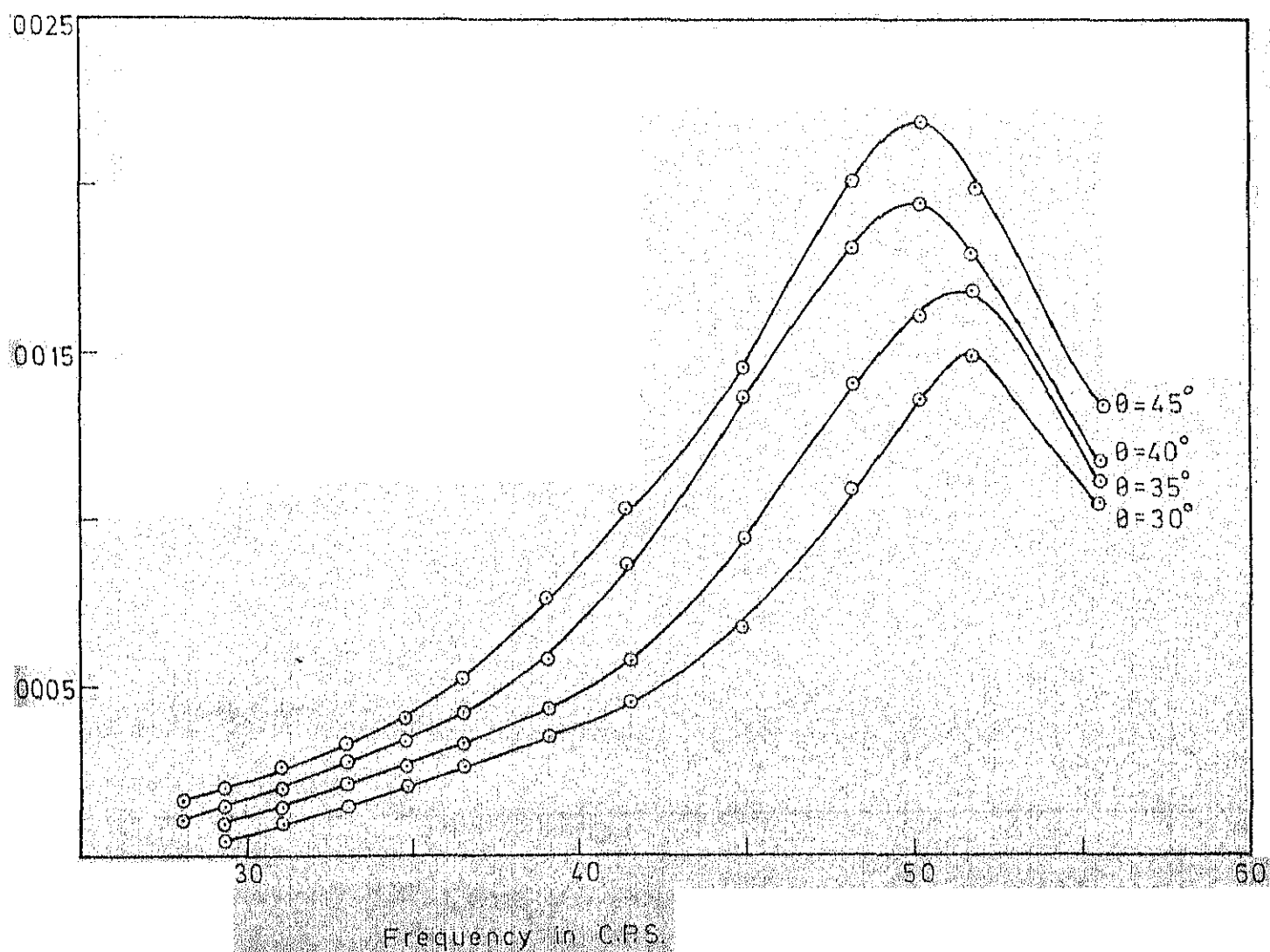


FIG. 6.8 FREQUENCY VS. DISPLACEMENT, BASE-3, BACKFILLED BY SAND, 4' DEEP

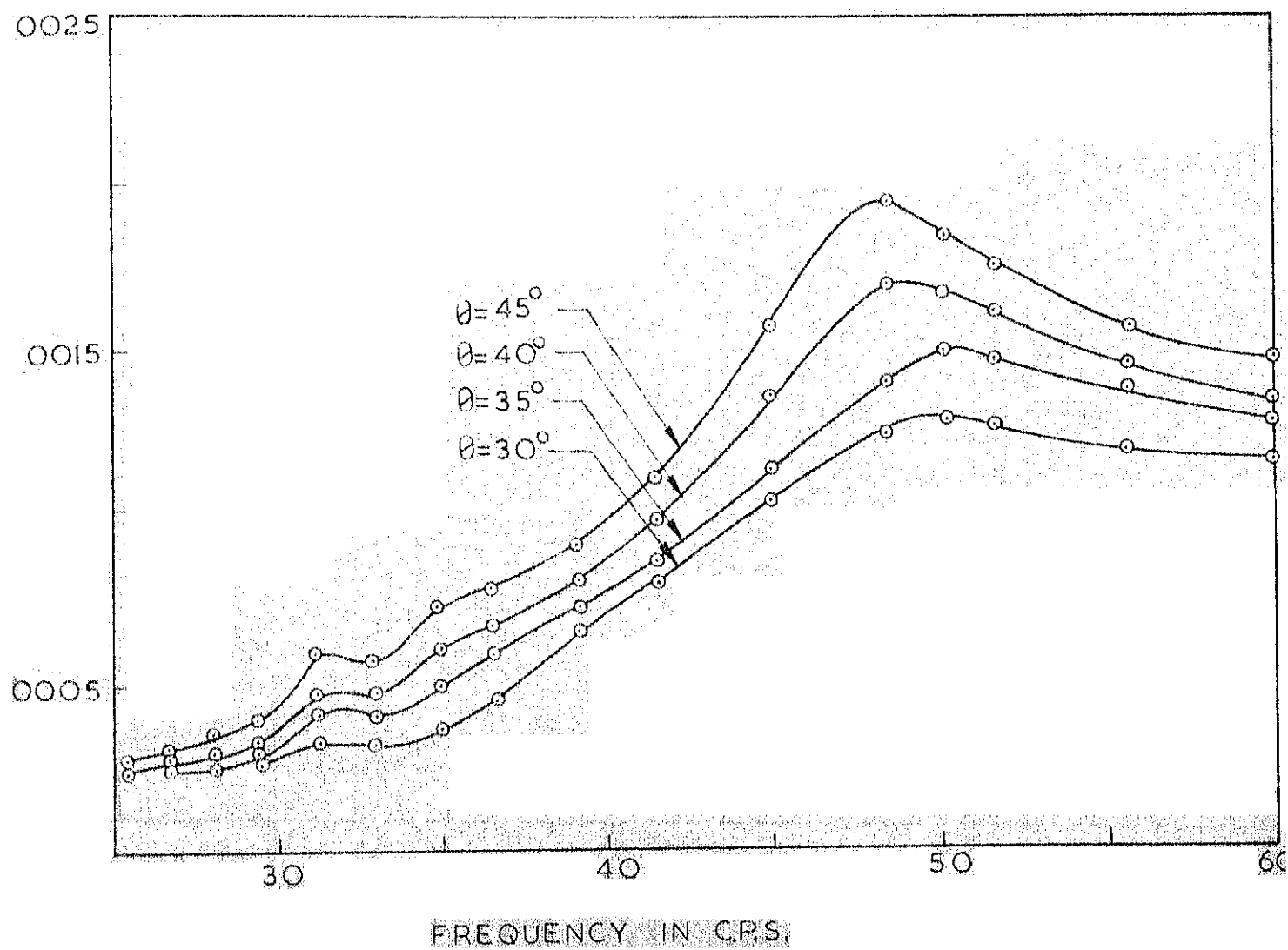


FIG. 6.9 FREQUENCY VS. DISPLACEMENT, BASE-4, BACKFILLED BY SAND-6^{3/4}' DEEP.

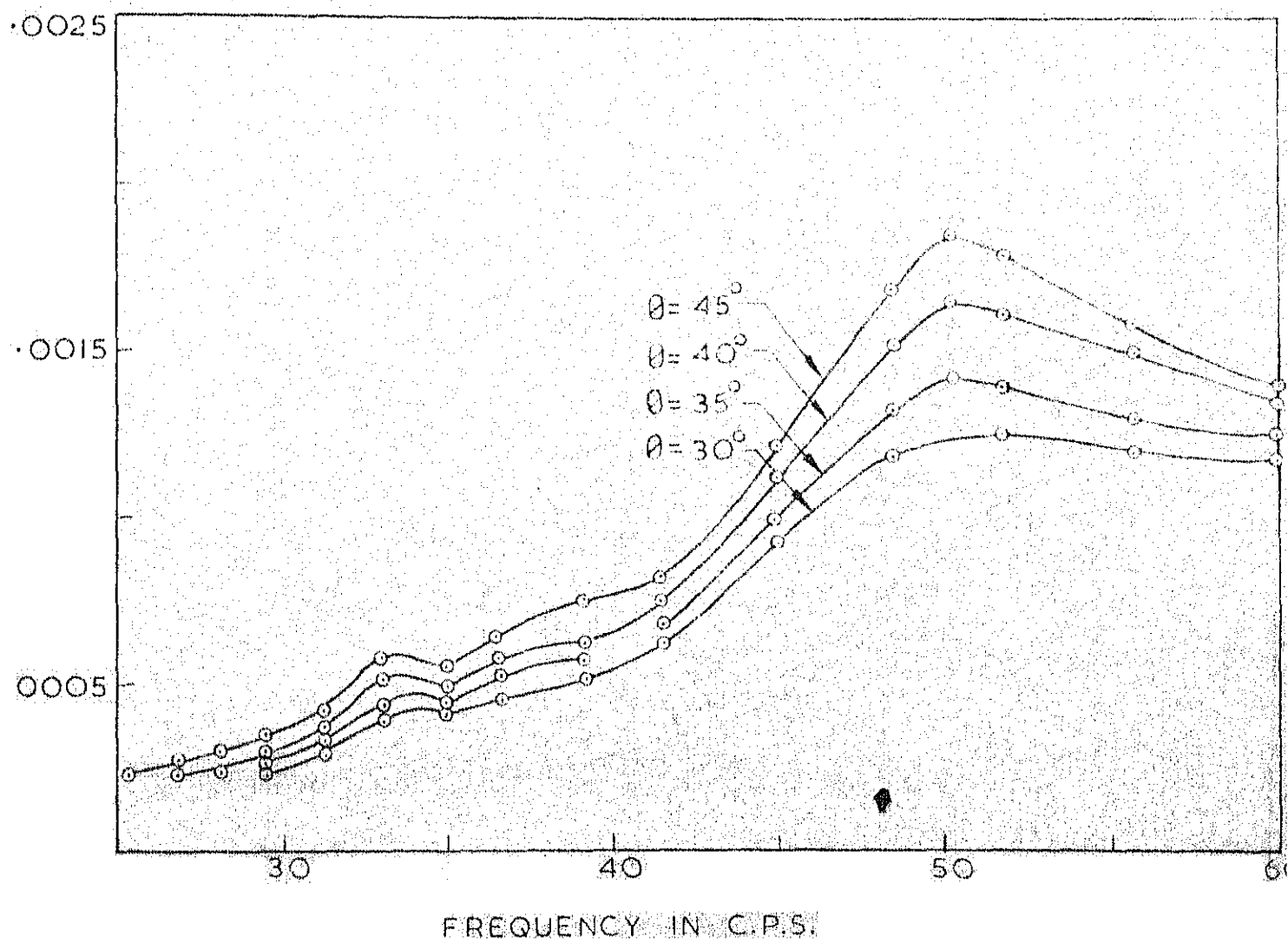


FIG. 6.10 FREQUENCY VS. DISPLACEMENT, BASE-4, BACKFILLED BY SAND- $13\frac{1}{2}$ DEEP.

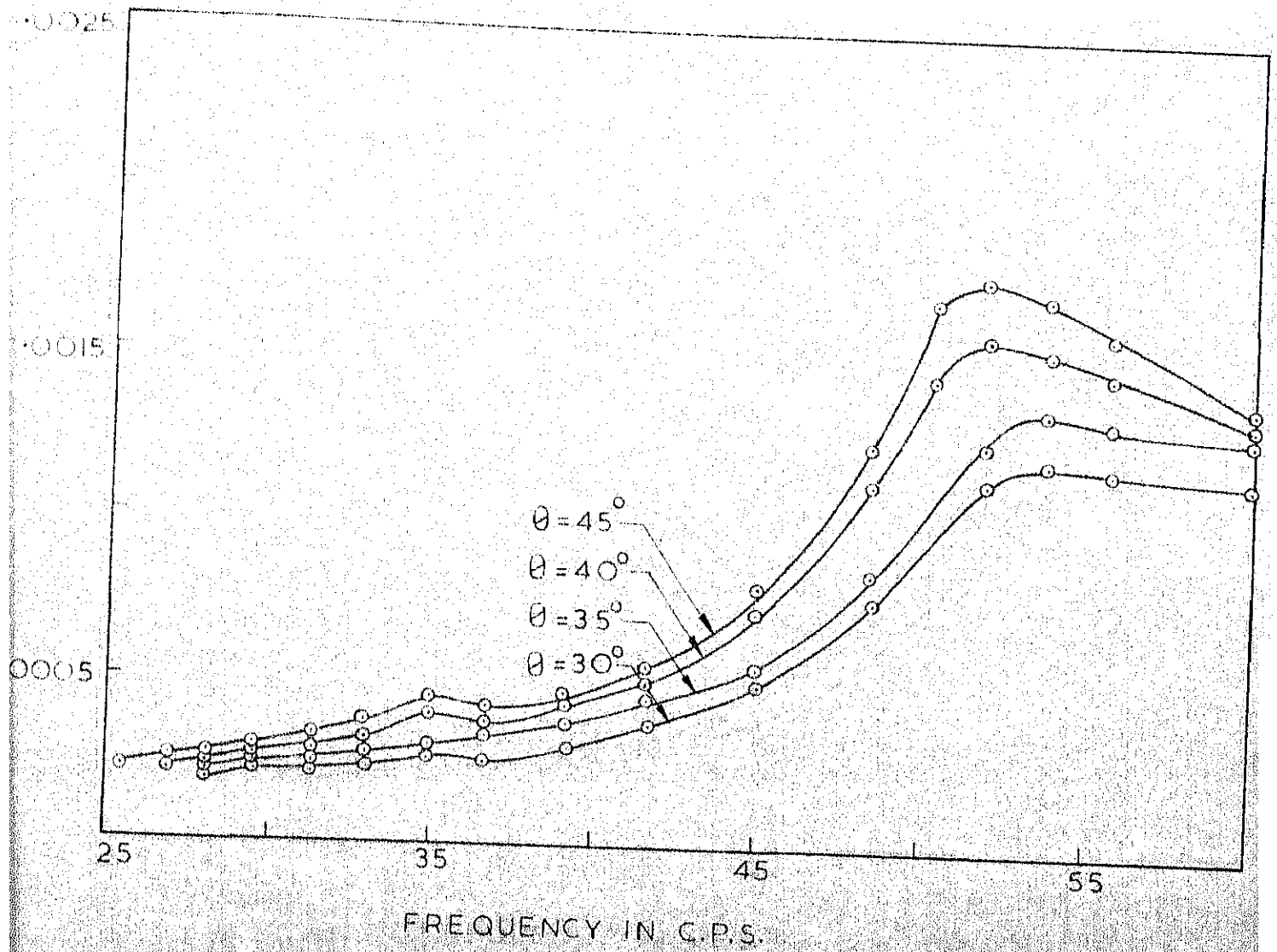


FIG. 6.11 FREQUENCY VS. DISPLACEMENT, BASE-4, BACKFILLED BY SAND-20 1/4" DEEP.

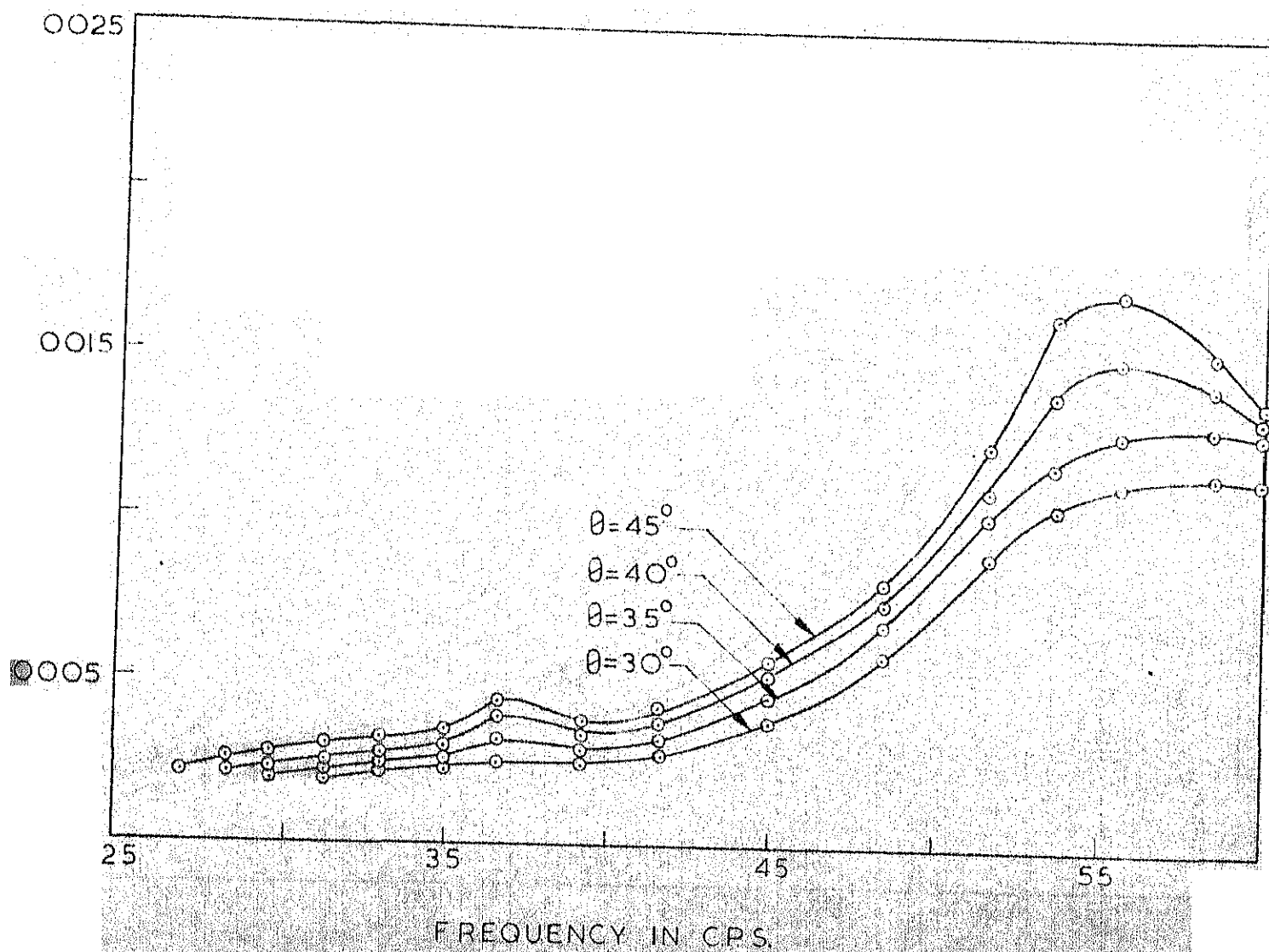


FIG. 6.12 FREQUENCY VS DISPLACEMENT, BASE-4, BACKFILLED BY SAND-27' DEEP.

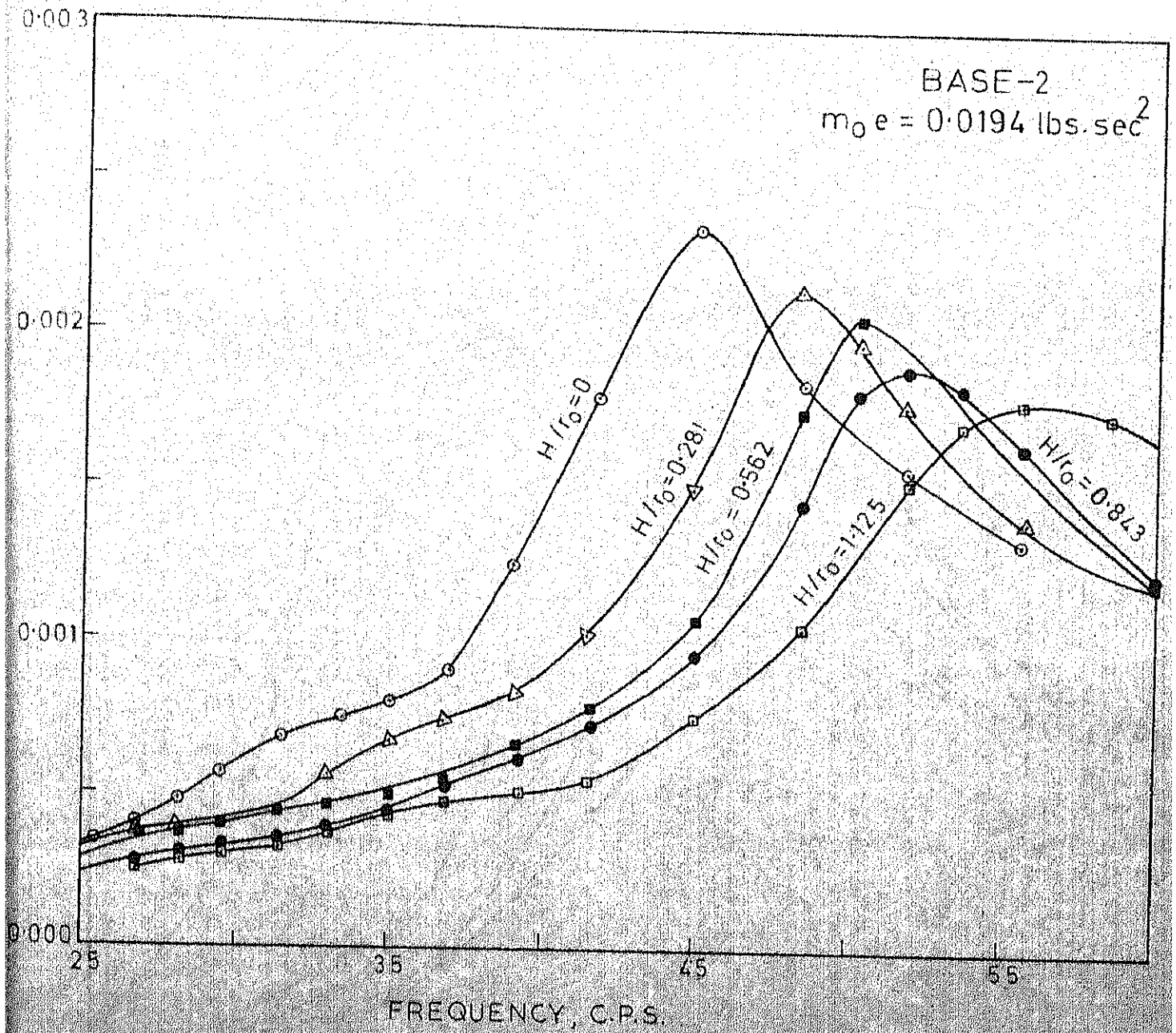


FIG. 6.13 COMPARISON OF RESPONSE CURVES FOR BASE-2 WITH DIFFERENT EMBEDMENT FACTORS.

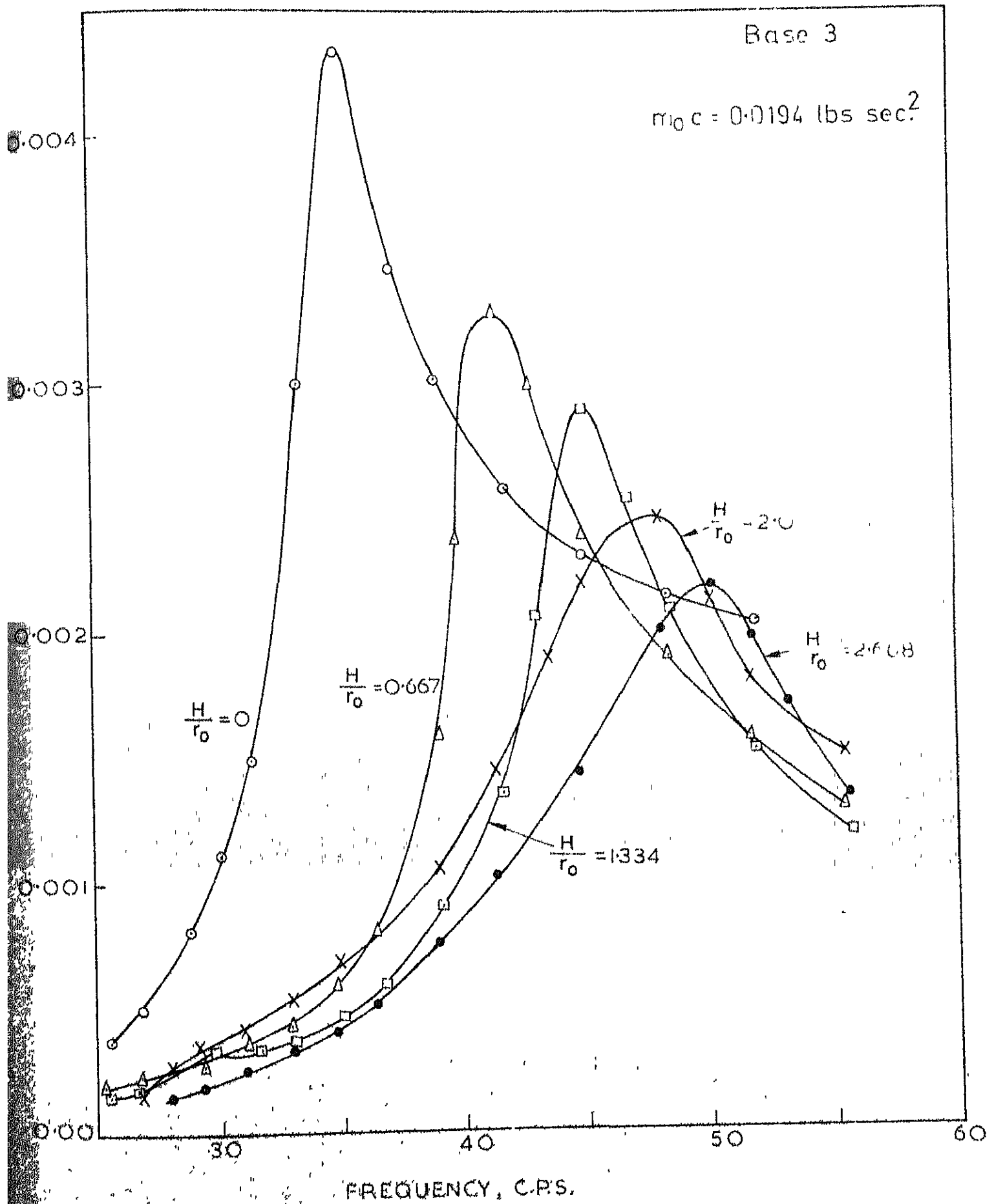


FIG. 6.14 COMPARISON OF RESPONSE CURVES FOR BASE-3 WITH DIFFERENT EMBEDMENT FACTORS.

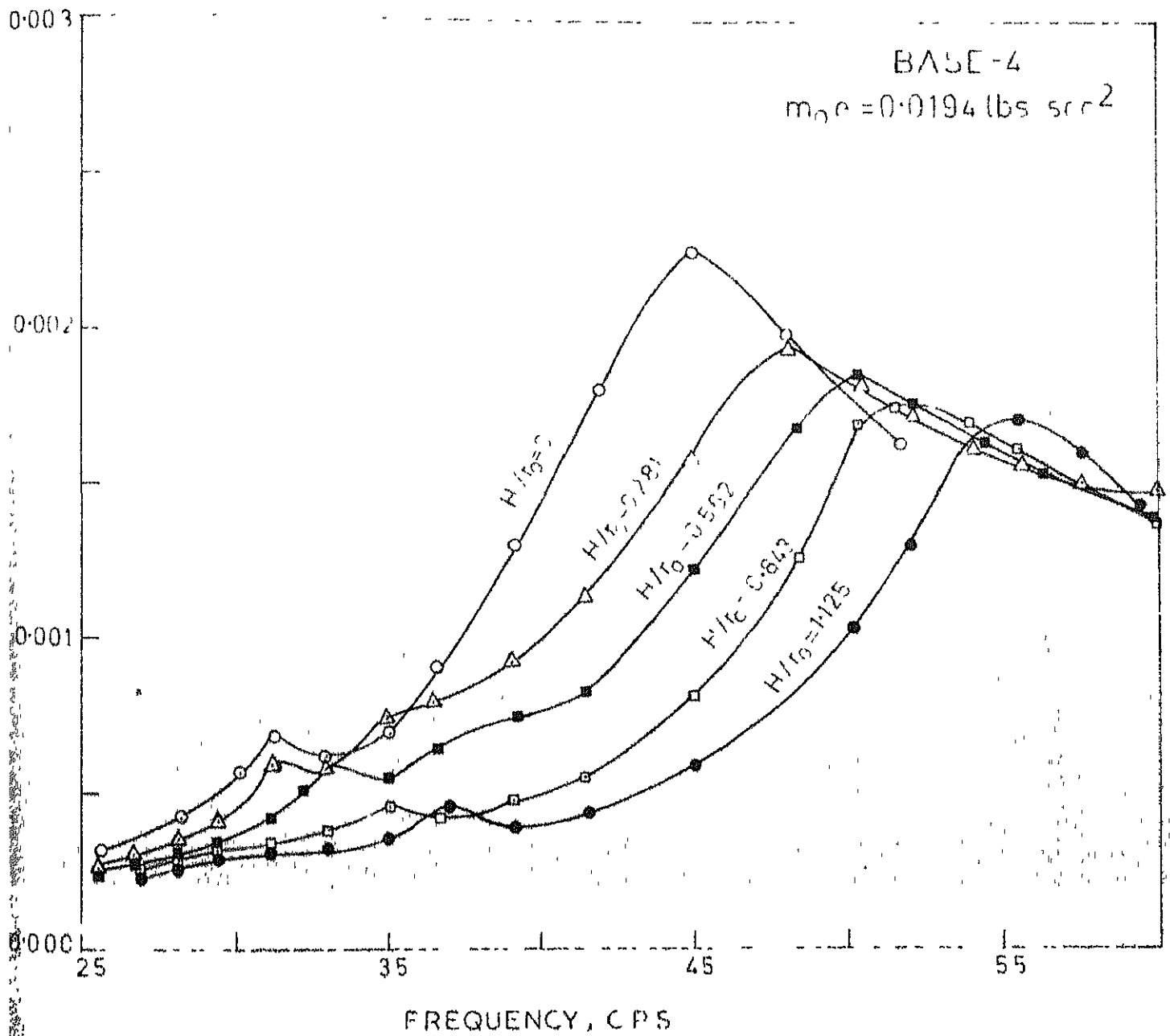


FIG. 6.15 COMPARISON OF RESPONSE CURVES FOR BASE-4 WITH DIFFERENT EMBEDMENT FACTORS.

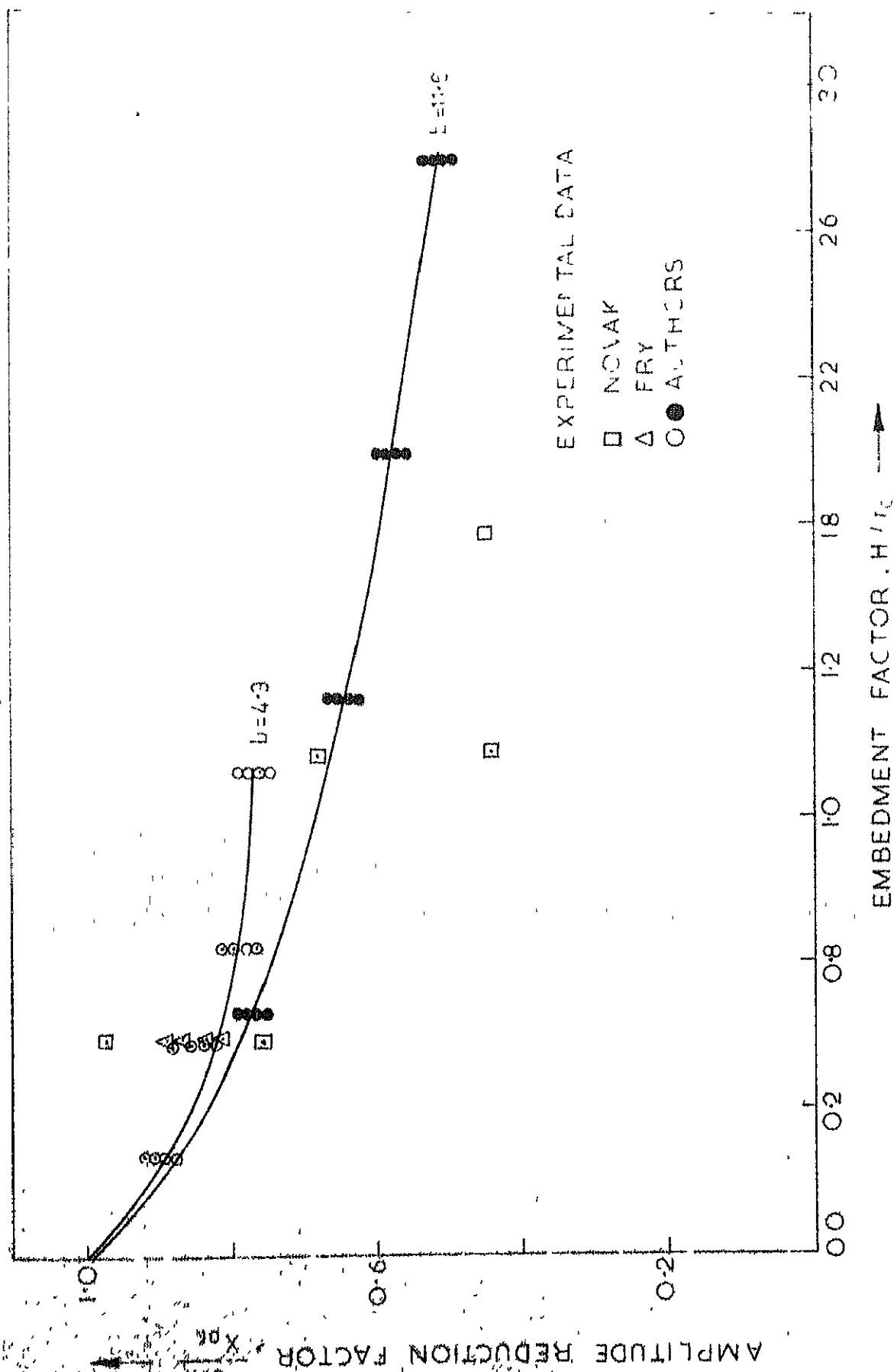


FIG. 6.16 OBSERVED AMPLITUDE REDUCTION FACTOR VS EMBEDMENT FACTOR.

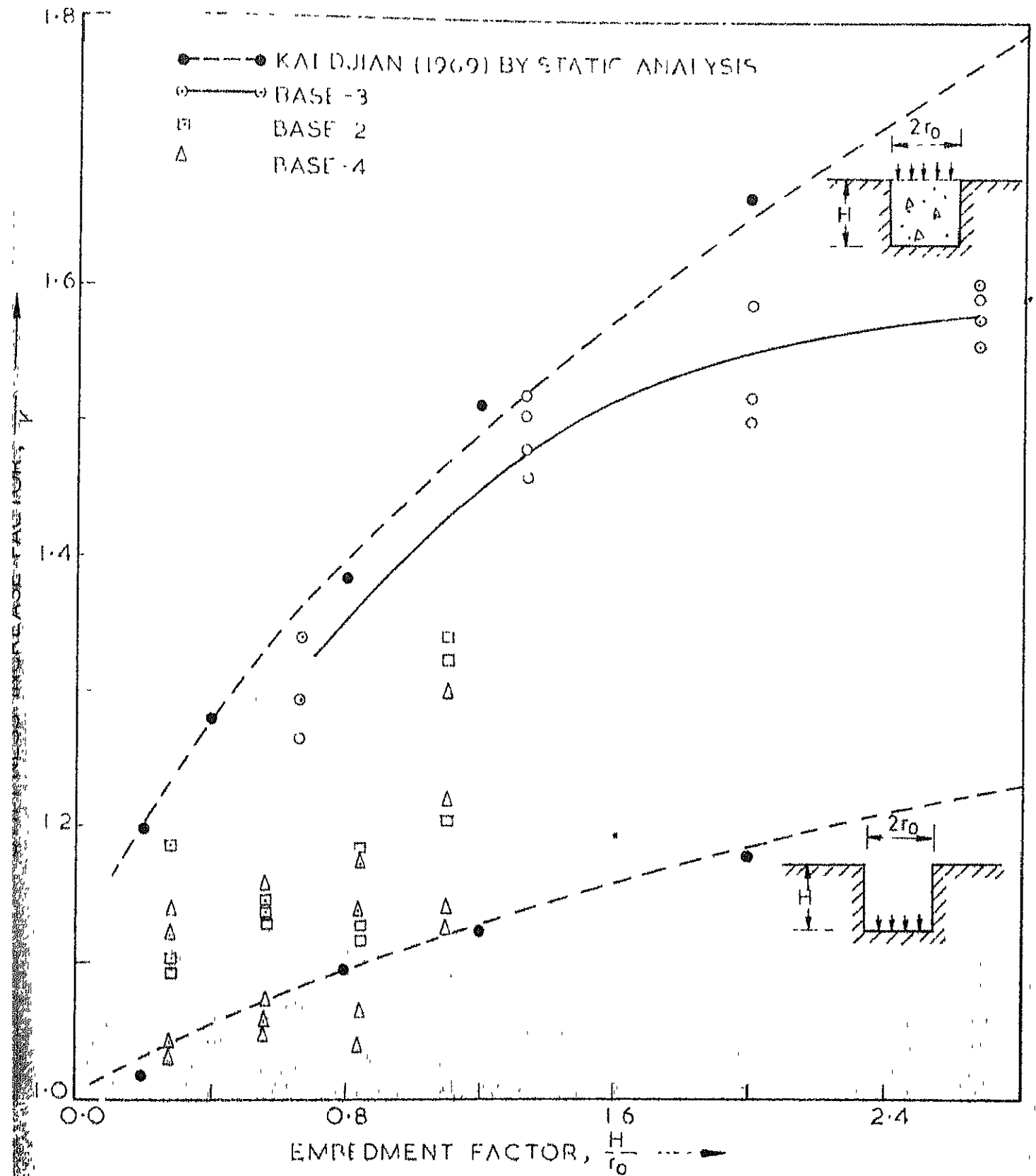


FIG. 6.18 OBSERVED INCREASE IN THE EFFECTIVE STIFFNESS OF THE SOIL-FOUNDATION SYSTEM WITH EMBEDMENT

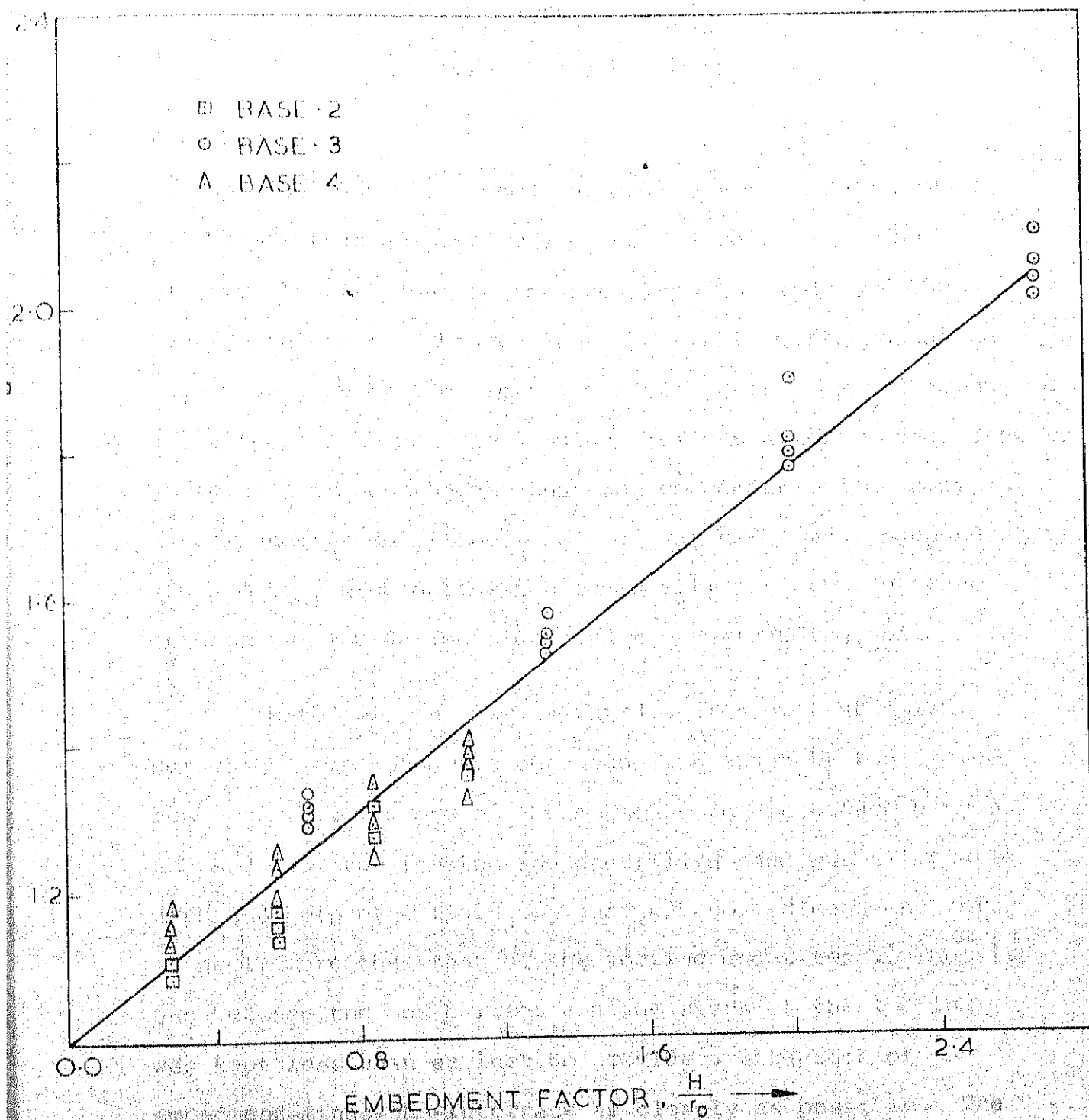


FIG. 6.19 OBSERVED INCREASE IN THE EFFECTIVE VISCOUS DAMPING OF THE SOIL-FOUNDATION SYSTEM WITH

CHAPTER 7

TESTS WITH SURCHARGE

7.1 GENERAL

The effect of embedment of footings, as described in the previous chapter, may be considered due to the additional frictional resistance along the sides of the footing and to the changes in the overall stiffness and the effective mass of the vibrating system caused by the surcharge or overburden around the footing, besides several other factors. Therefore, it was thought that the embedment effect could be better understood if the effect of surcharge was independently studied by a procedure which could eliminate the interface between the foundation sides and the surrounding soil.

With this in view, a third series of tests with surcharge were conducted on Bases-1, 2 and 5 by two different methods. In one of the methods, the interface between the sides of the footing and backfilled sand was eliminated with the help of a rigid box barrier whose dimensions were slightly more than that of the footing under test. The air gap between the box barrier and the sides of the footing was kept less than an inch to provide a situation of embedment-minus-the-interface as closely as possible. The surcharge was increased in regular increments by the back-filling of sand into the space between the periphery of the

rigid box enclosure and the reexcavated pit.

The effect of surcharge was studied by a different method in which sand bags were placed all around the footing so that the gap between the footing and the edge of sand bags was approximately six inches. The surcharge was increased in regular increments by piling up sand bags, layer above layer. The dynamic response of the footing for various layers of surcharge consisting of sand bags was obtained by exciting the footing into steady-state vertical oscillations in the same manner as described in Section 3.3.4.

7.2 TEST RESULTS

The dynamic response of the footings for various depths of surcharge was obtained at several selected eccentric settings of the rotating masses, as was done earlier. Typical frequency-displacement curves obtained by the sand bag method, in the case of Base-5 are illustrated in Figures 7.1 to 7.7. The results of tests conducted on Bases-1, 2 and 5 by the two methods described in Section 7.1 have been presented by plotting the maximum amplitudes at resonance and the resonant frequencies against the number of surcharge layers in the case of sand bags and the height of surcharge in the case of backfilled sand, for convenience. These results are illustrated in Figures 7.8 to 7.12.

Some interesting observations were made regarding the change of maximum amplitudes at resonance with increasing number of surcharge layers. Initially, the resonant amplitudes were found to decrease rapidly upto a specific number of surcharge layers which can be called as the 'optimum surcharge value'. The resonant amplitudes were, however, found to increase with every further increment in the number of surcharge layers after surpassing the so called 'optimum surcharge value'. The increase in the resonant amplitudes were observed upto a specific number of surcharge layers which can be called as the 'critical surcharge value'. The resonant amplitudes were, however, found to remain more or less constant after surpassing the so called 'critical surcharge value'. On the other hand, the resonant frequencies increased with the number of surcharge layers initially, but, later, was found to decrease with further increase of surcharge. This, rather a peculiar phenomenon at first sight, occurred consistently for all the bases at several exciting force levels, as illustrated in Figures 7.8 to 7.12.

An attempt was made to generalise the test results by defining a surcharge factor as the ratio of the intensity of surcharge pressure surrounding the footing to the static pressure below the base of the footing. Thus, the optimum surcharge factors for Bases-1, 2 and 5 were found to be 0.18 , 0.28 and 0.08 respectively. Similarly the critical

surcharge factors for Bases-1, 2 and 5 were found to be 0.47 , 0.70 and 0.39 respectively.

7.3 DISCUSSION ON TEST RESULTS

It may be rather too early to draw broad conclusions from the numerical values of optimum surcharge values found from the surcharge tests conducted on some concrete footings in the present investigation. This is especially so as the numerical values may hold good only for the particular conditions and circumstances under which the tests were conducted. However, the results of these tests indicate, atleast qualitatively, that the manipulation of the amount of surcharge around a vibrating footing may be used for bringing down the resonant amplitudes of motion. Further experimental investigations under more controlled conditions can establish the precise values of optimum surcharge factors in terms of the geometry of the foundation and other pertinent parameters. As such, the value of these investigations has a good potential in places where corrective measures are to be suggested to improve the performance of machines whose foundations are designed by the rule of thumb or without proper field investigations.

The effect of surcharge, as described in the previous paragraphs, may be attributed to the changes in the confining

pressure and the effective mass associated with the vibrations. For instance, the trend in the variation of the resonant amplitudes of motion with respect to the first few increases in the surcharge can be explained by the fact that the confining pressure below the base has increased. The increase in the confining pressure may be expected to cause an increase in the overall stiffness of the system and hence the decrease of resonant amplitudes and increase of resonant frequencies. The reduction in maximum amplitudes, however, would cease at some stage and the amplitudes at resonance will begin to increase because of the reduced damping, caused by an increase in the associated mass of the vibrating system in the form of further increments in surcharge. The same reason explains the decrease of resonant frequencies. In other words, the amplitudes of motion at resonance will increase and the resonance frequencies will decrease with further increments in surcharge, i.e., beyond the so called 'optimum surcharge factor', due to the increase in the effective mass ratio, b , of the vibrating system. The rate of increase of resonant amplitudes was found to become negligible after surpassing the so called 'critical surcharge factor'. This apparently stable state was attained, perhaps by the combined effect of the varying confining pressure in the soil below the base and the changes in the effective mass associated with the vibrating system.

However, further research efforts in this direction are desirable to understand fully the effects of surcharge on the steady-state response of footings and its significance in the area of corrective measures which are adopted to improve the performance of existing machine foundations.

It may be of interest to note that the tests with surcharge were undertaken in order to estimate the share of influence of surcharge on the dynamic response of embedded footings. Though the effect of surcharge is not explicitly taken into consideration by the proposed theoretical model for embedded footings, explained in Chapter 8, the influence of the same is implicit in the procedure suggested for the evaluation of the constant frictional force mobilized along the interface between the foundation walls and the surrounding soil, as explained in Section 8.4 of Chapter 8.

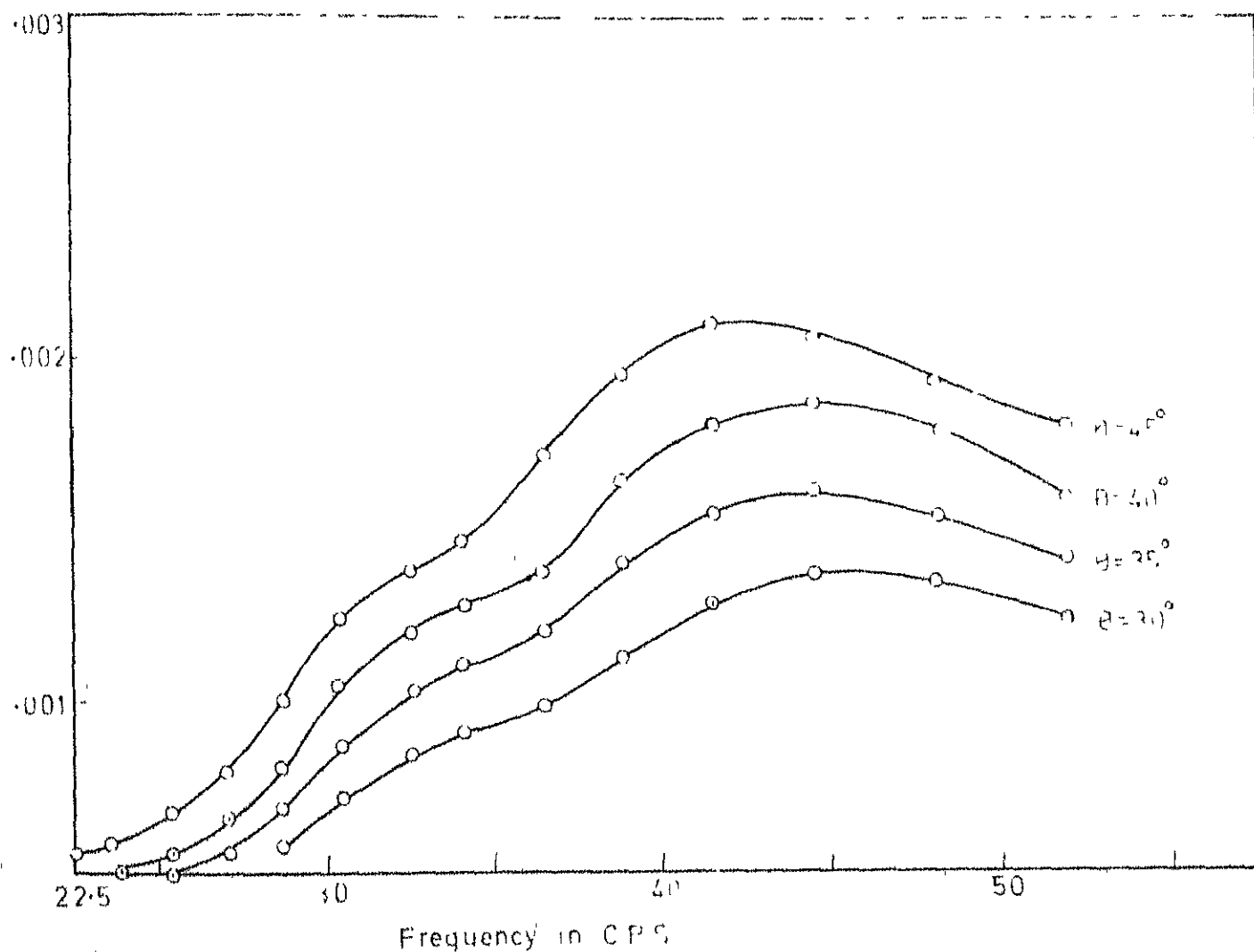


FIG. 7.1 FREQUENCY VS DISPLACEMENT, BASE-5 WITH 1 LAYER OF SURCHARGE
 NOTE: 1 LAYER OF SURCHARGE CONSISTS OF 20 SAND BAGS AROUND THE BASE

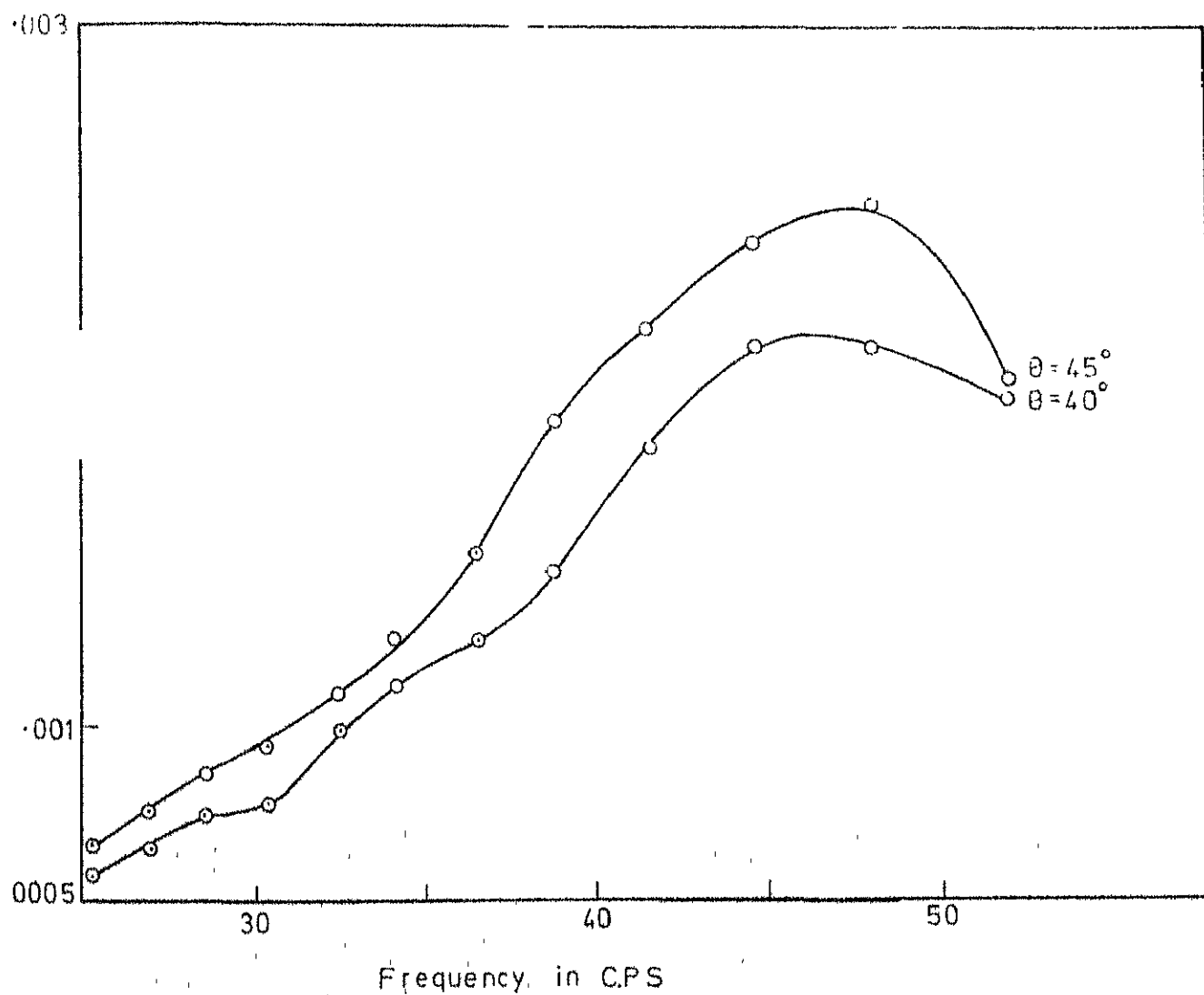


FIG 7.2 FREQUENCY VS DISPLACEMENT, BASE-5 WITH 2 LAYERS OF SURCHARGE

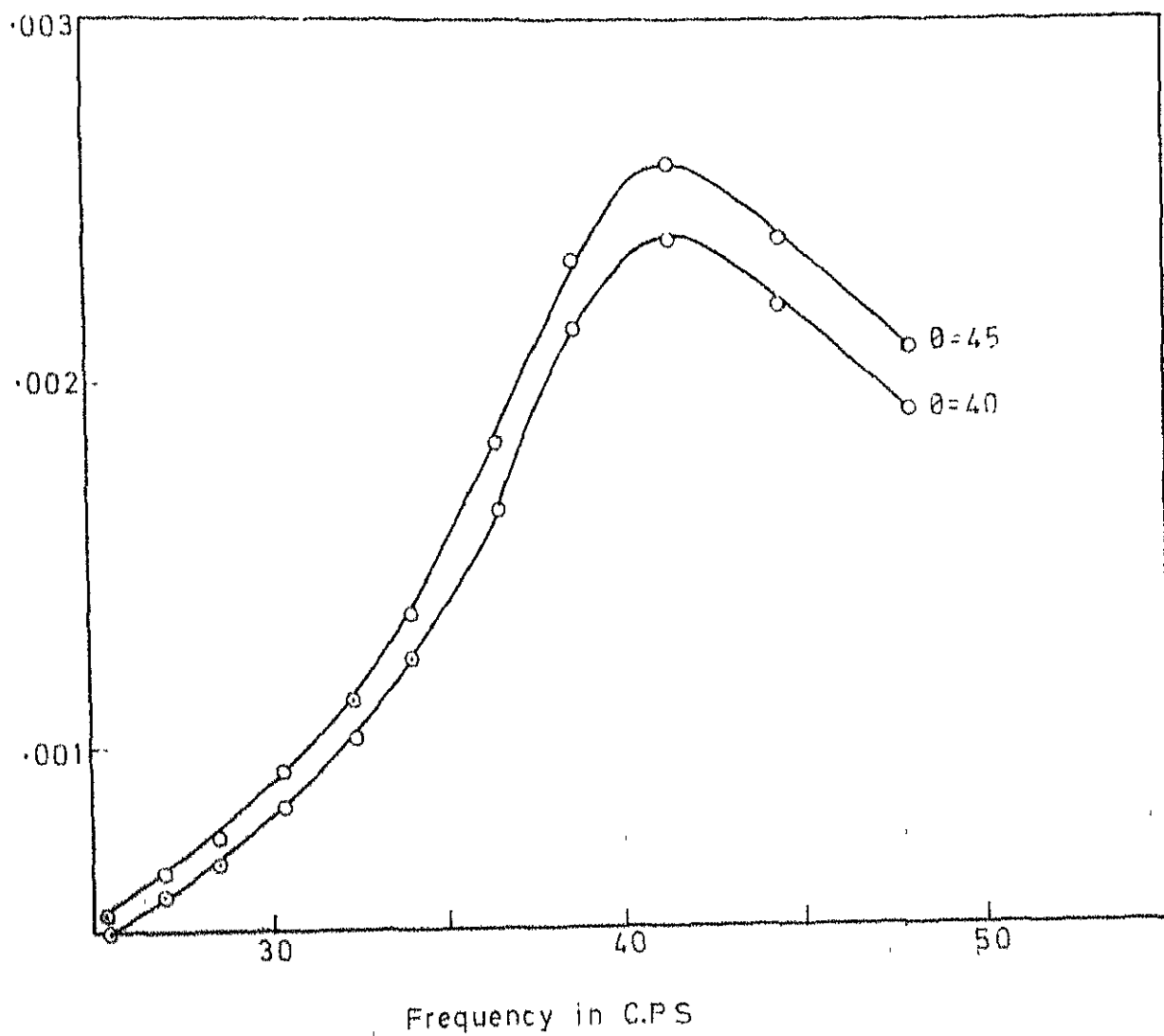


FIG. 7.3 FREQUENCY VS DISPLACEMENT, BASE-5 WITH 3 LAYERS OF SURCHARGE

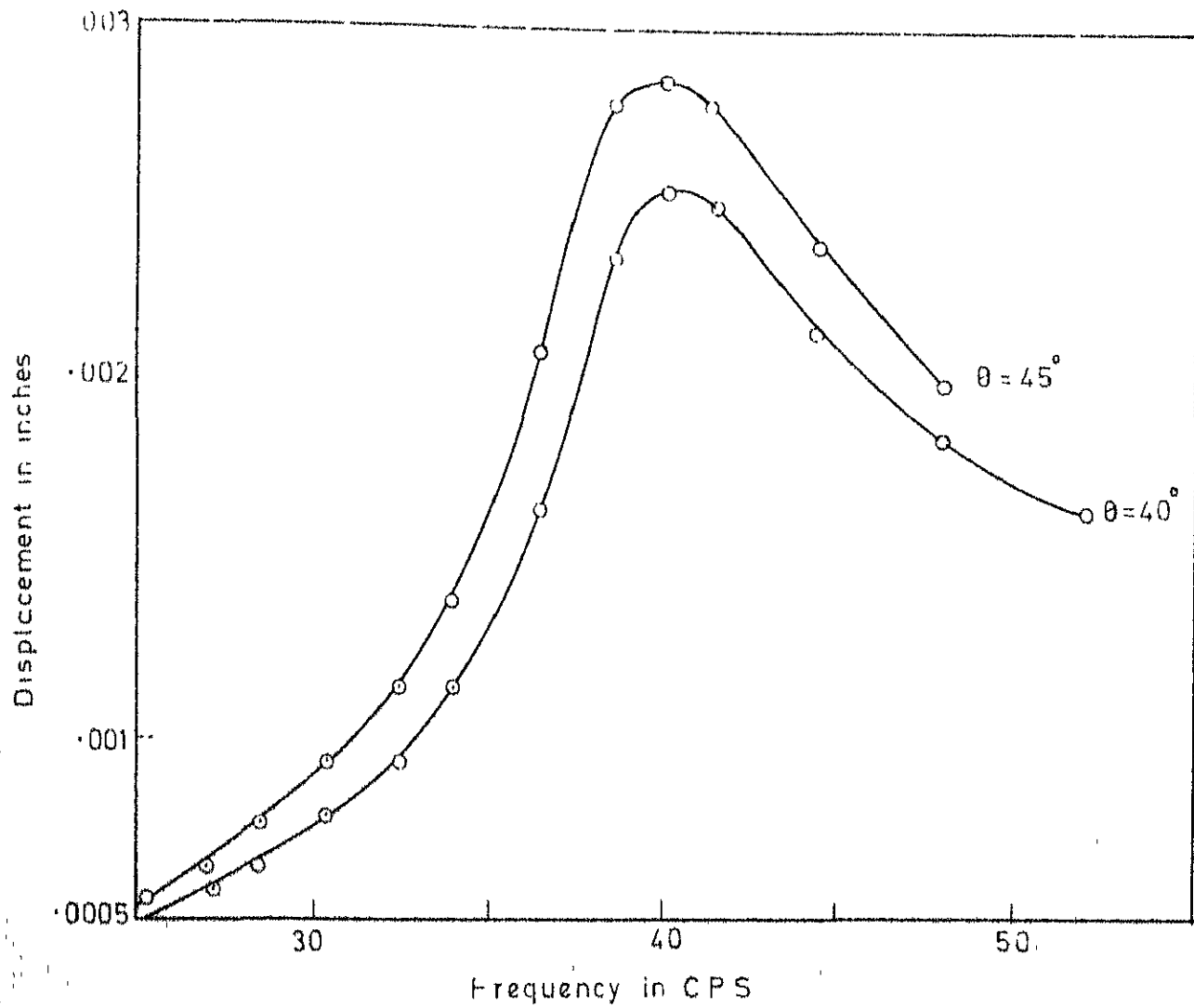


FIG. 7.4 FREQUENCY VS DISPLACEMENT, BASE-5
WITH 4 LAYERS OF SURCHARGE

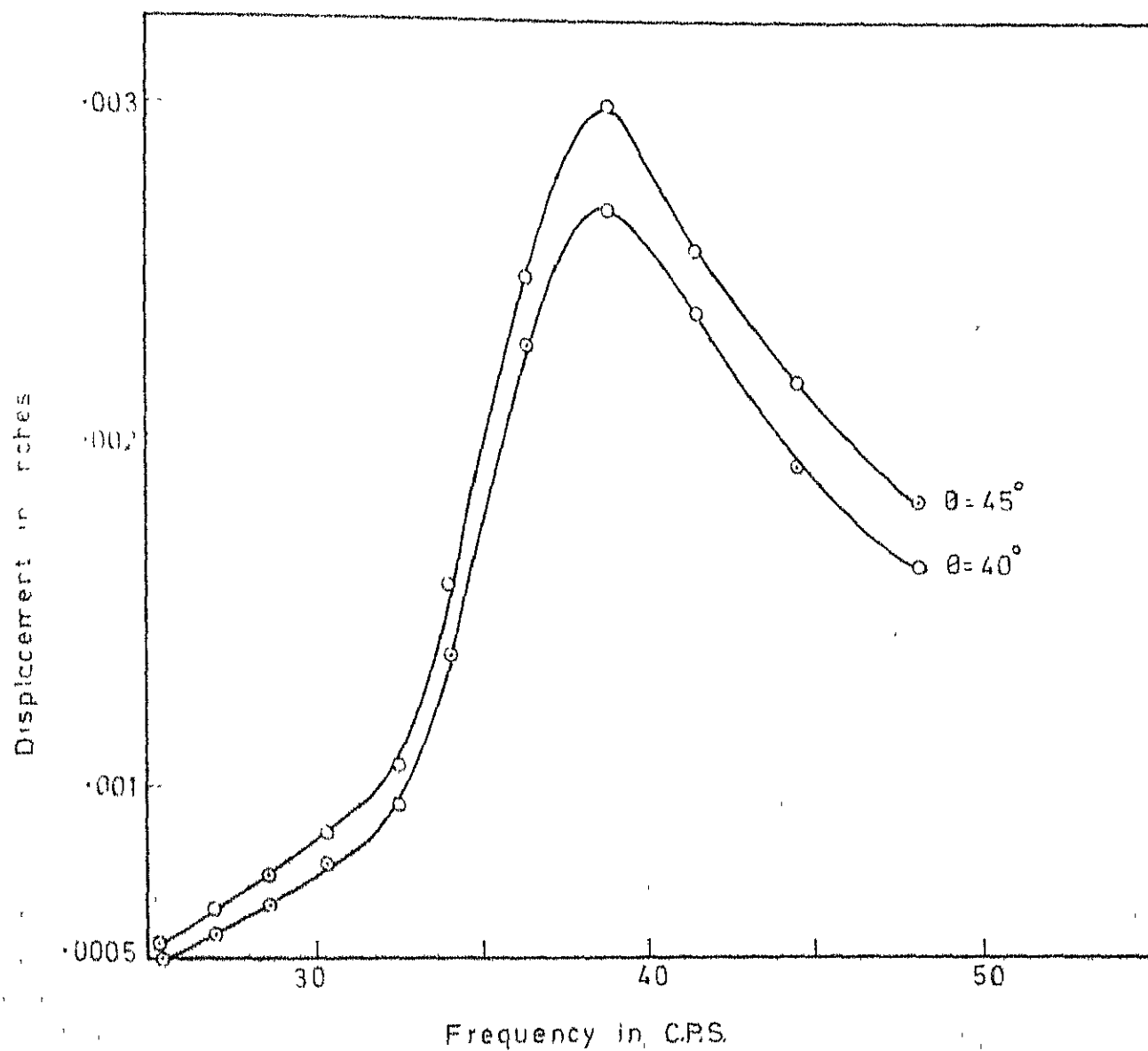


FIG. 7.5 FREQUENCY VS DISPLACEMENT, BASE-5 WITH 5 LAYERS OF SURCHARGE

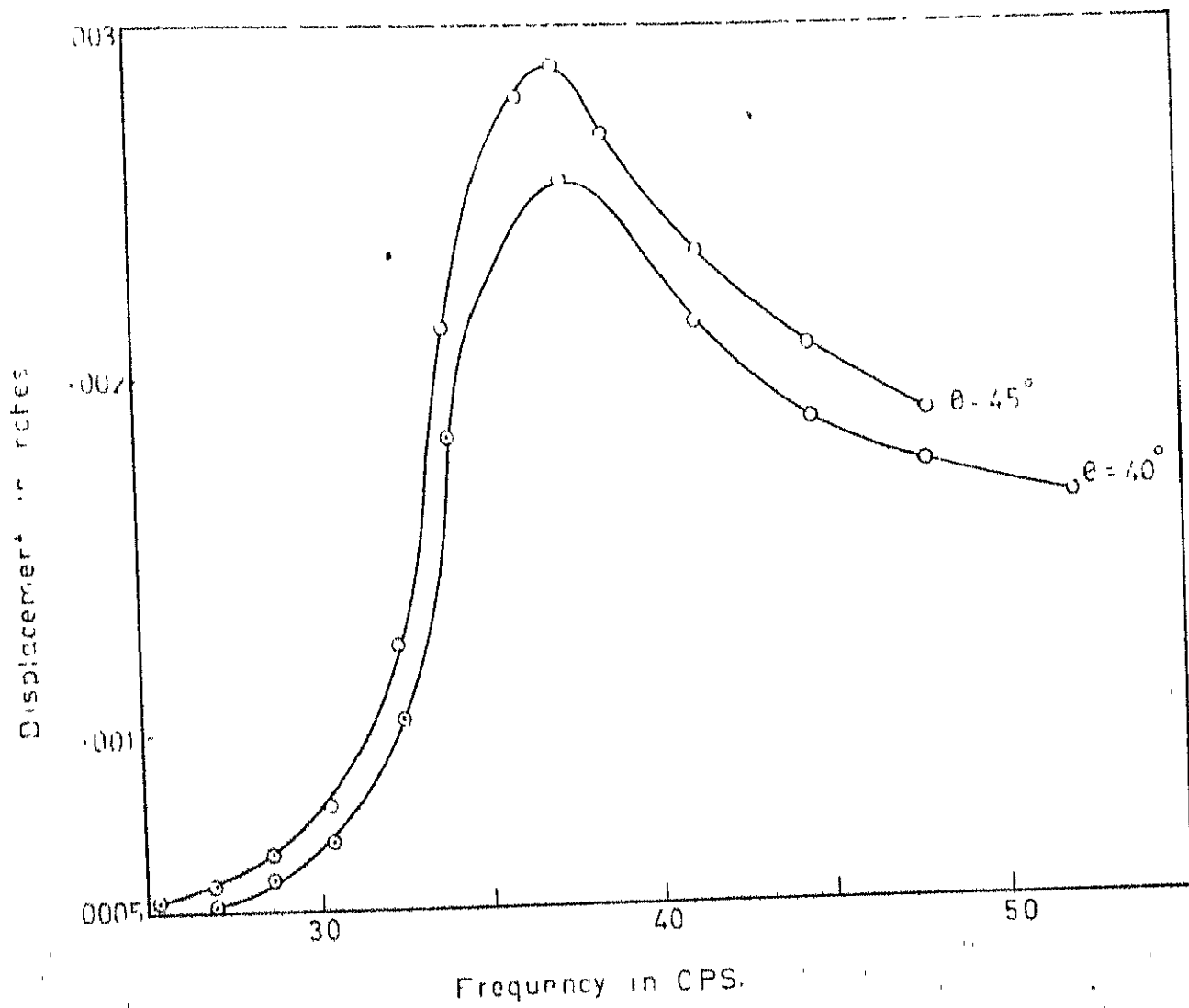


FIG 7.6 FREQUENCY VS DISPLACEMENT, BASE-5 WITH 6 LAYERS OF SURCHARGE

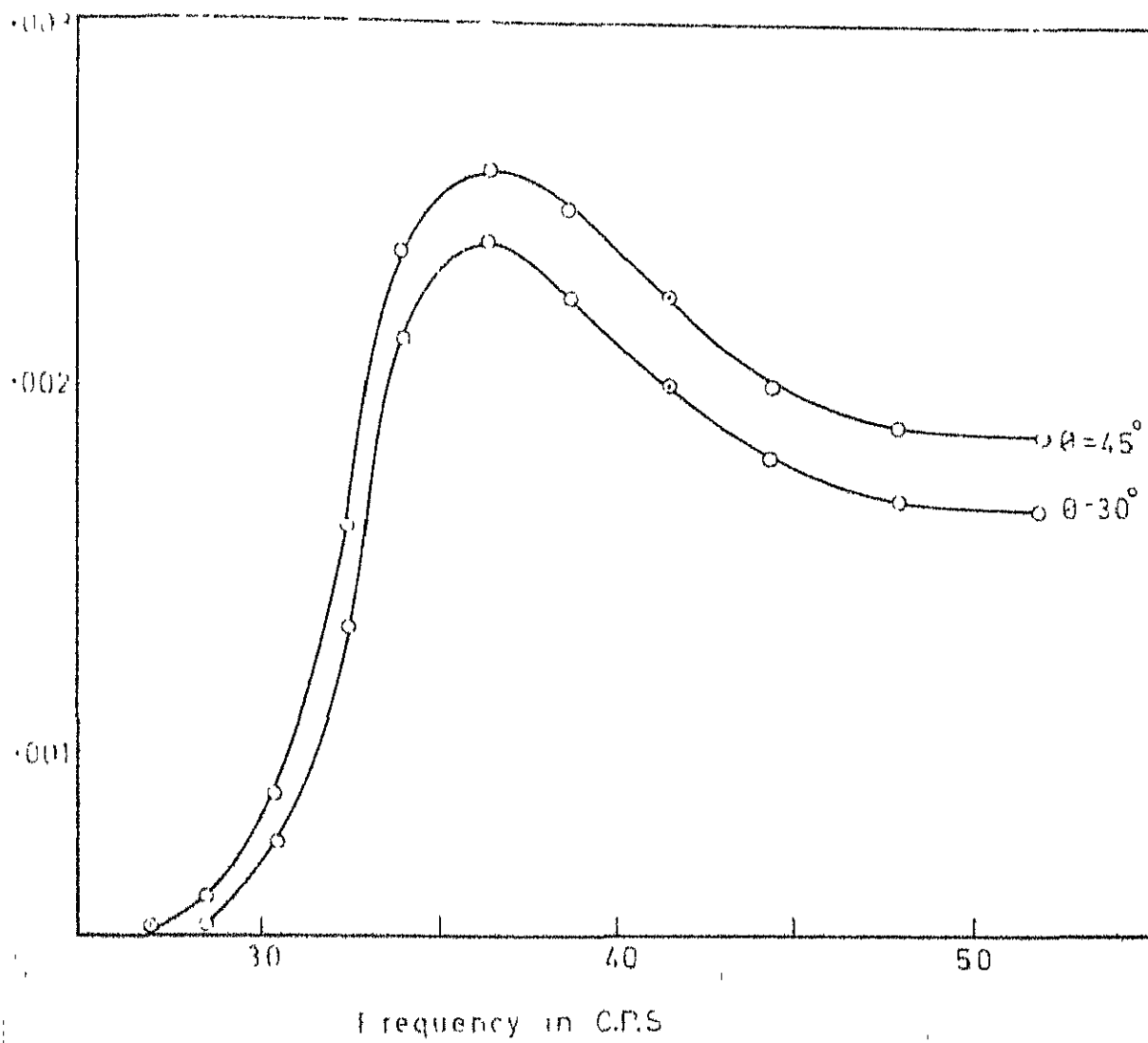
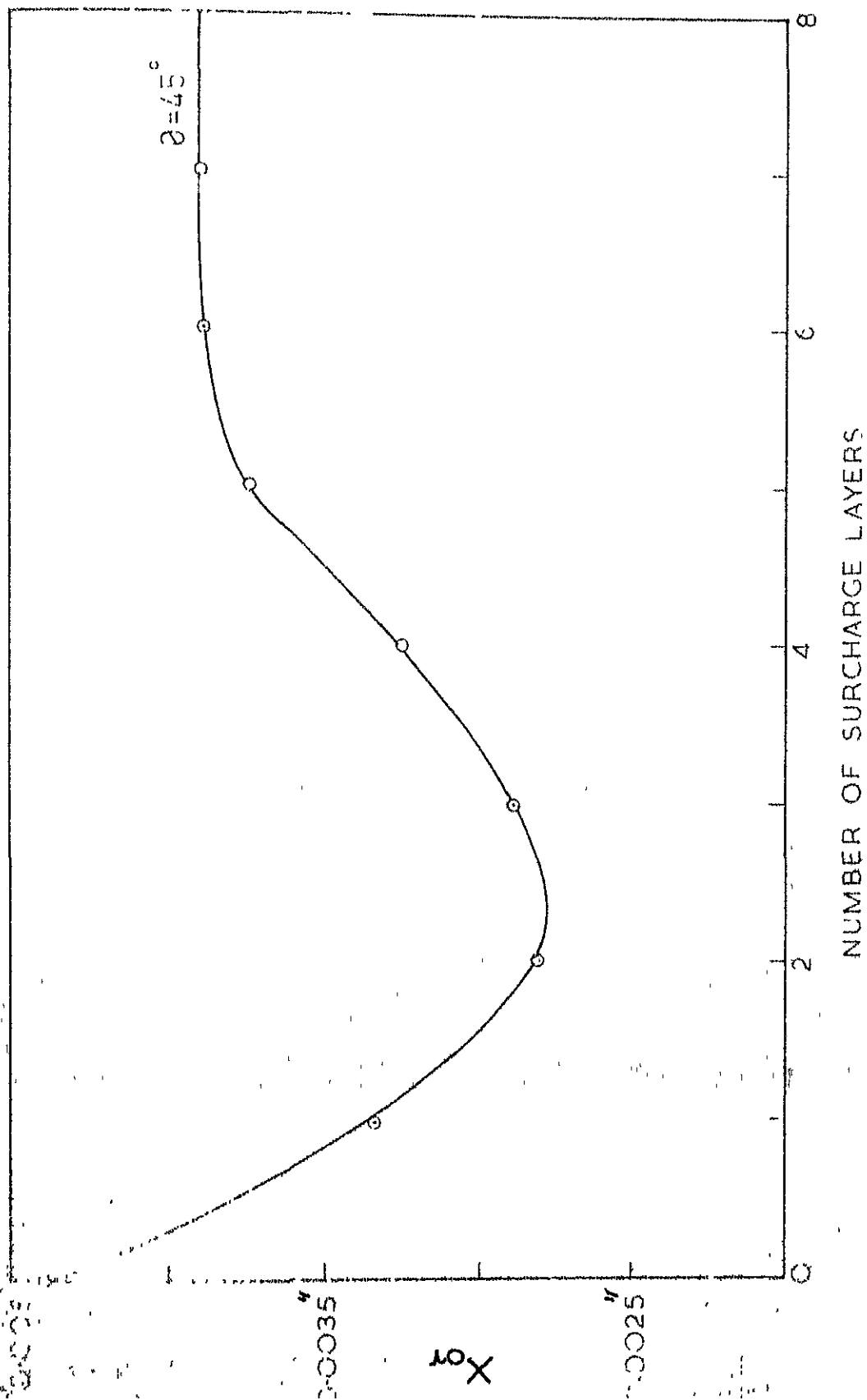
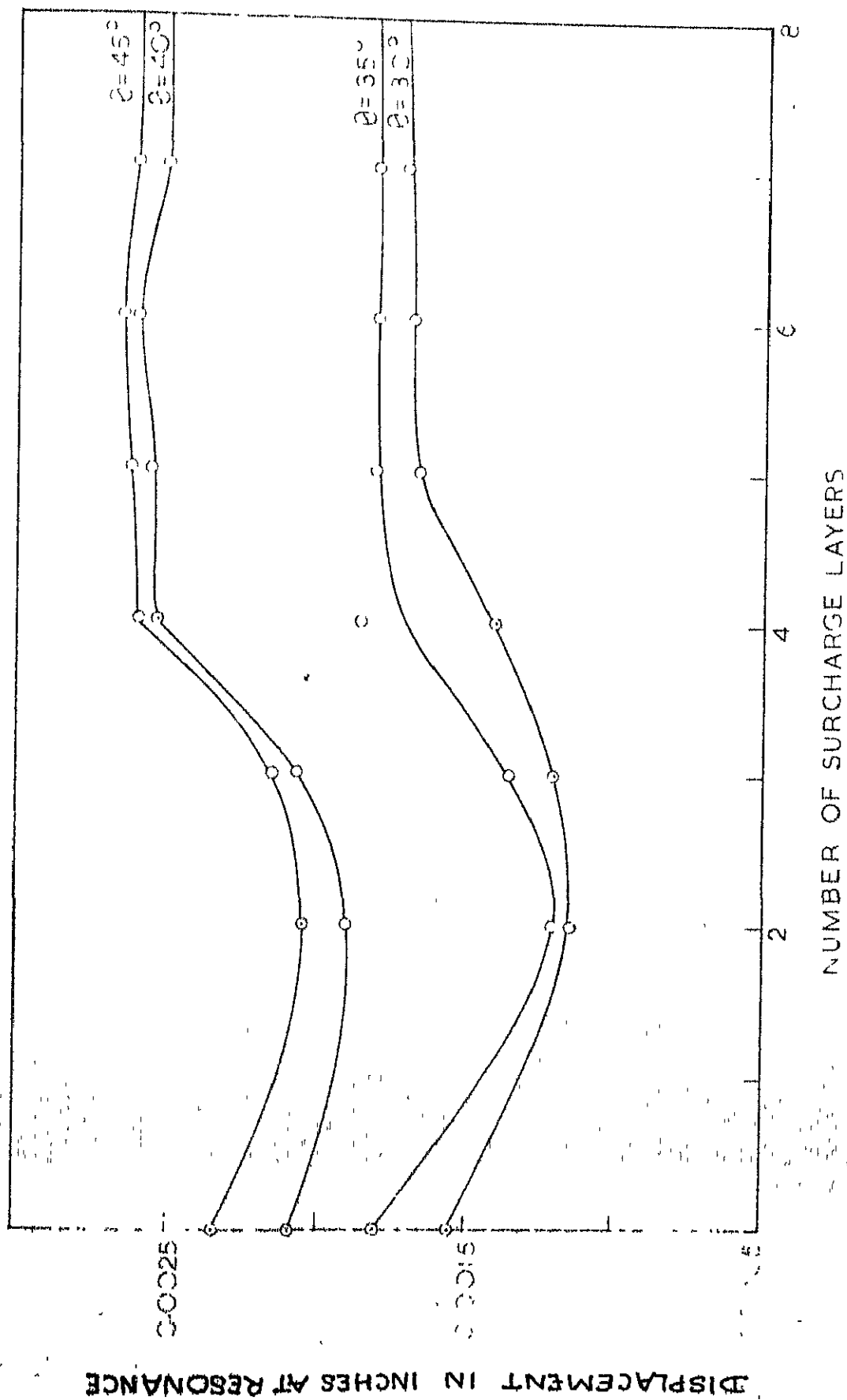


FIG. 7.7 FREQUENCY VS DISPLACEMENT, BASE-5
WITH 7 LAYERS OF SURCHARGE

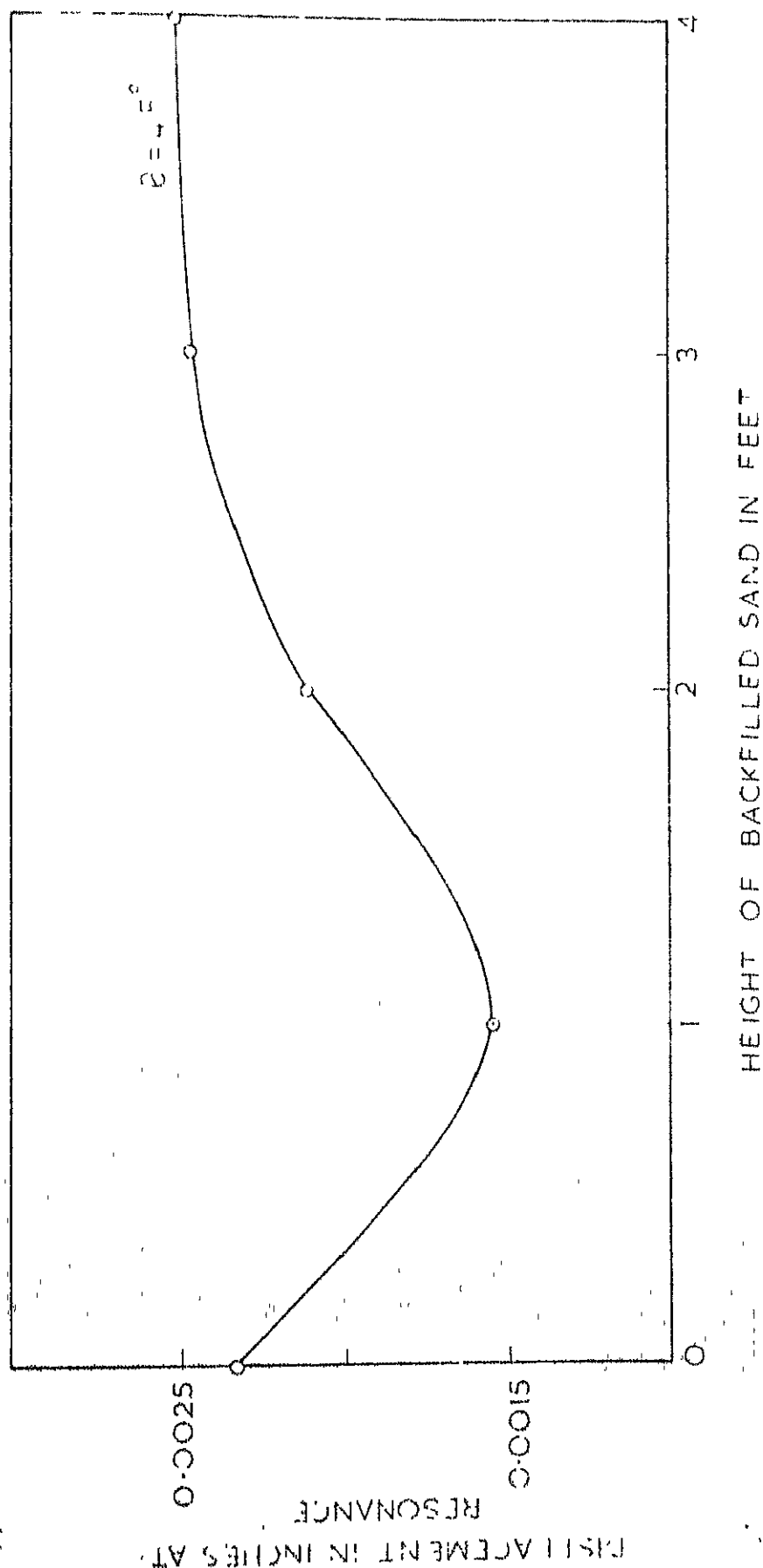


NOTE: EACH LAYER OF SURCHARGE CONSISTS OF 20 SAND BAGS PLACED ALL AROUND THE BASE

FIG 7.8 EFFECT OF SURCHARGE ON MAXIMUM AMPLITUDES AT RESONANCE, BASE-1.

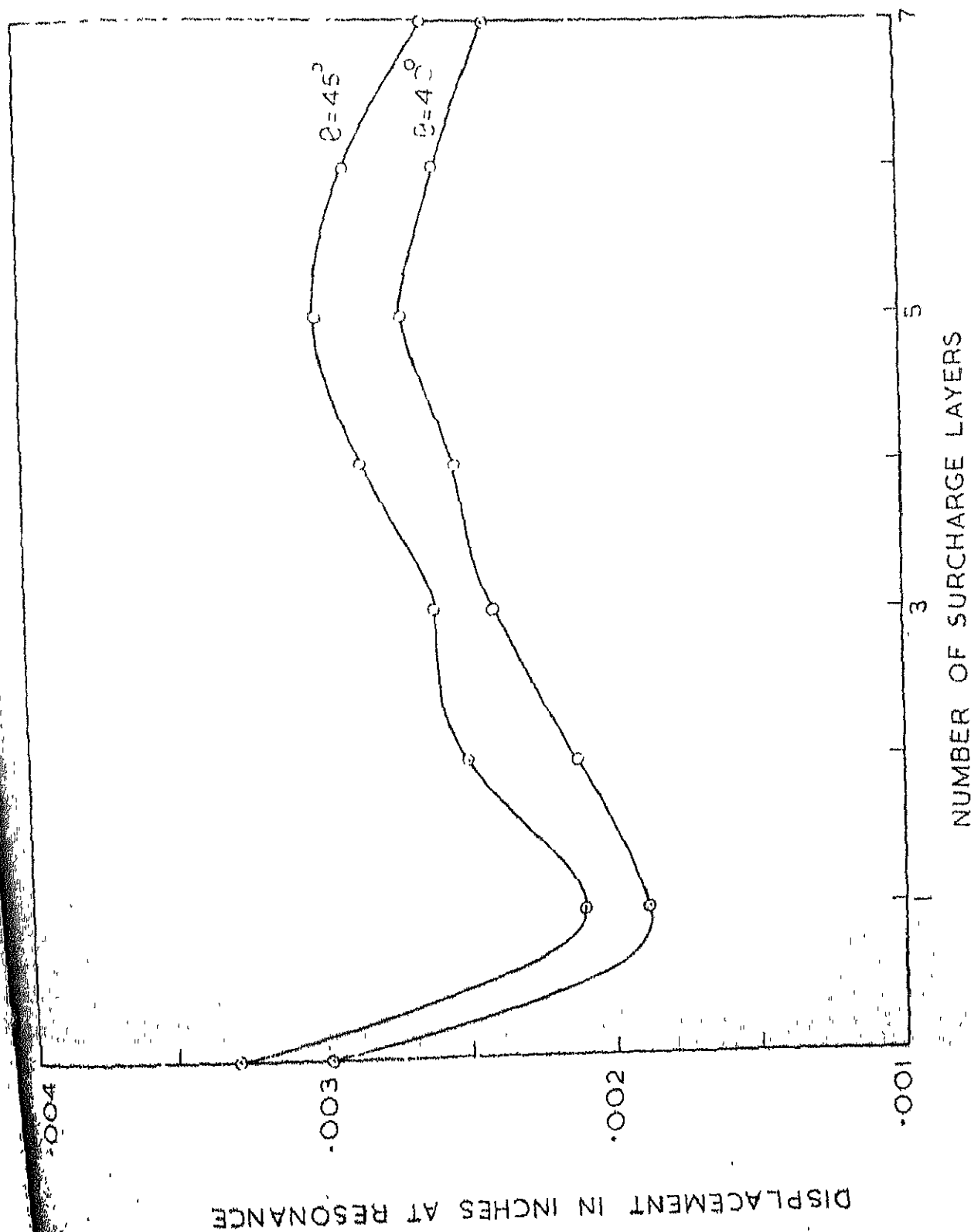


7.9 EFFECT OF SURCHARGE ON MAXIMUM AMPLITUDES AT RESONANCE, BASE-2



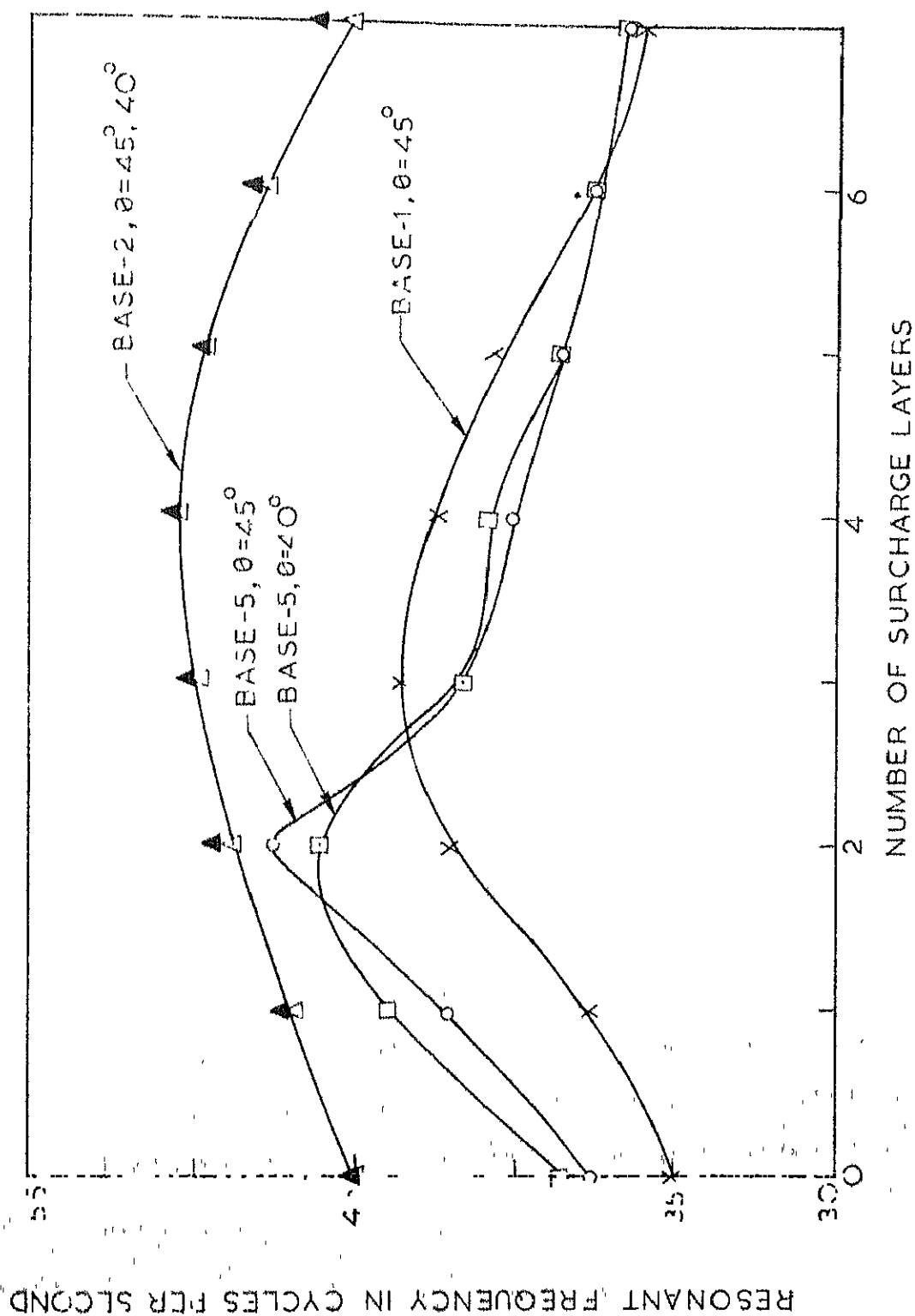
NOTE: THE CONTACT BETWEEN THE BACKFILLED SAND AND THE FOOTING SIDES WAS ELIMINATED BY MEANS OF A RIGID BOX ENCLOSURE AROUND THE BASE

FIG. 7.10 EFFECT OF SURCHARGE ON MAXIMUM AMPLITUDES AT RESONANCE, CASE-2



NOTE: EACH LAYER OF SURCHARGE CONSISTS OF 20 SAND BAGS PLACED ALL AROUND THE BASE

FIG. 7.11 EFFECT OF SURCHARGE ON MAXIMUM AMPLITUDES AT RESONANCE. BASF-5



NOTE: IN THE CASE OF BASES-1 AND 5, ONE LAYER OF SURCHARGE CONSISTS OF 20 SAND BAGS, IN THE CASE BASE-2, ONE LAYER OF SURCHARGE CONSISTS OF 24 SAND BAGS, PLACED ALL AROUND THE BASE

FIG.7.12 EFFECT OF SURCHARGE ON RESONANT FREQUENCIES

CHAPTER 8

THE PROPOSED THEORETICAL MODEL

8.1 GENERAL

The theoretical models which were reviewed in Section 2.5.3 cannot fully explain the actual performance of embedded footings because of the highly simplified assumptions made regarding the shape of the footing, the quality of the footing contact with the surrounding soil and the idealised properties of the half-space in which the footing is embedded. Because of the magnitude of uncertainties involved in actual practice, it seems justifiable to choose such a model whose parameters can be adjusted to findings from field tests. The single-degree-of-freedom mass-spring-dashpot analogue, based on the elastic half-space theory, no doubt, has all the advantages for such adjustments. But this model is already made vulnerable for its inability to accommodate some of the serious departures from the theory encountered in practice such as those due to the nonlinear nature of the response of footings with higher dynamic force levels, the effects of variation of soil properties with depth and the effects of base size and shape of the footing. Therefore, any attempts at including the effect of embedment also into the same model will only add to the already existing doubts. In view of

all these practical difficulties, a new lumped parameter model which can deal with the effects of embedment in an independent manner has been suggested in this dissertation.

8.2 EFFECT OF EMBEDMENT

The embedment of footing results in the increase of total foundation surface subjected to the influence of soil reactions. The soil-footing interface due to embedment is an unavoidable source of interfacial friction between the two surfaces and consequently, an increase in the dissipation of energy of foundation vibrations in the form of a constant friction damping can be expected. The sides of the footing and the soil with a common interface are held together by a clamping pressure which depends on the lateral earth pressure as well as the physical characteristics of the interface formed by the foundation surface and the surrounding soil. When a variable external load is applied, the shear stress on the interface is augmented. Slip eventually occurs when the variable load exceeds the clamping pressure. This implies that the points on the opposite sides of the interface experience small relative displacements. When such a motion occurs along the interface, one is usually justified in neglecting the elastic deformations and in treating the contacting elements as rigid.

The estimation of the energy dissipation at the soil-footing interface as a result of frictional forces that are brought into play is thus very important. The nature and the amount of these frictional forces would, however, depend on the mode of vibrations, the relative depth of embedment, the area of side contact, the density of the surrounding soil, the nature of contact between the foundation sides and the surrounding soil and the effects of surcharge around the embedded footing. Therefore, any attempt at formulating a theoretical model to describe the dynamic behaviour of an embedded footing should take into consideration all the above important phenomena. The model at the same time should be able to distinguish between the behaviour of footing embedded in cohesionless and cohesive soil media.

8.3 THE PROPOSED THEORETICAL MODEL

8.3.1 General Remarks

The preceding discussions indicate that the effect of embedment of footing results in an increase of the effective damping force due to the skin friction force mobilized between the vertical surface of the footing and the surrounding soil. Therefore, a logical choice would be to include a Coulomb friction damper as a lumped parameter to the simplified single-degree-of-freedom analogue described

earlier in Section 2.4. This parameter can describe completely the effects of embedment in an independent manner taking into consideration the material properties of the soil and the geometry of the footing. In the following paragraphs, it is demonstrated that the Coulomb friction damper, as an analogue, is as versatile as the dashpot which is chosen to represent the energy dissipation of a footing, vibrating on the surface of the half-space.

Assuming that the vertical oscillations of a rigid circular footing embedded in the soil can be approximated by the simplified analogue described in Eq. 2.38 (Section 2.4.3, Chapter 2) with the addition of a Coulomb friction damper, F , as shown in Figur. 8.1(b), the differential equation of motion for such a system can be written as

$$M \ddot{X} + C \dot{X} + K X \pm F = Q(t) \quad (8.1)$$

in which ' F ' is a constant friction force resisting the motion of the vibrating mass, M .

The constant friction force has the sign of velocity. The force always opposes motion and, consequently, changes sign at each half cycle. Therefore, a single continuous solution cannot be written to the differential equations of the type described in Eq. 8.1. Each part of the solution must be considered between the largest positive and negative displacements of each half cycle.

Nevertheless, a remarkable steady-state solution for maximum displacement was given by Den Hartog (13) for the case of vibrations under a constant sinusoidal force with constant friction. When the forcing function is frequency dependent as given by Eq. 2.19, the exact steady-state solution for Eq. 8.1 can be obtained by a procedure similar to that adopted by Den Hartog (13) with slight modifications. The solution procedure which involves lengthy trigonometric and exponential functions are briefly presented below for the case of a constant sinusoidal force, as solved by Den Hartog (13) as well as for the case of rotating-mass type of excitation, as extended in the present investigation. The final results are presented, for the first time, in a form suitable for the purposes of design and analysis.

8.3.2 Forced Vibrations with Constant Forcing Function

The differential equation of motion for the lumped mass-spring system with the combined viscous and Coulomb friction damping, excited by a force $P(t) = P_0 \cos(\omega t + \psi)$, as shown in Figure 8.1(b) can be written as

$$M \ddot{X} + C \dot{X} + K X \pm F = P_0 \cos(\omega t + \psi) \quad (8.2)$$

where the $+ F$ holds when the mass moves in $+ X$ direction and viceversa. The phase angle ψ in the forcing function has no meaning in a differential equation of the type described in Eq. 8.2 and is only included for the purpose of

subsequently writing the boundary conditions in a simple form. During the half cycle of motion, $0 < t < \pi/\omega$, the velocity is always negative, therefore $-F$ holds. Using the abbreviations,

$$(\Omega_0/K) = a; (F/K) = x_f; (K/M) = \omega_n^2 \quad (8.3)$$

the differential equation for that interval of time can be written as

$$\ddot{x} + \omega_n^2 (x - x_f) + (C/M) \dot{x} = a \omega_n^2 \cos(\omega t + \psi) \quad (8.4)$$

The general solution of Eq. 8.4 is known to be

$$x = \exp(-\omega_n D t) \left[C_1 \cos \omega_d t + C_2 \sin \omega_d t \right] + \frac{a}{q} \cos(\omega t + \epsilon) + x_f \quad (8.5)$$

where

$$\omega_d = \omega_n \sqrt{1 - D^2}, \text{ the damped natural frequency,}$$

$$q = \sqrt{\left(\frac{\beta^2 - 1}{\beta^2} \right)^2 + \left(\frac{2D}{\beta} \right)^2}, \text{ the inverse response function with viscous damping,}$$

$$D = \frac{C}{2\sqrt{KM}}, \text{ the viscous damping factor and}$$

$$\beta = \omega_n/\omega, \text{ the inverse frequency ratio; and}$$

$$\tan(\psi - \epsilon) = \frac{C\omega}{K - M\omega^2} \quad (8.6)$$

A steady-state nonstop motion has to fulfil the following boundary conditions.

$$\begin{aligned} t = 0 \quad x = x_0 \quad \dot{x} &= 0 \\ t = \frac{\pi}{\omega} \quad x = -x_0 \quad \dot{x} &= 0 \end{aligned} \quad (8.7)$$

These are four conditions and the general solution of Eq. 8.2 contains only two integration constants. The two superfluous equations will be used for determining the unknown quantities x_0 and ψ .

First C_1 and C_2 are eliminated by means of two conditions

$$\begin{aligned} \text{at } t = 0 \\ x = \exp(-\omega_h D t) \left[(x_0 - x_f) \cos \omega_d t \right. \\ \left. - \frac{a}{q} \cos \epsilon \cos \omega_d t + \frac{c}{2 \omega_d M} (x_0 - x_f) \sin \omega_d t \right. \\ \left. + \frac{a c}{2 \omega_d q M} \cos \epsilon \sin \omega_d t + \frac{a \omega}{\omega_d q} \sin \epsilon \sin \omega_d t \right] \\ + \frac{a}{q} \cos(\omega t + \epsilon) + x_f \end{aligned} \quad (8.8)$$

Then the two conditions at $t = \pi/\omega$ can be written in the form

$$\begin{aligned} A_1 \cos \epsilon + A_2 \sin \epsilon + A_3 &= 0 \\ A_4 \cos \epsilon + A_5 \sin \epsilon + A_6 &= 0 \end{aligned} \quad (8.9)$$

where

$$\begin{aligned} A_1 &= - \frac{a}{q} \exp\left(-\frac{\pi c}{2 M \omega}\right) \cos(\omega_d \pi/\omega) \\ &- \frac{a c}{2 \omega_d M q} \exp\left(-\pi c/2 M \omega\right) \sin(\omega_d \pi/\omega) - a/q \end{aligned} \quad (8.10)$$

$$A_2 = \frac{a\omega}{\omega_d q} \exp(-\pi c/2 M\omega) \sin(\omega_d \pi/\omega) \quad (8.11)$$

$$A_3 = (X_0 - X_f) \exp(-\pi c/2 M\omega) \cos(\omega_d \pi/\omega) + X_f + X_0 \\ + (c/2 \omega_d M) (X_f - X_0) \exp(-\pi c/2 M\omega) \sin(\omega_d \pi/\omega) \quad (8.12)$$

$$A_4 = \frac{a}{q} \exp(-\pi c/2 M\omega) \sin \frac{\omega_d \pi}{\omega} \left(\frac{c^2}{4 M^2 \omega_d} + \omega_d \right) \quad (8.13)$$

$$A_5 = \frac{a\omega}{q} \left[1 + \exp(-\pi c/2 M\omega) \cos(\omega_d \pi/\omega) \right. \\ \left. - (c/2 M \omega_d) \exp(-\pi c/2 M\omega) \sin(\omega_d \pi/\omega) \right] \quad (8.14)$$

$$A_6 = - (X_0 - X_f) \exp(-\pi c/2 M\omega) \sin \frac{\omega_d \pi}{\omega} \left(\frac{c^2}{4 M^2 \omega_d} + \omega_d \right) \quad (8.15)$$

From Eq. 8.9, it can be deduced

$$\sin \epsilon = \frac{A_3 A_4 - A_1 A_6}{A_1 A_5 - A_2 A_4} \quad \text{and} \quad \cos \epsilon = \frac{A_2 A_6 - A_3 A_5}{A_1 A_5 - A_2 A_4} \quad (8.16)$$

Substituting the values just given in Eqs. 8.10 to 8.15 in

Eq. 8.16, we get

$$\sin \epsilon = -q S \frac{X_f}{a} \cos \epsilon = q \left(\frac{X_0}{a} + R \frac{X_f}{a} \right) \quad (8.17)$$

where R and S are functions independent of Coulomb damping

which can be expanded as

$$R = \frac{\sinh(\beta \pi D) - \sqrt{(D^2)/(1-D^2)} \sin \beta \pi \sqrt{1-D^2}}{\cosh(\beta \pi D) + \cos(\beta \pi \sqrt{1-D^2})} \quad (8.18)$$

and

$$S = \frac{\beta}{\sqrt{1-D^2}} \frac{\sin(\beta \pi \sqrt{1-D^2})}{\cosh(\beta \pi D) + \cos(\beta \pi \sqrt{1-D^2})} \quad (8.19)$$

Eliminating ϵ from Eq. 8.17, we get

$$\frac{X_c}{a} = -R \left(\frac{X_f}{a} \right) + \sqrt{\frac{1}{q^2} - S^2 \left(\frac{X_f}{a} \right)^2} \quad (8.20)$$

Eq. 8.20 is an expression for the amplitude of motion and will reduce to Eq. 2.15 in the absence of Coulomb friction, F . It may be recalled, Eq. 2.15 defines the dimensionless amplitude factor for the case of the mass supported by a spring and a dashpot and excited by a constant sinusoidal forcing function. The phase angle can be obtained from Eqs. 8.16 and 8.6.

Eq. 8.20 defines the complete solution for the steady-state, non-stop motion for the differential equation of motion described in Eq. 8.2. The results of Eq. 8.20 are plotted above the broken lines in Figures 8.2(a) to 8.2(j) for various values of viscous damping factor, D and the Coulomb friction factor, F/Q_0 .

It is interesting to note that if the frictional force is large enough, a single cycle of motion may consist of regions of motion and regions of standstill. Den Hartog (13) extended the solution procedure to cover motions with one stop per half cycle to obtain the amplitudes of motion in the region below the broken lines of Figures 8.2(a) to 8.2(j). Therefore, it is important to note that Eq. 8.20 gives the complete solution for non-stop motion and is valid when the following conditions are satisfied.

$$\frac{x_n}{a} \geq \frac{(I - R)}{\sqrt{q^2 (s^2 + I^2)}} \quad (8.21)$$

and

$$\frac{x_f}{a} \geq \frac{1}{\sqrt{q^2 (s^2 + I^2)}} \quad (8.22)$$

in which

$$I = 2\beta D S + \beta^2 (1 + R) \quad (8.23)$$

Eqs. 8.21 and 8.22 are valid for all values of $\omega/\omega_n \geq 0.5$ and the boundary for non-stop motion as shown by the broken lines of Figures 8.2(a) to 8.2(j) is determined using Eq. 8.21.

It may be noted that ψ is the phase angle between the displacement and the exciting force vector. After a

sufficient length of time, a steady, periodic but nonharmonic motion of frequency, ω will be established. Since the motion is nonharmonic, it is clear that the phase angle applies only to the maxima of exciting force, Q_0 and amplitude of displacement, X_0 . This does not mean that the problem is nonlinear. According to Cunningham (12), "the problem of a vibrating mass with Coulomb or dry friction can be assumed to be linear but with an abrupt jump taking place when the velocity changes sign. Considered as a single equation, the problem is nonlinear. However, it may be thought of as two linear equations. Such a problem is said to be linear in segments or piecewise linear. The problem can, therefore, be solved by fitting together solutions of strictly linear equations which can be found with no difficulty".

3.3.3 Forced Vibrations with Rotating-Mass-Type Excitation

The harmonic exciting force caused by an eccentric mass has a force amplitude, $Q_0 = m_0 e \omega^2$. The steady-state solution of Eq. 8.2 with $Q_0 = m_0 e \omega^2$ can be written as

$$\frac{X_0}{\frac{m_0 e \omega^2}{K}} = -R\left(\frac{F}{m_0 e \omega^2}\right) + \sqrt{\frac{1}{q^2} - S^2 \left(\frac{F}{m_0 e \omega^2}\right)^2} \quad (8.24)$$

Eq. 8.24 can be rearranged as

$$\frac{M X_o}{m_o e} = \left(\frac{\omega}{\omega_n} \right)^2 \left[-R \left(\frac{F}{m_o e \omega^2} \right) + \sqrt{\frac{1}{q^2} - s^2 \left(\frac{F}{m_o e \omega^2} \right)^2} \right] \quad (8.25)$$

Eq. 8.25 is, however, not suitable for the presentation of solutions in the form of dimensionless quantities as presented in Figures 8.2(a) to 8.2(j) for the previous case. This is because, a nondimensional friction parameter which does not vary with the exciting frequency is still not defined.

Defining a nondimensional parameter, $\frac{F}{m_o e \omega_n^2}$, as the friction factor, Eq. 8.25 can be written as

$$\frac{M X_o}{m_o e} = \left(\frac{\omega}{\omega_n} \right)^2 \left[-R \beta^2 \frac{F}{m_o e \omega_n^2} + \sqrt{\frac{1}{q^2} - s^2 \beta^4 \left(\frac{F}{m_o e \omega_n^2} \right)^2} \right] \quad (8.26)$$

Eq. 8.26 is in a convenient form so that the nondimensional amplitude factor, $\frac{M X_o}{m_o e}$ can be plotted against the frequency ratio, $\frac{\omega}{\omega_n}$ for various values of viscous damping factor, D and Coulomb friction factor, $\frac{F}{m_o e \omega_n^2}$. The results of Eq. 8.26 are illustrated in Figures 8.3(a) to 8.3(j). As before, Eq. 8.26 gives the complete solution for non-stop motion and is valid when the following conditions are satisfied.

$$\frac{M X_o}{m_o e} \geq \left(\frac{\omega}{\omega_n} \right)^2 \frac{(I - R)}{\sqrt{q^2 (s^2 + I^2)}} \quad (8.27)$$

and

$$\frac{F}{m_0 e \omega_n^2} \geq \left(\frac{\omega}{\omega_n} \right)^2 \frac{1}{\sqrt{q^2 (s^2 + 1^2)}} \quad (8.28)$$

Eqs. 8.27 and 8.28 are valid for all values of $(\omega/\omega_n) \geq 0.5$ and the boundary for non-stop motion as shown by the broken lines of Figures 8.3(a) to 8.3(j) is determined by Eq. 8.27.

The results of Figures 8.2(a) to 8.2(j) and Figures 8.3(a) to 8.3(j) are replotted in a form suitable for ready use, for purposes of design and analyses. The nondimensional resonant amplitudes of motion, $\frac{x_{or}}{Q_0 / K}$ and $\frac{M x_{or}}{m_0 e}$ are plotted against friction factors, $\frac{F}{Q_0}$ and $\frac{F}{m_0 e \omega_n^2}$ for various viscous damping factors, D , in Figures 8.4 and 8.6 respectively.

Similarly, the nondimensional frequency ratio at resonance, $\frac{\omega_r}{\omega_n}$ are plotted against friction factors, $\frac{F}{Q_0}$ and $\frac{F}{m_0 e \omega_n^2}$ for various viscous damping factors, D in Figures 8.5 and 8.7 respectively.

It can be seen from Figure 8.6 and Figure 8.7 that the resonant amplitudes of motion decreases with the increase of the friction factor, $\frac{F}{m_0 e \omega_n^2}$ and the resonant frequency increases with the friction factor respectively. This trend conforms with the observed results of field vibratory tests

on embedded footings where rotating-mass-type of vibrators were used. Therefore, the proposed theoretical model can be used to predict the dynamic response of embedded footings provided all the lumped parameters, K , C and F can be pre-determined from the properties of the soil and the geometry of the foundation.

As described in Section 2.4.3, the parameters K and C can be evaluated, if the values of shear modulus, G , Poisson's ratio, μ , mass density, ρ of the soil and mass ratio, b of the footing are known. This means, that if the total frictional force mobilized between the sides of the footing and the surrounding soil or fill material is known, the dynamic response of the embedded footing can be predicted. The engineer is then faced with the problem of determining the constant frictional force. Fortunately some test data are available from which a reasonable procedure for evaluating the interfacial frictional force between the various types of soils and footing surfaces can be established.

8.4 EVALUATION OF THE CONSTANT FRICTIONAL FORCE

As previously mentioned, the interfacial friction that can be developed along the interface between the sides of the footing and the surrounding soil depends, mainly on the physical characteristics of the interface between the soil and the walls of the foundation besides the lateral earth pressure acting normal to the interface.

For a footing embedded in cohesionless soil, the total amount of constant interfacial friction that would be mobilized during vibrations can be written as

$$F = \frac{1}{2} K_0 \gamma H^2 \mu_f L \quad (8.29)$$

in which K_0 is the coefficient of lateral earth pressure at rest, γ is the bulk density of the soil in which the footing is embedded, H is the depth of embedment into the soil, μ_f is the coefficient of kinematic wall friction between the soil and the surface of foundation walls and L is the perimeter length of the embedded footing.

Similarly, for a footing embedded in a purely cohesive soil, the total amount of interfacial friction that would be mobilized during vibrations can be written as

$$F = C_a H L \quad (8.30)$$

in which C_a is the wall adhesion between the soil and the surface of the foundation wall, under dynamic conditions.

Thus, for a footing embedded in a 'c - ϕ ' soil, the total amount of interfacial friction that would be mobilized during vibrations can be written as

$$F = \left(\frac{1}{2} K_0 \gamma H^2 \mu_f + C_a H \right) L \quad (8.31)$$

It may be noted that in Eq. 8.29 and Eq. 8.31 the lateral earth pressure coefficient at rest, K_0 has been suggested for the vertical mode of vibrations. However,

lateral pressure values which are intermediate between the active and passive cases are entirely possible, especially when the mode of vibrations is not purely vertical.

The coefficient of kinematic friction, μ_f depends on the nature of the surfaces of bodies which rub against each other. In the case of metal surfaces, a substantial amount of published literature on the magnitudes of sliding and rolling friction is available. However, in the field of foundation engineering where one is confronted with the interface of rough concrete surfaces with various types of soils, the coefficient of wall friction is normally taken as $\tan(\frac{2}{3} \phi)$ in which ϕ is the angle of internal friction of the soil. This assumption is found satisfactory for the purpose of analysis of static problems. Since the coefficient of kinematic friction is always less than the coefficient of static friction the magnitude of μ_f can be taken as $\tan(\frac{1}{3} \phi)$ for the purpose of analysis of dynamic problems. The value of μ_f between rough concrete surfaces and most granular and 'c - ϕ ' soils would, thus, fall within a reasonable range of 0.15 to 0.2, depending on the angle of internal friction of the soil.

At this stage, the availability of experimental data is too scant to stipulate specific numerical values for the wall adhesion, C_a under dynamic conditions. However, some

data published by Novak (45) who conducted a series of tests on footings embedded in loess-loam soil, are analysed in the light of the proposed theoretical model to obtain the extent of wall adhesion mobilised under dynamic conditions. The analysis indicated that in such a ' $c - \phi$ ' soil the magnitude of wall adhesion, C_a was of the order of 1 to 2 % of the actual cohesive strength of the soil. Further experimental research on the dynamic behaviour of footings embedded in cohesive soils is desirable to elucidate this observation.

8.5 COMPARISON WITH EXPERIMENTS

In order to predict the values of resonant amplitudes of motion and the resonant frequencies of an embedded footing by means of the proposed theoretical model, described in Eq. 8.1 appropriate values of K , D and F should be evaluated. It may, however, be noted that one of the assumptions of the proposed theoretical model is that no change is effected either in the spring constant, K or the damping factor, D as a result of embedment of the footing. Therefore, the parameters K and D should be evaluated on the basis of the results of steady-state vibration tests on footings which are not embedded or on the basis of the in situ dynamic soil properties obtained from a seismic investigation of the test site.

As previously mentioned in Section 5.2 of Chapter 5, the lumped parameters K and D for each of the test bases

were evaluated on the basis of the results of steady-state vibration tests as well as seismic investigations. The results of these investigations are tabulated in Tables 5.1 and 5.2. For a known damping factor, D and the friction factor, $F/(m_0 e \omega_n^2)$, the decrease in resonant amplitude of motion and the increase in resonant frequency of an embedded footing can be predicted with the use of Figures 8.6 and 8.7 respectively. The constant frictional force, F , developed by any of the Bases-2, 3 and 4, for a given height of back-filled material, H , was calculated as per Eq. 8.29 in which the lateral earth pressure at rest, $K_0 = 0.4$; the bulk density of the compacted sand fill, γ , being approximately equal to 100 pounds per cubic feet; and the coefficient of kinematic friction, $\mu_f = \tan(30/3)^\circ = 0.18$. The values of F , so obtained are tabulated in Table 8.1. The analysis of data reported by Fry (16) was also carried out using Eq. 8.29 in which $K_0 = 0.4$; $\gamma = 100$ pounds per cubic feet and $\mu_f = 0.18$. The friction factors, $F/(m_0 e \omega_n^2)$ for each of the bases at corresponding eccentricity moments, $m_0 e$ and natural frequencies, ω_n can therefore be evaluated and are tabulated in Table 8.1. The predicted values of dimensionless amplitude at resonance, $(M X_{or}/m_0 e)$, resonant amplitude of motion, X_{or} , frequency ratio, (ω_r/ω_n) and resonant frequency, ω_r are tabulated in columns (3, 4, 5 and 6) of Table 8.1 respectively. The experimentally observed

values of dimensionless amplitude at resonance, $(M X_{or}/m_0 e)$, resonant amplitude of motion, X_{or} , frequency ratio, (ω_r/ω_n) and resonant frequency, ω_r are tabulated in columns (7, 8, 9 and 10) of Table 8.1 respectively.

Sufficient test data are not available for the case of cohesive soils to examine the extent of correlation with Eqs. 8.30 and 8.31. However, the results of tests on embedded footings reported by Novak (45) are analysed in the light of the present hypothesis. In this case the reported soil parameters are : $\phi = 31.5^\circ$; $c = 0.35$ kilograms per square centimeters; degree of saturation = 0.56 to 0.76 ; and porosity number = 38.7 to 41.6 % (Therefore $\gamma = 116$ pounds per cubic feet). Assuming $k_o = 0.4$; $\mu_f = \tan(31.5/3)^\circ$ a very satisfactory correlation with Eq. 8.31 is established if wall adhesion, C_a under dynamic condition is taken as about 1 % of the effective cohesion. The results are tabulated in Table 8.1.

The numerical steps involved for one set of computations is illustrated in Appendix A as an example.

Thus, the field test data obtained in the present investigation as well as those published by Novak (45) and

Fry (16) are compared with the values predicted by the proposed theoretical model and are illustrated in Figures 8.8(a) through 8.8(h). The correlation between the available experimental data and the predicted values is found to be quite satisfactory.

TABLE 8.1 COMPARISON BETWEEN THE PREDICTED AND OBSERVED DYNAMIC RESPONSE OF EMBEDDED FOOTINGS.

Base-2 Evaluation of Frictional Force, F (lbs.)									
Depth of Embedment H in Feet	Perimeter Length L in Feet	H/r _o		(From Eq. 9.29) F in Pounds					
0.562	12.56	0.281		14.3					
1.125		0.562		57.2					
1.687		0.843		128.7					
2.250		1.125		228.8					
m _o e= 0.0194 lb.-sec ² ; α = 1.21 ; D= 0.307 ; ω _n = 254.5 sec ⁻¹									
H/r _o	F	Predicted Values of				Observed Values of			
	m _o eω _n ²	$\frac{MX_{or}}{m_{oe}}$	X _{or} in inches	$\frac{\omega_r}{\omega_n}$	ω _r rads. per sec.	$\frac{MX_{or}}{m_{oe}}$	X _{or} in inches	$\frac{\omega_r}{\omega_n}$	ω _r rads. per sec.
(1)	(2)	(3)	(4)	(5)	(6)	(7)	(8)	(9)	(10)
0.281	0.011	1.70	0.00230	1.11	282	1.56	0.00215	1.20	305
0.562	0.046	1.63	0.00220	1.13	288	1.49	0.00205	1.24	316
0.843	0.102	1.55	0.00210	1.16	295	1.38	0.00190	1.28	325
1.125	0.182	1.43	0.00195	1.22	310	1.31	0.00180	1.37	350

Contd.....

Table 8.1 contd...

$m_0 e = 0.0174 \text{ lb.-sec}^2 ; \alpha = 1.21 ; D = 0.309 ; \omega_n = 254.2 \text{ sec}^{-1}$									
(1)	(2)	(3)	(4)	(5)	(6)	(7)	(8)	(9)	(10)
0.281	0.013	1.70	0.00210	1.11	282	1.54	0.00190	1.20	305
0.562	0.051	1.62	0.00200	1.13	288	1.48	0.00180	1.24	316
0.843	0.114	1.52	0.00190	1.17	298	1.36	0.00170	1.28	325
1.125	0.203	1.40	0.00170	1.24	315	1.30	0.00160	1.37	350
$m_0 e = 0.0152 \text{ lb.-sec}^2 ; \alpha = 1.21 ; D = 0.311 ; \omega_n = 253.8 \text{ sec}^{-1}$									
0.281	0.015	1.70	0.00180	1.11	282	1.55	0.00167	1.24	316
0.562	0.059	1.60	0.00170	1.13	286	1.48	0.00160	1.24	316
0.843	0.132	1.50	0.00160	1.18	299	1.34	0.00145	1.33	338
1.125	0.234	1.37	0.00150	1.27	322	1.30	0.00140	1.44	367
$m_0 e = 0.0131 \text{ lb.-sec}^2 ; \alpha = 1.21 ; D = 0.310 ; \omega_n = 253.9 \text{ sec}^{-1}$									
0.281	0.017	1.67	0.00155	1.12	284	1.56	0.00145	1.24	316
0.562	0.068	1.60	0.00150	1.14	289	1.51	0.00140	1.28	325
0.843	0.153	1.47	0.00140	1.20	304	1.34	0.00125	1.33	338
1.125	0.271	1.33	0.00120	1.30	330	1.29	0.00120	1.44	367

Contd.....

Table 8.1 contd...

 $m_0 e = 0.0194 \text{ lb.-sec}^2 ; \mathcal{L} = 1.00 ; D = 0.383 ; \omega_n = 237.4 \text{ sec.}^{-1}$

(1)	(2)	(3)	(4)	(5)	(6)	(7)	(8)	(9)	(10)
0.281	0.013	1.37	0.00228	1.21	287	1.29	0.00215	1.28	305
0.562	0.053	1.33	0.00220	1.24	294	1.23	0.00205	1.33	316
0.843	0.118	1.27	0.00212	1.31	311	1.14	0.00190	1.37	325
1.125	0.210	1.20	0.00199	1.43	339	1.08	0.00180	1.48	350

 $m_0 e = 0.0174 \text{ lb.-sec}^2 ; \mathcal{L} = 1.00 ; D = 0.335 ; \omega_n = 236.9 \text{ sec.}^{-1}$

0.281	0.015	1.37	0.00205	1.21	286	1.27	0.00190	1.28	305
0.562	0.059	1.32	0.00198	1.25	296	1.22	0.00182	1.33	316
0.843	0.132	1.25	0.00187	1.33	315	1.12	0.00168	1.37	325
1.125	0.235	1.18	0.00177	1.47	348	1.07	0.00160	1.48	350

 $m_0 e = 0.0152 \text{ lb.-sec}^2 ; \mathcal{L} = 1.00 ; D = 0.388 ; \omega_n = 236.3 \text{ sec.}^{-1}$

0.281	0.017	1.37	0.00179	1.21	286	1.28	0.00167	1.33	316
0.562	0.067	1.32	0.00172	1.26	298	1.23	0.00160	1.33	316
0.843	0.152	1.25	0.00163	1.35	319	1.11	0.00145	1.42	338
1.125	0.270	1.16	0.00151	1.54	364	1.07	0.00140	1.55	367

Contd.....

Table 8.1 contd...

$m_0 e = 0.0131 \text{ lb.-sec}^2$; $\alpha = 1.00$; $D = 0.337$; $\omega_n = 236.5 \text{ sec.}^{-1}$

(1)	(2)	(3)	(4)	(5)	(6)	(7)	(8)	(9)	(10)
0.281	0.020	1.37	0.00154	1.21	286	1.29	0.00145	1.33	316
0.562	0.078	1.30	0.00146	1.27	300	1.24	0.00140	1.33	325
0.843	0.175	1.22	0.00138	1.38	326	1.11	0.00125	1.42	338
1.125	0.312	1.14	0.00128	1.61	381	1.07	0.00120	1.55	367

$m_0 e = 0.0194$; By Lysmer's Analogue, $D = 0.434$; $\omega_n = 246.0 \text{ sec.}^{-1}$

0.281	0.012	1.25	0.00208	1.28	315	1.29	0.00215	1.24	305
0.562	0.049	1.23	0.00204	1.32	324	1.23	0.00205	1.28	316
0.843	0.110	1.20	0.00199	1.40	344	1.14	0.00190	1.32	325
1.125	0.195	1.15	0.00191	1.55	381	1.08	0.00180	1.42	350

$m_0 e = 0.0174$; By Lysmer's Analogue, $D = 0.434$; $\omega_n = 246.0 \text{ sec.}^{-1}$

0.281	0.014	1.25	0.00187	1.28	315	1.27	0.00190	1.24	305
0.562	0.055	1.23	0.00183	1.33	327	1.22	0.00182	1.28	316
0.843	0.122	1.19	0.00178	1.42	349	1.12	0.00168	1.32	325
1.125	0.218	1.13	0.00169	1.59	391	1.07	0.00160	1.42	350

Contd.....

Table 8.1 contd...

$m_0 e = 0.0152$; By Lysmer's Analogue, $D = 0.434$; $\omega_n = 246.0 \text{ sec.}^{-1}$

(1)	(2)	(3)	(4)	(5)	(6)	(7)	(8)	(9)	(10)
0.281	0.016	1.25	0.00163	1.28	315	1.28	0.00167	1.28	316
0.562	0.062	1.22	0.00159	1.34	330	1.23	0.00160	1.28	316
0.843	0.140	1.17	0.00152	1.45	356	1.11	0.00145	1.37	338
1.125	0.249	1.12	0.00144	1.65	405	1.07	0.00140	1.49	367

$m_0 e = 0.0131$; By Lysmer's Analogue, $D = 0.434$; $\omega_n = 246.0 \text{ sec.}^{-1}$

0.281	0.018	1.25	0.00140	1.29	317	1.29	0.00145	1.28	316
0.562	0.072	1.22	0.00137	1.37	332	1.24	0.00140	1.32	325
0.843	0.163	1.15	0.00129	1.49	366	1.11	0.00125	1.37	338
1.125	0.290	1.10	0.00123	1.75	430	1.07	0.00120	1.49	367

Base-3 Evaluation of Frictional Force, F (lbs.)

Depth of Embedment H in Feet	Perimeter Length L in Feet	H/r_0	(From Eq. 9.29) F in Pounds
1.0	10.66	0.667	38.4
2.0		1.334	153.6
3.0		2.000	345.6
4.0		2.668	614.4

Contd.....

Table 8.1 contd....

 $m_0 e = 0.0194 \text{ lb.-sec}^2 ; \alpha = 1.09 ; D = 0.173 ; \omega_n = 212.7 \text{ sec.}^{-1}$

(1)	(2)	(3)	(4)	(5)	(6)	(7)	(8)	(9)	(10)
0.667	0.044	2.65	0.00400	1.04	222	2.16	0.00330	1.23	261
1.334	0.175	2.25	0.00340	1.07	228	1.90	0.00290	1.32	282
2.000	0.394	1.65	0.00250	1.18	251	1.60	0.00245	1.42	303
2.668	0.700	1.22	0.00190	1.54	328	1.44	0.00220	1.48	315

 $m_0 e = 0.0174 \text{ lb.-sec}^2 ; \alpha = 1.09 ; D = 0.181 ; \omega_n = 212.5 \text{ sec.}^{-1}$

0.667	0.049	2.63	0.00360	1.04	222	2.15	0.00295	1.23	261
1.334	0.196	2.17	0.00290	1.08	230	1.83	0.00250	1.32	282
2.000	0.440	1.57	0.00220	1.21	257	1.61	0.00220	1.42	303
2.668	0.730	1.20	0.00170	1.67	355	1.42	0.00195	1.48	315

 $m_0 e = 0.0152 \text{ lb.-sec}^2 ; \alpha = 1.09 ; D = 0.187 ; \omega_n = 216.5 \text{ sec.}^{-1}$

6.667	0.054	2.60	0.00310	1.04	225	2.13	0.00255	1.21	261
1.334	0.215	2.12	0.00250	1.09	236	1.80	0.00215	1.32	287
2.000	0.483	1.50	0.00180	1.25	271	1.59	0.00190	1.40	303
2.668	0.860	1.16	0.00140	1.83	396	1.42	0.00170	1.50	325

Contd.....

Table 8.1 contd...

 $m_0 e = 0.0131 \text{ lb.-sec.}^2 ; \alpha = 1.09 ; D = 0.184 ; \omega_n = 218.3 \text{ sec.}^{-1}$

(1)	(2)	(3)	(4)	(5)	(6)	(7)	(8)	(9)	(10)
0.667	0.061	2.60	0.00270	1.04	227	2.13	0.00220	1.20	261
1.334	0.246	2.05	0.00210	1.10	240	1.34	0.00190	1.35	294
2.000	0.550	1.40	0.00150	1.32	288	1.60	0.00165	1.39	303
2.668	0.980	1.12	0.00110	2.05	447	1.45	0.00150	1.50	325

 $m_0 e = 0.0194 \text{ lb.-sec.}^2 ; \alpha = 1.00 ; D = 0.195 ; \omega_n = 211.3 \text{ sec.}^{-1}$

0.667	0.045	2.40	0.0040	1.05	222	1.98	0.00330	1.23	261
1.334	0.178	2.05	0.00340	1.09	230	1.74	0.00290	1.32	282
2.000	0.400	1.55	0.00260	1.21	256	1.47	0.00245	1.42	303
2.668	0.710	1.20	0.00200	1.62	342	1.32	0.00220	1.47	315

 $m_0 e = 0.0174 \text{ lb.-sec.}^2 ; \alpha = 1.00 ; D = 0.198 ; \omega_n = 211.0 \text{ sec.}^{-1}$

0.667	0.050	2.40	0.00360	1.05	222	1.98	0.00295	1.23	261
1.334	0.198	2.00	0.00300	1.09	230	1.67	0.00250	1.32	282
2.000	0.446	1.45	0.00220	1.25	264	1.47	0.00220	1.42	303
2.668	0.794	1.15	0.00170	1.77	374	1.31	0.00195	1.47	315

Contd.....

Table 8.1 contd...

 $m_0 e = 0.0152 \text{ lb.-sec.}^2$; $\alpha = 1.00$; $D = 0.205$; $\omega_n = 214.8 \text{ sec.}^{-1}$

(1)	(2)	(3)	(4)	(5)	(6)	(7)	(8)	(9)	(10)
0.667	0.055	2.40	0.00310	1.05	226	1.95	0.00255	1.23	261
1.334	0.220	1.95	0.00250	1.10	236	1.65	0.00215	1.34	287
2.000	0.493	1.40	0.00180	1.30	279	1.46	0.00190	1.42	303
2.668	0.880	1.15	0.00150	1.95	418	1.30	0.00170	1.52	325

 $m_0 e = 0.0131 \text{ lb.-sec.}^2$; $\alpha = 1.00$; $D = 0.201$; $\omega_n = 216.7 \text{ sec.}^{-1}$

0.667	0.062	2.35	0.00260	1.05	228	1.96	0.00220	1.23	261
1.334	0.250	1.90	0.00210	1.12	243	1.69	0.00190	1.37	294
2.000	0.562	1.30	0.00150	1.39	302	1.47	0.00165	1.42	303
2.668	0.999	1.16	0.00120	2.17	470	1.33	0.00150	1.52	325

 $m_0 e = 0.0194$; By Lysmer's Analogue, $D = 0.282$; $\omega_n = 213.0 \text{ sec.}^{-1}$

0.667	0.044	1.75	0.00290	1.10	234	1.98	0.00330	1.23	261
1.334	0.180	1.52	0.00252	1.18	251	1.74	0.00290	1.33	282
2.000	0.400	1.25	0.00208	1.41	300	1.47	0.00245	1.42	303
2.668	0.700	1.11	0.00184	1.95	415	1.32	0.00220	1.48	315

Contd.....

Table 8.1 contd...

$m_0 e = 0.0174$; By Lysmer's Analogue, $D = 0.282$; $\omega_n = 213.0 \text{ sec.}^{-1}$									
(1)	(2)	(3)	(4)	(5)	(6)	(7)	(8)	(9)	(10)
0.667	0.048	1.74	0.00260	1.10	234	1.93	0.00295	1.23	261
1.334	0.195	1.50	0.00224	1.19	254	1.67	0.00250	1.33	282
2.000	0.437	1.23	0.00184	1.45	309	1.47	0.00220	1.42	303
2.668	0.780	1.09	0.00163	2.10	447	1.31	0.00195	1.48	315
$m_0 e = 0.0152$; By Lysmer's Analogue, $D = 0.282$; $\omega_n = 213.0 \text{ sec.}^{-1}$									
0.667	0.056	1.74	0.00226	1.11	236	1.95	0.00255	1.23	261
1.334	0.223	1.46	0.00191	1.21	258	1.65	0.00215	1.35	287
2.000	0.500	1.19	0.00155	1.56	332	1.46	0.00190	1.42	303
2.668	0.890	1.06	0.00138	2.33	496	1.30	0.00170	1.52	325
$m_0 e = 0.0131$; By Lysmer's Analogue, $D = 0.282$; $\omega_n = 213.0 \text{ sec.}^{-1}$									
0.667	0.065	1.72	0.00193	1.11	236	1.96	0.00220	1.23	261
1.334	0.258	1.42	0.00160	1.24	264	1.69	0.00190	1.38	294
2.000	0.580	1.15	0.00129	1.70	362	1.47	0.00165	1.42	303
2.668	1.030	1.05	0.00118	2.56	545	1.33	0.00150	1.52	325

Contd.....

Table 8.1 contd...

Base-4 Evaluation of Frictional Force, F (lbs.)									
Depth of Embedment H in Feet	Perimeter Length L in Feet		H/r ₀		(From Eq. 8.29) F in Pounds				
0.562	14.16		0.281		16.2				
1.125			0.562		64.8				
1.687			0.843		145.8				
2.250			1.125		259.2				
$m_0 e = 0.0194 \text{ lb.-sec.}^2$; $\alpha = 1.21$; $D = 0.323$; $\omega_n = 251.4 \text{ sec.}^{-1}$									
(1)	(2)	(3)	(4)	(5)	(6)	(7)	(8)	(9)	(10)
0.281	0.013	1.60	0.00220	1.13	284	1.42	0.00195	1.21	305
0.562	0.053	1.55	0.00210	1.15	289	1.34	0.00185	1.25	316
0.843	0.120	1.45	0.00200	1.20	302	1.27	0.00175	1.29	325
1.125	0.210	1.35	0.00185	1.28	322	1.24	0.00170	1.39	350
$m_0 e = 0.0174 \text{ lb.-sec.}^2$; $\alpha = 1.21$; $D = 0.336$; $\omega_n = 248.7 \text{ sec.}^{-1}$									
0.281	0.015	1.56	0.00190	1.14	284	1.38	0.00170	1.22	305
0.562	0.060	1.50	0.00185	1.18	293	1.34	0.00165	1.27	316
0.843	0.135	1.40	0.00170	1.23	306	1.28	0.00157	1.31	325
1.125	0.240	1.30	0.00160	1.34	333	1.22	0.00150	1.41	350

Contd.....

Table 8.1 contd...

 $m_{oe} = 0.0152$; lb.-sec.² ; $\alpha_c = 1.21$; $D = 0.337$; $\omega_n = 248.5 \text{ sec}^{-1}$

(1)	(2)	(3)	(4)	(5)	(6)	(7)	(8)	(9)	(10)
0.281	0.017	1.55	0.00165	1.15	286	1.39	0.00150	1.27	316
0.562	0.069	1.50	0.00160	1.18	294	1.32	0.00142	1.31	325
0.843	0.155	1.38	0.00150	1.25	311	1.27	0.00137	1.36	338
1.125	0.276	1.25	0.00135	1.38	343	1.21	0.00130	1.48	367

 $m_{oe} = 0.0131$ lb.-sec.² ; $\alpha_c = 1.21$; $D = 0.341$; $\omega_n = 247.6 \text{ sec}^{-1}$

0.281	0.020	1.53	0.00140	1.15	284	1.40	0.00130	1.27	316
0.562	0.081	1.45	0.00135	1.20	297	1.34	0.00125	1.31	325
0.843	0.183	1.33	0.00125	1.28	316	1.29	0.00120	1.36	338
1.125	0.324	1.20	0.00110	1.46	361	1.24	0.00115	1.48	367

 $m_{oe} = 0.0194$ lb.-sec.² ; $\alpha_c = 1.00$; $D = 0.404$; $\omega_n = 231.8 \text{ sec}^{-1}$

0.281	0.016	1.30	0.00216	1.25	289	1.17	0.00195	1.31	305
0.562	0.062	1.25	0.00208	1.31	303	1.11	0.00185	1.36	316
0.843	0.140	1.20	0.00200	1.41	327	1.05	0.00175	1.40	325
1.125	0.250	1.14	0.00190	1.60	370	1.02	0.00170	1.51	350

Contd.....

Table 8.1 contd....

$m_0 e = 0.0174 \text{ lb.-sec.}^2 ; \alpha = 1.00 ; D = 0.422 ; \omega_n = 226.6 \text{ sec.}^{-1}$									
(1)	(2)	(3)	(4)	(5)	(6)	(7)	(8)	(9)	(10)
0.281	0.018	1.30	0.00194	1.26	286	1.14	0.00170	1.34	305
0.562	0.072	1.25	0.00187	1.32	299	1.11	0.00165	1.39	316
0.843	0.162	1.17	0.00175	1.44	326	1.06	0.00157	1.43	325
1.125	0.290	1.12	0.00167	1.69	383	1.01	0.00150	1.54	350
$m_0 e = 0.0152 \text{ lb.-sec.}^2 ; \alpha = 1.00 ; D = 0.424 ; \omega_n = 226.3 \text{ sec.}^{-1}$									
0.281	0.021	1.29	0.00168	1.26	285	1.15	0.00150	1.39	316
0.562	0.083	1.23	0.00160	1.33	301	1.09	0.00142	1.44	325
0.843	0.187	1.15	0.00150	1.49	337	1.05	0.00137	1.49	338
1.125	0.330	1.10	0.00143	1.78	403	1.00	0.00130	1.62	367
$m_0 e = 0.0131 \text{ lb.-sec.}^2 ; \alpha = 1.00 ; D = 0.430 ; \omega_n = 225.0 \text{ sec.}^{-1}$									
0.281	0.024	1.28	0.00144	1.26	284	1.16	0.00130	1.40	316
0.562	0.094	1.22	0.00138	1.35	304	1.11	0.00125	1.45	325
0.843	0.214	1.15	0.00129	1.53	344	1.07	0.00120	1.50	338
1.125	0.380	1.08	0.00121	1.90	427	1.02	0.00115	1.64	367

Contd.....

Table 8.1 contd...

$m_{oe} = 0.0194$; By Lysmer's Analogue, $D = 0.434$; $\omega_n = 246.0 \text{ sec}^{-1}$

(1)	(2)	(3)	(4)	(5)	(6)	(7)	(8)	(9)	(10)
0.281	0.014	1.26	0.00210	1.28	314	1.17	0.00195	1.24	305
0.562	0.055	1.23	0.00214	1.33	327	1.11	0.00185	1.28	316
0.843	0.124	1.18	0.00196	1.43	352	1.05	0.00175	1.32	325
1.125	0.221	1.13	0.00188	1.60	393	1.02	0.00170	1.42	350

$m_{oe} = 0.0174$; By Lysmer's Analogue, $D = 0.434$; $\omega_n = 246.0 \text{ sec}^{-1}$

0.281	0.015	1.26	0.00188	1.28	314	1.14	0.00170	1.24	305
0.562	0.062	1.23	0.00184	1.34	330	1.11	0.00165	1.28	316
0.843	0.139	1.17	0.00175	1.45	356	1.05	0.00157	1.32	325
1.125	0.247	1.12	0.00167	1.65	405	1.01	0.00150	1.42	350

$m_{oe} = 0.0152$; By Lysmer's Analogue, $D = 0.434$; $\omega_n = 246.0 \text{ sec}^{-1}$

0.281	0.018	1.25	0.00163	1.29	317	1.15	0.00150	1.28	316
0.562	0.071	1.22	0.00159	1.35	332	1.09	0.00142	1.32	325
0.843	0.158	1.16	0.00151	1.48	364	1.05	0.00137	1.37	338
1.125	0.282	1.16	0.00144	1.72	423	1.00	0.00130	1.49	367

Contd.....

Table 8.1 contd.....

$m_0 e = 0.0131$; By Lysmer's Analogue, $D = 0.434$; $(\omega)_n = 246.0 \text{ sec}^{-1}$									
(1)	(2)	(3)	(4)	(5)	(6)	(7)	(8)	(9)	(10)
0.281	0.021	1.25	0.00141	1.29	317	1.16	0.00130	1.28	316
0.562	0.082	1.21	0.00136	1.36	334	1.11	0.00125	1.32	325
0.843	0.184	1.15	0.00129	1.53	376	1.07	0.00120	1.37	338
1.125	0.327	1.09	0.00123	1.83	450	1.02	0.00115	1.49	367
Eglin Base Data, After Fry (1963) ; Evaluation of Frictional Force, F (lbs.)									
Weight of Footing + Vibrator in Pounds	Base Size in Feet	Depth of Embedment H in Feet	Perimeter Length L in Feet	H/ r_0	F in Pounds				
30970	7.30 dia	2.08	22.9	0.57	360				
$m_0 e = 1.468 \text{ lb.-sec.}^2$; $\alpha = 1.23$; $D = 0.330$; $(\omega)_n = 83.5 \text{ sec.}^{-1}$									
(1)	(2)	(3)	(4)	(5)	(6)	(7)	(8)	(9)	(10)
0.00	0.00	-	-	-	-	1.59	0.0235	1.13	94.3
0.57	0.035	1.55	0.0230	1.15	96.0	1.41	0.0210	1.20	100.5

Contd.....

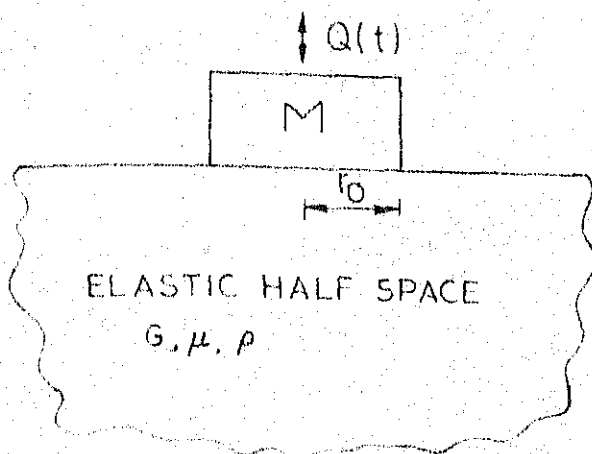
Table 8.1 contd....

$m_0 e = 1.106 \text{ lb.-sec.}^2 ; \mathcal{L} = 1.23 ; D = 0.330 ; \omega_n = 83.5 \text{ sec.}^{-1}$									
(1)	(2)	(3)	(4)	(5)	(6)	(7)	(8)	(9)	(10)
0.00	0.00	-	-	-	-	1.60	0.0178	1.13	94.3
0.57	0.047	1.54	0.0170	1.16	96.8	1.35	0.0150	1.20	100.5
$m_0 e = 0.735 \text{ lb.-sec.}^2 ; \mathcal{L} = 1.23 ; D = 0.330 ; \omega_n = 83.5 \text{ sec.}^{-1}$									
0.00	0.00	-	-	-	-	1.61	0.0120	1.13	94.3
0.57	0.070	1.50	0.0110	1.17	97.7	1.34	0.0100	1.24	103.6
$m_0 e = 0.363 \text{ lb.-sec.}^2 ; \mathcal{L} = 1.23 ; D = 0.330 ; \omega_n = 88.5 \text{ sec.}^{-1}$									
0.00	0.00	-	-	-	-	1.60	0.0062	1.13	100.5
0.57	0.125	1.43	0.0056	1.21	107.0	1.44	0.0056	1.20	106.8
$m_0 e = 1.468 \text{ lb.-sec.}^2 ; \mathcal{L} = 1.00 ; D = 0.420 ; \omega_n = 76.0 \text{ sec.}^{-1}$									
0.00	0.00	-	-	-	-	1.29	0.0235	1.24	94.3
0.57	0.0425	1.27	0.0230	1.29	98.0	1.15	0.0210	1.32	100.5
$m_0 e = 1.106 \text{ lb.-sec.}^2 ; \mathcal{L} = 1.00 ; D = 0.420 ; \omega_n = 76.0 \text{ sec.}^{-1}$									
0.00	0.00	-	-	-	-	1.30	0.0178	1.24	94.3
0.57	0.0565	1.26	0.0170	1.30	98.8	1.10	0.0150	1.32	100.5

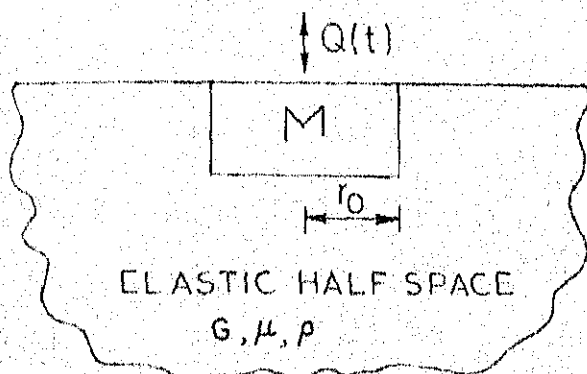
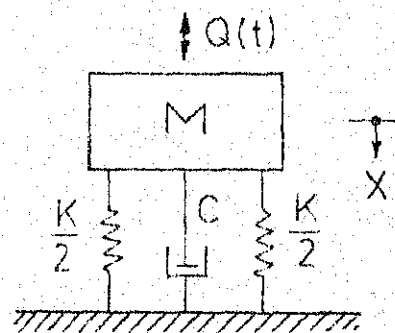
Contd.....

Table 8.1 contd....

$m_0e = 0.735 \text{ lb.-sec.}^2$; $\alpha = 1.00$; $D = 0.420$; $\omega_n = 76.0 \text{ sec.}^{-1}$									
(1)	(2)	(3)	(4)	(5)	(6)	(7)	(8)	(9)	(10)
0.00	0.00	-	-	-	-	1.31	0.0120	1.24	94.3
0.57	0.0845	1.23	0.0110	1.34	102.0	1.09	0.0100	1.37	103.6
$m_0e = 0.368 \text{ lb.-sec.}^2$; $\alpha = 1.00$; $D = 0.420$; $\omega_n = 81.0 \text{ sec.}^{-1}$									
0.00	0.00	-	-	-	-	1.30	0.0062	1.24	100.5
0.57	0.148	1.19	0.0057	1.42	115.0	1.17	0.0056	1.32	106.8
Data After Novak (1970) ; Evaluation of Frictional Force, F (lbs.)									
Weight of Footing + Vibrator in Pounds	Base Size in Feet	Depth of Embedment H in Feet	Perimeter Length L in Feet	H/r ₀	F in Pounds				
5500	3.28	1.094	13.124	0.591	164.0				
	by 3.28	2.187		1.182	466.0				
$m_0e = 0.0259 \text{ lb.-sec.}^2$; $\alpha = 1.15$; $D = 0.163$; $\omega_n = 208.8 \text{ sec.}^{-1}$									
0.00	0.00	-	-	-	-	3.11	0.00492	1.03	215
0.591	0.145	2.60	0.00411	1.05	219	2.36	0.00374	1.32	276
1.182	0.412	1.75	0.00277	1.15	240	1.36	0.00216	1.70	355
$m_0e = 0.0259 \text{ lb.-sec.}^2$; $\alpha = 1.00$; $D = 0.188$; $\omega_n = 206.8 \text{ sec.}^{-1}$									
0.00	0.00	-	-	-	-	2.70	0.00492	1.04	215
0.591	0.147	2.25	0.00410	1.07	222	2.06	0.00374	1.33	276
1.182	0.420	1.56	0.00284	1.20	248	1.19	0.00216	1.72	355



(a)



(b)

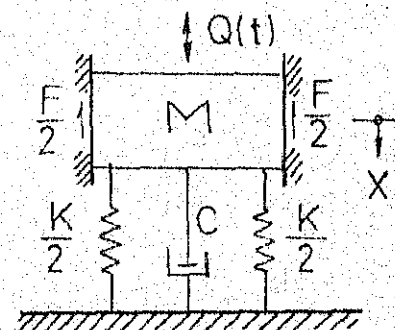


FIG. 8.1 THE ELASTIC HALF-SPACE MODEL AND THE EQUIVALENT SINGLE-DEGREE-OF-FREEDOM ANALOGUE. a) A RIGID CIRCULAR FOOTING ON SURFACE OF SOIL. b) A RIGID CIRCULAR FOOTING EMBEDDED IN SOIL.

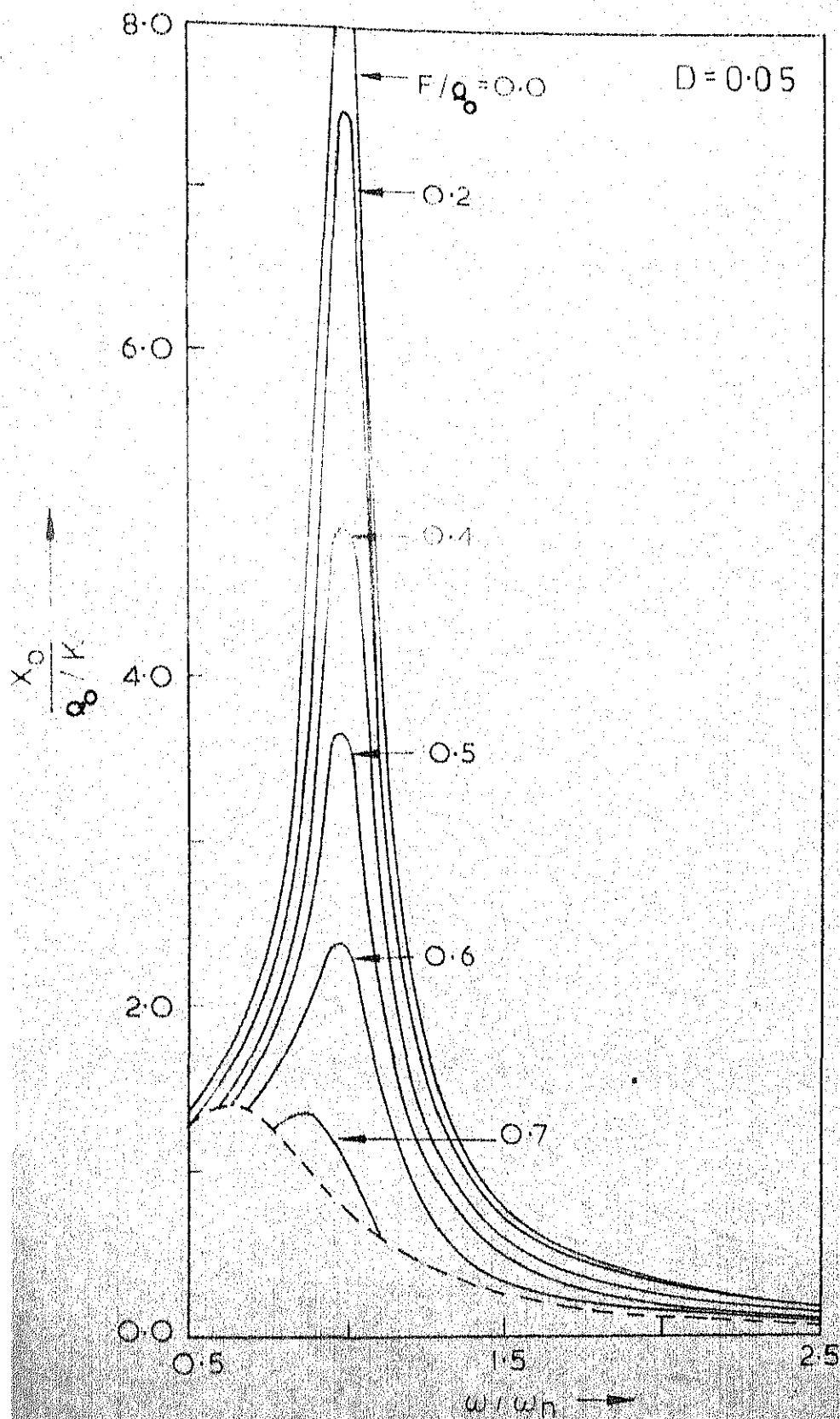


FIG. 8.2 AMPLITUDE-FREQUENCY RELATIONS FOR A LUMPED MASS-SPRING
(a) SYSTEM WITH COMBINED VISCOUS AND COULOMB FRICTION
DAMPING FOR CONSTANT AMPLITUDE EXCITING FORCE

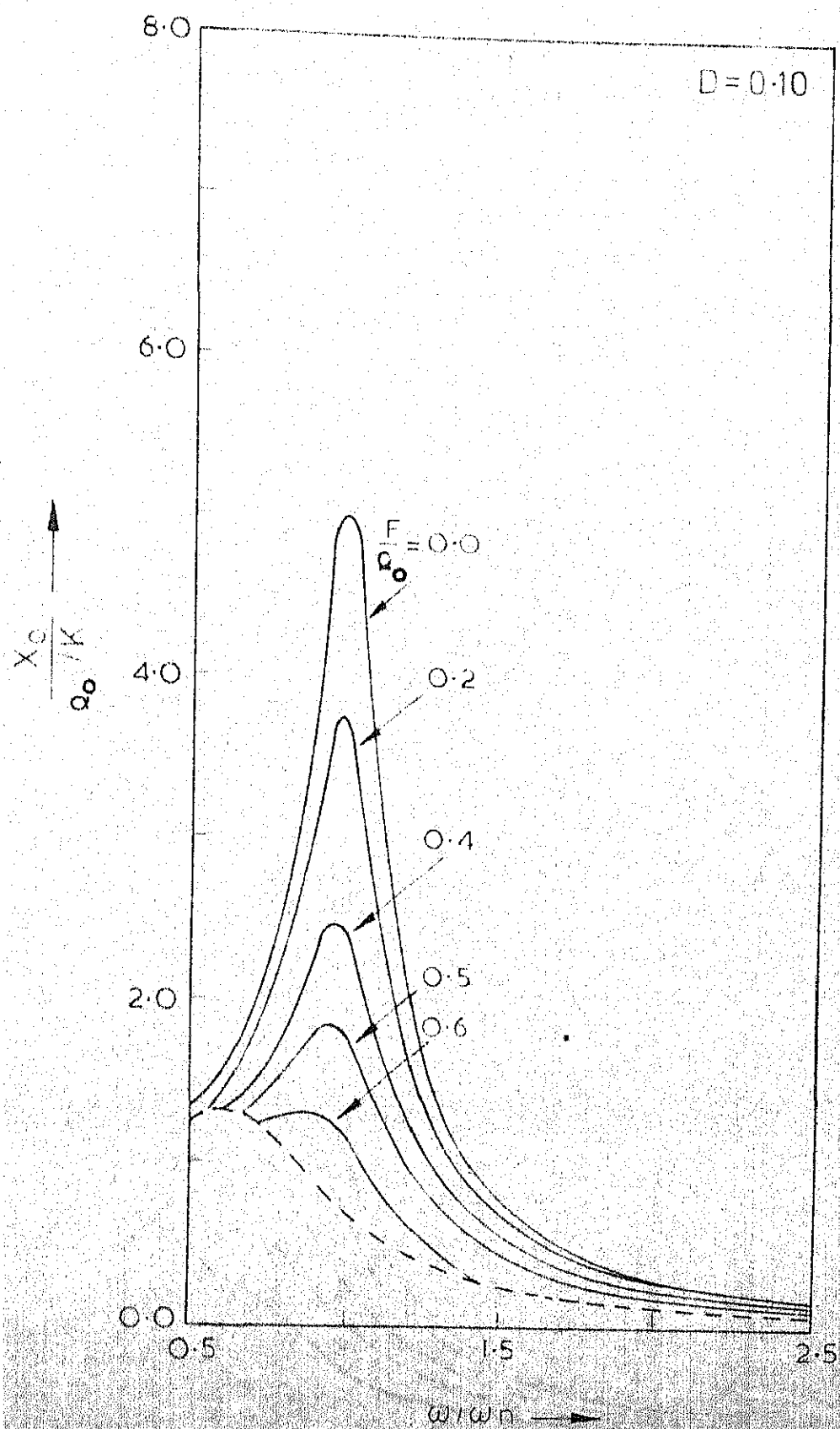


FIG. 8.2(b)

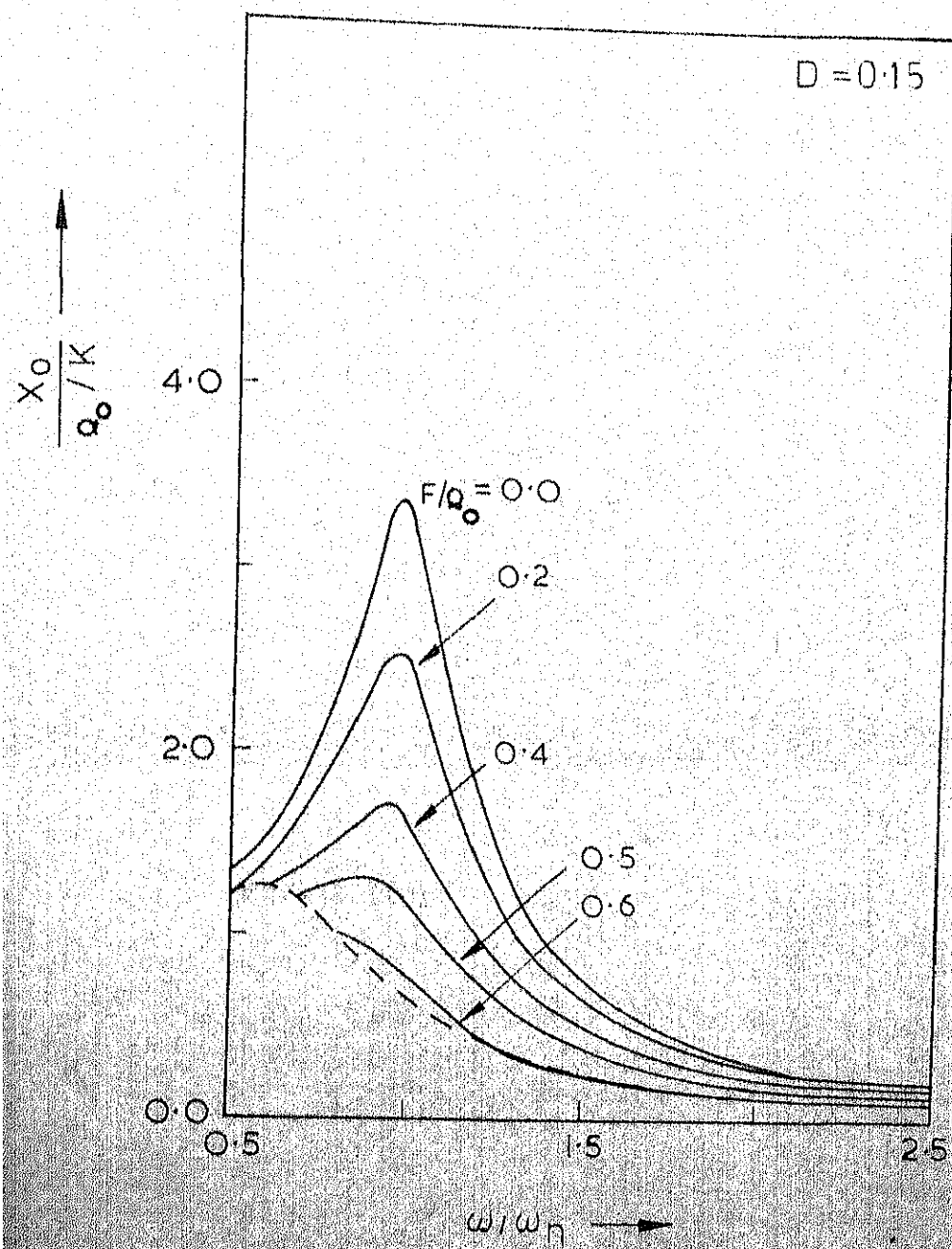


FIG. 8.2(c)

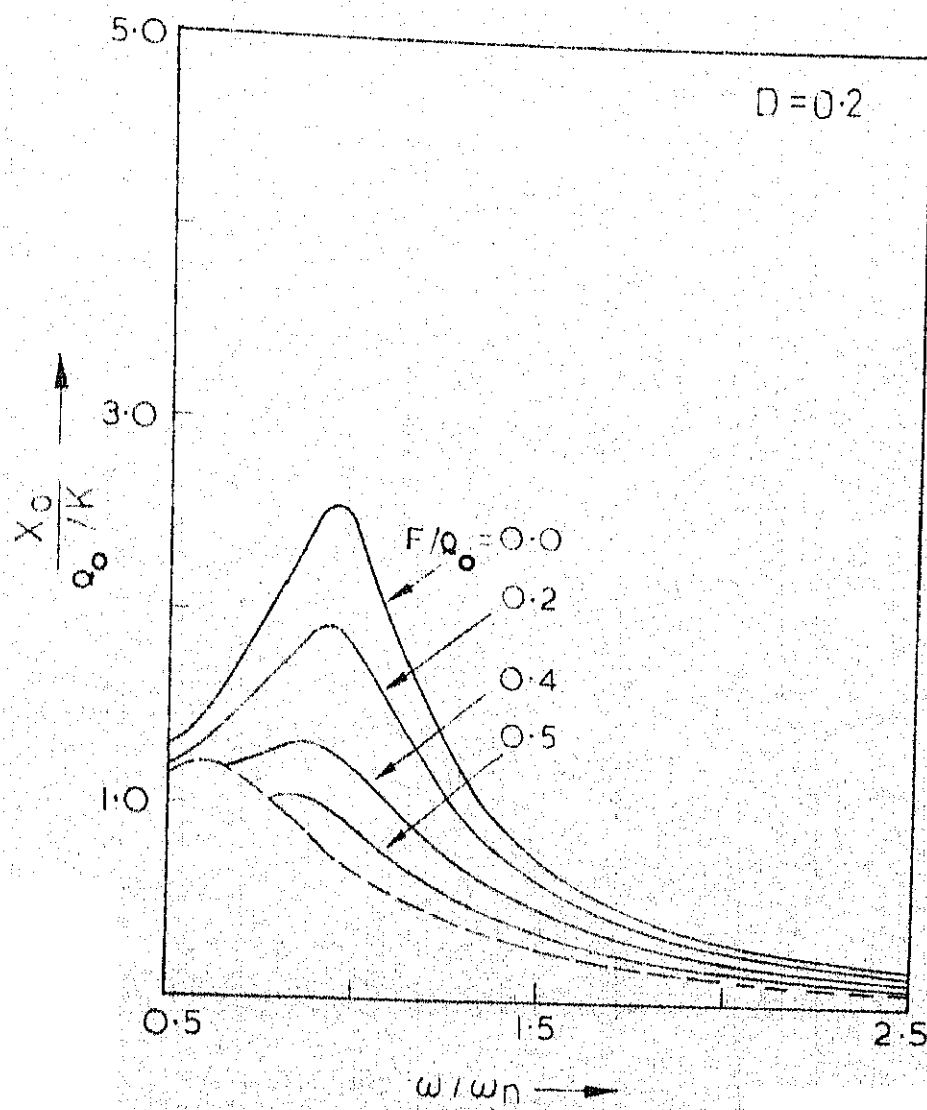


FIG. 8.2(d)

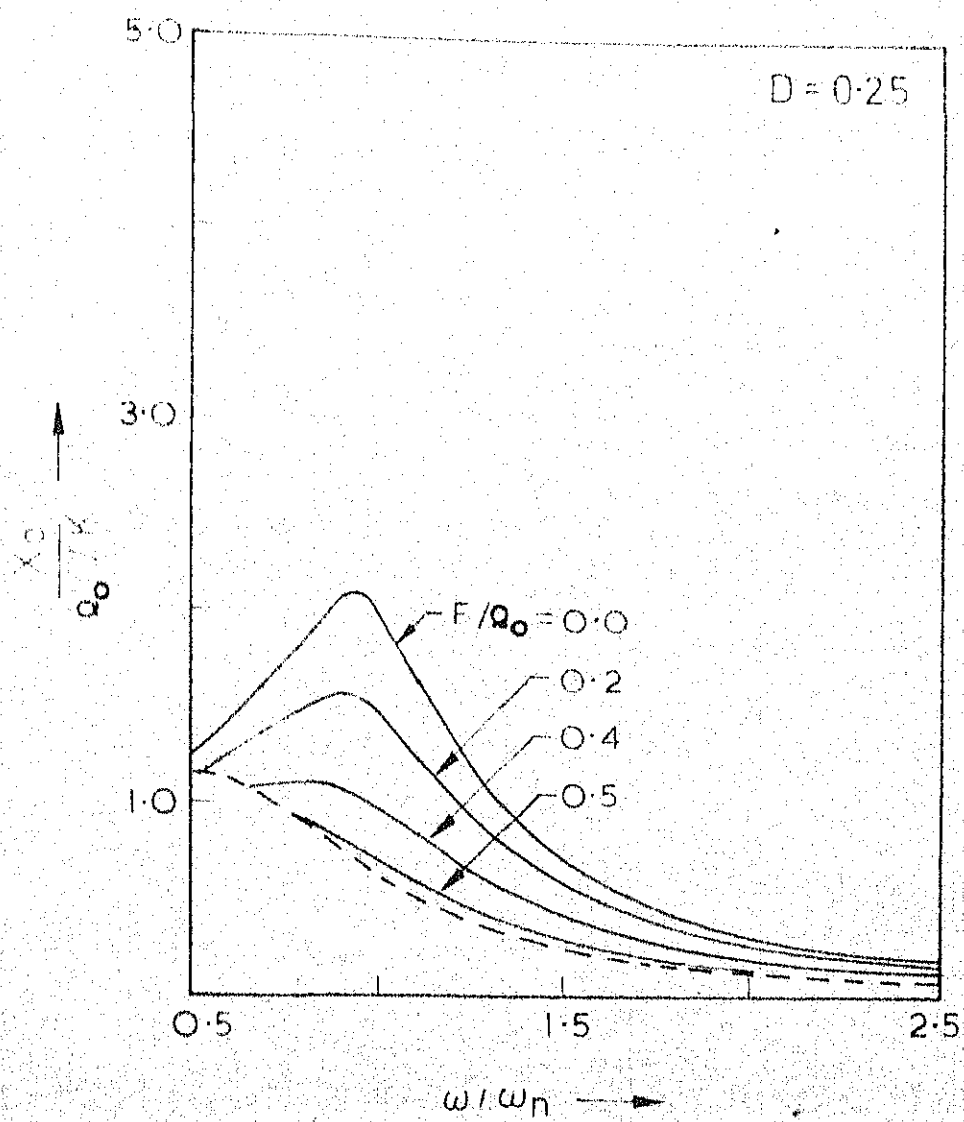


FIG. 8.2(e)

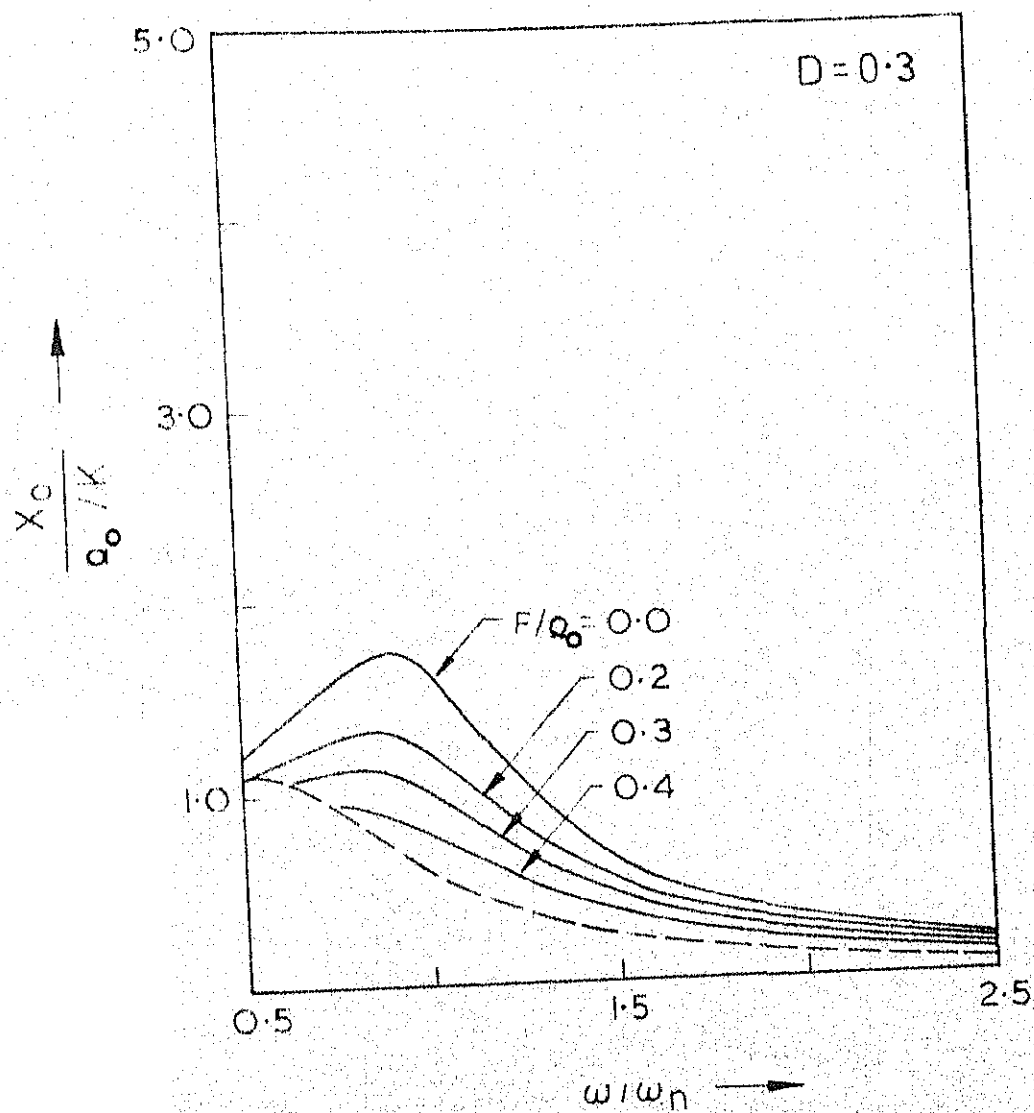


FIG. 8.2(f)

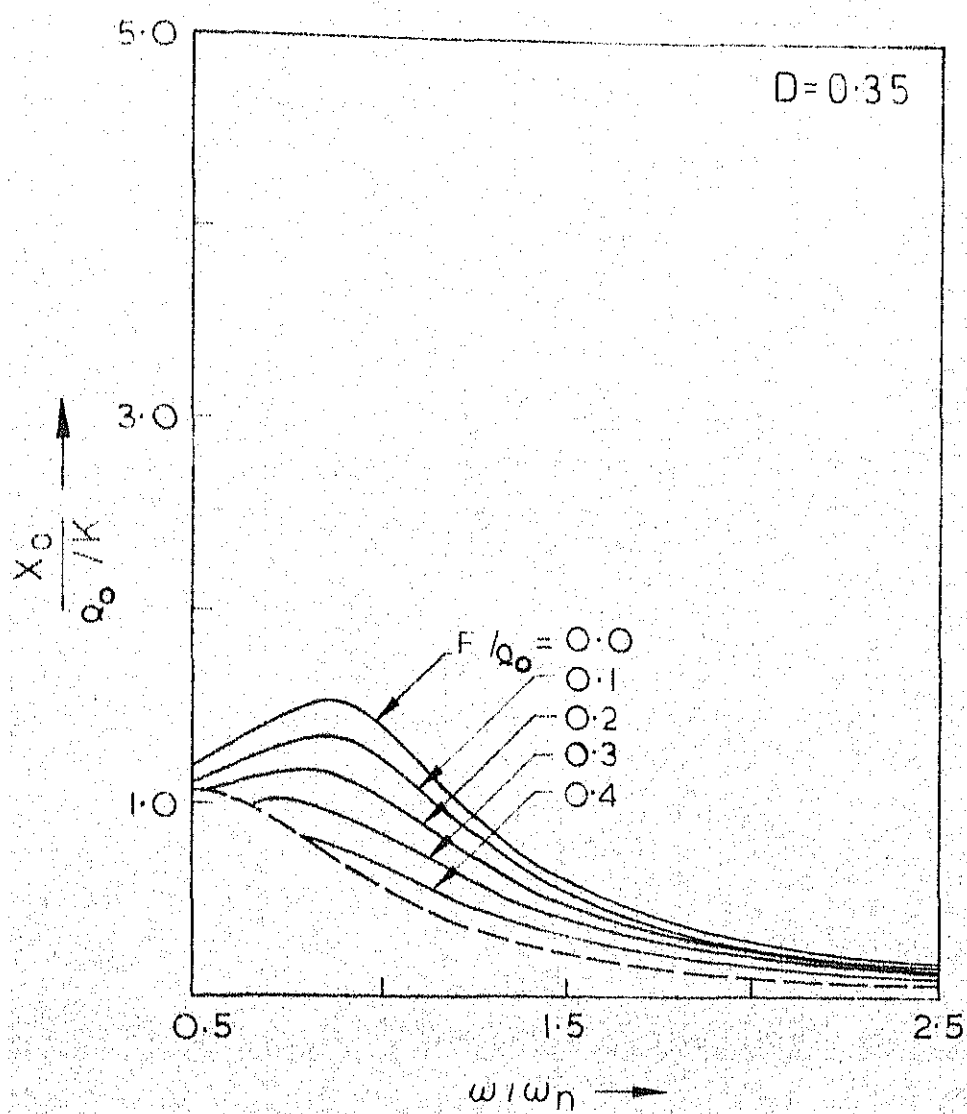


FIG. 8.2(g)

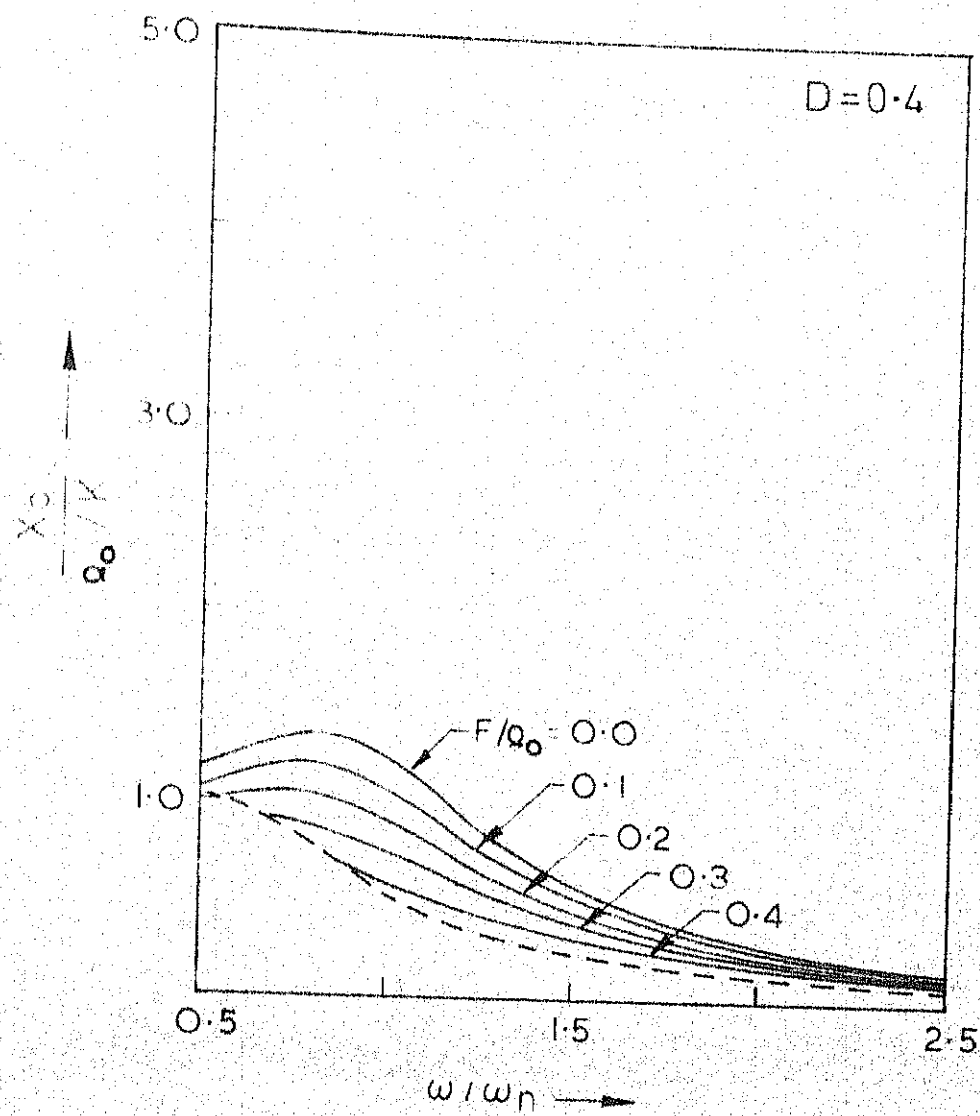


FIG. 8.2(h)

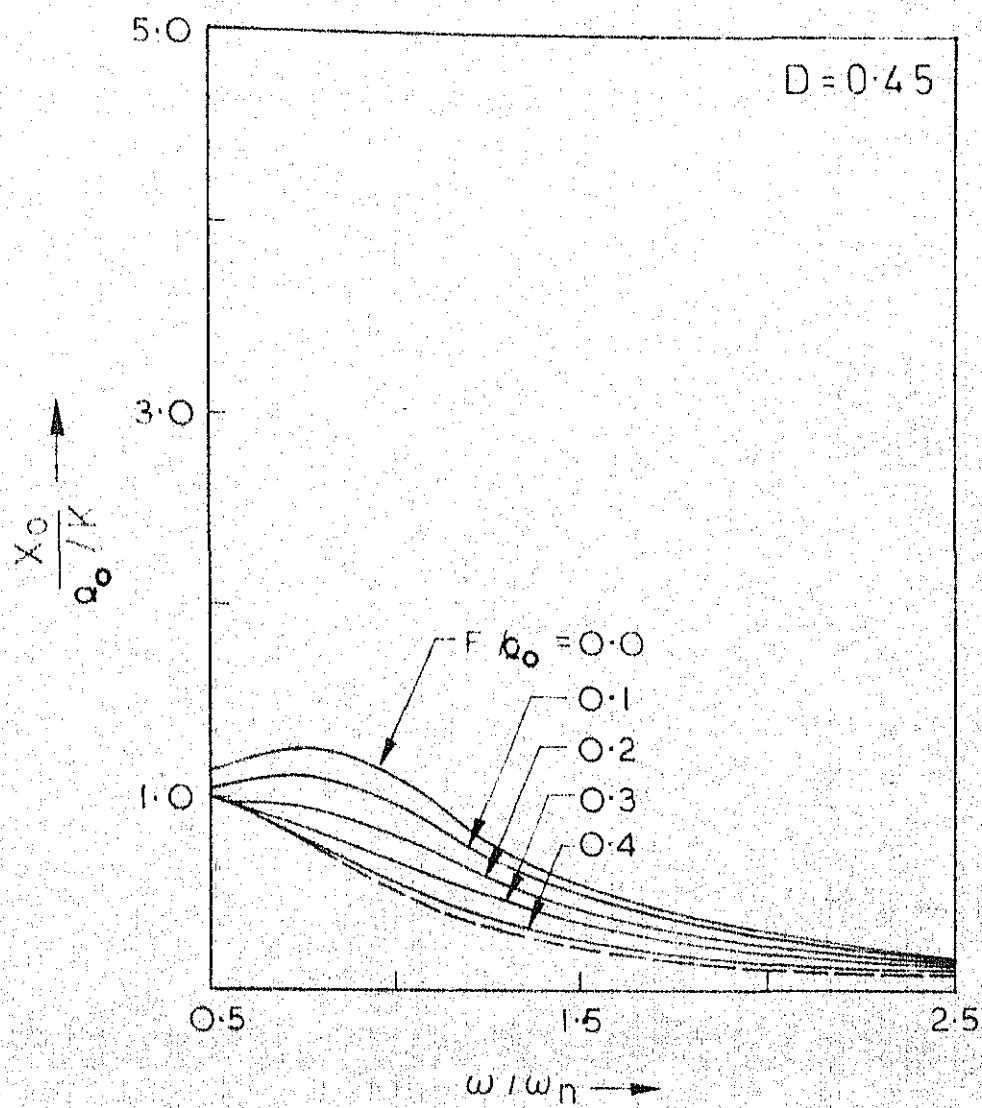


FIG. 8.2(1)

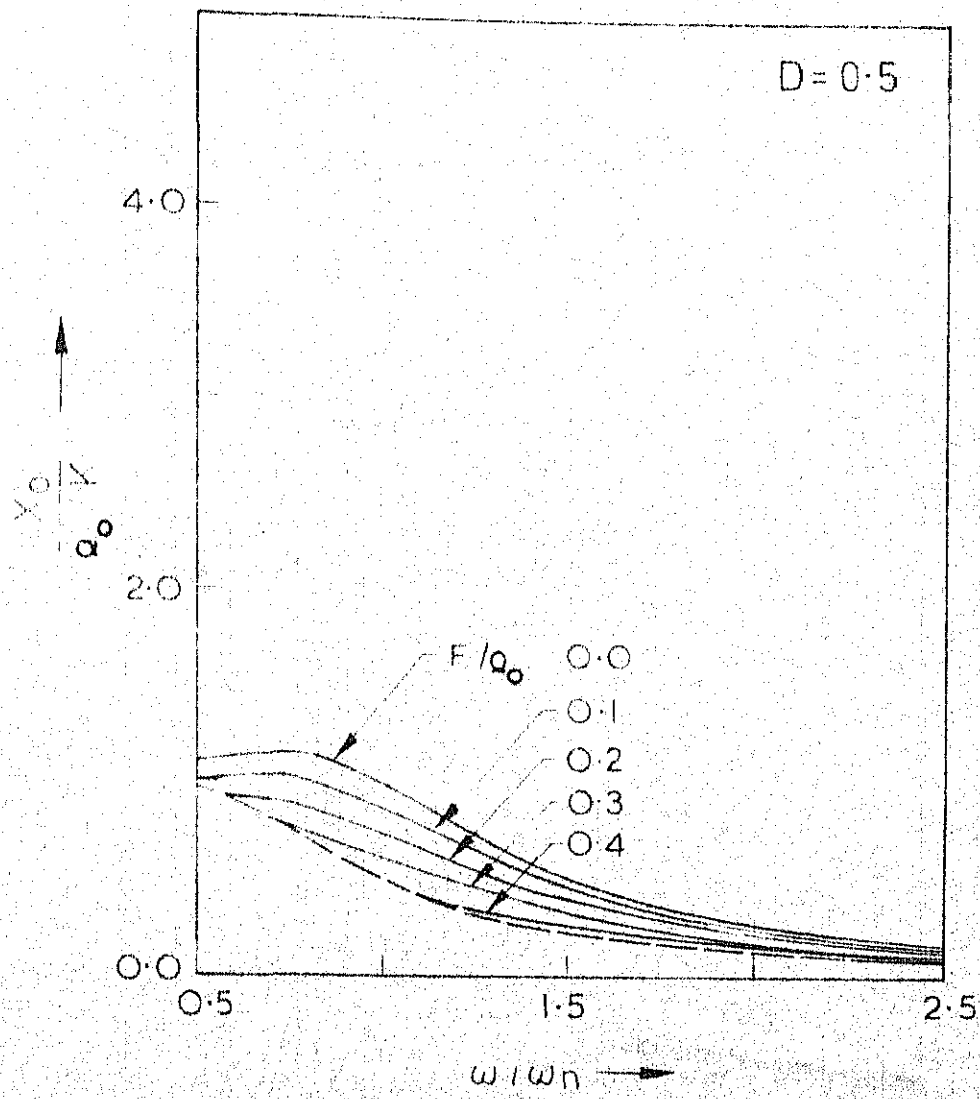
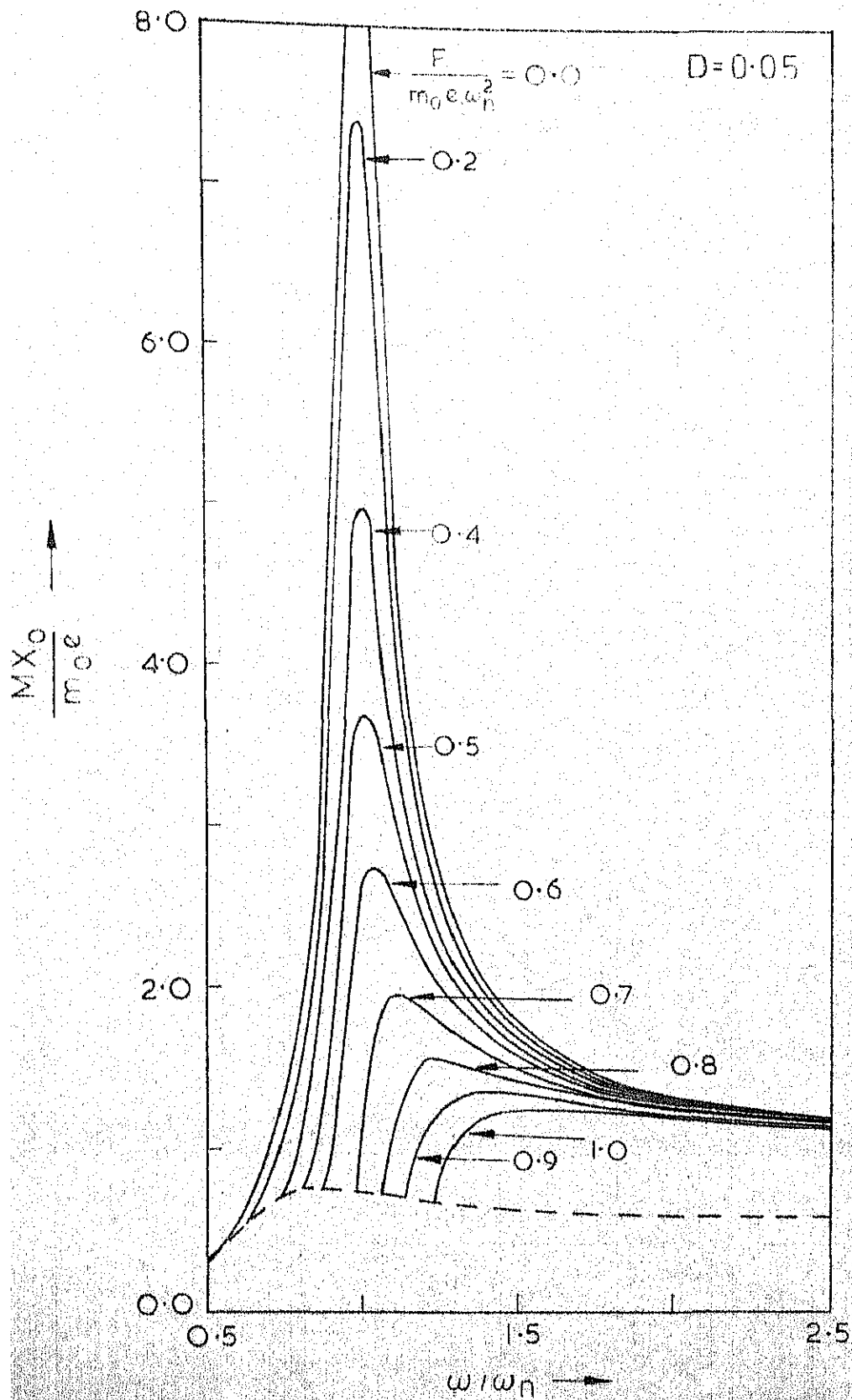


FIG. 8.2(j)



G.8.3 (a) AMPLITUDE-FREQUENCY RELATIONS FOR A LUMPED MASS-SPRING SYSTEM WITH COMBINED VISCOUS AND COULOMB FRICTION DAMPING FOR EXCITING FORCE DUE TO ECCENTRIC ROTATING MASSES

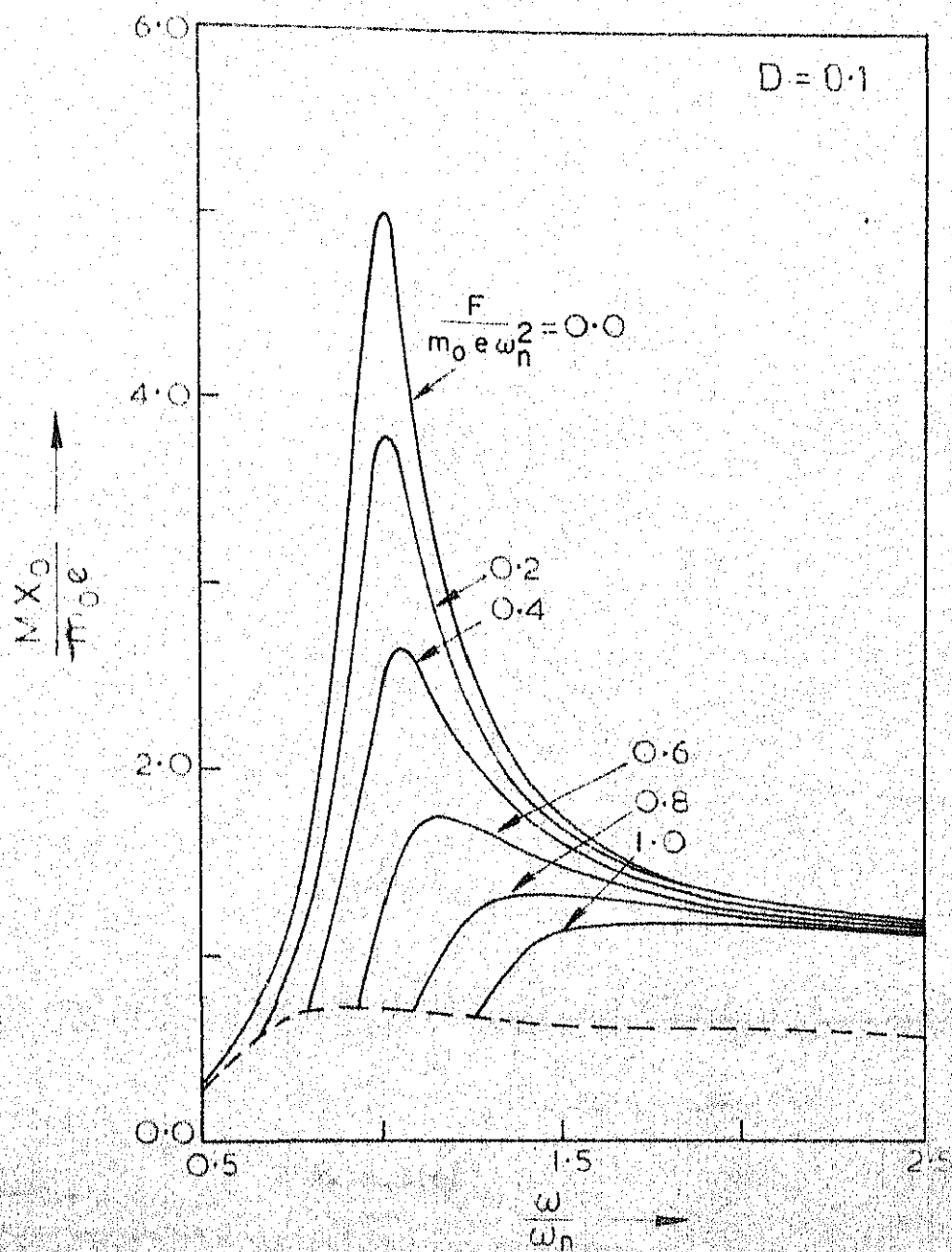


FIG. 8.3(b).

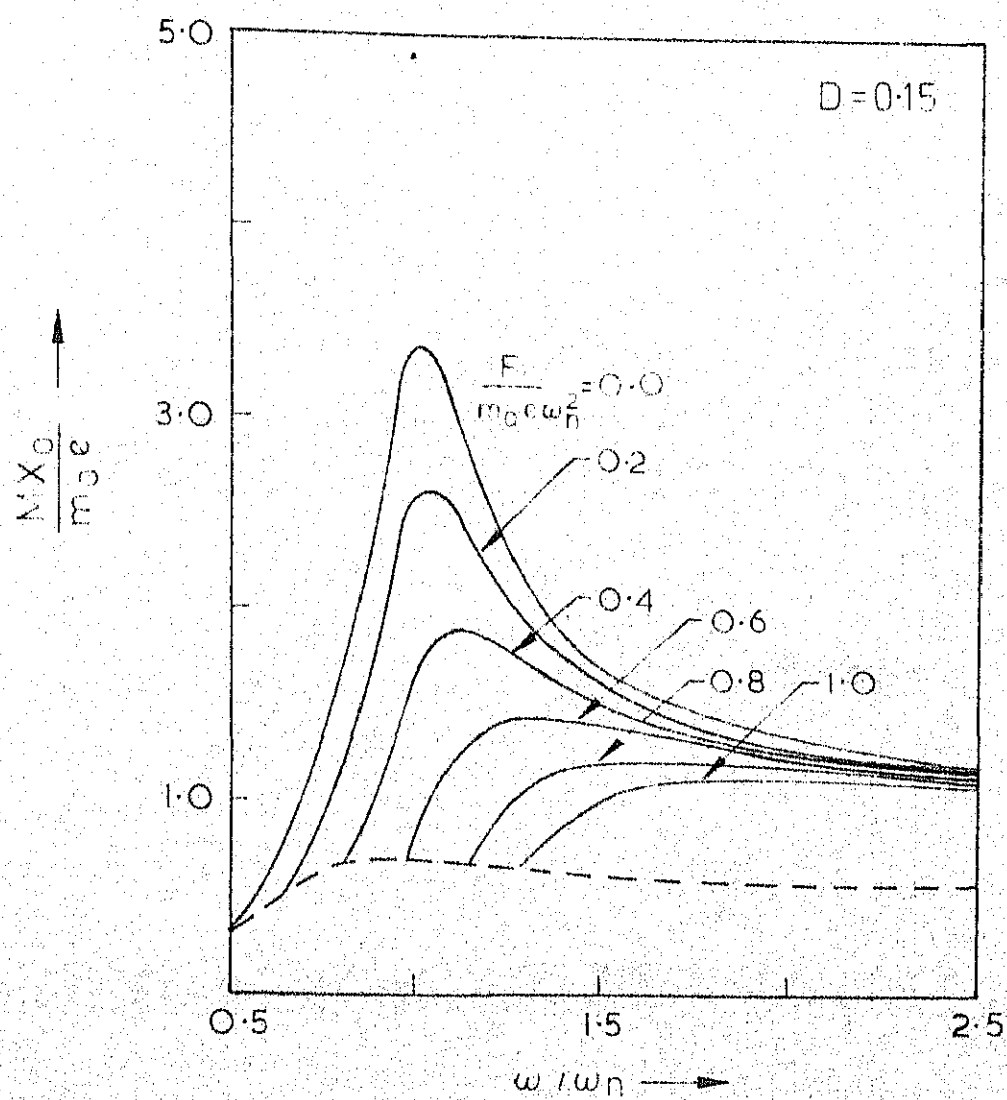


FIG. 8.3(c)

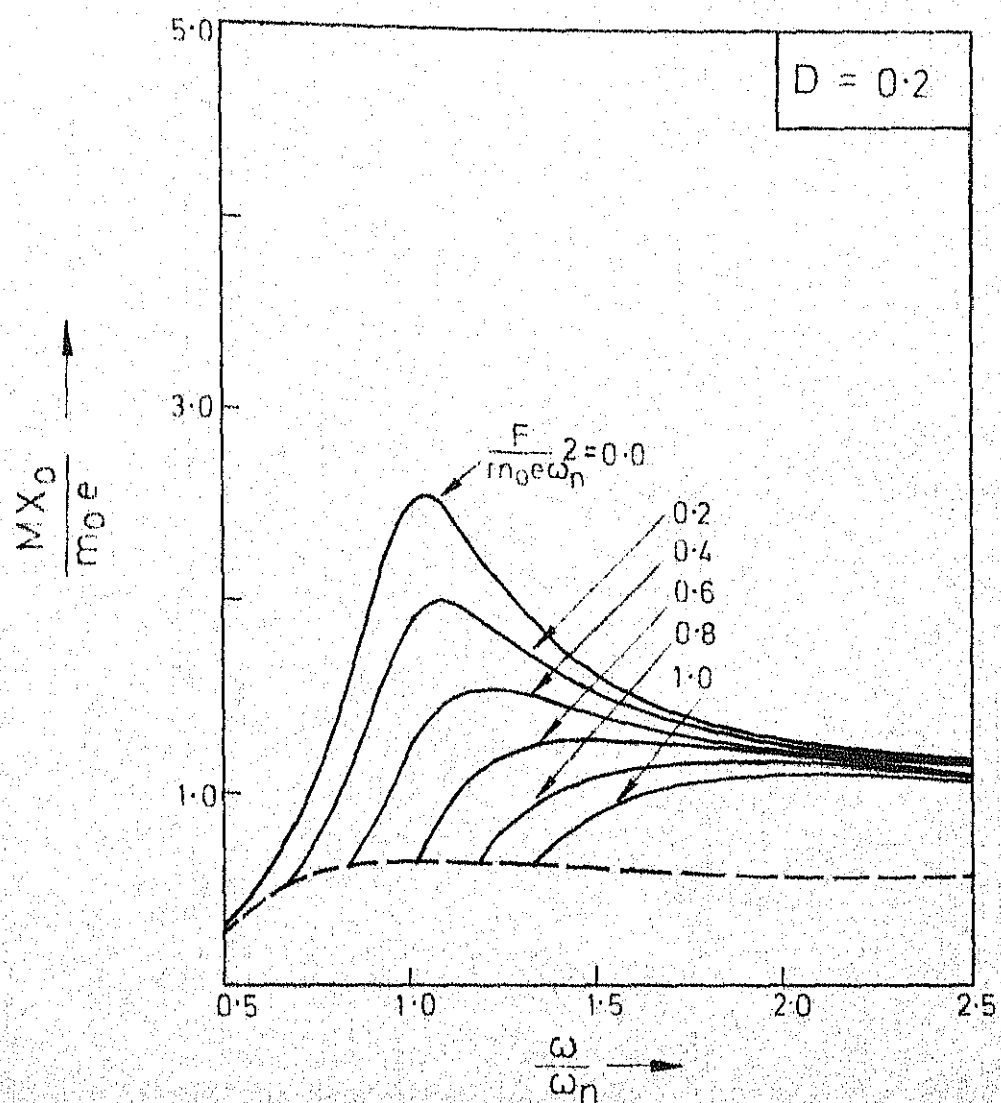


FIG. 8.3(d).

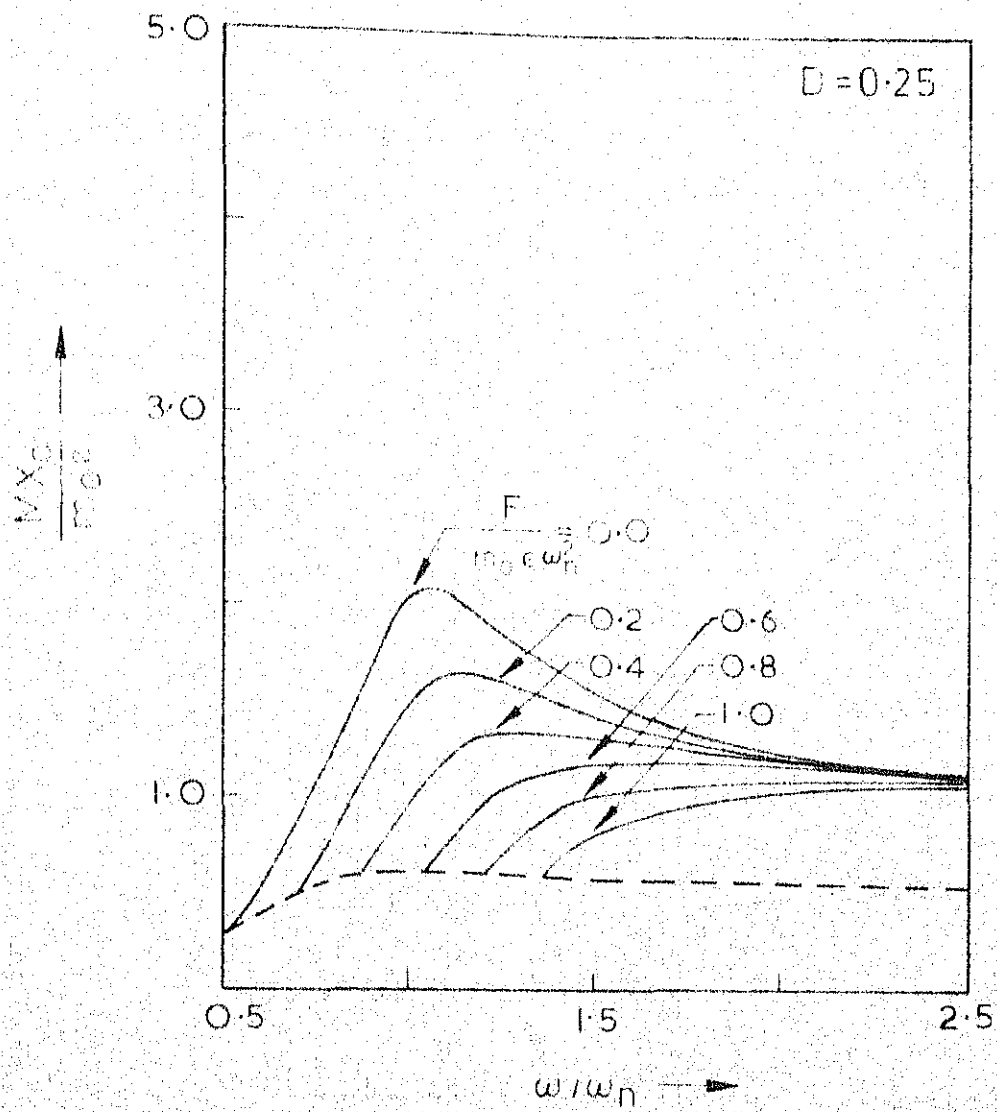


FIG. 8.3(e)

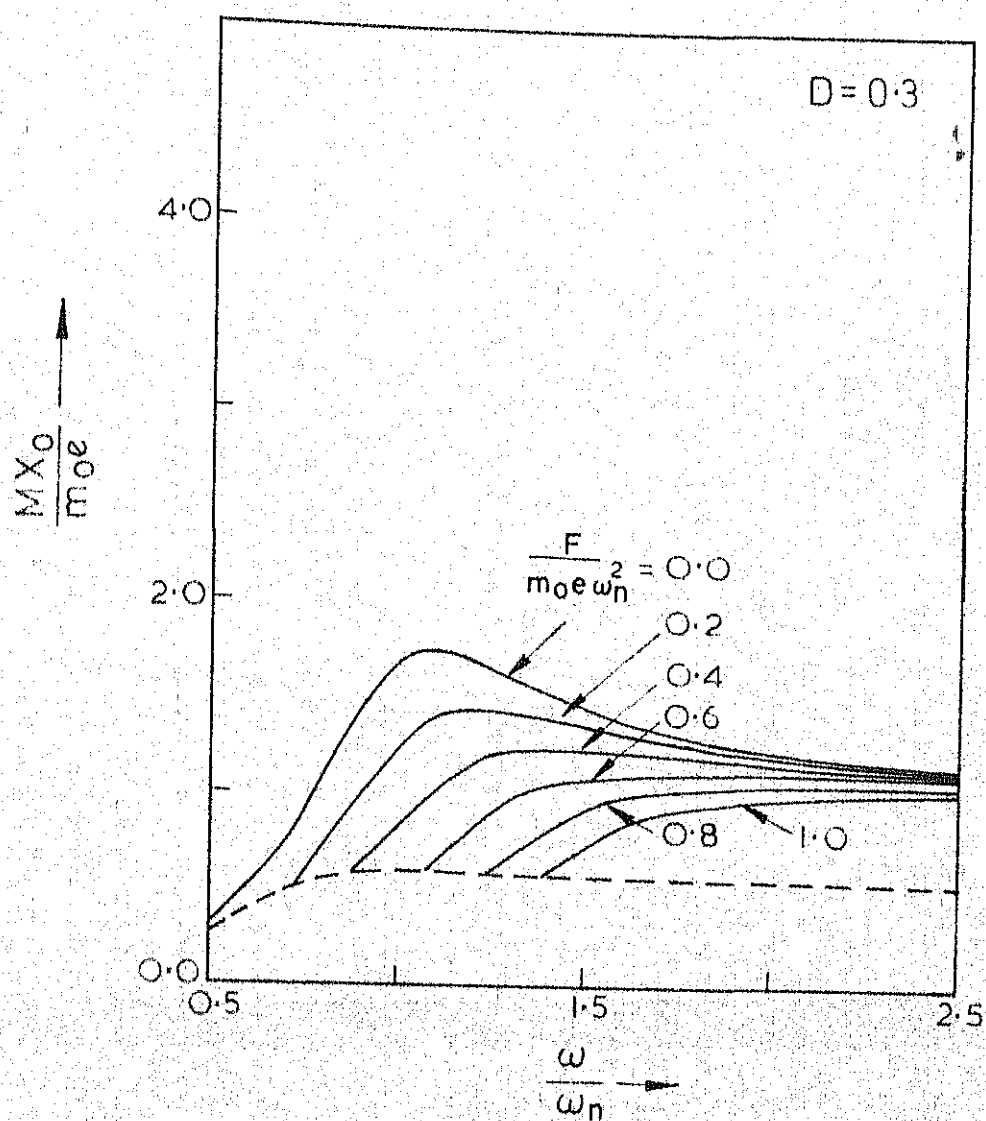


FIG. 8.3(f).

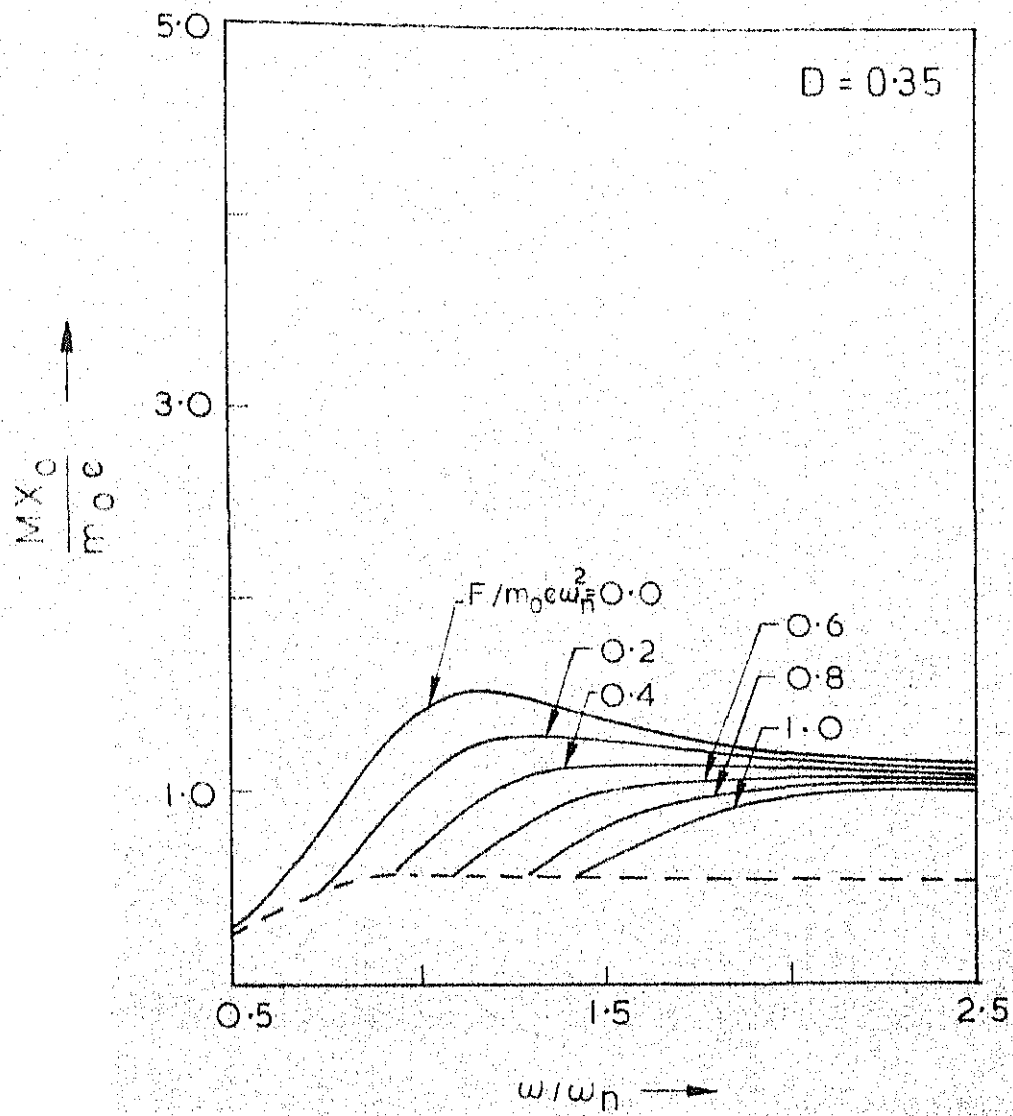


FIG. 8.3(g)

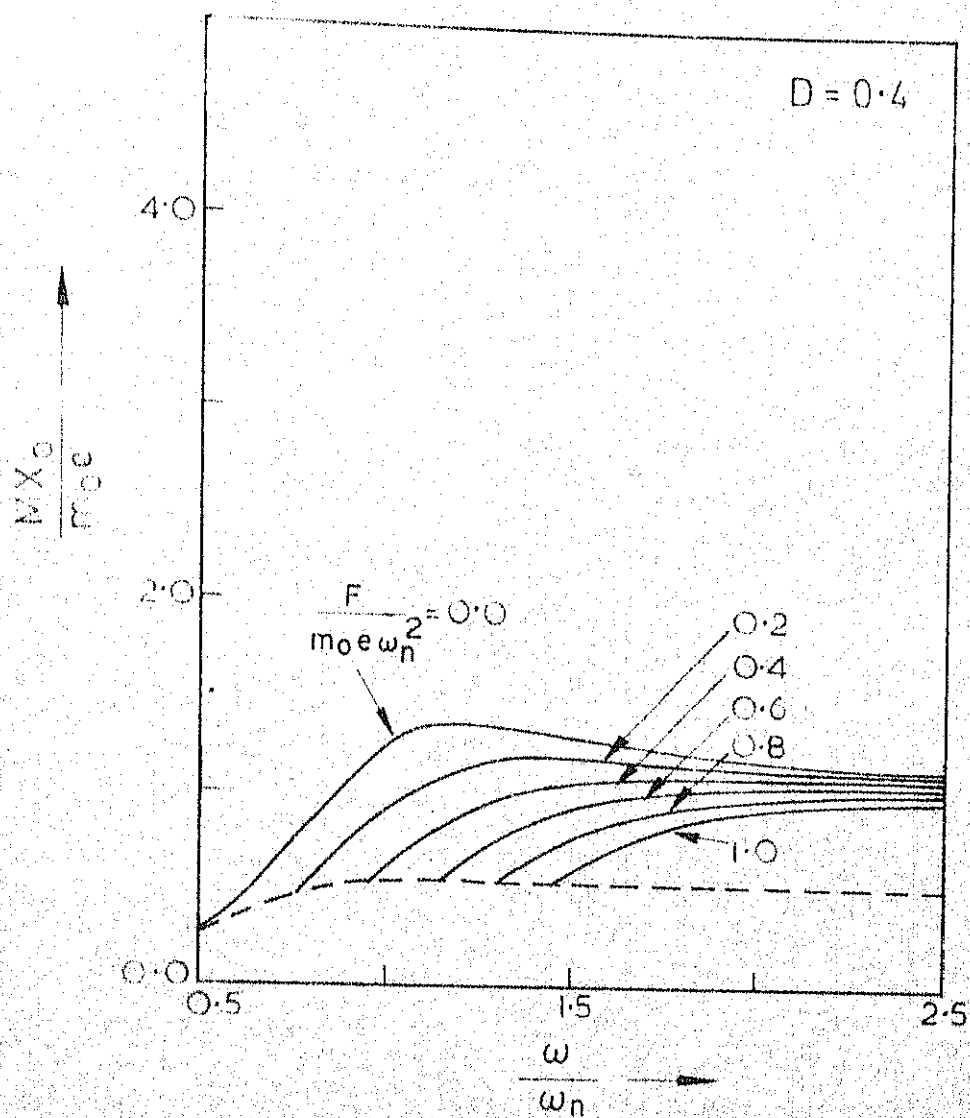


FIG. 8.3(h).

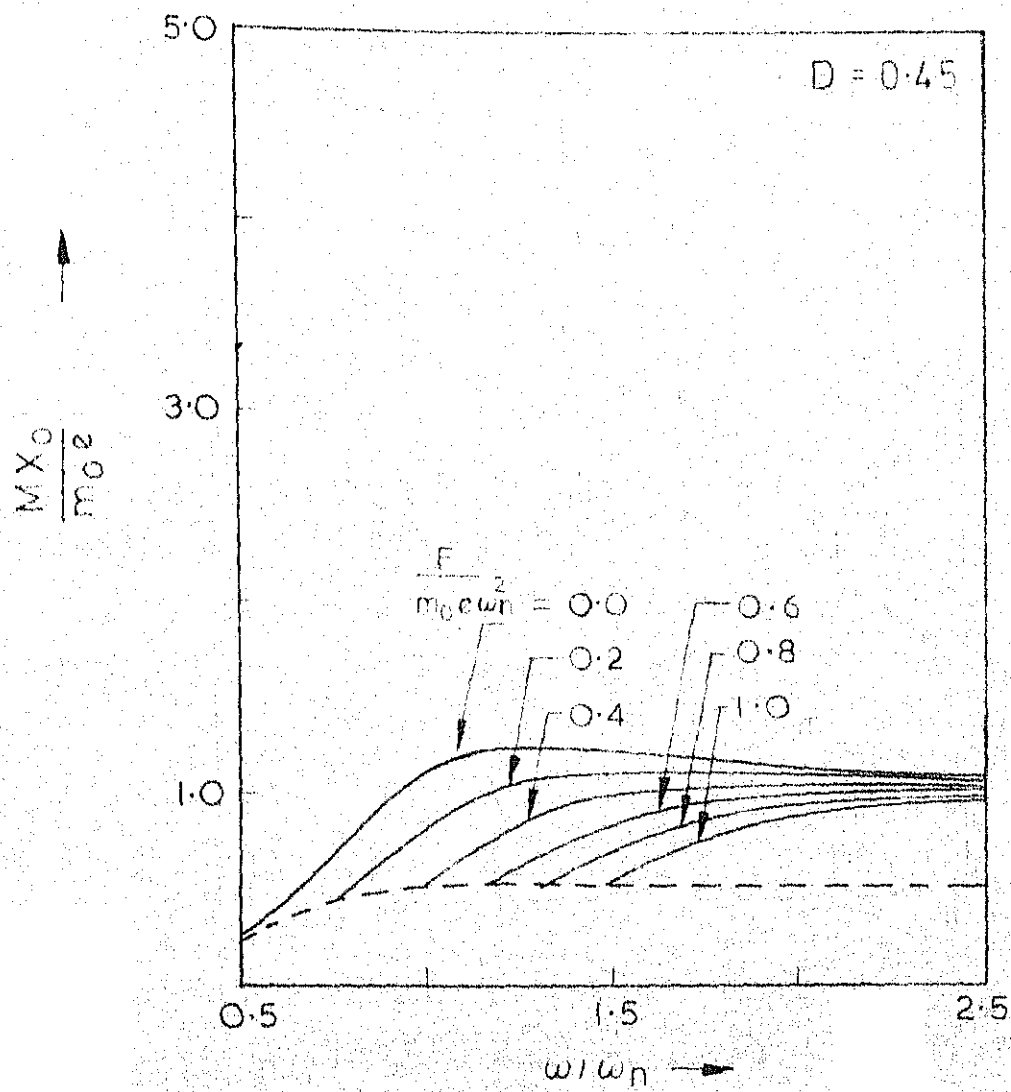


FIG. 8.3(1)

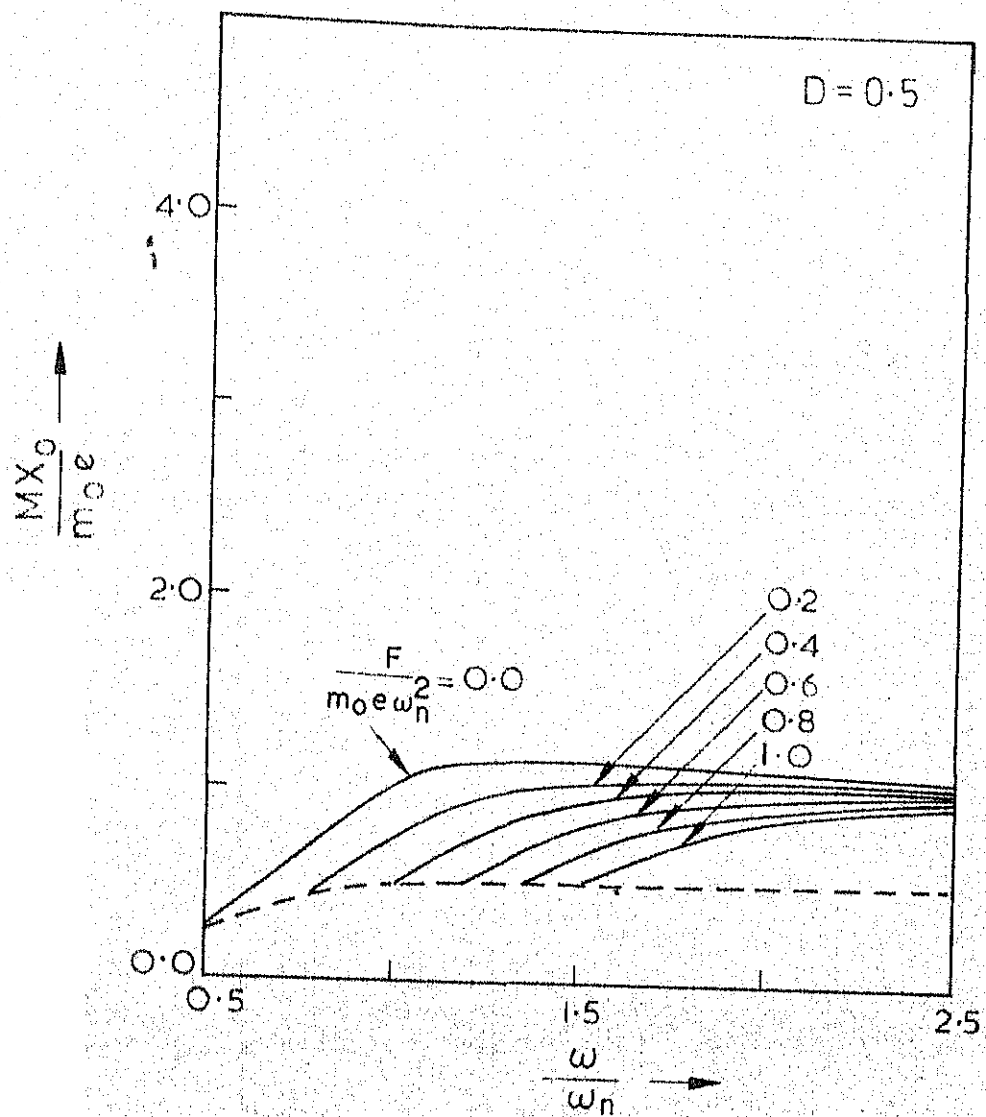


FIG. 8.3(j).

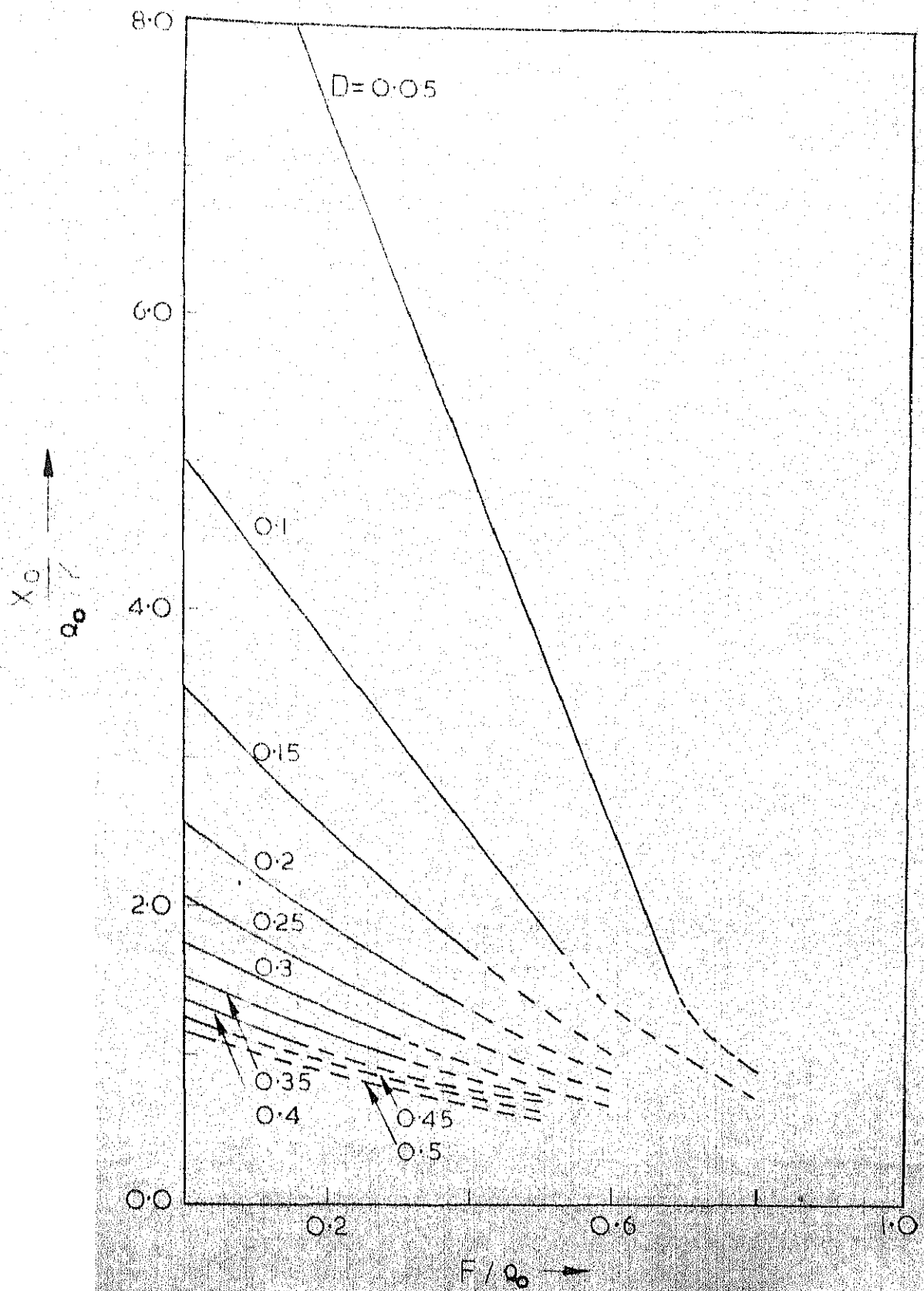


FIG. 8.4 DECREASE OF MAXIMUM AMPLITUDES AT RESONANCE WITH COULOMB FRICTION FACTOR FOR CONSTANT AMPLITUDE OF EXCITING FORCE

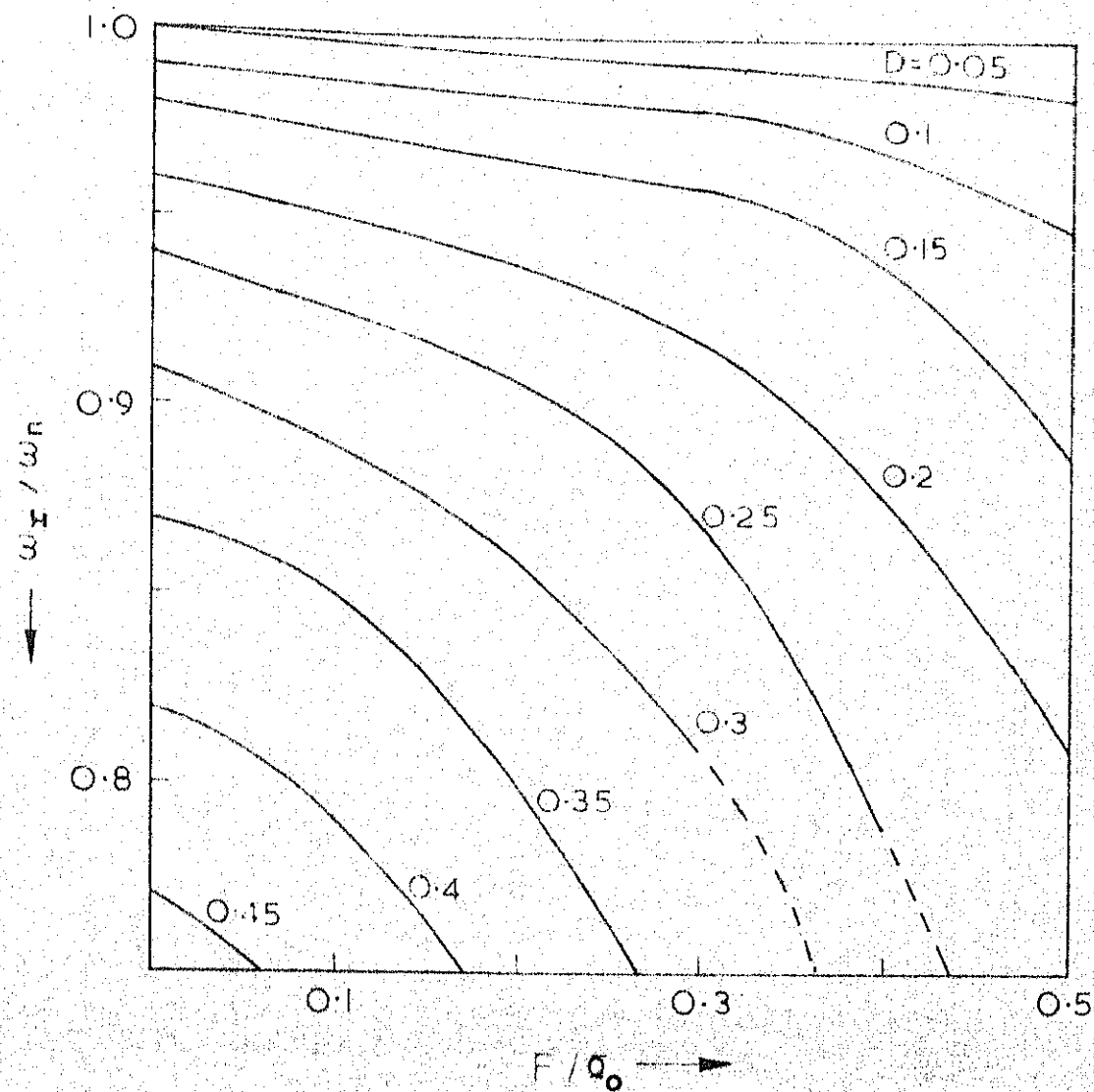
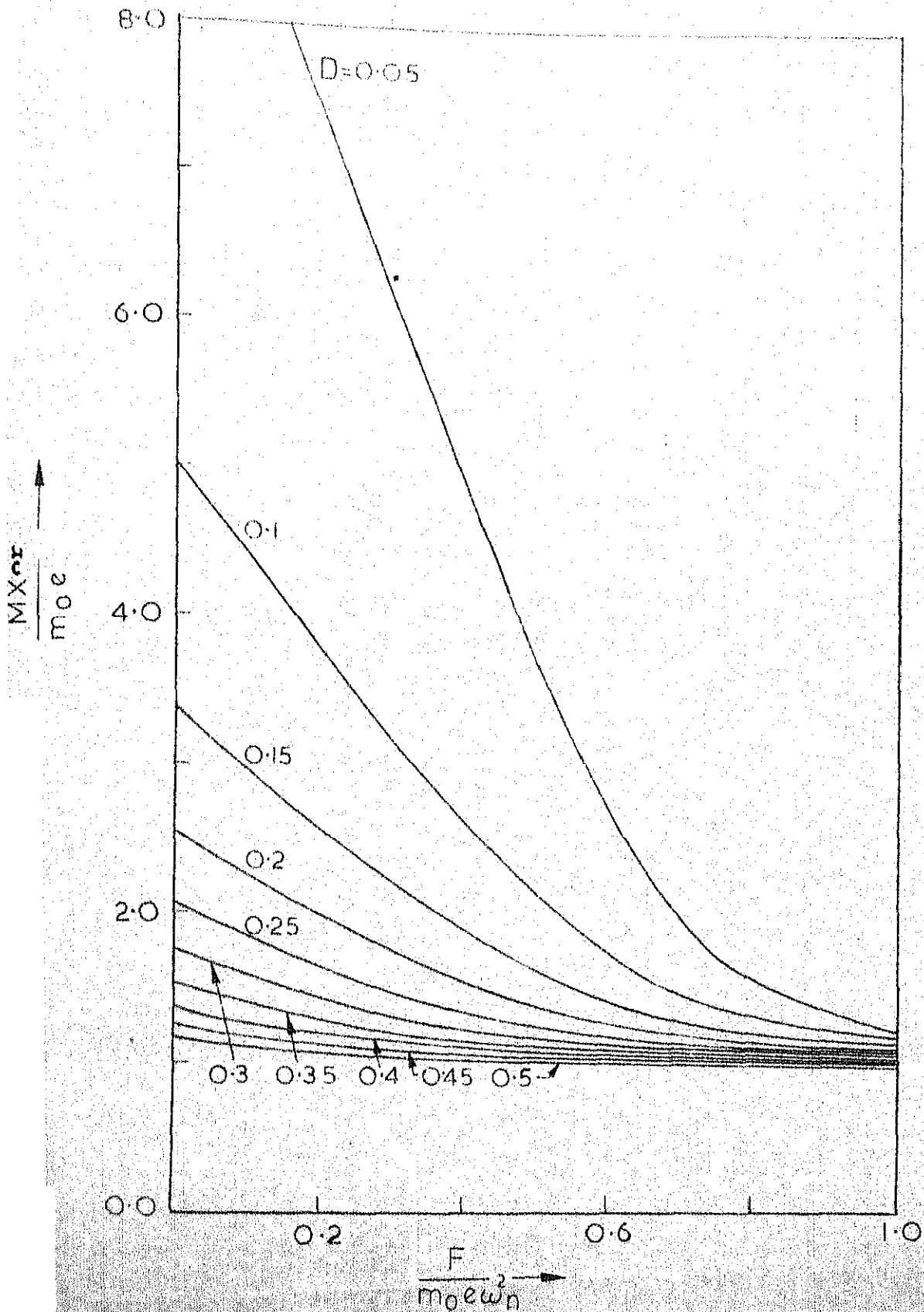


FIG. 8.5 DECREASE OF RESONANT FREQUENCY WITH COULOMB FRICTION FACTOR FOR CONSTANT AMPLITUDE OF EXCITING FORCE



G. 8.6 DECREASE OF MAXIMUM AMPLITUDES AT RESONANCE WITH COULOMB FRICTION FACTOR FOR EXCITING FORCE DUE TO ECCENTRIC ROTATING MASSES

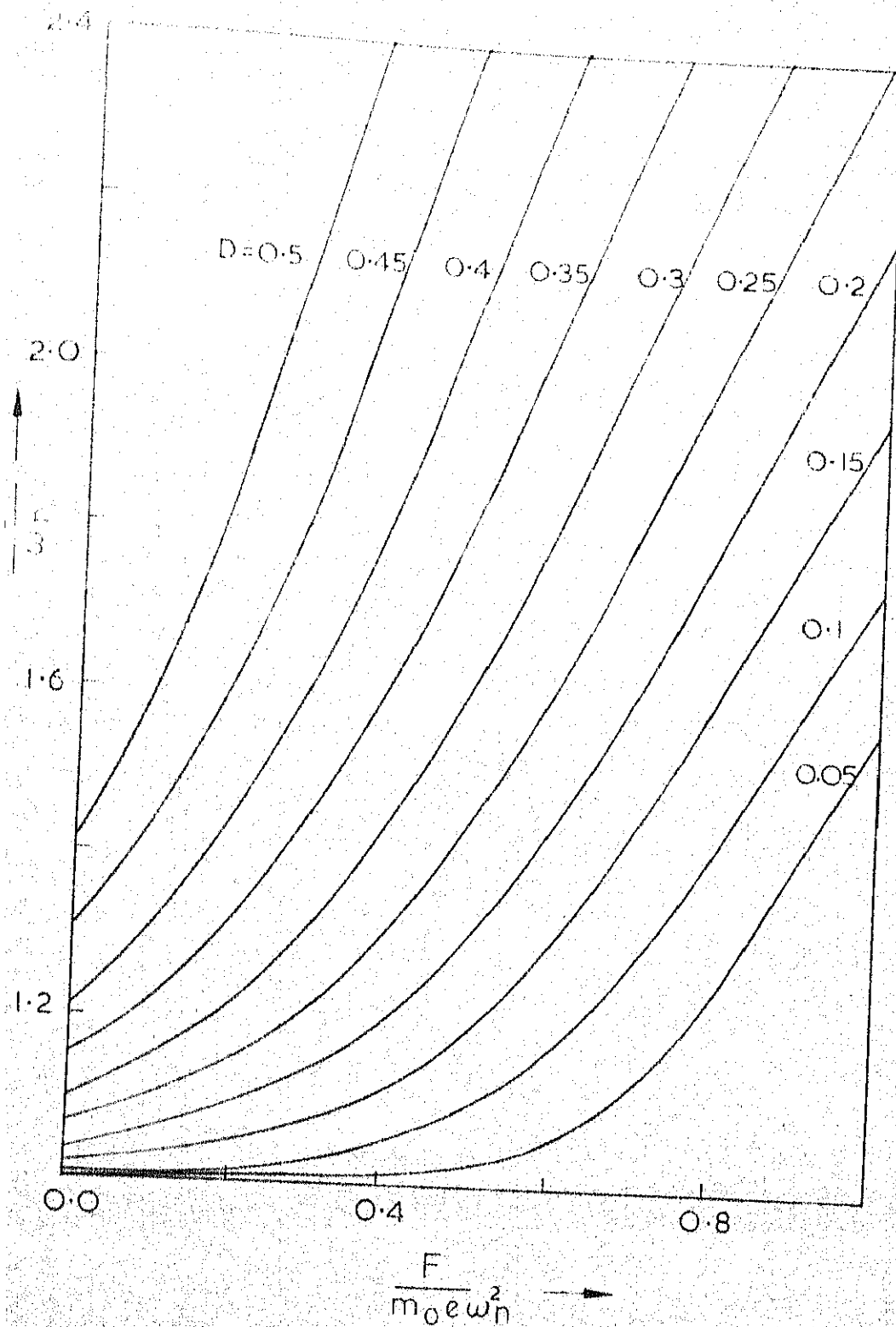


FIG. 8.7 INCREASE OF RESONANT FREQUENCY WITH COULOMB FRICTION FACTOR FOR EXCITING FORCE DUE TO ECCENTRIC ROTATING MASSES

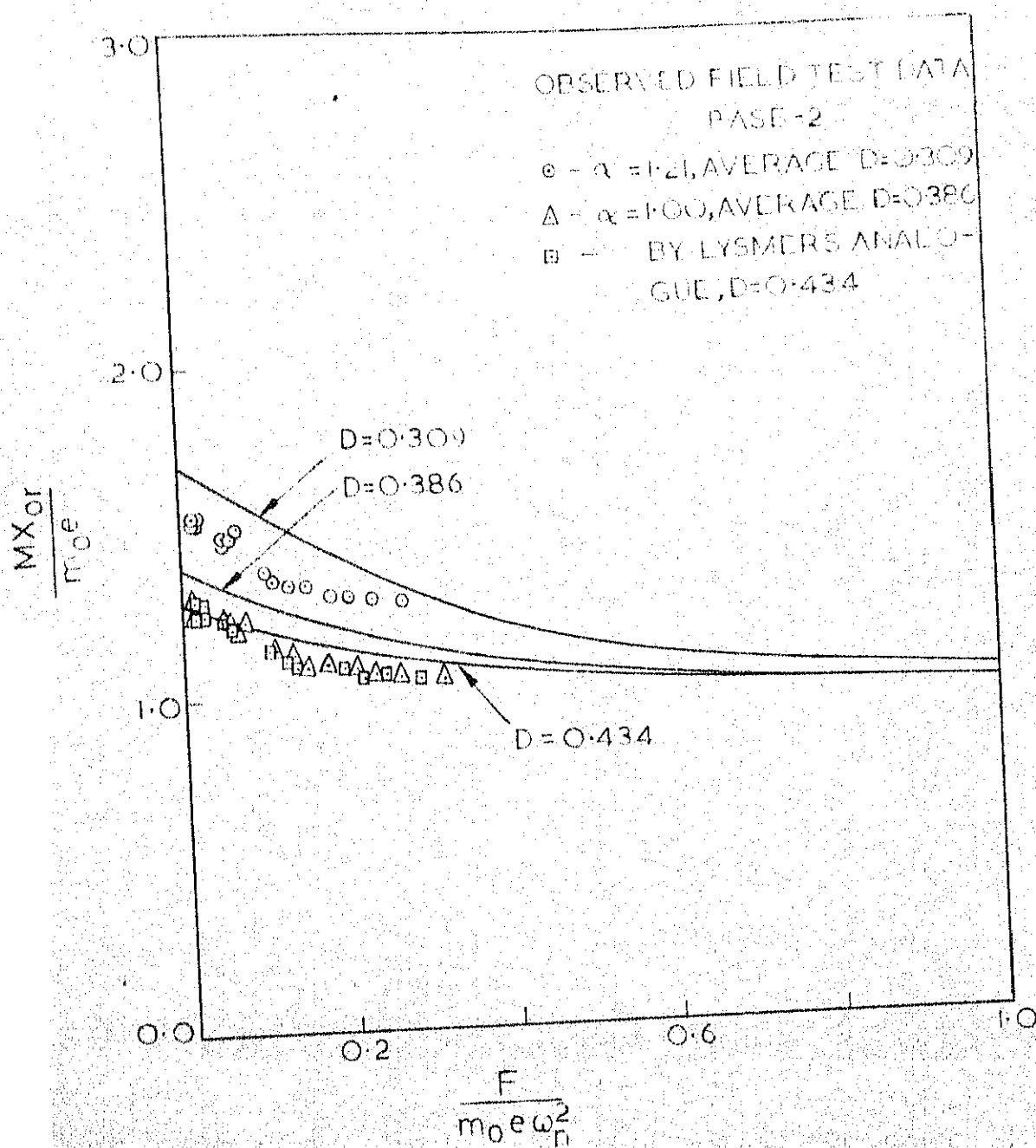


FIG. 8-8(a) CORRELATION BETWEEN THE PREDICTED AND OBSERVED AMPLITUDES AT RESONANCE FOR AN EMBEDDED FOOTING (BASE-2)

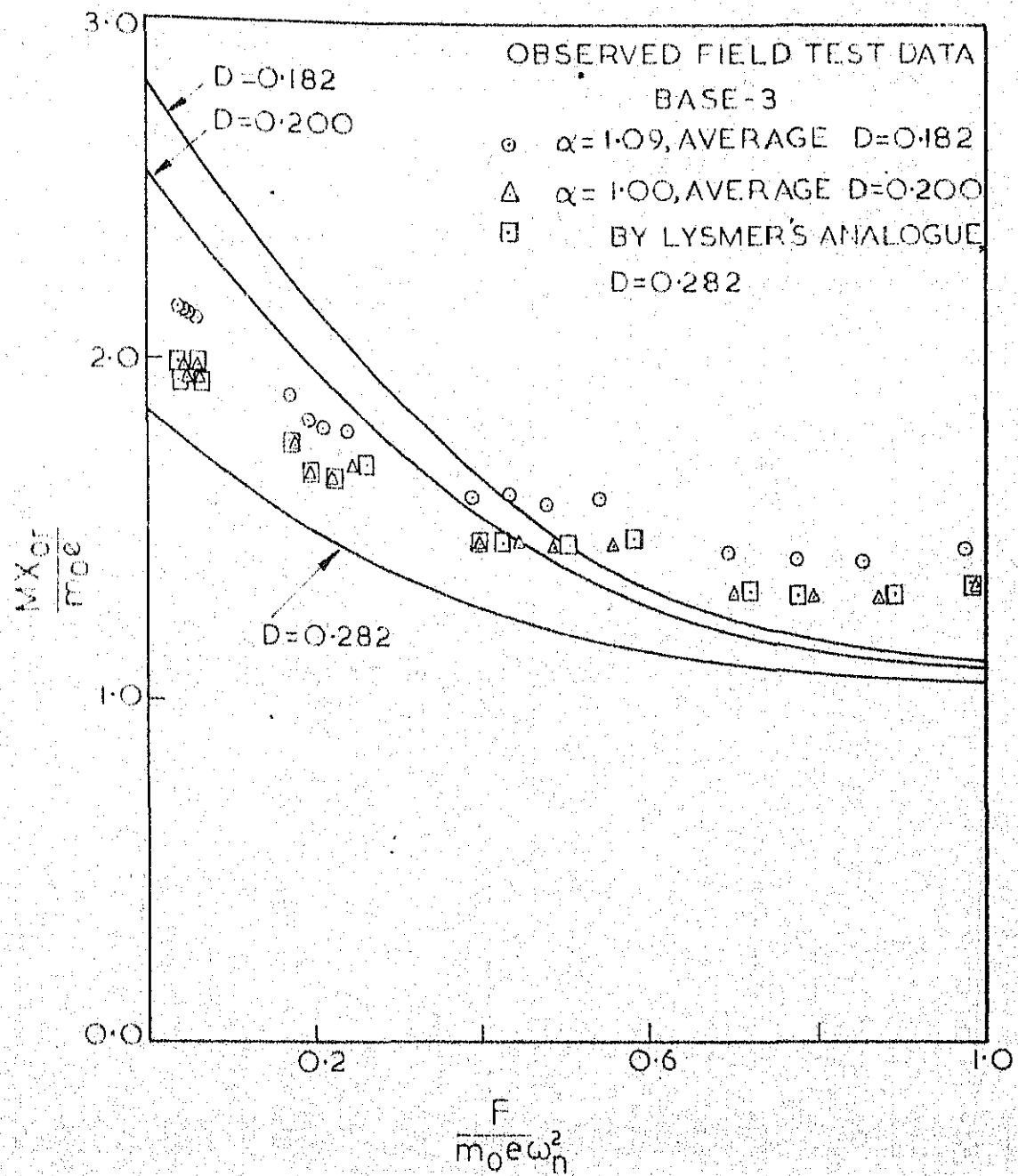


FIG.8-8(b) CORRELATION BETWEEN THE PREDICTED AND OBSERVED AMPLITUDES AT RESONANCE FOR AN EMBEDDED FOOTING (BASE-3)

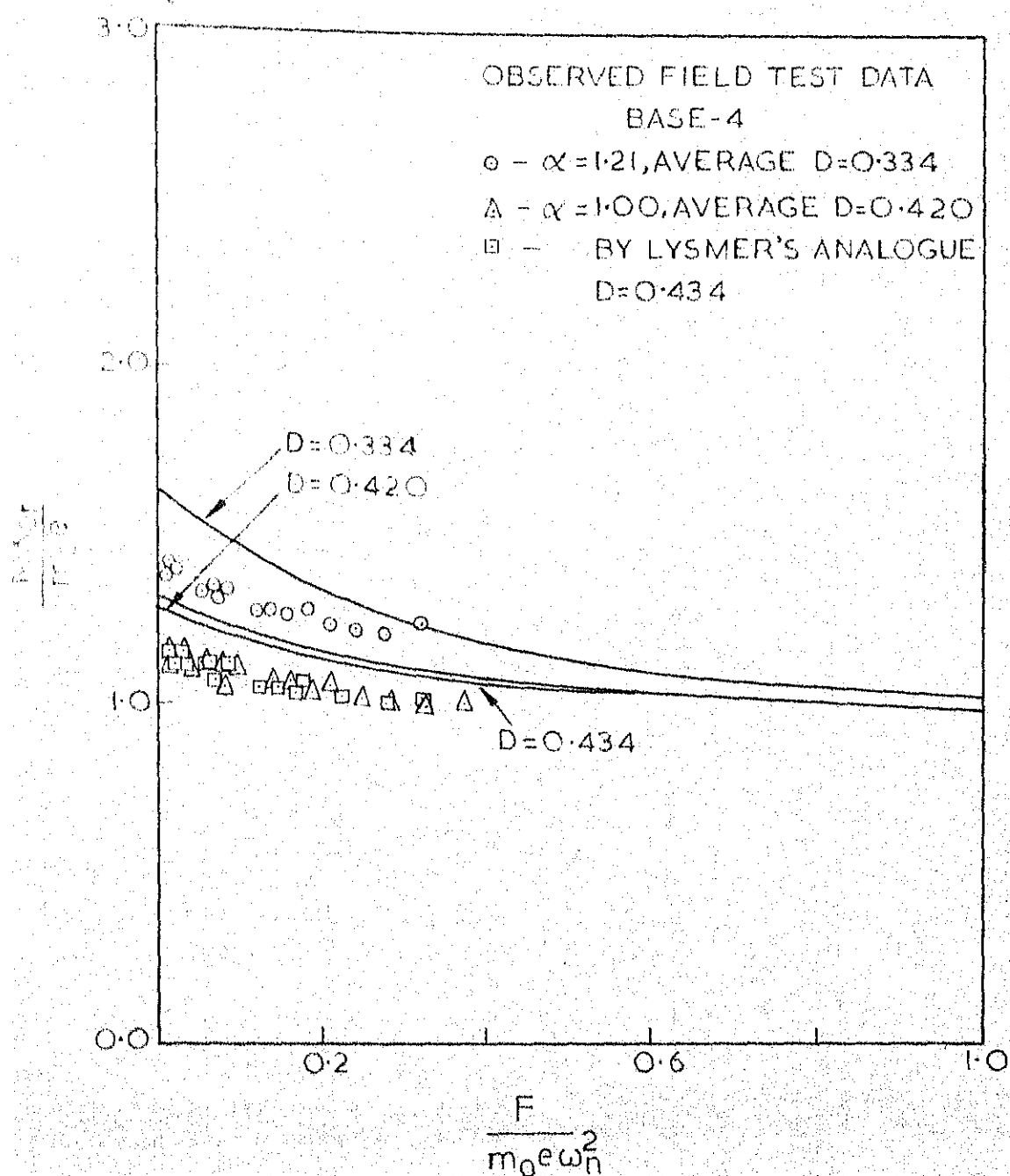


FIG.8.8(c) CORRELATION BETWEEN THE PREDICTED AND OBSERVED AMPLITUDES AT RESONANCE FOR AN EMBEDDED FOOTING (BASE-4)

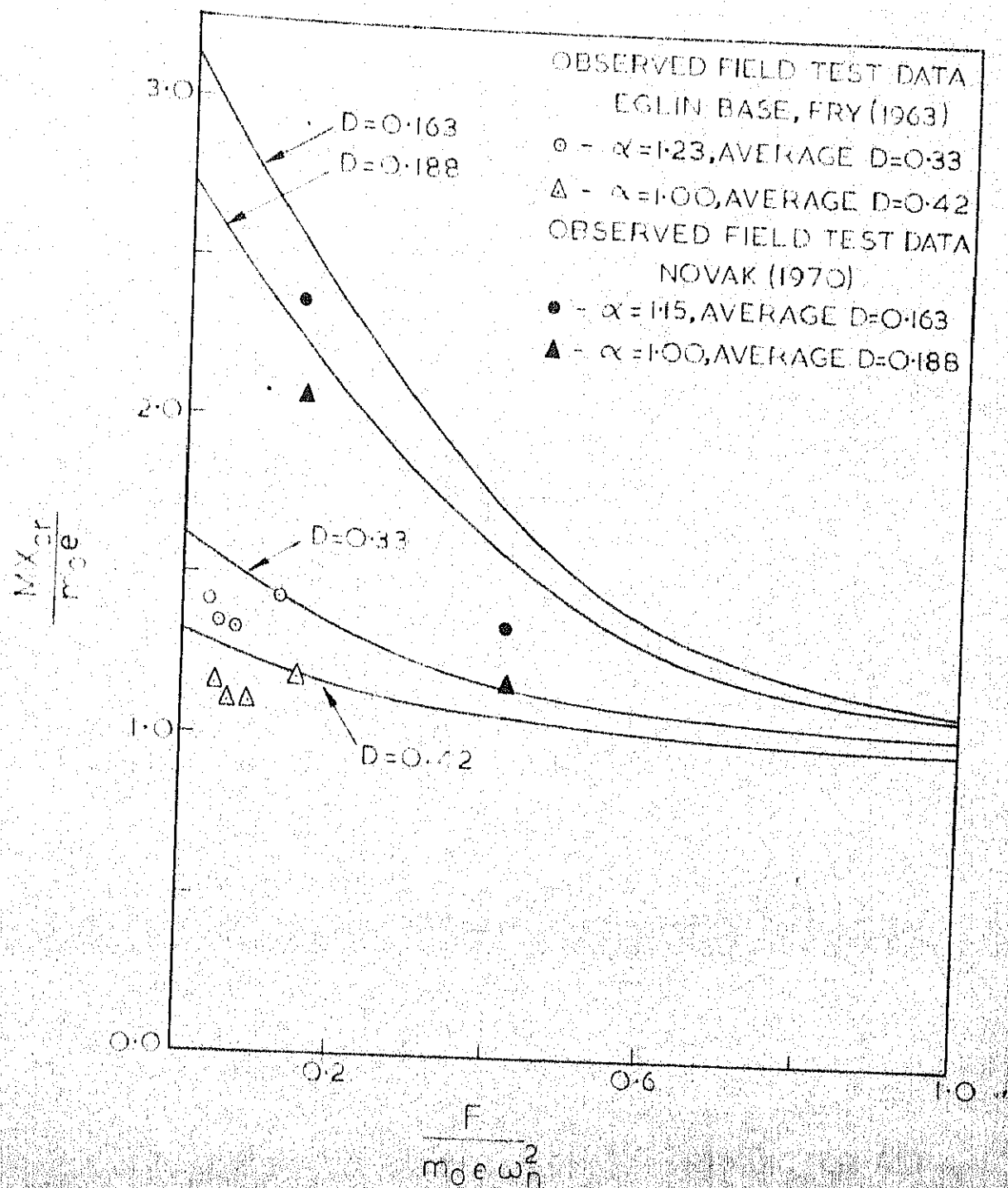


FIG. 8.8(d) CORRELATION BETWEEN THE PREDICTED AND OBSERVED AMPLITUDES AT RESONANCE FOR EMBEDDED FOOTINGS [DATA FROM FRY (1963) AND NOVAK (1970)]

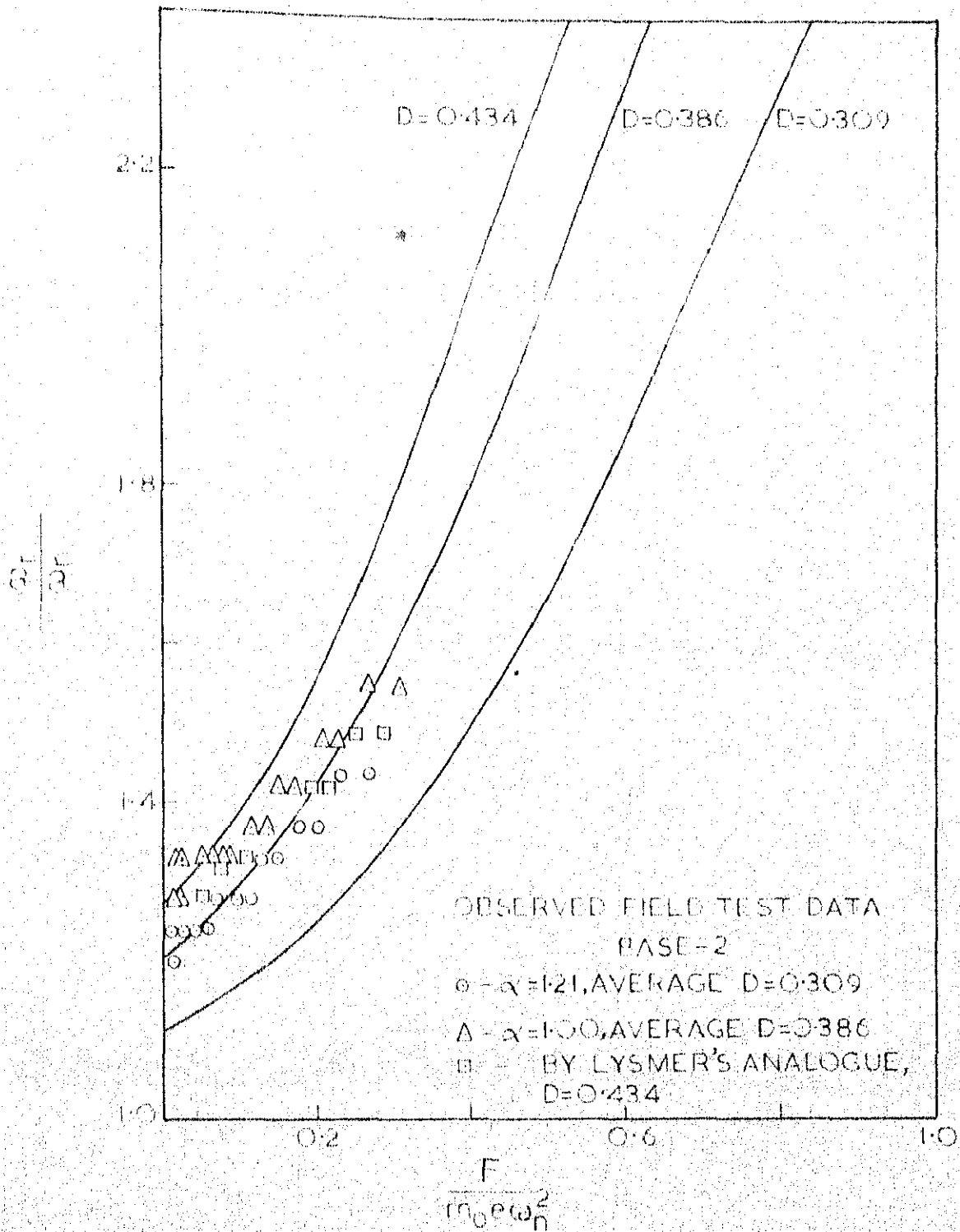


FIG. 8.8(e) CORRELATION BETWEEN THE PREDICTED AND OBSERVED RESONANT FREQUENCIES FOR AN EMBEDDED FOOTING (BASE-2)

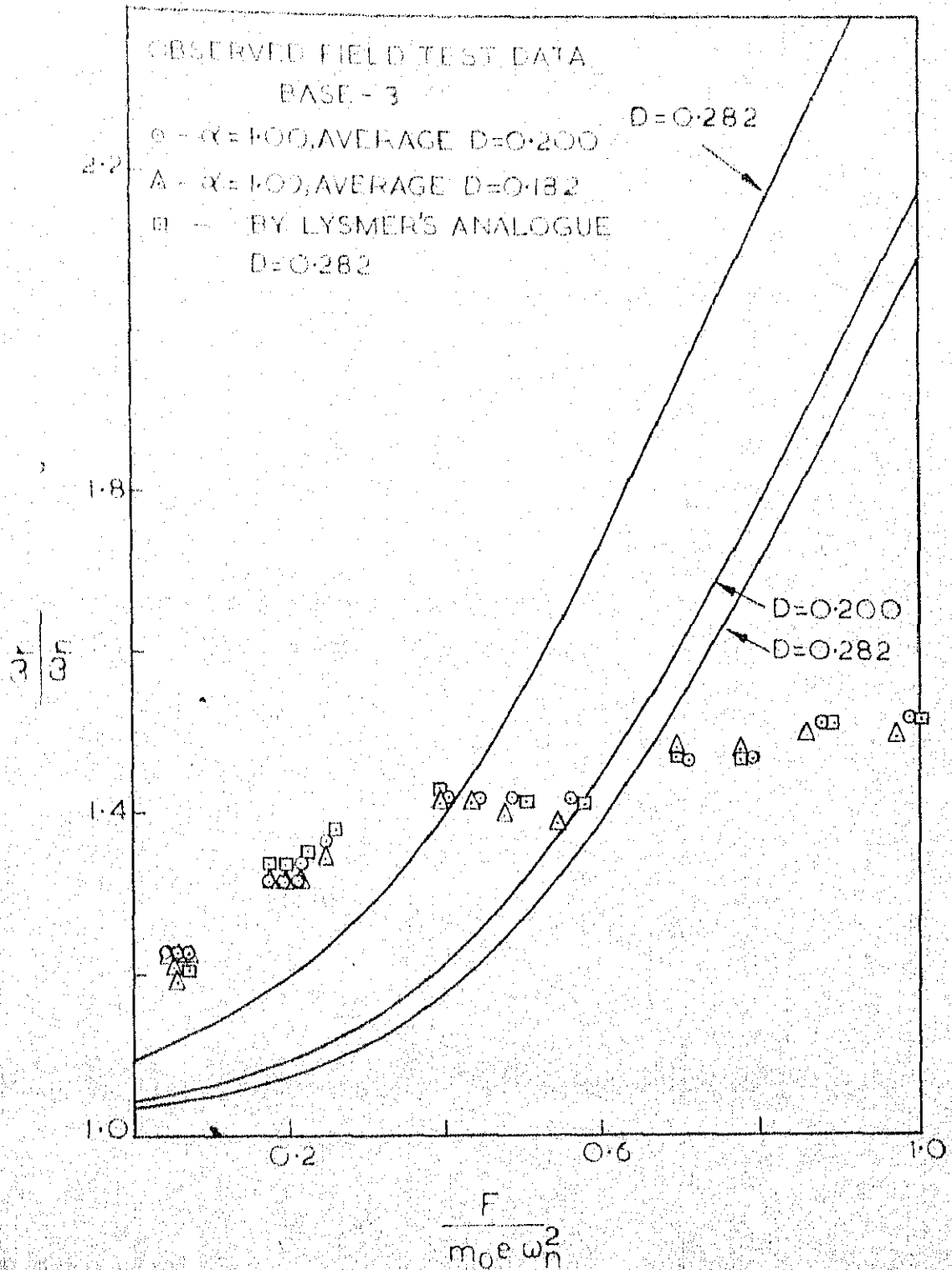


FIG. 8.8 (f) CORRELATION BETWEEN THE PREDICTED AND OBSERVED RESONANT FREQUENCIES FOR AN EMBEDDED FOOTING (BASE-3)

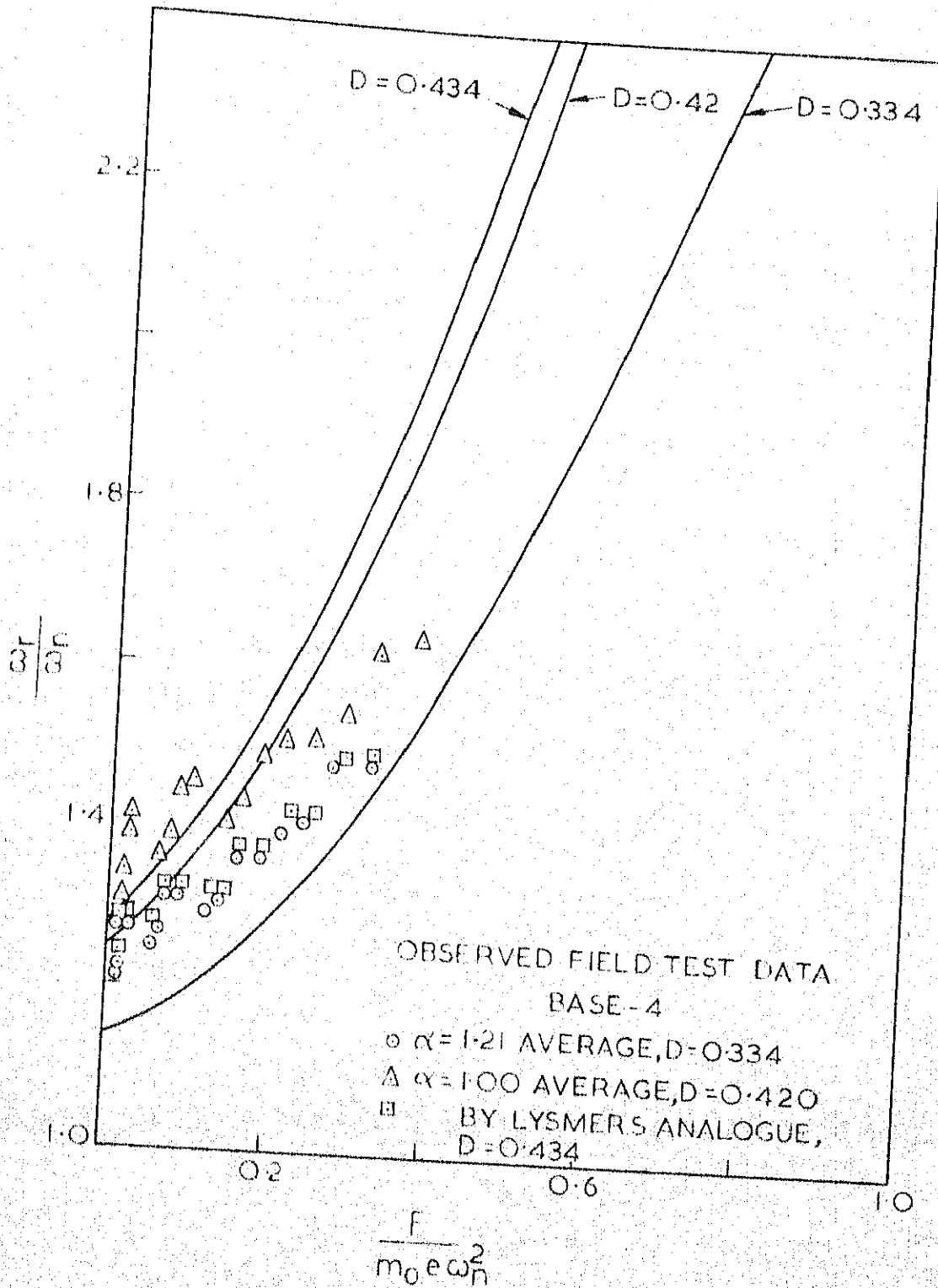


FIG. 8-8(g) CORRELATION BETWEEN THE PREDICTED AND OBSERVED RESONANT FREQUENCIES FOR AN EMBEDDED FOOTING (BASE-4)

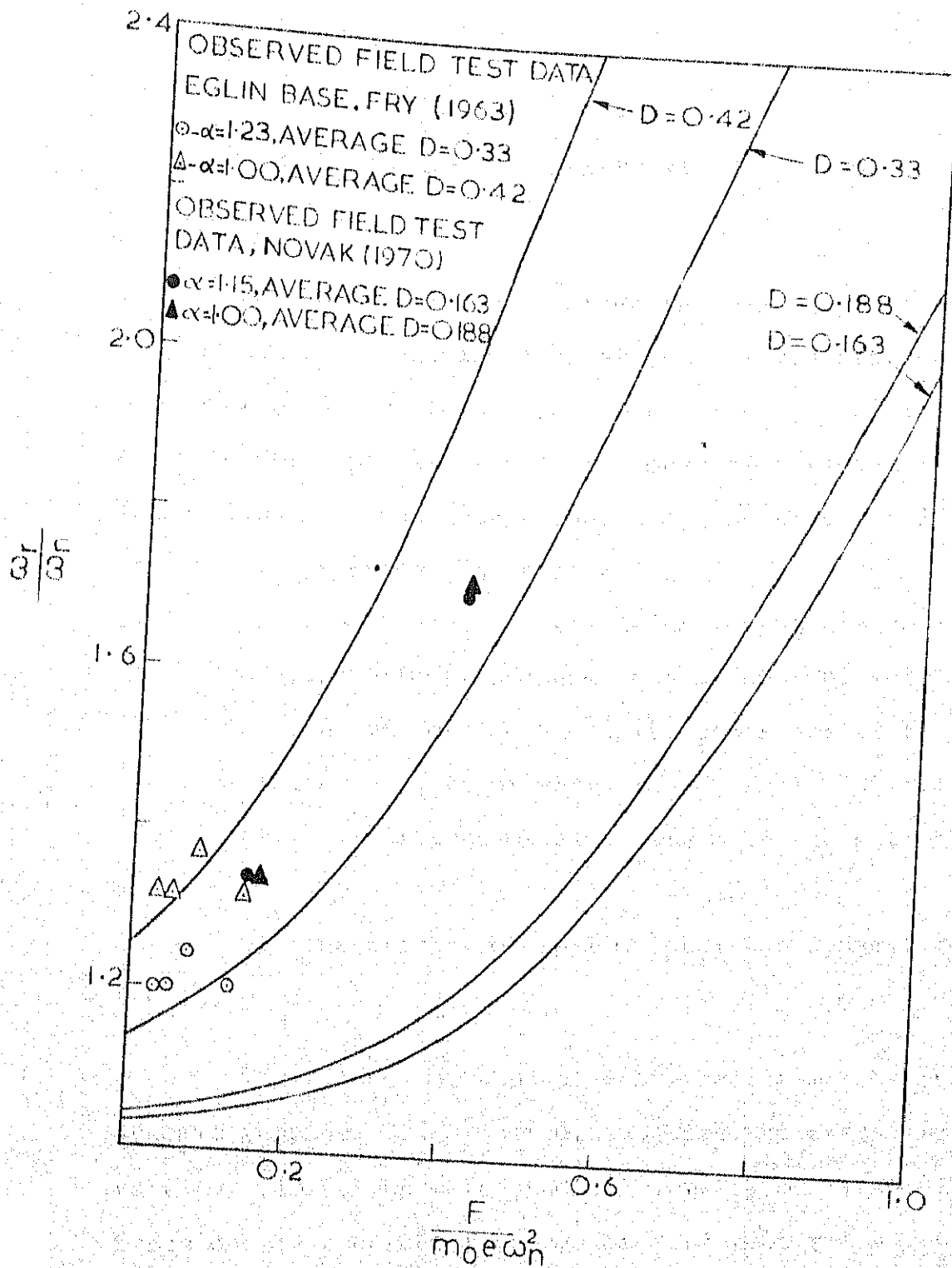


FIG. 8.8(h) CORRELATION BETWEEN THE PREDICTED AND OBSERVED RESONANT FREQUENCIES FOR EMBEDDED FOOTINGS [DATA FROM FRY(1963) AND NOVAK (1970)]

CHAPTER 9

CONCLUDING DISCUSSIONS WITH RECOMMENDATIONS

9.1 GENERAL

The investigation reported in this dissertation, was undertaken to examine some of the serious departures encountered in the field from the theories which are in vogue to describe the dynamic response of a vibrating foundation. The main deviations from the theory which are observed in practice can be listed as:

- 1) the effects due to the embedment of the footing;
- 2) the effects of surcharge around the footing;
- 3) the effects of base size and shape of the footing;
- 4) the effects of variation of soil properties;
- 5) the effects of extremely moist conditions of soil;
- 6) the effects of soil under large dynamic force levels; etc.

The effects of the above listed parameters on the dynamic response of a footing, subjected to steady-state vertical vibrations were studied by means of field vibratory tests on six concrete footings of different shapes and sizes, constructed at several locations to provide a variety of soil conditions below the bases. The steady-state test data were supplemented by a thorough seismic investigation of the

test site, both area-wise and depth-wise, by means of surface refraction surveying and cross-hole investigations. It is hoped that the seismic investigation of the test area enhanced the value of the steady-state vibratory test data, providing scope for interpretation of the test results in the right perspective.

9.2 THE EFFECT OF EMBEDMENT

It is recognised that the single-degree-of-freedom system of lumped parameters is a grossly simplified representation of the footing vibrating on a soil continuum, but such a system can be employed with ease and sufficient accuracy to predict as well as analyse the responses. For instance, it was shown in Chapter 8 that the dynamic response of an embedded footing could be represented mathematically by a single-degree-of-freedom lumped mass-spring system with combined viscous and Coulomb friction damping where the values of these parameters could be determined from the dimensions and properties of the foundation, the elastic medium below the base of the footing and the material surrounding the sides of the footing. Even though this mathematical representation is a gross simplification of the real system, the ability of the model to provide a satisfactory dynamic analysis cannot be doubted.

The effect of embedment on the steady-state response of a footing subjected to vertical vibrations was discussed in Chapter 6 with the help of data obtained from a programme of field vibratory tests on concrete footings. The results of these tests indicated a decrease of maximum amplitudes of motion and an increase of resonant frequencies as a consequence of embedment of footings into the soil. The test results, however, did not agree with the observations of Chae (10) who reported that the amplitude reduction factor when plotted against embedment factor, was essentially independent of the mass ratio, b , of the footing. This can be explained by the previously mentioned fact that the foundation response greatly depends on the depth of embedment, the area of side contact, the density of the surrounding soil and the physical characteristics of the interface between foundation walls and the surrounding soil. This implies that the response of an embedded foundation, for a given embedment factor and mass ratio, can vary depending on the area of contact of the backfilled soil with the foundation walls. Therefore, footings with circular, square and rectangular base shapes, but with same base area, may show different responses for the same height of embedment, under identical circumstances. Also, the area of contact of the backfilled soil with the foundation sides is affected by suitable changes in the mass ratio for a given embedment

factor. In such a case, the amplitude reduction factor cannot be independent of mass ratio, even if plotted against embedment factor. The observed dynamic response of embedded footings of different mass ratios, as illustrated in Figure 6.16 of Chapter 6, confirms this fact.

The present investigation dealt exclusively with the steady-state vertical vibrations. The effect of embedment for horizontal and rocking types of motion may be much more pronounced than that for vertical or torsional modes. The simple extension of the proposed lumped parameter model described in Chapter 8, to analyse or predict the dynamic response of embedded footings under torsional mode should be possible provided appropriate changes are made for the rotational motion. The application of the proposed lumped parameter model to rocking and horizontal modes is possible only if an acceptable procedure to determine the frictional moments or forces mobilized along the interface is evolved on the basis of experimental observations. It should, however, be noted that further field tests are needed to establish the influence of embedment, particularly for the rocking mode.

The proposed theoretical model, described in Chapter can also be used for analysing the dynamic response of embedded footings under transient excitation by means of

Well known techniques such as the phase-plane analysis (55).

9.3 THE EFFECT OF SURCHARGE

The effect of this parameter on the dynamic response of a footing has been reported, perhaps, for the first time by means of field experiments as described in Chapter 7. It is rather intriguing that the effect of surcharge has not been studied as an independent parameter in any of the experimental investigations reported so far.

The existence of the so called 'optimum surcharge value', reported in Chapter 7, calls for further experimental research effort. The results qualitatively indicate that by manipulating the amount of surcharge around a footing, it is possible to bring down the amplitudes of motion at resonance. The observed phenomenon is significant and may lead to new possibilities in the area of corrective measures which are applied to improve the performance of machines or other structures whose foundations had been designed by the rule of thumb or without adequate field investigations.

The existence of the so called 'optimum surcharge value' and the 'critical surcharge values' observed during the surcharge tests, were explained with the concepts of changing confining pressure and the effective mass associated with the vibrating system. These arguments are, however,

intuitive and it may be possible to come up with different reasons for explaining the same phenomenon.

9.4 THE EFFECT OF BASE SIZE AND SHAPE

The effect of base size on the dynamic response of foundation-soil systems has been studied exhaustively by a number of other investigators (16, 45) besides the present one reported in this dissertation. The trend of the results reported in Section 5.5 of Chapter 5, in general, confirms the findings of similar investigations reported elsewhere (16, 45).

It may be recalled that the mass of the footings in the present investigation was same for each of the bases. However, the base size and shape were different for different footings. The observed dynamic response of the footings, for a particular eccentricity moment of the vibrator, as illustrated in Figure 5.3 to 5.6, indicates that an increase in the base area of the footing results in the decrease of resonant amplitudes and increase of resonant frequencies. Though this trend conforms with the results of the elastic half-space theory qualitatively, the agreement with respect to quantities is not satisfactory. The disagreement becomes more and more pronounced as the base area gets larger and larger. This particular field behaviour has been confirmed by a review of experimental works by Novak (45). Richart,

Hall and Woods (55) have reviewed the field investigations conducted by the U.S. Army Engineers Waterways Experiment Station (16) in which they have summarized the results of the entire test programme of vertical vibrations of the model footings, totalling about 94 tests. They observed that the overall agreement between the results of field tests and the theory was within a factor of 2 ($\pm 100\%$), which is considered good for dynamic problems. The reason for such discrepancies has been attributed to local failures and compaction of the supporting soil during some parts of the test programme. The deviation of test results from the theory can also be attributed to the changes in the soil properties with depth. Since the elastic moduli of even relatively deep layers of homogeneous soils increase with depth as a result of confining pressure, the actual soil media behaving as a layered system, whose properties vary progressively with depth, cannot be ruled out. Such a situation hardly justifies the assumption of the theory that the soil can be represented by an isotropic, homogeneous and elastic half-space.

It is, however, heartening to note that circular and equivalent square footings of same base area, show more or less the same dynamic response under identical situations. More field tests with rectangular and other shapes of footings

energy at different boundaries inside the soil media is too complicated to explain the involved phenomenon at the present state of the art. It can, however, safely be concluded that it is advantageous to locate the base of a machine foundation on top of the hardest layer of soil possible, if the same exists within a reasonable depth below the ground surface. Further field investigations in this direction or case histories to prove this point may be significant for the development of the profession.

9.6 THE EFFECT OF MOISTURE IN SOILS

The study of the effect of extreme wet conditions of the soil on the dynamic behaviour of foundation-soil systems has not received much attention, especially under field conditions. A typical set of data obtained for Base-1, under wet conditions, demonstrated the effect of near saturation of the soil upto a depth of 1.5 to 2 feet below the level of the base, on both the resonant frequencies and resonant amplitudes. The resonant frequencies were observed to be less than those observed for tests during dry conditions. Also the maximum amplitudes of motion at resonance registered a slight increase. This implied a decrease in the effective stiffness of the system which, according to the elastic half-space theory, is directly proportional to the shear modulus of the soil. However, Biot's theory indicates that pore

fluids cannot transmit shear waves. Therefore, the only influences of the pore water on the propagation of shear waves in the soil structure are through the changes in the unit weight of the soil and inertia forces. This reasoning, however, does not fully explain the softening character of the system which in other words should amount to a decrease in the shear modulus of the soil. Further field investigations under saturated conditions of the soil are very desirable to investigate the implications of Biot's theory. The study is important by itself as the design of a machine foundation should take into consideration the fluctuation of the ground water table which may be seasonal or irregular as that due to a flood or tide.

9.7 THE EFFECT OF SOIL UNDER LARGE DYNAMIC FORCE LEVELS

It was observed from the results of tests described in Section 5.3 of Chapter 5, that the foundation-soil system appeared to behave as though it were a softening system with increasing dynamic force levels. Several investigators (1, 18, 39, 46, 58) have come forward with various theoretical models by suggesting different types of nonlinear resistance functions and nonlinear damping functions. These methods may not be of much help unless standard field or laboratory procedures are established to identify the type of nonlinearity involved in various kinds of soils. Much research effort is needed in this direction.

CHAPTER 10

SUMMARY AND CONCLUSIONS

The deviation of the observed results from the elastic half-space method as a result of certain departures from the idealized assumptions of the simple theory was studied with the help of data obtained from a comprehensive programme of field vibratory tests on concrete footings in conjunction with a thorough seismic investigation of the test site.

The steady-state vertical vibration tests revealed the following observations:

- 1) The foundation-soil system appeared to behave as though it were a softening nonlinear system with increasing dynamic force levels.

- 2) Tests conducted during extremely wet conditions registered a corresponding decrease of resonant frequencies and a slight increase of resonant amplitudes. This showed that the effective stiffness of the silty clay soil at the test site had decreased due to the presence of excessive moisture.

- 3) Mass of the footing remaining same, an increase in the base area resulted in the decrease of resonant amplitudes and an increase of resonant frequencies. Though this trend conformed with the results of the half-space

theory qualitatively, there was some disagreement in quantitative aspects.

4) Circular and equivalent square footings of same base area, in general, showed the same dynamic response when the soil conditions below the footings remained same.

5) The dynamic response of a footing constructed on top of a relatively hard layer of silty clay with kankar or limestone nodules showed relatively lower amplitudes of motion at resonance and appreciably higher resonant frequencies, indicating a relatively greater stiffness of the soil below the footing.

6) The surcharge studies indicated the presence of a so called 'optimum surcharge value', the knowledge of which can be utilized to bring down the amplitudes of motion of a footing by a manipulation of the amount of surcharge around the footing.

The effect of embedment was studied by backfilling of wellgraded sand into excavated pits. The steady-state vertical vibration tests, in general, indicated a decrease of maximum amplitudes of motion and an increase of resonant frequencies as a consequence of embedment of footing into the soil.

A single-degree-of-freedom mass-spring-dashpot analogue with the inclusion of a Coulomb friction damper

has been suggested to explain the dynamic behaviour of embedded foundations. A simple procedure by which the constant frictional force of the Coulomb friction damper can be evaluated, has been described. The suggested procedure can take into consideration the depth of embedment, the area of side contact, the density of the surrounding soil and the physical characteristics of the interface between foundation walls and the surrounding soil.

The field test data obtained from the present investigation as well as those published by other investigators elsewhere are compared with the values predicted by the proposed theoretical model. The correlation between the available experimental data and the predicted values is quite satisfactory. The theoretical results, presented in dimensionless form, can be readily used for purposes of design and analyses.

REFERENCES

- 1 Alpan, I. (1961), "Machine Foundation and Soil Resistance", *Geotechnique*, Vol. XI, p. 95.
- 2 Arnold, R.M., Bycroft, G.N., and Warburton, G.B. (1955), "Forced Vibrations of a Body on an Infinite Elastic Solid", *J. Appl. Mech., Trans. ASME*, Vol. 77, pp. 391-401.
- 3 Awojobi, A.O., Grootenhuis, P. (1965), "Vibrations of Rigid Bodies on Semi-Infinite Elastic Media", *Proceedings of the Royal Society of London, Series A*, Vol. 287, pp. 27-63.
- 4 Balakrishna Rao, H.A., and Nagaraj, C.N. (1960), "A New Method for Predicting the Natural Frequency of Soil-Foundation System", *The Structural Engineer*, pp. 310-316.
- 5 Baranov, V.A. (1967), "On the Calculation of Excited Vibration of an Embedded Foundation", (in Russian), *Almanac Voprosy Dinamiki i Prochnosti*, No. 14, Polytechnical Institute of Riga, pp. 195-209.
- 6 Barkan, D.D. (1962), Dynamics of Bases and Foundations (translated from the Russian by L. Drashevskaya, and translation edited by G.P. Tschebotarioff), McGraw-Hill Book Co. (New York), 434 pp.

- 13 Den Hartog, J.P. (1931), "Forced Vibrations with Combined Coulomb and Viscous Friction", Transactions, American Society of Mechanical Engineers, APM-53-9, Vol. 53, pp. 107-115.
- 14 Elorduy, J., Nieto, J.A., and Szekely, E.M. (1967), "Dynamic Response of Bases of Arbitrary Shape Subjected to Periodic Vertical Loading", Proc. International Symposium on Wave Propagation and Dynamic Properties of Earth Materials, Albuquerque, N.M., Aug.
- 15 Ewing, W.M., Jardetzky, W.S., and Press, F. (1957), Elastic Waves in Layered Media, McGraw-Hill Book Co. (New York), 380 pp.
- 16 Fry, Z.B. (1963), "Development and Evaluation of Soil Bearing Capacity, Foundations of Structures", WES, Tech. Rep. No. 3-632, Report No. 1. Jul.
- 17 Funston, N.E. (1966), "The Vibrations of Foundations with Various Types of Subgrade Support", Thesis presented to University of Illinois, in partial fulfillment of the requirements for the Degree of Doctor of Philosophy.
- 18 Funston, N.E., and Hall, W.J. (1967), "Footing Vibration with Nonlinear Subgrade Support", J. Soil Mech. and Found. Div., Proc. ASCE, Vol. 93, No. SM 5, Sept., pp. 191-211.

- 19 Gokhale, K.V.G.K. (1971), "A Case Study for Hydro-Geological Investigations in Planning for Ground Water Exploration", Proceedings of the Water Resources Seminar, Indian Institute of Science, Bangalore, May, pp. B 11.1-B 11.7.
- 20 Grant, F.S., and West, G.F. (1965), Interpretation Theory in Applied Geophysics, McGraw-Hill Book Co. (New York), 584 pp.
- 21 Griffiths, D.H., and King, R.F. (1965), Applied Geophysics for Engineers and Geologists, Pergamon Press (New York), 223 pp.
- 22 Hall, J.R., Jr. (1967), "Coupled Rocking and Sliding Oscillations of Rigid Circular Footings", Proc. International Symposium on Wave Propagation and Dynamic Properties of Earth Materials, Albuquerque, N.M., Aug.
- 23 Hall, J.R., Jr. and Richart, F.E., Jr. (1963), "Dissipation of Elastic Wave Energy in Granular Soils", J. Soil Mech. and Found. Div., Proc. ASCE, Vol. 89, No. SM 6, Nov., pp. 27-56.
- 24 Hardin, B.O. (1965), "The Nature of Damping in Sands", J. Soil Mech. and Found. Div., Proc. ASCE, Vol. 91, No. SM 1, Jan., pp. 63-97.

- 25 Hardin, B.O., and Black, W.L. (1966), "Sand Stiffness Under Various Triaxial Stresses", J. Soil Mech. and Found. Div. Proc. ASCE, Vol. 92, No. SM 2, March, pp. 27-42.
- 26 Hardin, B.O., and Black, W.L. (1968), "Vibration Modulus of Normally Consolidated Clay", J. Soil Mech. and Found. Div., Proc. ASCE, Vol. 94, No. SM 2, March, pp. 353-369.
- 27 Hardin, B.O., and Music, J. (1965), "Apparatus for Vibration During the Triaxial Test", Symposium on Instrumentation and Apparatus for Soils and Rocks, ASTM STP, No. 392.
- 28 Hardin, B.O., and Richart, F.E., Jr. (1963), "Elastic Wave Velocities in Granular Soils", J. Soil Mech. and Found. Div., Proc. ASCE, Vol. 89, No. SM 1, Feb., pp. 33-65.
- 29 Hertwig, A., Früh, G., and Lorenz, H. (1933), "Die Ermittlung der für das Bauwesen wichtigsten Eigenschaften des Bodens durch erzwungene Schwingungen", DEGEBO No. 1, J. Springer (Berlin), 45 pp.
- 30 Heukelom, W., and Foster, C.R. (1960), "Dynamic Testing of Pavements", J. Soil Mech. and Found. Div., Proc. ASCE, Vol. 86, No. SM 1, part 1, Feb., pp. 1-28.

- 31 Hsieh, T.K. (1962), "Foundation Vibrations", Proc. Institution of Civil Engineers, Vol. 22, pp. 211-226.
- 32 Jain, A.K. (1971), "Dynamic Behaviour of Embedded Foundations", Thesis, presented to Indian Institute of Technology, Kanpur, in partial fulfillment of the requirements for the degree of Master of Technology.
- 33 Jones, R. (1958), "In-Situ Measurement of the Dynamic Properties of Soil by Vibration Methods", Geotechnique, Vol. 8, No. 1, Mar., pp. 1-21.
- 34 Kaldjian, M.J. (1969), Discussion of "Design Procedures for Dynamically Loaded Foundations", by R.V. Whitman and F.E. Richart, Jr., Paper No. 5569, J. Soil Mech. and Found. Div. Proc. ASCE, Vol. 95, No. SM 1, Jan., pp. 364-366.
- 35 Kaldjian, M.J. (1971), "Torsional Stiffness of Embedded Footings", J. Soil Mech. and Found. Div. Proc. ASCE, Vol. 97, No. SM 7, July, pp. 969-980.
- 36 Kobori, T. (1962), "Dynamical Response of Rectangular Foundations on an Elastic Half-Space", Proc. Japanese National Symposium on Earthquake Eng., pp. 81-86.
- 37 Kolsky, H. (1963), Stress Waves in Solids, Dover Publications, Inc. (New York) and Clarendon Press (Oxford), 1953, 213 pp.

- 38 Lamb, H. (1904), "On the Propagation of Tremors over the Surface of an Elastic Solid", Philosophical Transactions of the Royal Society, London, Ser. A, Vol. 203, pp. 1-42.
- 39 Lorenz, H. (1953), "Elasticity and Damping Effects of Oscillating Bodies on Soil", Symposium on Dynamic Testing of Soils, ASTM STP No. 156, pp. 113-122.
- 40 Lysmer, J. (1965), Vertical Motion of Rigid Footings, Dept. of Civil Eng., Univ. of Michigan Report to WES Contract Report No. 3-115 under Contract No. DA-22-079-eng-340; also a Ph.D. dissertation, Univ. of Michigan, Aug.
- 41 Lysmer, J., Kuhlemeyer, R.L. (1969), "Finite Dynamic Model for Infinite Media", J. Engineering Mechanics Division, ASCE, Vol. 95, Proc. Paper 6719, Aug. pp. 859-877.
- 42 Lysmer, J., and Richart, F.E., Jr. (1966), "Dynamic Response of Footings to Vertical Loading", J. Soil Mech. and Found. Div., Proc. ASCE, Vol. 92, No. SM 1, Jan., pp. 65-91.
- 43 Maxwell, A.A., and Fry, Z.B. (1967), "A Procedure for Determining Elastic Moduli of In-Situ Soils by Dynamic Techniques", Proc. International Symposium on Wave Propagation and Dynamic Properties of Earth Materials, New Mexico, pp. 913-921.

- 44 McNeill, R.L. (1969), "Machine Foundations-The State of the Art Paper", Soil Dynamics Speciality Session, 7th International Conf. on Soil Mech. and Foundation Engg. Aug., Mexico City.
- 45 Novak, M. (1970), "Prediction of Footing Vibrations", J. Soil Mech. and Found. Div., ASCE, Vol. 96, No. SM 3, Proc. paper 7268, May, pp. 837-861.
- 46 Novak, M. (1971), "Data Reduction From Nonlinear Response Curves", J. Engineering Mechanics Division, Proceedings of the ASCE, Vol. 97, No. EM 4, Proc. paper 8300, Aug., pp. 1187-1204.
- 47 Novak, M. (1970), Discussion of "Finite Dynamic Model to Infinite Media", by Lysmer, J. and Kuhlemeyer, R.L., Proc. paper 6719, Aug., 1969, Journal of the Engineering Mechanics Division, Proc. of the ASCE, Vol. 96, No. EM 2, April, pp. 186-188.
- 48 Pauw, A. (1953), "A Dynamic Analogy for Foundation-Soil Systems", Symposium on Dynamic Testing of Soils, ASTM Special Technical Publication No. 156, July, p. 90.
- 49 Prange, B. (1965), "Ein Beitrag Zum Problem der Spannungsmessung im Halbraum", disseration, Technischen Hochschule Karlsruhe, Germany, O. Berenz (Karlsruhe), 159 pp.

- 50 Quinlan, P.M. (1953), "The Elastic Theory of Soil Dynamics", Symposium on Dynamic Testing of Soils, ASTM STP No. 156, pp. 3-34.
- 51 Reissner, E. (1936), "Stationare, Axialsymmetrische durch eine Schüttelnde Masse erregte Schwingungen eines homogenen elastischen Halbraumes", Ingenieur-Archiv, Vol. 7, Part 6, Dec., pp. 381-396.
- 52 Reissner, E. (1937), "Freie und erzwungene Torsionschwingungen des elastischen Halbraumes," Ingenieur-Archiv, Vol. 8, No. 4, pp. 229-245.
- 53 Reissner, E., and Sagoci, H.F. (1944), "Forced Torsional Oscillations of an Elastic Half-Space", J. of Appl. Phys., Vol. 15, pp. 652-662.
- 54 Richart, F.E., Jr. (1962), "Foundation Vibrations", Trans. ASCE, Vol. 127, Part 1, pp. 863-898.
- 55 Richart, F.E., Jr., Hall, J.R., Jr., and Woods, R.D. (1970), Vibrations of Soils and Foundations, Prentice-Hall, Inc. (Englewood Cliffs, New Jersey), 414 pp.
- 56 Robson, J.D. (1957), "Effects of Non-linearity on the Resonant Frequency of a Body on Soil", 9th International Congress on Theoretical and Applied Mechanics, Vol. 7, p. 344.

- 57 Sung, T.Y. (1953), "Vibrations in Semi-Infinite Solids due to Periodic Surface Loadings", Symposium on Dynamic Testing of Soils, ASTM-STP No. 156, pp. 35-64.
- 58 Toshkov, E. (1963), "Design of Forging Hammer Foundations, with respect to the Coacting Soil Masses", Proc. of the Symposium RILEM, Budapest, Hungary, Vol. 1, pp. 265-277.
- 59 Thomson, W.T., and Kobori, T. (1963), "Dynamical Compliance of Rectangular Foundations on an Elastic Half-Space", J. Appl. Mech., Trans. ASME, Dec., pp. 579-584.
- 60 Timoshenko, S.P., and Goodier, J.N. (1951), Theory of Elasticity, McGraw-Hill Book Co. (New York), 506 pp.
- 61 Warburton, G.B. (1957), "Forced Vibration of a Body Upon an Elastic Stratum", J. Appl. Mech., Trans. ASME, Vol. 24, pp. 55-58.
- 62 Whitman, R.V. (1966), "Analysis of Foundation Vibrations", Vibration in Civil Engineering, London, Butterworths, pp. 159-179.

APPENDIX A

A TYPICAL SET OF NUMERICAL COMPUTATIONS

- 1 Prediction of the Dynamic Response of Base-3 by Lysmer's Analogue.

Data

r_0 = Equivalent radius of the base = 1.5 ft.

W = Weight of the footing + vibrator = 4500 lbs.

$m_0 e$ = Eccentricity moment of the vibrator = 0.0194 lbs.-sec.²

γ = Unit weight of the soil at the test site = 110 lbs./ft.³

G = Dynamic shear modulus of the soil = 5500 lbs./sq. in.

μ = Poisson's ratio of the soil = 0.25

Computations

$b = W / (\rho r_0^3) = \text{Mass ratio} = 12.1$

$B = b (1 - \mu) / 4 = \text{Lysmer's modified mass ratio} = 2.27$

$D = \frac{0.425}{\sqrt{B}} = \text{Damping factor} = 0.282$

$K = \frac{4Gr_0}{1 - \mu} = \text{Static spring constant} = 528,000 \text{ lbs./in.}$

$M = \frac{W}{g} = \text{Mass of the footing - vibrator system}$
 $= 11.65 \text{ lbs./in./sec.}^2$

$\omega_n = \sqrt{\frac{K}{M}} = \text{Natural circular frequency} = 213 \text{ rads./sec.}$

$\omega_r = \frac{\omega_n}{\sqrt{1 - 2D^2}} = \text{Resonant circular frequency} = 232 \text{ rads./sec.}$

$$\frac{MX_{or}}{m_0e} = \frac{1}{2D\sqrt{1-D^2}} = \text{Nondimensional resonant amplitude of motion} = 1.848$$

X_{or} = Resonant amplitude of motion = 0.00308 in.

- 2 Evaluation of K and D (Base-3) by means of Frequency-Displacement Curves, Illustrated in Figure 5.5.

Data

W = Weight of footing and vibrator = 4500 lbs.

m_0e = Eccentricity moment of the vibrator = 0.0194 lbs.-sec².

X_{or} = Resonant amplitude of displacement = 0.00435 in.

$(\omega)_r$ = Resonant circular frequency = 220 rads./sec.

Computations

a) For a rotating mass type vibrator, the amplitude of motion at resonance is defined by

$$\frac{MX_{or}}{m_0e} = \frac{1}{2D\sqrt{1-D^2}} \quad (\text{see Eq. 2.22})$$

In the present case, $M = W/g = 11.65 \text{ lbs./in./sec}^2$;

$X_{or} = 0.00435 \text{ in.}$; and $m_0e = 0.0194 \text{ lbs.-sec}^2$.

By substituting in Eq. 2.22 , we get

$$2.614 = \frac{1}{2D\sqrt{1-D^2}}$$

Solving for D , we get

$$D = 0.195$$

For a rotating mass type vibrator, the resonant frequency occurs at a frequency ratio

$$\frac{\omega_r}{\omega_n} = \frac{1}{\sqrt{1-2D^2}} \quad (\text{see Eq. 2.21})$$

Substituting the value of $D = 0.195$ and $\omega_r = 220$ rads./sec. in Eq. 2.21, we get

$$\omega_n = \sqrt{K/M} = 211.3 \text{ rads./sec.}$$

Therefore, $K = (211.3)^2 \times 11.65 = 520,007$ lbs./in.

b) The above computations can be carried out by assuming a suitable coefficient of mass increase, α , to account for the amount of in-phase mass of soil associated with the vibrations of the footing. As described earlier, a suitable coefficient of apparent mass increase, α , as given by Funston (17) was assumed in the present study. In the present case $\alpha = 1.09$

The amplitude of motion at resonance is, now, defined as

$$\frac{MX_{or}}{m_0 e} = \frac{1}{2D\sqrt{1-D^2}} = 2.85$$

Solving for D , we get

$$D = 0.178$$

Substituting the value of $D = 0.178$ and $\omega_r = 220$ rads./sec. in Eq. 2.21, we get

$$\omega_n = \sqrt{\frac{K}{\alpha M}} = 212.7 \text{ rads./sec.}$$

Therefore, $K = (212.7)^2 \times 1.09 \times 11.65 = 574,529$ lbs./in.

3 Prediction of the Dynamic Response of an Embedded Footing (Base-3) by the Proposed Theoretical Model.

a) Evaluation of Constant Frictional Force, F .

Data

L = Perimeter length of the footing = 10.66 ft.

H = Depth of embedment = 2.0 ft.

K_0 = Coefficient of lateral earth pressure at rest = 0.4

γ = Unit weight of the backfilled sand = 100 lbs./ft.³

μ_f = Coefficient of kinematic wall friction = 0.18

Computations

The total amount of frictional force mobilized during vibrations in the vertical mode can be written as

$$\begin{aligned} F &= \frac{1}{2} I_0 \gamma H^2 \mu_f L && \text{(see Eq. 8.29)} \\ &= 0.5 \times 0.4 \times 100 \times 4 \times 0.18 \times 10.66 \\ &= 153.6 \text{ lbs.} \end{aligned}$$

b) Prediction of the Dynamic Response.

Data

$m_0 e$ = Eccentricity moment of the vibrator = 0.0194 lbs.-sec.²

M = W/g = 11.65 lbs./in./sec.²

α = Coefficient of apparent mass increase = 1.09

D = Damping factor = 0.178

$\omega_n = \sqrt{K/\alpha M}$ = natural frequency = 212.7 rads./sec.

Computations

The amplitude of motion of the embedded footing at resonance and the resonant frequency of the vibrating system can be found out directly by using the graphically presented solutions, illustrated in Figures 8.6 and 8.7 respectively. The friction factor, $F/(m_0 e \omega_n^2)$ is the main parameter which is to be computed in order to calculate the amplitude of motion at resonance and the resonant frequency using Figures 8.6 and 8.7.

$$\text{Thus, } \frac{F}{m_0 e \omega_n^2} = \frac{153.6}{0.0194 \times (212.7)^2} = 0.175$$

The graphical relation of $(MX_{or}) / (m_0 e)$ vs $F/(m_0 e \omega_n^2)$ for the given damping factor, $D = 0.178$, can be found either by interpolating between the curves established for $D = 0.15$ and $D = 0.20$, as illustrated in Figures 8.6 and 8.7, or directly by means of the closed form solution described in Eq. 8.26. The latter approach would, however, require the services of a digital computer in order to locate the resonant amplitudes of motion and the resonant frequency quickly.

Thus, for a friction factor, $F/(m_0 e \omega_n^2) = 0.175$ and $D = 0.178$, the nondimensional amplitude factor at resonance, $(MX_{or}) / (m_0 e)$ is found to be 2.25 and the frequency ratio at resonance, ω_r / ω_n is found to be 1.07.

It may be noted that the total mass of the vibrating system, in the present case = ∞M .

Therefore, $(\infty M X_{or}) / (m_o e) = 2.25$,

and hence $X_{or} = 0.0034$ in.

Also, $\omega_r / \omega_n = 1.07$.

Therefore, $\omega_r = 228$ rads./sec.

APPENDIX B

LIST OF EQUIPMENTS AND THEIR MANUFACTURERS

1. Mechanical Vibrator

Commercial Name: LA-1 Oscillator.
 Capacity: \pm 1600 Lb., @ 1800 R.P.M.
 Maximum Speed: 3600 R.P.M.
 Manufacturer: Wiedemann Division, The Warner and Swasey Company. U.S.A.

2. Variable Speed Motor

Commercial Name: U.S. Varidrive Motor.
 Capacity: 3 H.P., 3 Phase., 50 Cycles., 400 V.,
 Minimum R.P.M. = 375., Maximum
 R.P.M. = 3750.
 Manufacturer: U.S. Electrical Motors Division,
 Emerson Electric Co., Old Gate Lane.,
 Milford, Conn. 06460 , U.S.A.

3. Transducers

a) Velocity Type

Commercial Name: MB Vibration Pickup, Types: 100 ,
 124 , 125 , 126 , and 127.
 Natural Frequency: 4.75 C.P.S.

Manufacturer: MB Electronix, A Division of Textron
 Electronics, Inc., P.O. Box 1825 ,
 New Haven 8 , Conn., U.S.A.

b) Acceleration Type

Commercial Name: Piezoelectric, Accelerometer-Type
 Pickups, Type 1560-P52.

Range for Flat
 Frequency Response: 2-20000 C.P.S.

Manufacturer: General Radio Company, West Concord,
Massachusetts, U.S.A.

4. Oscilloscope

Commercial Name: Type 564 Storage Oscilloscope.

Special Features: Two Separate Storage Screens, can be
Operated in a Variety of Modes
Including Differential, Multi-trace,
Wide-band, Sampling and Delayed Sweep;
Convenient for Detailed Viewing and
Photography.

Manufacturer: Tektronix, Inc., S.W. Millikan Way.,
P.O. Box 500., Beaverton., Oregon.,
U.S.A.

5. Vibration Meters

a) Commercial Name: MB Vibration Meter, Model M6.

Manufacturer: MB Electronics, A Division of
Textron Electronics, Inc., P.O. Box
1825, New Haven 8 , Conn., U.S.A.

b) Commercial Name: Type 1553-AK Vibration Meter.

Manufacturer: General Radio Company, West Concord,
Massachusetts, U.S.A.

VITA

N.R. Krishnaswamy was born on 25 August 1942 in Shimoga, Mysore State. He attended Secondary School at the Government High School, Chikballapur, Mysore State and passed the Public Examination for the Mysore Secondary School-Leaving Certificate in June 1958. From June 1958 to April 1959, he attended the Pre-University Course of Mysore University at National College, Bangalore and passed the Pre-University Examination in June 1959. He enrolled in the University College of Engineering, Bangalore in 1959 and received from Bangalore University, the B.E. degree in Civil Engineering in 1965. He was admitted to the Indian Institute of Technology, Kanpur, as a graduate student in July 1966 and was awarded an M. Tech. degree in Civil Engineering in June 1968. He continued his graduate study at the Indian Institute of Technology, Kanpur and enrolled in the Ph.D Programme in July 1968.

His professional experience includes work with the Central Public Works Department of the Government of India, Nagpur as a Graduate Section Officer from February 1966 to July 1966. He has been working as a Senior Research Assistant in the Civil Engineering Department at Indian Institute of Technology, Kanpur since September 1968.

He served the Society of Civil Engineers, Indian Institute of Technology, Kanpur as a Vice-President, during the Academic Year 1967-68.

Date Slip

This book is to be returned on the date last stamped.

[illegible]

CD 6.72.9

CE-1979-D-KR1-810

It may be noted that the total mass of the vibrating system, in the present case = $\mathcal{O}M$.

Therefore, $(\mathcal{O}Mx_{or})/(m_0e) = 2.25$,

and hence $x_{or} = 0.0034$ in.

Also, $\omega_r / \omega_n = 1.07$.

Therefore, $\omega_r = 228$ rads./sec.

APPENDIX B

LIST OF EQUIPMENTS AND THEIR MANUFACTURERS

1. Mechanical Vibrator

Commercial Name: LA-1 Oscillator.

Capacity: \pm 1600 Lb., @ 1800 R.P.M.

Maximum Speed: 3600 R.P.M.

Manufacturer: Wiedemann Division, The Warner and Swasey Company, U.S.A.

2. Variable Speed Motor

Commercial Name: U.S. Varidrive Motor.

Capacity: 3 H.P., 3 Phase., 50 Cycles., 400 V.,
Minimum R.P.M. = 375., Maximum
R.P.M. = 3750.

Manufacturer: U.S. Electrical Motors Division,
Emerson Electric Co., Old Tate Lane.,
Milford, Conn. 06460, U.S.A.

3. Transducers

a) Velocity Type

Commercial Name: MB Vibration Pickup, Types: 100 ,
124 , 125 , 126 , and 127.

Natural Frequency: 4.75 C.P.S.

Manufacturer: MB Electronics, A Division of Textron
Electronics, Inc., P.O. Box 1825 ,
New Haven 8 , Conn., U.S.A.

b) Acceleration Type

Commercial Name: Piezoelectric, Accelerometer-Type
Pickups, Type 1560-P52.

Range for Flat
Frequency Response: 2-20000 C.P.S.

Manufacturer: General Radio Company, West Concord,
Massachusetts, U.S.A.

4. Oscilloscope

Commercial Name: Type 564 Storage Oscilloscope.

Special Features: Two Seperate Storage Screens, can be
Operated in a Variety of Modes
Including Differential, Multi-trace,
Wide-band, Sampling and Delayed Sweep;
Convenient for Detailed Viewing and
Photography.

Manufacturer: Tektronix, Inc., S.W. Millikan Way.,
P.O. Box 500., Beaverton., Oregon.,
U.S.A.

5. Vibration Meters

a) Commercial Name: MB Vibration Meter, Model M6.

Manufacturer: MB Electronics, A Division of
Textron Electronics, Inc., P.O. Box
1825, New Haven 8 , Conn., U.S.A.

b) Commercial Name: Type 1553-AK Vibration Meter.

Manufacturer: General Radio Company, West Concord,
Massachusetts, U.S.A.

VITA

N.R. Krishnaswamy was born on 25 August 1942 in Shimoga, Mysore State. He attended Secondary School at the Government High School, Chikballapur, Mysore State and passed the Public Examination for the Mysore Secondary School-Leaving Certificate in June 1958. From June 1958 to April 1959, he attended the Pre-University Course of Mysore University at National College, Bangalore and passed the Pre-University Examination in June 1959. He enrolled in the University College of Engineering, Bangalore in 1959 and received from Bangalore University, the B.E. degree in Civil Engineering in 1965. He was admitted to the Indian Institute of Technology, Kanpur, as a graduate student in July 1966 and was awarded an M. Tech. degree in Civil Engineering in June 1968. He continued his graduate study at the Indian Institute of Technology, Kanpur and enrolled in the Ph.D. Programme in July 1968.

His professional experience includes work with the Central Public Works Department of the Government of India, Nagpur as a Graduate Section Officer from February 1966 to July 1966. He has been working as a Senior Research Assistant in the Civil Engineering Department at Indian Institute of Technology, Kanpur since September 1968.

He served the Society of Civil Engineers, Indian Institute of Technology, Kanpur as a Vice-President, during the Academic Year 1967-68.

